HIGHWAY RESEARCH RECORD

Number 405

Soils and Bases: Characteristics, Classification, and Planning

16 reports
prepared for the
51st Annual Meeting

Subject Areas

25	Pavement Design
33	Construction
61	Exploration-Classification (Soils)
62	Foundations (Soils)
63	Mechanics (Earth Mass)
64	Soil Science

HIGHWAY RESEARCH BOARD
DIVISION OF ENGINEERING NATIONAL RESEARCH COUNCIL
NATIONAL ACADEMY OF SCIENCES—NATIONAL ACADEMY OF ENGINEERING

Washington, D.C. 1972

NOTICE

The studies reported herein were not undertaken under the aegis of the National Academy of Sciences or the National Research Council. The papers report research work of the authors done at the institution named by the authors. The papers were offered to the Highway Research Board of the National Research Council for publication and are published herein in the interest of the dissemination of information from research, one of the major functions of the HRB.

Before publication, each paper was reviewed by members of the HRB committee named as its sponsor and was accepted as objective, useful, and suitable for publication by NRC. The members of the committee were selected for their individual scholarly competence and judgment, with due consideration for the balance and breadth of disciplines. Responsibility for the publication of these reports rests with the sponsoring committee; however, the opinions and conclusions expressed in the reports are those of the individual authors and not necessarily those of the sponsoring committee, the HRB, or the NRC.

Although these reports are not submitted for approval to the Academy membership or to the Council of the Academy, each report is reviewed and processed according to procedures established and monitored by the Academy's Report Review Committee.

ISBN 0-309-02077-8

Price: $4.60

Available from

Highway Research Board
National Academy of Sciences
2101 Constitution Avenue, N.W.
Washington, D.C. 20418

CONTENTS

FOREWORD

The multiciplicity of problems faced by the soils engineer in a transportation-oriented department is illustrated in this RECORD, which includes papers on topics that are as widely separated as the effect of negative skin friction on piles and the capability of an unsurfaced roadway.

This RECORD also includes papers of interest to the bridge engineer. Those papers deal with influence values for vertical stress distribution beneath uniformly loaded circles, uncertainty of settlement analysis, vertical sand drains, and dragdown due to negative skin friction.

The planner and those responsible for route location will be interested in the applications of air-photo interpretation to the definition of soils problems and of the generalized regional concept to highway soils considerations.

Transportation departments, increasingly involved in the design of roads in wilderness areas, will find the road capability study report helpful.

The more sophisticated material characteristics, methods of arriving at trade-offs through values of relative strength, and improved soil bituminous mix design are discussed in several papers that will benefit the materials engineer and the structural pavement designer. Safety and convenience are improved with improved methods of in situ strength evaluation.

COEFFICIENTS OF RELATIVE STRENGTH FOR IOWA GRANULAR BASE MATERIALS

K. L. Bergeson and J. M. Hoover, Department of Civil Engineering and Engineering Research Institute, Iowa State University

The purpose of this investigation was to use the consolidated-undrained triaxial test to relate untreated and asphalt-treated Iowa granular base materials to those used in the AASHO Road Test. The primary objectives were to (a) obtain a measure of the relative behavior of Iowa materials from different aggregate sources for comparison with 2 AASHO Road Test materials also subjected to the same triaxial test technique and (b) develop a laboratory triaxial test technique and form of analysis to indicate a granular materials variability for ascertaining an assigned coefficient of relative strength. Results indicated that volumetric strain-axial strain relations were appropriate evaluation parameters for determining coefficient of relative strength at what was termed minimum volume failure criteria; minimum volume is considered as a point of "proportional limit" when viewed in conjunction with a stress-strain diagram.

•PERFORMANCE of a flexible pavement structure is related to the physical properties and supporting capacity of the various structural components. The AASHO Interim Guide for the Design of Flexible Pavement Structures, based on the pavement performance-serviceability concept developed from the AASHO Road Test, uses the physical properties and supporting capacity of granular base materials through an evaluation of the coefficient of relative strength of the materials. The term "coefficient of relative strength" implies that materials vary in their physical properties and, thus, affect the supporting capacity of the pavement structure. The coefficients developed from the AASHO Road Test are indicative of a material's variance.

The purpose of this investigation was to use the consolidated-undrained triaxial test to relate untreated and bituminous-treated Iowa granular base materials to those used in the AASHO Road Test. The primary objectives were to

1. Obtain a measure of the relative behavior of Iowa materials from different aggregate sources for comparison with 2 AASHO Road Test materials also subjected to the same triaxial test technique, and
2. Develop a laboratory triaxial test technique and form of analysis to indicate a granular materials variability for ascertaining an assigned coefficient of relative strength (CORS).

MATERIALS

Twenty-one materials of varying aggregate types and sources were studied. All untreated aggregates and bituminous-treated field mixes were furnished through cooperation of the Iowa State Highway Commission (ISHC).

Bituminous-treated, field-mixed samples were obtained by ISHC personnel from construction batch plants immediately following mixing with asphalt. Aggregates used for all laboratory mixes were obtained by sampling prior to batching or from stockpiled

Sponsored by Committee on Strength and Deformation Characteristics of Pavement Sections.

materials. Asphalt cement for the laboratory mixes, penetration grade 120 to 150, was also furnished by the ISHC.

Samples of AASHO Road Test base material, obtained from the road test site, were provided in a limited quantity. The base material included a hard dolomitic limestone, recommended by the ISHC for use in an untreated condition, and a coarse-graded gravel, recommended for use in a bituminous-treated condition.

SPECIMEN PREPARATION

All 4-in. diameter by 8-in. high cylindrical test specimens were prepared by a vibratory compaction procedure using an electromagnetic vibrator operating at a constant frequency of 3,600 cycles/min and an amplitude of 0.368 mm, a surcharge weight of 35 lb, and a vibration duration of 2 min. This procedure, previously reported by Hoover et al. (1), minimizes aggregate degradation and segregation while producing uniform densities comparable to other methods. Figure 1 shows the specimen preparation procedure.

Bituminous-Treated Materials

Laboratory- and field-mixed materials were molded and tested in a similar manner. The major difference was in the initial preparation and combining with asphalt of the laboratory mixes of known gradation and then molding as a 1-step operation. The field-mixed samples, by contrast, had to be reheated from a previously mixed condition and relatively unknown gradation and asphalt content.

Aggregates for the laboratory-mixed materials were blended and adjusted, if needed, to meet ISHC recommended gradations within ±2 percent of each sieve fraction. Test specimens were molded at the asphalt content recommended by the ISHC.

AASHO coarse-graded gravel material, as obtained from the test road, was separated into individual sieve fractions, blended, and adjusted to within 1 standard deviation from the AASHO mean gradation for bituminous-treated base material as given in the road test report (11, Table 37, p. 74). Test specimens were molded at 5 percent asphalt content.

All bituminous-treated specimens were air-cured at about 75 F for a minimum of 7 days prior to testing.

Untreated Materials

Seven materials were selected for use in an untreated condition, as representative of the various aggregate types. Each was blended and adjusted in the same manner as the laboratory-mixed, bituminous-treated materials. A moisture-density curve was established for the adjusted blend, and test specimens were molded at optimum moisture. When compaction was complete, all specimens were wrapped in 2 layers of Saran Wrap with a taped layer of aluminum foil and placed in a curing room at about 75 F and 100 percent relative humidity until testing.

AASHO crushed-limestone material was blended and adjusted to within 1 standard deviation from the mean gradation for untreated crushed limestone base material as given in the road test report (11, Table 31, p. 68). Test specimens were molded at 6 percent moisture content.

TESTING PROCEDURE

This investigation utilized the consolidated-undrained triaxial test for all specimens. All testing was conducted at a deformation rate of 0.01 in./min. Pore pressure, volume change, and axial load readings were taken at vertical deflection intervals of every 0.01 to 0.2 in., every 0.025 to 0.4 in., and every 0.05 to 0.6 in. deflection. Specimen volume changes were measured to a precision of 0.01 $in.^3$. Both positive and negative pore pressures could be measured.

A minimum of 4 tests were performed within each mix type (field mix, 4 percent laboratory mix, 5 percent laboratory mix, and selected untreated mixes) at 10-, 20-, 30-, and 40-psi lateral pressure.

Figure 2 shows the bituminous-treated materials test procedure. The test procedure for the untreated materials was similar except that specimens (a) could not be saturated and (b) were not heated but maintained at room temperature.

METHOD OF ANALYSIS

Failure Criterion

Results of this investigation were analyzed on the basis of 2 criteria of failure.

1. Minimum volume (MV) is defined as that point of loading at which the specimen has consolidated to its smallest volume during triaxial shear. As the specimen is loaded, volume decreases to some minimum value, and pore pressure in the undrained specimen increases to its maximum positive value. It is believed that at this point failure has begun and may be considered a "proportional limit" when viewed in conjunction with a stress-strain curve. On further axial loading volume increases, an interparticle sliding or crushing or both will begin. Pore pressure will also decrease. Further illustrations of this concept are presented by Fish and Hoover (2) and Ferguson and Hoover (3).
2. Maximum effective stress ratio (MESR) is defined as that point in a triaxial shear test at which the effective stress ratio $(\bar{\sigma}_1 - \bar{\sigma}_3)/\bar{\sigma}_3$ is at a maximum. Effective stresses are intergranular stresses corrected for pore pressures. At MESR the specimen volume has increased substantially, and negative pore pressure normally exists. Further illustrations of this concept are presented by Fish and Hoover (2) and Best and Hoover (4).

Calculations

An IBM 360/65 computer program was used to determine stress, strain, volume change, and pore-pressure conditions at each data point in the shear portion of the triaxial test. This program was also capable of producing plots of effective stress ratio, percentage of volume change, and pore pressure versus percentage of axial strain. Values of cohesion, friction angle, modulus of deformation (2), and Poisson's ratio were determined from each series of tests and output of the appropriate failure criterion.

Statistical Analysis

An IBM 360/65 computer program capable of generating correlation coefficients among a large number of variables, having an equally large number of observations of each variable, was used as one means of analyzing the large volume of triaxial test results. The correlation coefficients were output in matrix form.

The coefficient of correlation is a good measure of linear correlation between 2 variables. It must be emphasized, however, that the correlation coefficients developed are indicative of linear trends only. A low correlation coefficient means only that no significant linear trend exists; consequently, a nonlinear relation may exist. The coefficient may vary from +1 to -1. A positive value indicates positive linear correlation; a negative value indicates negative linear correlation.

Correlation matrices were produced separately for the field mixes, 4 percent laboratory mixes, 5 percent laboratory mixes, and the untreated mixes at 10-, 20-, 30-, and 40-psi lateral pressure.

Flow charts indicating variables used for the correlation matrices at minimum volume and maximum effective stress ratio failure criteria are shown in Figures 3 and 4 respectively. Definitions of the variables shown in the flow charts are as follows:

Name	Abbreviation	Number
Asphalt content	AC	1
Optimum moisture content	Opt. MC	1
Sand equivalent	S. Eq.	2
Percentage passing No. 200 sieve	-No. 200	3

Figure 1. Specimen preparation.

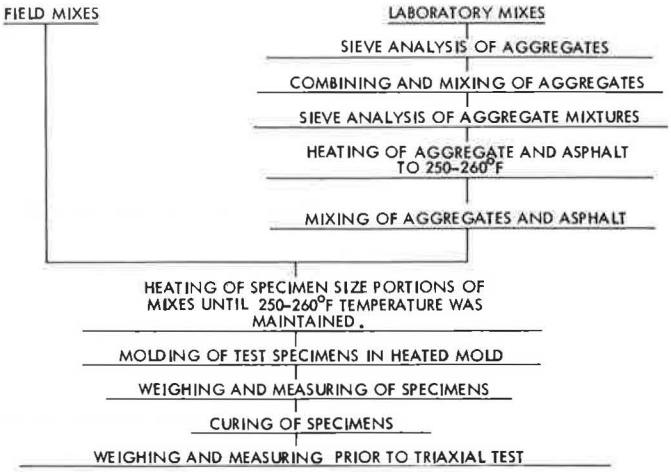

Figure 2. Test procedure for bituminous-treated materials.

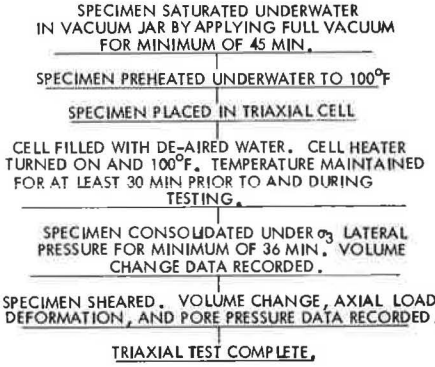

Figure 3. Variables used at minimum volume conditions for correlation determinations.

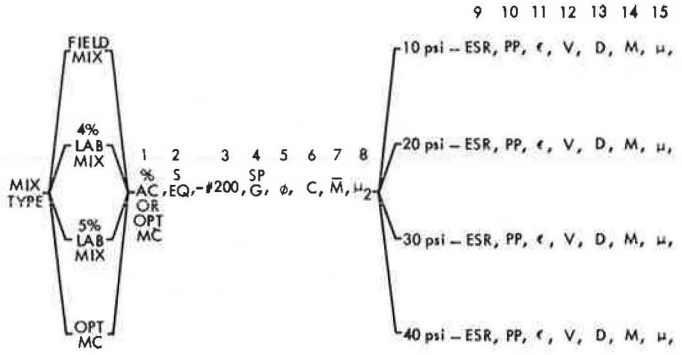

Figure 4. Variables used at maximum effective stress ratio conditions for correlation determinations.

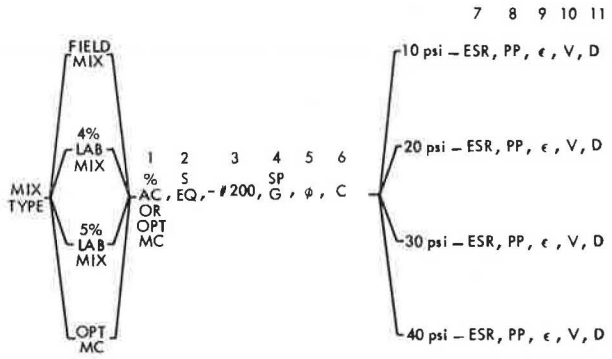

Name	Abbreviation	Number
Specific gravity	Sp. G.	4
Angle of internal friction	ϕ	5
Cohesion	C	6
Average modulus of deformation (2)	$\overline{M}$	7
Poisson's ratio (2, Eq. 21)	μ_2	8
Effective stress ratio	ESR	9
Pore pressure	PP	10
Axial strain	ϵ	11
Volumetric strain	V	12
Density	D	13
Modulus of deformation	M	14
Poisson's ratio (2, Eq. 13)	μ	15

In addition to the variables gathered from the triaxial tests, the following properties, as determined by the ISHC, were included as variables for the correlation matrices: specific gravity, sand equivalent, and percentage passing the No. 200 sieve for the field mixes.

The AASHO materials were not included as a part of any of the correlation matrices since they were considered strictly as control samples.

The primary purpose of this phase of analysis was to determine which pair, or pairs, of variables exhibited a significant degree of correlation and was consistent among the various materials. The value of these variables could then be compared to the value of the same variables of the AASHO control mixes, and ranked accordingly, in order to obtain the coefficient of relative strength (CORS).

RESULTS

Minimum Volume Criteria

Investigation of correlation matrices developed for the various mix types (field, 4 percent laboratory, 5 percent labortory, and untreated) at minimum volume failure conditions indicated that the highest degree of correlation was obtained between volumetric strain (defined as the percentage ratio of unit volume change to original volume at start of shear phase of triaxial test) and axial strain (defined as the percentage ratio of axial deformation to original axial length at start of shear phase). Volumetric strain and axial strain referred to here are at the point of minimum volume failure criteria.

The correlations between volumetric strain and axial strain (V-ϵ) were consistent for all lateral pressures within each mix type and among mix types. Figures 5 through 7 show the V-ϵ regression lines for the various mix types at 10-psi lateral pressure. Figure 8 shows the combined V-ϵ regression line for the untreated materials at 10-, 20-, and 30-psi lateral pressure.

Least squares linear regressions were performed on values of volumetric strain and axial strain within the mix types of each lateral pressure. Results are given in Table 1.

Slopes of the volumetric strain-axial strain lines, as determined by regression, remained relatively consistent among treated mixes within a given lateral pressure though there appeared to be a decrease in slope with increase in lateral pressure for the treated mixes.

Slopes of volumetric strain-axial strain lines for the untreated mixes were considerably greater than for treated mixes and appeared to increase with lateral pressure.

The volumetric strain-axial strain regression lines for the 10-, 20-, and 30-psi lateral pressures for untreated and treated mixes, shown in Figure 9, were used for qualitative observations. It can be shown that, when Poisson's ratio is 0, volumetric strain is equal to axial strain and lateral strain is 0. It can also be shown that, when Poisson's ratio equals 0.5, volumetric strain is 0 (incompressible) and axial strain equals twice the lateral strain. These conditions are shown in Figure 9.

Figure 5. Volumetric strain versus axial strain for 4 percent laboratory mix at minimum volume and 10-psi lateral pressure.

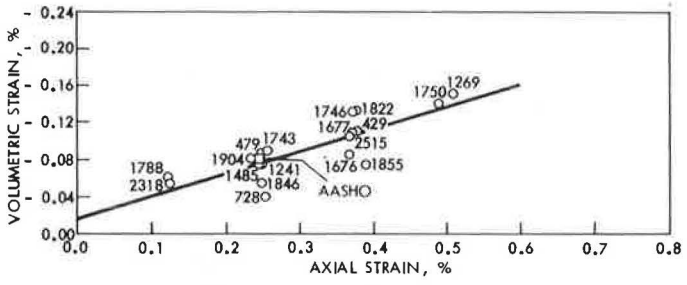

Figure 6. Volumetric strain versus axial strain for 5 percent laboratory mix at minimum volume and 10-psi lateral pressure.

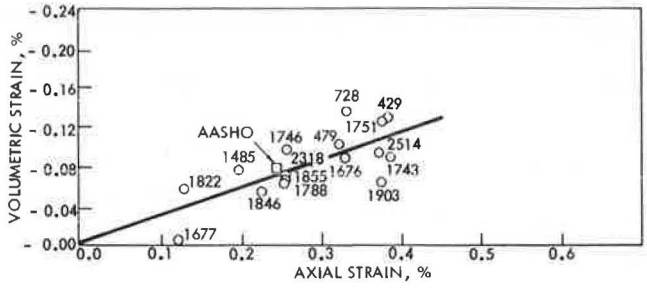

Figure 7. Volumetric strain versus axial strain for field mix at minimum volume and 10-psi lateral pressure.

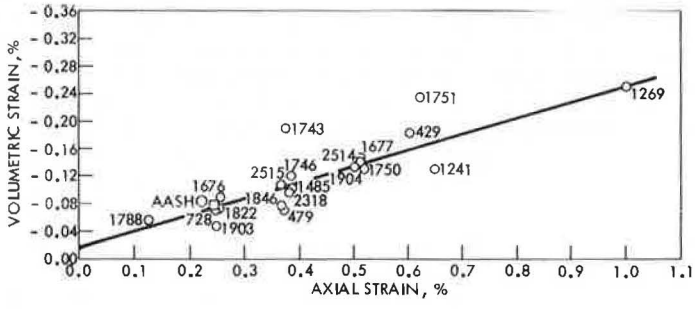

Figure 8. Volumetric strain versus axial strain for untreated mix with optimum moisture content at minimum volume and 10-, 20-, and 30-psi lateral pressures.

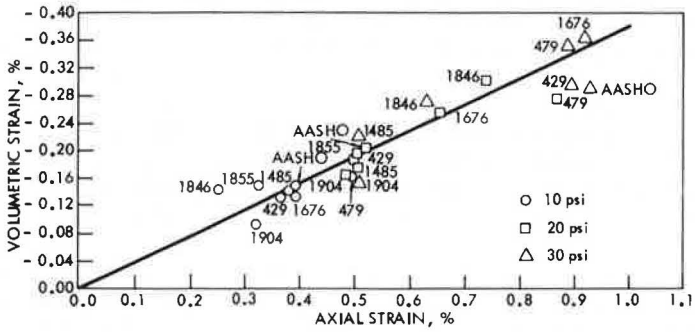

Table 1. Regression results.

Mix	Lateral Pressure	Intercept	Slope	Correlation Coefficient
Field	10	-0.016	-0.243	0.855
	20	-0.012	-0.234	0.841
	30	-0.030	-0.190	0.948
	40	-0.022	-0.228	0.931
4 percent laboratory	10	-0.017	-0.243	0.816
	20	-0.026	-0.203	0.943
	30	-0.050	-0.179	0.973
	40	-0.048	-0.186	0.986
5 percent laboratory	10	-0.006	-0.267	0.722
	20	-0.010	-0.241	0.860
	30	-0.049	-0.167	0.881
	40	-0.060	-0.191	0.945
Optimum moisture content	10	-0.094	-0.118	0.400
	20	-0.028	-0.321	0.903
	30	-0.023	-0.353	0.899
	40	-0.012	-0.377	0.966

Note: AASHO values were not included in the regressions.

Figure 9. Volumetric strain and axial strain characteristics based on minimum volume criteria.

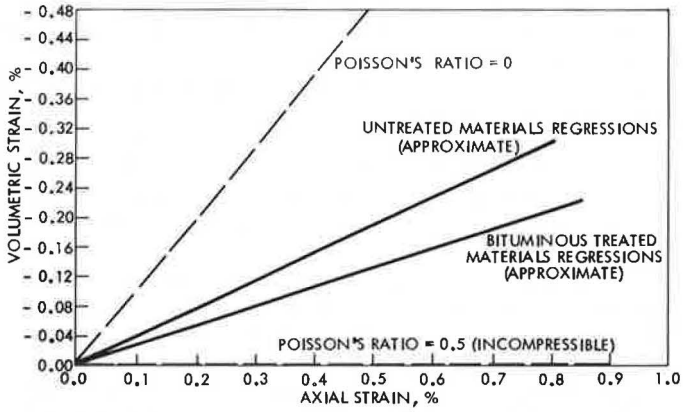

Untreated materials exhibited greater slopes than treated materials, indicating that at a given value of axial strain the amount of volume decrease is greater for the untreated materials. It also indicates that both materials exhibited a limited amount of lateral strain although volume was decreasing. Treated materials underwent more lateral strain, at a given axial strain, than untreated materials.

The variation in slopes between the untreated and treated materials can be attributed to test temperature (the treated materials were tested at 100 F), density difference from untreated to treated condition, degree of saturation, or asphalt content. If the temperature difference at testing is assumed to be the cause of the deviation, that should allow the asphalt-treated specimens to undergo volume decrease without lateral strain easier than if they were tested at room temperature. This, however, would only tend to lessen the deviation since temperature, if it is contributing, is tending to equalize and not cause the variance.

Dry densities of the untreated specimens were generally higher than those of treated specimens of the same material. This is probably due to the asphalt increasing specimen volume by separation of soil particles with a film of asphalt and fines, thereby decreasing the specimen weight. Also, the cohesive property of asphalt does not allow so much freedom for particle reorientation during compaction as water in the untreated specimens. If density is thus assumed to cause the deviation in volumetric strain at a given vertical strain, it can be reasoned that the less dense specimen of a given material would normally have a greater void ratio and consequently should be able to undergo a volume decrease without lateral strain easier than denser specimens. This again would tend to equalize the deviation and not contribute to it.

All field- and laboratory-mixed bituminous-treated materials were vacuum saturated. As previously indicated, the untreated material specimens could not be saturated. The latter was due to complete disintegration of the specimens under vacuum saturation and severe flotation removal of fines when capillary saturated. Calculated degree of saturation of the untreated materials ranged from less than 60 to near 95 percent saturation. Theoretically, materials at a low percentage of saturation should undergo a greater volumetric strain than materials at a higher percentage of saturation. No correlation was found between calculated degree of saturation and volumetric strain. Instead, untreated materials of high saturation exhibited both high and low volumetric strain. Similar data were noted for the low degree of saturation in untreated materials.

Thus, by the process of elimination it can be concluded that the primary cause of deviation in regression slopes of the treated materials to the untreated materials is the asphalt itself. It should not be concluded, however, that density and temperature have no effect whatsoever. Instead, the effect of these variables would appear to decrease the deviation. This behavior can possibly be explained by the fact that the cohesive properties of the asphalt tend to lock the individual particles together in a matrix of asphalt and fine material. During the initial shear portion of a test, when the specimen is being further consolidated, the particles are less able to reorient themselves into a more compact state without a greater amount of lateral strain than the untreated specimens, even though the latter are less dense initially.

Figure 9 shows that more solid materials such as concrete mixtures will have slopes of volumetric strain-axial strain approaching the line representing Poisson's ratio equal to 0. Such materials exhibit very little lateral strain on loading, while stability is primarily dependent on individual material properties. The other extreme is fluids and fluid mixtures that are nearly incompressible and will have slopes of volumetric strain-axial strain approaching Poisson's ratio of 0.5. Fluids are entirely dependent on lateral restraint to support loads.

From the data shown in Figure 9, one can imagine a succession of lines beginning at Poisson's ratio equal to 0 and representing materials that derive stability from individual material properties and continuing to the line representing Poisson's ratio equal to 0.5 and representing materials deriving their stability primarily from lateral restraint. As the slope of this line decreases, stability becomes more dependent on some form of lateral restraint. Asphaltic concrete is a fluid-solid mixture (Fig. 9) and is more dependent on lateral restraint for stability than on individual material properties.

In a study of cement-treated granular base materials, Ferguson and Hoover (3) advanced the hypothesis that the stability of untreated granular bases may be a function of lateral restraint existing prior to loading and of its ability to increase the restraint through resistance to lateral expansion. The results of this study appear to confirm this hypothesis, extending it to include bituminous-treated base materials.

A study of the shear strength parameters of cohesion and friction angle at minimum volume for the 7 materials used in the treated and untreated condition revealed that the addition of asphalt generally reduced the angle of friction and slightly increased cohesion but did not substantially alter overall shear strength characteristics. This indicates that strength alone does not account for the differences in stabilities of bituminous-treated and untreated base materials.

A mechanism that may account, in part, for the stability differences and may not be so nearly dependent on strength is suggested. Under similar field conditions bituminous-treated materials will exhibit more lateral strain per given amount of vertical strain than untreated materials. This would give rise to greater lateral support from adjacent material for the bituminous-treated materials and, hence, greater stability by virtue of being more able to undergo lateral strain.

A study by Csanyi and Fung (5) concluded that there was no direct relation between performance of an asphaltic mix and its stability regardless of the method used to determine stability. This indicates that, although asphaltic mixes may meet stability requirements and may not fail in terms of shear, they may fail in performance from rutting and channeling. It, therefore, seems that some measure of rutting potential is needed that would also be a measure of strength. The volumetric strain-axial strain characteristics of a particular material would seem to satisfy these requirements. A material that has a high value of volumetric strain-axial strain at minimum volume must undergo more densification and decrease in volume before reaching the condition where lateral strain will provide additional support. This material will have begun to fail in performance as a result of densification, which is the beginning of rutting. A material having a low value of volumetric strain-axial strain will need to densify very little before reaching the condition of additional lateral support.

The discussion given above also indicates that compaction and sufficient lateral support are variables that affect the stability of bituminous-treated base materials to a large degree. Nichols (6) concluded in a flexible pavement research project in Virginia that deflections and performance seemed more closely allied with compaction than with pavement design characteristics. Arena et al. (7) concluded in a compaction study that sections of pavement rolled under pressures of 85 psi had rutted far less after 3 years of exposure to heavy traffic than those rolled at 55 to 75 psi. This indicates that compaction of an asphalt-treated material is a critical factor contributing to the stability of that material and substantiates the use of minimum volume criteria and volumetric strain-axial strain characteristics as a means of evaluating stability and performance.

CORS Based on Volumetric Strain-Axial Strain

CORS were determined at 10-, 20-, and 30-psi lateral pressures. AASHO bituminous-treated gravel and untreated crushed stone were assigned CORS of 0.34 and 0.14 respectively in accordance with the AASHO Interim Guide for the Design of Flexible Pavement Structures. Each material was ranked according to its value of volumetric strain-axial strain ($V\text{-}\epsilon$), at minimum volume, on triangular charts of 10-, 20-, and 30-psi lateral pressure. Figure 10 shows the chart used for 10-psi lateral pressure. It is readily noted that the final development of these charts relied on a straight-line relation between only 2 points of control, i.e., the 2 AASHO samples recommended and supplied to the project. The charts are used as follows:

1. Volumetric strain and axial strain, as computed from the consolidated undrained triaxial shear test data at the point of minimum volume during shear, are respectively entered from the left and right sides of the chart; and
2. At the intersection of the values given above, a line is projected down and to the left, to the CORS scale.

Tables 2, 3, and 4 give the CORS determined for each material and mix type from charts similar to that shown in Figure 10. (Several CORS were determined as slightly negative values from the triangular charts but are given in Tables 2, 3, and 4 as 0.) The validity of the CORS thus determined can be fully ascertained only after extensive analysis of the pavement field performance where each material and mix type have been used.

However, it is obvious from data given in Tables 2, 3, and 4 that definite physical property and supporting capacity differences exist among the various materials and mix types. The CORS from untreated to either 4 or 5 percent laboratory mix show that an optimum asphalt content could be significantly less than 4 percent for some mixes or higher than 5 percent for other mixes. Comparison of untreated with treated CORS generally shows the benefit of addition of asphalt.

Three pairs of field and laboratory mixes each used the same aggregate source, i. e., mixes 1750-1751, 1903-1904, and 2514-2515 (respectively limestone-dolomite, gravel, and limestone). The variation of CORS due to asphalt content is apparent between the laboratory and field mixes for each of these materials (Tables 2 and 3). Table 3 gives little variance in CORS with asphalt treatment of these materials, probably because of the increase in lateral restraint, as later explained in this paper.

Comparison of the untreated 4 and 5 percent treated laboratory mixes with their respective field mixes is difficult, however. Major inconsistencies of comparison of the field mixes and their closest laboratory-mix asphalt content were noted during analyses. These inconsistencies were apparently related to gradation differences (extracted gradation varied from recommended gradation) and the effects of reheating the mixtures. A study by Hveem (8) indicates that asphalts harden and become more brittle (lowering of initial penetration) on cooling from an elevated temperature. Therefore, on reheating and cooling an unknown additional amount of brittleness may have been introduced in the field-mixed samples.

There was no discernible trend for the variation of CORS with aggregate type. Some gravels had a very low CORS, material 1269 in particular, while some had relatively high CORS. Material 1750, a dolomitic limestone, had a low CORS, while other dolomitic materials had high CORS. The traffic simulator study by Csanyi et al. (5) concluded that asphaltic mixes using softer aggregates tend to be displaced under traffic less than mixes with harder aggregates and that there is no direct relation between stability and trafficability of a particular mix. It would appear then that some mixes containing soft aggregates could perform better under traffic than those containing hard aggregates and vice versa.

The flexible pavement research study by Nichols (6) concluded that deflections and performance seemed more closely allied with compaction than with pavement design characteristics. From this it would seem that deflections would decrease and performance would increase with increasing density of the base course material. Figure 11 shows that, in general, CORS of the various materials increased with increasing density. A similar plot of density versus CORS of the field mixes was very erratic and was considered indicative of the effect of asphalt brittleness due to reheating and recooling.

Figure 12 shows a general trend for increasing CORS with increasing modulus of deformation (2) for the laboratory mixes only at 10-psi lateral pressure. This plot indicates that volumetric strain-axial strain at minimum volume is a measure of strength. A similar plot of modulus of deformation versus CORS of the field mixes was very erratic and was again considered indicative of the effect of asphalt brittleness.

Comparison of the CORS for each individual material and mix type from 10- to 20- to 30-psi lateral pressures shows less variation in value than originally anticipated. At least a partial reason for this behavior is that the range of volumetric strain-axial strain at minimum volume between untreated and treated materials increased with increasing lateral pressure. A similar increase occurred between the 2 AASHO materials, thus tending to provide similar CORS for the various materials of each of the 3 lateral pressures.

It can be reasoned that, as lateral restraint (pressure) is increased to a point of near total confinement, all materials will tend to behave similarly and their individual

Figure 10. Triangular chart for determining CORS at 10-psi lateral pressure.

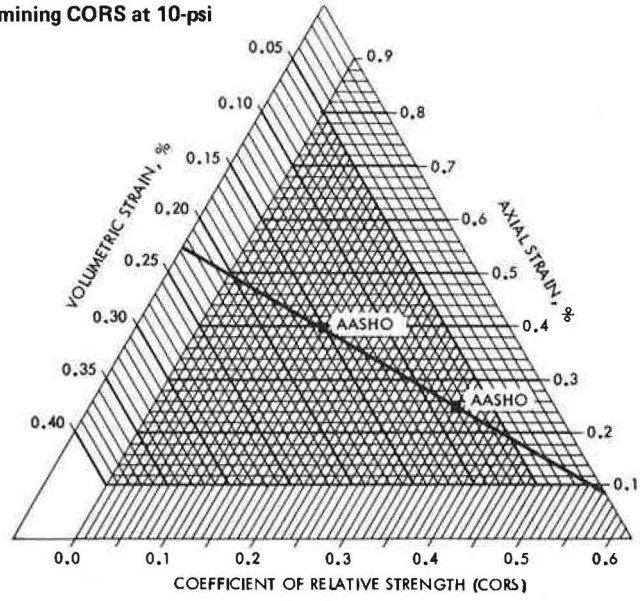

Table 2. CORS based on volumetric strain-axial strain at minimum volume and 10-psi lateral pressure.

Material			Laboratory Mix		
Type	Number	Field Mix	4 Percent	5 Percent	Untreated
Limestone	429	0	0.22	0.20	0.19
Dolomite	479	0.26	0.33	0.25	0.06
Dolomite-chert	728	0.35	0.39	0.21	ND[b]
Gravel	1241	0	0.34	—[a]	ND
Gravel	1269	0	0.05	—[a]	ND
Gravel-sand	1485	0.21	0.34	0.38	0.16
Limestone	1676	0.32	0.25	0.27	0.16
Limestone	1677	0.07	0.21	0.54	ND
Limestone	1743	0.10	0.33	0.23	ND
Limestone	1746	0.19	0.17	0.31	ND
Limestone-dolomite	1750	0.09	0.09	—[a]	ND
	1751	0	—[a]	0.19	ND
Dolomite-chert	1788	0.45	0.45	0.36	ND
Dolomite	1822	0.34	0.17	0.45	ND
Limestone	1846	0.26	0.38	0.37	0.25
Dolomite-chert	1855	0.48	0.25	0.35	0.19
Gravel	1903	0.38	—[a]	0.28	ND
	1904	0.15	0.35	—[a]	0.27
Limestone	2318	0.22	0.47	0.34	ND
Limestone	2514	0.07	—[a]	0.24	ND
	2515	0.20	0.22	—[a]	ND

[a]Not recommended for testing by ISHC. [b]Not determined.

Table 3. CORS based on volumetric strain-axial strain at minimum volume and 20-psi lateral pressure.

Material			Laboratory Mix		
Type	Number	Field Mix	4 Percent	5 Percent	Untreated
Limestone	429	0.04	0	0.32	0.14
Dolomite	479	0.24	0.35	0.34	0
Dolomite-chert	728	0.47	0.25	0.35	ND[b]
Gravel	1241	0.09	0.32	—[a]	ND
Gravel	1269	0	0	—[a]	ND
Gravel-sand	1485	0.46	0.36	0.21	0.18
Limestone	1676	0.24	0.35	0.38	0
Limestone	1677	0.25	0.13	0.10	ND
Limestone	1743	0.22	0.34	0.21	ND
Limestone	1746	0.33	0.16	0.14	ND
Limestone-dolomite	1750	0.23	0.12	—[a]	ND
	1751	0.08	—	0.23	ND
Dolomite-chert	1788	0.45	0.43	0.27	ND
Dolomite	1822	0.17	0.18	0.35	ND
Limestone	1846	0.27	0.28	0.31	0
Dolomite-chert	1855	0.37	0.35	0.40	0.16
Gravel	1903	0.20	—[a]	0.45	ND
	1904	0.37	0.35	—[a]	0.21
Limestone	2318	0.45	0.45	0.26	ND
Limestone	2514	0.28	—[a]	0.34	ND
	2515	0.16	0.24	—[a]	ND

[a]Not recommended for testing by ISHC. [b]Not determined.

Table 4. CORS based on volumetric strain-axial strain at minimum volume and 30-psi lateral pressure.

Material			Laboratory Mix		
Type	Number	Field Mix	4 Percent	5 Percent	Untreated
Limestone	429	0.15	0.22	0.28	0.15
Dolomite	479	0.34	0.29	0.37	0.12
Dolomite-chert	728	0.31	0.34	0.47	ND[b]
Gravel	1241	0.30	0.29	—[a]	ND
Gravel	1269	0	0	—[a]	ND
Gravel-sand	1485	0.36	0.33	0.36	0.28
Limestone	1676	0.26	0.31	0.37	0.12
Limestone	1677	0.18	0.06	ND	ND
Limestone	1743	0.29	0.32	0.07	ND
Limestone	1746	0.28	0.26	0.29	ND
Limestone-dolomite	1750	0.22	0	—[a]	ND
	1751	0.22	—[a]	0.06	ND
Dolomite-chert	1788	0.25	0.34	0.31	ND
Dolomite	1822	0.32	0.25	0.31	ND
Limestone	1846	0.29	0.37	0.32	0.22
Dolomite-chert	1855	0.36	0.37	0.37	0.31
Gravel	1903	0.25	—[a]	0.29	ND
	1904	0.33	0.33	—[a]	0.30
Limestone	2318	0.35	0.33	0.34	ND
Limestone	2514	0.29	—[a]	0.29	ND
	2515	0.25	0.28	—[a]	ND

[a]Not recommended for testing by ISHC. [b]Not determined.

Figure 11. Density versus CORS based on volumetric strain-axial strain at minimum volume and 10-psi lateral pressure.

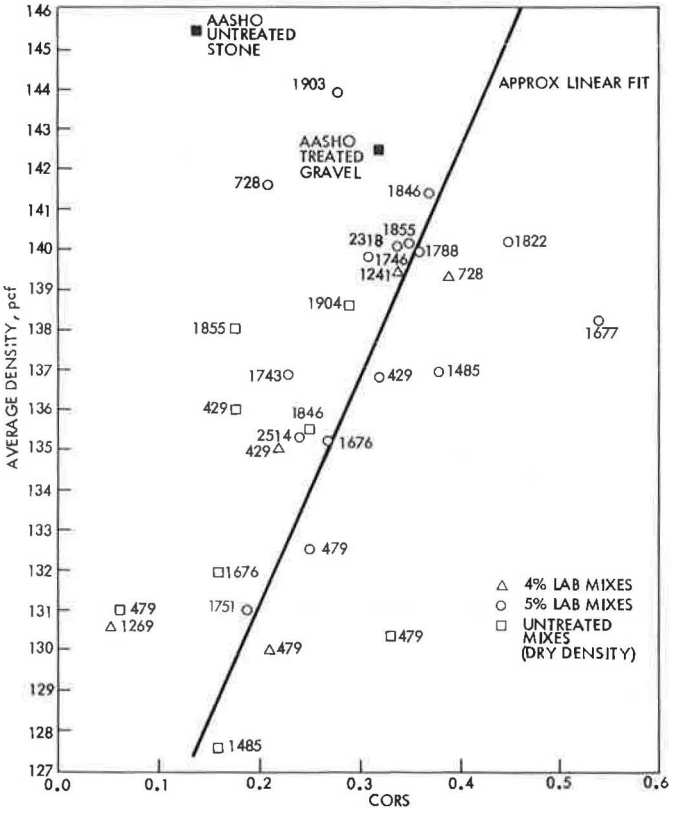

properties will have much less effect than at low lateral pressures. Such reasoning substantiates the use of volumetric strain-axial strain as a means of flexible pavement materials evaluation. However, the variation of CORS with lateral pressure indicates that a knowledge of the lateral pressures that would exist in the field under design loads must be known for the CORS to be valid. Currently there are very few data available that indicate what lateral pressures are developed in flexible pavement structures. A very rough approximation using a Boussinesq solution, assuming Poisson's ratio as 0.5, a 100-psi point load, a 6-in. depth, and offset distance of 1 ft, yielded about 13 psi. It must be recognized that none of the assumptions underlying the Boussinesq solution is met in flexible pavement structures and that Poisson's ratio is not 0.5 for soils. A decrease of Poisson's ratio, however, decreases calculated lateral stresses. Fish and Hoover (2) indicated that Poisson's ratio for the treated materials at minimum volume was about ±0.40. The untreated materials in this study had a Poisson's ratio of about ±0.30. It is, therefore, likely that the lateral stress developed would be less than the very approximate figure of 13 psi calculated above. From the previous discussion it appears that the most applicable values of CORS would be those obtained at 10-psi lateral pressure.

Variations in CORS within a particular material may occur because of individual test variations and the recording of test data at set increments of strain and may lead to some minor inconsistencies in the CORS determined for a material. Readings in the minimum volume portion of the triaxial test were taken at intervals of 0.010-in. deflection. For an 8-in. specimen height, 0.010 in. between readings is about 1 percent axial strain. Volume change readings were recordable to 0.01 in. of variation in water level in a 1-in. diameter tube. For a sample volume of 100 $in.^3$, a movement of 0.01 in. in the volume change tube is about 0.01 percent volumetric strain. Volumetric strain, therefore, changed more slowly than axial strain in this portion of the test, increasing the importance for precise determination of axial strain at which minimum volume occurs. It would be desirable in future studies to obtain continuous monitoring of volume change and axial deflection in order to firmly fix the point of minimum volume more accurately.

The concept presented in the preceding paragraph can be noted in the volumetric strain-axial strain data shown in Figures 5 through 8. Many points on the plots appear to be grouped vertically. This results from the test data being taken at set intervals of axial deflection during the shear phase of the test. Continuous and even more precise recording of test data would tend to separate the vertical nature of the plot and result in greater precision of pinpointing a CORS value in the laboratory when the techniques described in this report are used.

It should be reemphasized that the values of CORS obtained in this study are based on a very limited number of tests of the AASHO control materials. The quantity of material available was extremely limited. Four tests were run on each AASHO material at 10-, 20-, 30-, and 40-psi lateral pressure. This resulted in the CORS at each lateral pressure being determined on the basis of 2 points (Fig. 10), one for the AASHO untreated and one for the AASHO treated materials.

CORS Based on Other Variables

As previously indicated, the highest degree of correlation of data was obtained between volumetric strain and axial strain at minimum volume. For comparative purposes only, CORS were developed for other variables at minimum volume conditions by using data showing lesser degrees of correlation than volumetric strain-axial strain. Development and use procedures were somewhat different from those noted with the triangular chart (Fig. 10) because a single variable was plotted against the 2 AASHO-CORS, and the CORS for each material and mix type were thus determined on the basis of that single variable. CORS were determined for the individual variables of volumetric strain, axial strain, modulus of deformation, effective stress ratio, and average modulus of deformation, each at 10-psi lateral pressure and minimum volume.

Reasonably good comparisons of single variable CORS based on the volumetric strain ($\Delta V/V$) and axial strain ϵ at minimum volume were noted with those given in Table 2. Such comparisons indicate the potential of a simplified triaxial technique for determina-

tion of CORS using 10-psi lateral pressure and calculating only the precise axial strain at the precise, but continuously monitored, point of minimum volume.

CORS determined by using the modulus of deformation (2) at 10-psi lateral pressure varied widely within each mix type and material as well as among the various materials. The average modulus of deformation (2) CORS were not consistent with those determined by using the modulus at 10 psi and still varied widely within a material for the different mix types although the variability among materials was considerably less.

CORS determined for 10-psi lateral pressure by using the value of effective stress ratio at minimum volume indicated relatively high variability within a material for different mix types as well as among materials. A number of the field mix CORS were high, which may be a reflection of the brittleness of the reheated and recooled mixes when analyzed on a strength basis. It was generally concluded that CORS developed on the basis of a strength parameter alone did not appear valid.

Maximum Effective Stress Ratio Criteria

Specimen conditions at maximum effective stress ratio may not be as indicative of actual field conditions as those at minimum volume. Ferguson and Hoover (3) concluded that stresses at the condition of minimum volume in a triaxial shear test may be more closely related to actual field conditions than the stresses at maximum effective stress ratio. This conclusion appears especially valid in view of the relatively high value of Poisson's ratio (±0.4) for the bituminous-treated materials (2). Loading past the point of minimum volume results in a volume increase and consequently increased lateral strain. Under field conditions this increase of lateral strain would result in increased lateral pressure from adjacent material. In the triaxial test, lateral pressure remains constant, and therefore specimen conditions past the point of minimum volume might not be indicative of actual field response (4).

CORS Based on Effective Stress Ratio-Cohesion

A study of the correlation matrices developed for each mix type indicated that the only variables that had reasonably consistent correlations (between mix types) were effective stress ratio and cohesion (ESR-C). Correlations were consistent among mix types for the 10-psi tests but dropped considerably within a mix type with increasing lateral pressure. Any CORS that were to be developed on the basis of the effective stress ratio-cohesion variables would thus be highly dependent on existing lateral pressures.

Although the AASHO materials fit into the correlations at minimum volume criteria, they do not fit into the maximum effective stress ratio criteria. Instead of falling on the ESR-C regression lines, the AASHO materials lay well above the same. The densities of the AASHO treated and untreated specimens were higher than those of the Iowa materials. This is probably due, in part, to the very tight gradation control on the AASHO materials. It is believed that this density difference is the cause of the AASHO control points lying above the ESR-C regression. It was previously shown that the CORS determined on the basis of volumetric strain-axial strain were partially a function of density, i.e., in general as density increased CORS increased. The AASHO materials volumetric strain-axial strain values of minimum volume, however, compared favorably with their respective laboratory and field mixes. This indicates that, although volumetric strain-axial strain data are somewhat dependent on density, these data are nearly as sensitive to density changes as the strength criteria of ESR-C.

CORS were determined on ESR-C basis by using a triangular chart similar to that used for volumetric strain-axial strain at minimum volume. Table 5 gives the CORS thus determined at 10-psi lateral pressure (CORS shown as 0 were actually negative values). Field mixes are not included because of the high variability of the cohesion term. The extreme range of cohesion in the field mixes is probably the result of hardening of the asphalt and length of time prior to reheating for production of test specimens.

In general, there is only limited variation in CORS between materials and mix types (Table 5). Materials 1485 and 1846 indicate no basic change of CORS from untreated to either 4 or 5 percent asphalt treated. Material 1676 indicates a higher value of CORS for the untreated than either treated mix, a rather unrealistic situation. CORS

Figure 12. Modulus of deformation versus CORS based on volumetric strain-axial strain at minimum volume and 10-psi lateral pressure.

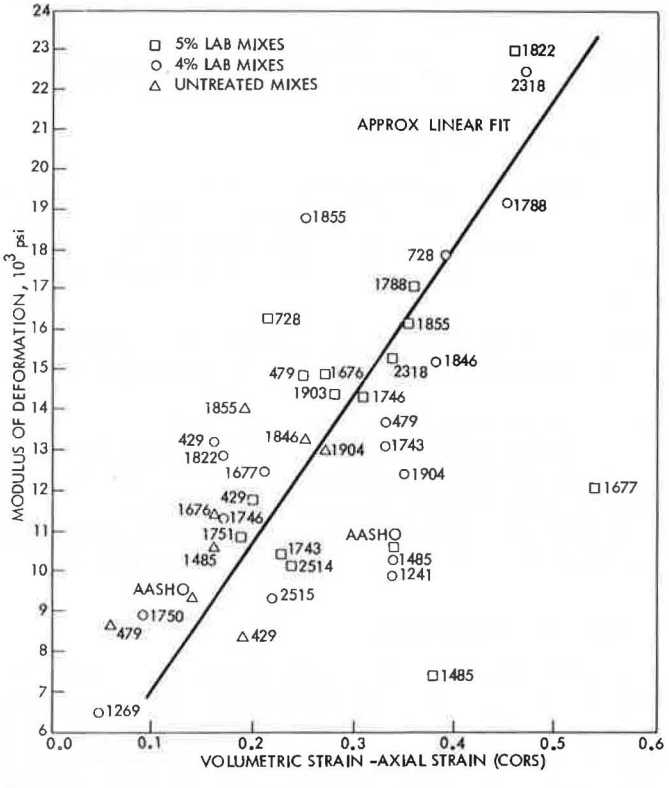

Table 5. CORS based on effective stress ratio-cohesion at maximum effective stress ratio criteria and 10-psi lateral pressure.

Material		Laboratory Mix		
Type	Number	4 Percent	5 Percent	Untreated
Limestone	429	0.29	0.23	0.18
Dolomite	479	0.25	0.16	9.24
Dolomite-chert	728	0.17	0	ND[b]
Gravel	1241	0.26	—[a]	ND
Gravel	1269	0.30	—[a]	ND
Gravel-sand	1485	0.37	0.39	0.32
Limestone	1676	0.05	0	0.16
Limestone	1677	0.22	0.20	ND[b]
Limestone	1743	0.26	0.31	ND
Limestone	1746	0.27	0.03	ND
Limestone-dolomite	1750	0.29	—[a]	ND
	1751	—[a]	0.23	ND
Dolomite-chert	1788	0.24	0.13	ND
Dolomite	1822	ND[b]	0	ND
Limestone	1846	0.25	0.23	0.24
Dolomite-chert	1855	0	0.14	0.07
Gravel	1903	—[a]	0.25	ND[b]
	1904	0.20	—[a]	0.14
Limestone	2318	0.13	0.17	ND[b]
Limestone	2514	—[a]	0.25	ND
	2515	0.29	—[a]	ND

[a]Not recommended for testing by ISHC. [b]Not determined.

for material 1855 ranged from 0.07 to a negative value to 0.14 for the untreated 4 and 5 percent laboratory mixes respectively. The 3 pairs of laboratory mixes, each using the same aggregate source—i. e., mixes 1750-1751, 1903-1904, and 2514-2515—show little variation between asphalt content or aggregate source.

As a consequence of the observations given above, CORS determined on the effective stress ratio-cohesion basis at MESR criteria do not appear valid for use in thickness design.

CONCLUSIONS

Coefficients of relative strength determined in this laboratory study are based on a very limited number of control values established from the AASHO materials and should be viewed with this in mind. The validity of the CORS determined can be fully ascertained only after extensive analysis of the pavement field performance where each material and mix type have been used.

1. Volumetric strain-axial strain relations appear to be appropriate evaluation parameters for determining coefficients of relative strength at minimum volume failure criteria.
2. Coefficients of relative strength determined on the basis of volumetric strain-axial strain tend to vary slightly with lateral pressure, all treated materials tending toward similar values of CORS as lateral pressure is increased. CORS determined at 10-psi lateral pressure are probably more indicative of actual field conditions.
3. Coefficients of relative strength determined on the basis of effective stress ratio-cohesion, at maximum effective stress ratio criteria, do not appear valid for use in thickness design.

ACKNOWLEDGMENTS

Sincere appreciation is extended to the sponsoring organizations—Iowa Highway Research Board, Iowa State Highway Commission, and Federal Highway Administration—and to S. E. Roberts and Bernard Ortgies, Iowa State Highway Commission, for their assistance and counseling. In addition, a special thanks is extended to personnel of the Engineering Research Institute, Iowa State University, for their untiring and valuable contributions to the research involved in this paper and the total project (10).

REFERENCES

1. Hoover, J. M., Kumar, S., and Best, T. W. Degradation Control of Crushed Stone Base Course Mixes During Laboratory Compaction. Highway Research Record 301, 1970, pp. 18-27.
2. Fish, R. O., and Hoover, J. M. Deformation Moduli of Asphalt Treated Granular Materials. Eng. Res. Institute, Iowa State Univ., Spec. Rept., 1969.
3. Ferguson, E. G., and Hoover, J. M. Effect of Portland Cement Treatment of Crushed Stone Base Materials as Observed From Triaxial Shear Tests. Highway Research Record 255, 1968, pp. 1-15.
4. Best, T. W., and Hoover, J. M. Stability of Granular Base Course Mixes Compacted to Modified Density. Eng. Res. Institute, Iowa State Univ., Spec. Rept., 1966.
5. Csanyi, L. H., and Fung, H. P. Traffic Simulator for Checking Mix Behavior. Highway Research Record 51, 1964, pp. 57-67.
6. Nichols, F. P. Flexible Pavement Research in Virginia. HRB Bull. 269, 1960, pp. 35-50.
7. Arena, P., Shah, S. G., and Adam, V. Compaction Type Tests for Asphaltic Concrete Pavement. Highway Div. Newsletter, ASCE, Feb. 1967, p. 5.
8. Hveem, F. N. Effects of Time and Temperature on Hardening of Asphalts. HRB Spec. Rept. 54, 1960, pp. 13-18.
9. Csanyi, L. H., Cox, R. E., and Teagle, C. R. Effect of Fillers on Asphaltic Concrete Mixes. Highway Research Record 51, 1964, pp. 68-88.
10. Hoover, J. M. Granular Base Materials for Flexible Pavements. Eng. Res. Institute, Iowa State Univ., Final Rept., 1970.
11. The AASHO Road Test: Report 2—Materials and Construction. HRB Spec. Rept. 61B, 1962.

RELATION OF STRESS TO STRAIN FOR A CRUSHED LIMESTONE BASE MATERIAL

William M. Moore, Sylvester C. Britton, and Frank H. Scrivner,
Texas Transportation Institute, Texas A&M University

ABRIDGMENT

•A TRULY rational system for the design of flexible pavements must include realistic physical equations—or computer-oriented procedures—from which traffic-induced stresses and deformations can be estimated. The first step in the derivation of such equations or procedures is to find, from laboratory and in situ testing, a set of basic relations between stress and strain from which one can predict, with acceptable accuracy, the deformations of flexible pavement materials subjected to any given state of stress. Many investigations have been devoted to a search for these basic relations within the laboratory. This is a report of one such investigation.

The physical data were acquired by a newly developed optical displacement tracker (Fig. 1). The instrument, commercially available from Martin Tracker Corporation, made it possible to measure the dynamic displacement vector at selected points on the periphery of a cylindrical triaxial test specimen of water-bound crushed limestone during rapid loading (Fig. 2). Except for brief infrequent intervals devoted to the acquisition of displacement data for selected combinations of lateral and vertical loadings, a 6-in. diameter by 8-in. high test specimen was subjected to a constant lateral pressure of 20 psi and a repetitive vertical pressure of 34 psi. The latter was applied and released within 0.2 sec and was repeated every 2 sec. A total of 2.5 million vertical load applications was made during the testing program.

The displacement data taken at points in the central region of the surface of the specimen—where the stresses were assumed to be reasonably uniform at any given instant—were converted to axial and circumferential strain components. The strain components were analyzed with respect to their relation to the applied pressures (Fig. 3). These strain data are believed to represent more reliably the deformation of triaxially loaded specimens than data obtained by any other method known to the authors. The measurement methods and the techniques used to develop strains are fully described in another paper (1). Table 1 gives values of resilient moduli determined for several typical conditions of loading.

Various stress-strain hypotheses proposed by other investigators were tried in an attempt to fit the observed stress-strain behavior. All were rejected. In general it was found that for brief periods of testing at a fixed confining pressure, a specimen appears to behave like an anisotropic elastic material. However, as the confining pressure is changed or the repetition of load is continued for a period of time, a specimen's pseudo anisotropic elastic constants vary. The writers were unable to formulate a rational mathematical hypothesis that would account for the variations due to both of these factors.

Based on measured axial and circumferential strains of crushed limestone specimens having moisutre contents near optimum, the following conclusions were apparent:

1. Laboratory specimens are anisotropic (that is, their stiffness in the axial direction is quite different from that in the radial direction);
2. The effect of changes in the rate of loading, within the range of about 200 to 600 psi per second, is small and probably insignificant;

Sponsored by Committee on Strength and Deformation Characteristics of Pavement Sections.

Figure 1. Optical displacement tracker (center), loading apparatus (right), and recorder (left).

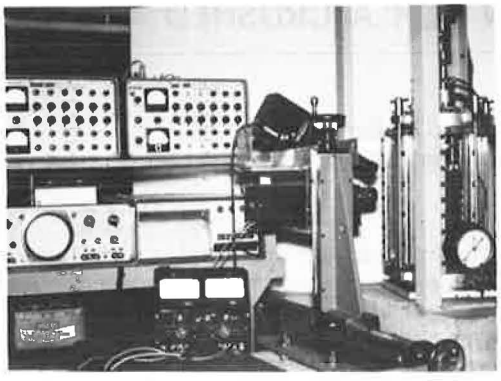

Figure 2. Triaxial test specimen with optical targets attached and ready for testing.

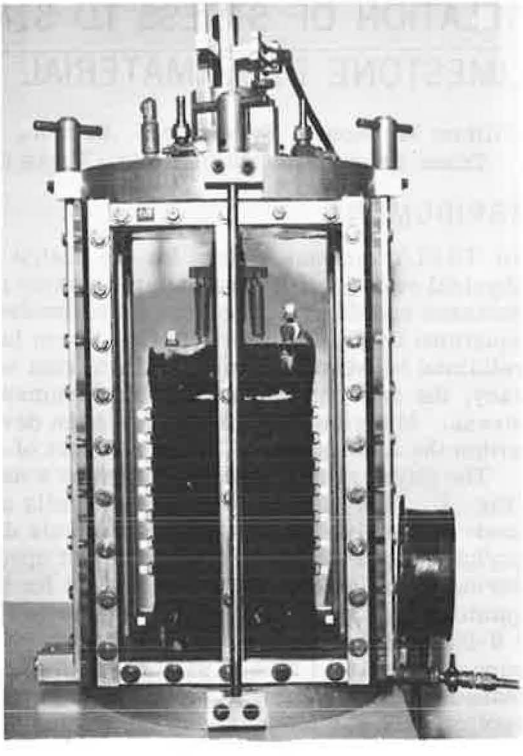

Table 1. Resilient modulus for lateral pressures of 10 and 30 psi.

Test	Average Number of Load Applications (millions)	Resilient Modulus 10 psi	Resilient Modulus 30 psi
1-6	0.06	70,600	160,200
7-12	0.27	98,500	199,700
13-18	0.77	170,600	342,400
19-24	2.49	332,900	503,000

Figure 3. Typical stress-strain data for tests 7-12.

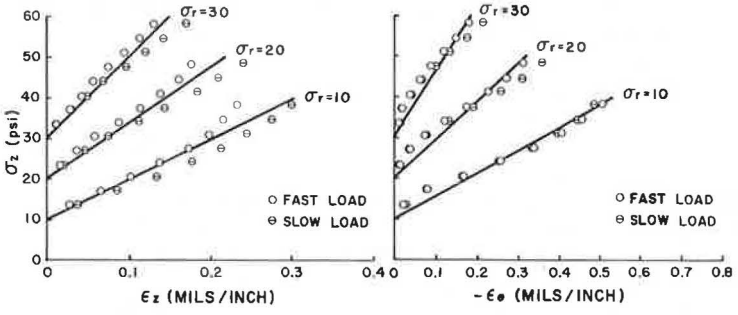

3. The stress-strain relations for laboratory specimens are significantly affected by their stress history; and
4. The axial strains observed were extremely small, resulting in resilient moduli much greater than reported by other investigators (however, they are believed to be correct for the test conditions).

REFERENCE

1. Moore, W. M., Swift, G., and Milberger, L. J. Deformation Measuring System for Repetitively Loaded, Large-Diameter Specimens of Granular Material. Highway Research Record 301, 1970, pp. 28-39.

EFFECT OF CHANGES IN GRADATION ON STRENGTH AND UNIT WEIGHT OF CRUSHED STONE BASE

Truman R. Jones, Jr., Edwin L. Otten, and Charles A. Machemehl, Jr.,
Vulcan Materials Company; and
T. A. Carlton, University of Alabama

ABRIDGMENT

•THIS report gives information on the changes in unit weight and strength for a crushed granite base when changes are made in the gradation.

The tests performed included compacted unit weight, CBR, and triaxial shear tests. The results of the tests indicate that crushed granite with a gradation inside the ASTM specification band included in the new ASTM Specification D 2940 71T, Graded Aggregate Material for Bases or Subbases for Highway or Airports, produces satisfactory shear strengths. The shear strength variation for gradations within the specification band was small. The highest shear strength was obtained on specimens conforming to an ASTM down-the-middle gradation. The results tended to show that increasing the percentage of material passing the No. 200 sieve causes a decrease in shear strength. The data appear to confirm the need to limit the percentage passing the No. 200 sieve to less than 10 percent and the percentage passing the No. 4 sieve to less than approximately 50 percent for a 2-in. topsized aggregate. Test results showed that the shear strength, as determined by the California bearing ratio test, was increased by a factor of slightly less than 2 when the compactive effort was increased from AASHO T 99 to AASHO T 180.

LABORATORY WORK

The tests were performed on a granite aggregate having a 2-in. topsize. This aggregate came from the Red Oak, Georgia, quarry owned by Vulcan Materials Company. The material properties as evaluated by the State Highway Department of Georgia using standard GHD test methods were as follows:

Property	Value
Los Angeles abrasion loss, percent	36
Specific gravity	
Bulk	2.64
Sat. surf. dry	2.66
Apparent	2.68
Absorption, percent	0.44
Magnesium sulfate roundness loss, percent	0.53

The initial testing program consisted of performing the standard AASHO T 99 and modified compaction AASHO T 180 tests on specimens with a laboratory-prepared gradation simulating the middle of the ASTM D 2940 71T grading band. CBR and triaxial tests were performed on specimens with this gradation in accordance with ASTM D 1883 and AASHO T 212 respectively. The same tests as mentioned above were performed on various laboratory-prepared gradations simulating a number of gradations meeting and not meeting ASTM and Georgia specifications, as follows:

Sponsored by Committee on Strength and Deformation Characteristics of Pavement Sections.

Gradation	Number
ASTM middle	2-B
ASTM fine	2-C
ASTM coarse	2-D
Georgia fine	2-E
70 percent passing No. 4	2-F
80 percent passing No. 4	2-J
ASTM 0 percent passing No. 200	2-K
ASTM 10 percent passing No. 200	2-L
ASTM 15 percent passing No. 200	2-M
ASTM 20 percent passing No. 200	2-N

Table 1 gives the gradations and the test results.

The gradation of the material was determined after each strength test was performed. The Texas triaxial test was slightly modified by increasing the compactive effort to make it similar to ASTM T 180 compactive effort. When possible, moisture tests were performed on the specimens after each test. The coarse material was very difficult to compact in the mold. Also, the specimens made with the coarse material would not stay together when it was extruded from the compaction cylinder. This was first solved by using rubber membranes. Later, a split cylinder mold was used to solve this problem. Several other changes or innovations or both were made in the laboratory equipment and testing procedures as follows:

1. No capillary pressure was used (1-psi lateral pressure required by AASHO T 212);
2. No capillary surcharge except a porous stone was used;
3. The specimens were compacted with the bottom porous stone in place and in a saturated condition so as not to remove water from the specimen during compaction;
4. Each specimen was prepared individually to conform to the specified gradation for that test; and
5. A 0-psi lateral pressure was used when the specimens were tested, while encased in the Texas triaxial cell, with the air valve open.

An analysis of the unit weights indicates that within the ASTM gradation band, if well-graded aggregates are compared, the unit weight of the gradation down-the-middle of the ASTM grading band is the highest. It also shows that moving to the coarse side of the ASTM gradation band reduces the density.

Attempts to compact samples of aggregates representing smooth gradations or well-graded aggregates outside the ASTM band on the coarse side were not possible because of the coarseness of the material. It is assumed that it would also be extremely difficult to compact such a base in the field. Figure 1 shows what happens to the unit weight of a base if the gradation curve remains parallel to a midpoint gradation but is continuously made finer. The results of the unit weights of the ASTM down-the-middle gradation, with the percentage passing the No. 200 sieve varied, are shown in Figure 2. It shows a distinct increase in unit weight as the percengage of material passing the No. 200 sieve increases. The results show that, if the topsize of an aggregate gradation is held constant and the fines are increased, the unit weight will likewise increase up to some point. This trend changed when the percentage of aggregate passing the No. 200 sieve was increased from 15 to 20 percent. Evidently at this point the fines, after filling all the voids, began to replace the coarse aggregate and thereby reduced the unit weight. The maximum compacted unit weight for the ASTM down-the-middle gradation appears to be its highest when the percentage of material passing the No. 200 sieve is increased to about 15 percent.

The data indicate that, for a gradation simulating ASTM down-the-middle, as material finer than the No. 200 sieve is added, the CBR strength of the material tends to decrease. This is shown in Figure 3.

The down-the-middle ASTM gradation increased from 206 to 377 or about 183 percent when the compaction effort was changed from AASHO T 99 to AASHO T 180. The CBR strength increased as the binder or percentage of material passing the No. 4 sieve

Table 1. Density, CBR, and maximum triaxial shear strength.

Item	ASTM Spec.	2-D	2-B	2-C	2-E	2-F	2-J	2-K	2-L	2-M	2-N
Gradation, cumulative percent passing											
2 in.	100	100	100	100	100	100	100	100	100	100	100
1½ in.	88-100	88.0	94.0	100	95.0	100	100	94.0	94.0	94.0	94.0
¾ in.	60-100	60.0	80.0	100	75.0	100	100	80.0	80.0	80.0	80.0
⅜ in.	40-77	40.0	58.5	77.0	62.5	87.0	89.0	58.5	58.5	58.5	58.5
No. 4	25-60	25.0	42.5	60.0	53.0	70.0	80.0	42.5	42.5	42.5	42.5
No. 10	—	15.0	—	41.0	45.0	51.0	61.0	—	—	—	—
No. 30	7-24	7.0	15.5	24.0	26.0	31.0	41.0	15.5	15.5	15.5	27.0
No. 200	0-10	0.0	5.0	10.0	10.0	13.0	25.0	0.0	10.0	15.0	20.0
Density (AASHO T-180), pcf		136	141[a]	138	139	137	134	142	144	146	142
Solid volume, percent		82	85	84	84	83	82	86	87	88	86
CBR values (AASHO T-180), percent		284	377	301	332	247	207	441	383	368	257
Maximum stress (AASHO T-212 at T-180 compaction), psi[b]											
Normal		146	254	229	217	158	102	159	159	186	125
Shear		68	123	103	104	73	46	74	74	88	57

[a]AASHO T-99 compaction also performed on this gradation resulted in density = 138 pcf; solid volume = 83 percent, and CBR = 206 percent.
[b]At 10-psi lateral pressure.

Figure 1. ASTM gradations parallel to grading bands.

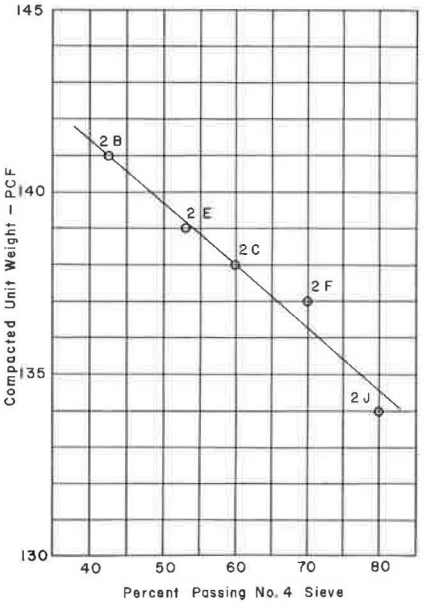

Figure 2. ASTM middle gradation except percentage passing No. 200 sieve.

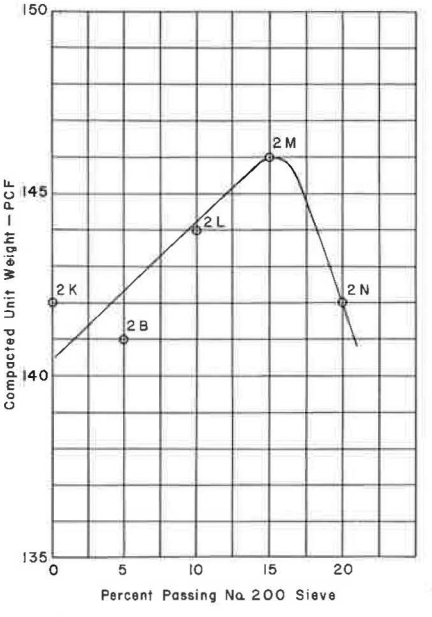

Figure 3. CBR and triaxial shear strengths versus percentage passing No. 200 sieve, ASTM middle gradation.

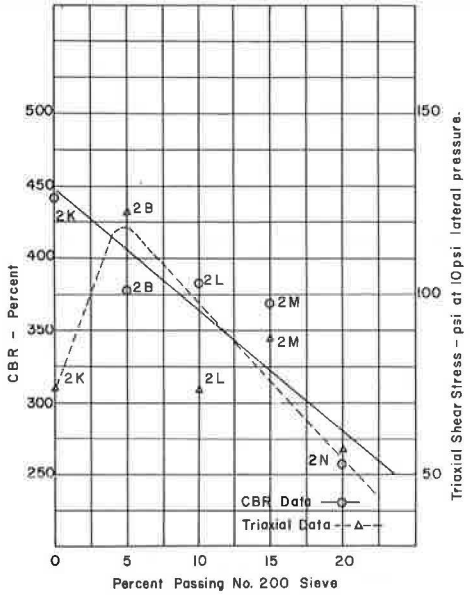

Figure 4. CBR and triaxial shear strengths versus percentage passing No. 4 sieve, all gradations.

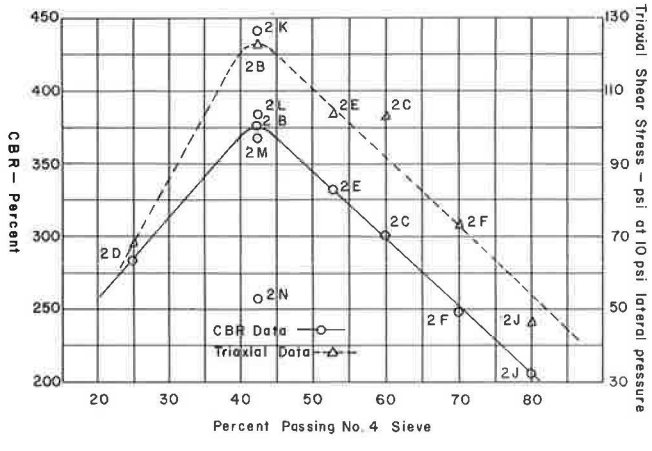

went from 25 to 42.5, the midpoint of the ASTM grading band, but then rapidly decreased as the binder was further increased. This is shown in Figure 4.

As expected, the triaxial test results showed that, as the lateral pressure increased, the maximum normal stress, the normal stress at 2 percent strain, and the maximum shear stress all increased. There is a general tendency for the triaxial strength to decrease slightly as the gradation curves move away from the ASTM midpoint. There is also a decrease in triaxial shear strength as the percentage of material passing the No. 200 sieve is increased for a down-the-middle ASTM specification (Fig. 3). There is a more definite trend of the decrease in triaxial strength as the percentage of material passing the No. 4 sieve is increased above the ASTM midpoint gradation of 42.5 percent (Fig. 4).

CONCLUSIONS AND SUGGESTIONS

The results of this research indicate that strengths considered satisfactory by current practice standards were obtained on the crushed stone granite that had gradations within the allowable limits of the new ASTM Specification D 2940 71T.

The midpoint of the ASTM specification appears to produce the highest strengths. The data showed that strengths decrease as the material passing the No. 200 sieve is increased above approximately 5 percent, the ASTM midpoint. The data confirm the limit of 10 percent used by the Corps of Engineers and specified in the ASTM D 2940. (These tests were accomplished by wet sieving.) Material with 40 to 50 percent passing the No. 4 sieve provided maximum strengths for this material. A good target for maximum strength appears to be the midpoint of the ASTM band, 42.5 percent. These suggestions are based on 2-in. topsized aggregate.

Gradations should not be designed for maximum unit weight because, as the fines are increased, the strength of the base may begin to decrease. Maximum laboratory unit weights were obtained when about 15 percent of the material passed the No. 200 sieve.

The results and suggestions given above are based on laboratory prepared and controlled gradations. To help ensure that field gradations simulate laboratory or specified gradations or both, highway departments and material suppliers can develop a statistical quality control program with the objective of establishing the accurate job mix tolerances. The strength of a stone base is highly dependent on its state of compaction, which can be accurately controlled and measured only when a consistent gradation is utilized.

The degree of compactive effort used on a base is very important to its strength. Increasing the compactive effort from AASHO T 99 to AASHO T 180 almost doubled the CBR strength for the material being tested. It is suggested that all crushed stone bases be compacted to the maximum possible density with 100 percent of AASHO T 180 set as a minimum acceptable value.

REFERENCES

1. Barksdale, R. D., and Leonards, G. A. Predicting Performance of Bituminous Surfaced Pavements. Proc. Second Internat. Conf. on Structural Design of Asphalt Pavements, Univ. of Michigan, Ann Arbor, July 1968.
2. Gray, J. E. Characteristics of Graded Base Course Aggregates Determined by Triaxial Tests. National Crushed Stone Association, Washington, D. C., Eng. Bull. 12, July 1962.
3. Factors Influencing Compaction Test Results. HRB Bull. 319, 1962.
4. Kalcheff, I. V. Some Important Properties of Graded Crushed Aggregate Mixtures for Use as Bases or Subbases. National Crushed Stone Association, Washington, D. C., 1968.
5. Machemehl, C. A., Jr. Effect of Aggregate Gradation on the Strength and Density of a Crushed Limestone Pavement Base Course. Univ. of Texas, MS thesis, Jan. 1964.
6. Yoder, E. J. Principles of Pavement Design. John Wiley and Sons, New York, 1959.

TESTS FOR SOIL CREEP

R. A. Lohnes, A. Millan, T. Demirel, and R. L. Handy,
Engineering Research Institute, Iowa State University

The Iowa bore-hole shear apparatus, modified to monitor time deformational behavior in soils, produced both primary and tertiary creep curves from in situ tests on soils. Laboratory simple shear tests produced comparable results. An examination of the concept of yield stress led to the speculation that true yield stress is one that produced secondary or linear creep curves. The secondary creep curves are a transition between primary and tertiary behavior. The creep rate from the bore-hole creep test became so nearly linear that the pseudo-Bingham yield stress computed from these tests is close to the true yield stress.

•THE OBJECTIVE of this research was to develop an in situ technique using the bore-hole shear test (1) to determine creep strength or yield stress for soils.

The early portion of the study was devoted to field tests on 3 soils: a sandy clay loam and a silt loam derived from glacial till and a loess (2). In the second phase of the research a simple shear apparatus was used to determine whether creep behavior observed with the bore-hole shear test was similar to that observed in laboratory tests. The third phase led to examination of the meaning of yield stress and an attempt to interpret this concept with rate process theory as applied to soils. As now used, this theory implies that deformations are proceeding continuously at extremely slow rates and that soil will deform at the very lowest of stresses.

BORE-HOLE CREEP TEST

The concept of a direct shear test for soil performed in the walls of a bore hole was first described by Handy and Fox in 1967 (1). A cylindrical head is inserted into a bored and trimmed 3-in. diameter hole. The head consists of 2 opposing 2- by 3-in. circumferentially grooved plates that can be expanded to engage the soil in the bore-hole wall with a measured contact pressure. The head, shown in Figure 1, is pulled axially up the hole, thereby creating a shear failure along zones parallel to the walls of the bore hole. The expansion force divided by one plate area gives normal stress, and the pulling force divided by both plate areas gives shear stress on the failure surface. The forces causing expansion and shear are applied by hydraulic or gas-operated pistons. Repetitions of expansion and pull result in linear relations on a graph of shear stress versus normal stress. In this manner a Mohr-Coulomb total stress failure envelope is generated. The values of cohesion and internal friction of sand, silt, and clay determined from the bore-hole shear test are realistic when compared to drained laboratory-determined values (1).

The pulling mechanism consists of a cable, chain, or rod attached to a yoke or a clamp acting against a base plate. For creep tests, a strain dial measuring deflection to 10^{-4} in. was attached to the pulling yoke with the dial stem pushing against the tripod as shown in Figure 2. As the soil creeps, the yoke moves upward relative to the stationary tripod allowing a deformation measurement parallel to the shear plane. Monitoring of time permits a deflection versus time curve to be plotted. A steel cantilever, mounted in contact with the strain dial stem and instrumented with SR-4 strain gauges connected to a battery-powered strain recorder, was used in some experiments. The

Sponsored by Committee on Embankments and Earth Slopes.

arrangement gave a direct plot of deflection versus time but allowed deflection measurements to only 10^{-3} in.

For all creep tests, both normal and shear stresses were held constant by using pressure regulators and CO_2 gas in the piston systems. The gauges and regulators hold stresses virtually constant and were adjustable to within about 0.4 psi. The tests consisted of measuring the deflection rate at constant normal and shear pressures.

The approach in the creep study was to apply constant normal and shearing stresses and monitor the time-deformation behavior of the soil as it crept at stresses below the shear strength. More than 100 creep tests, lasting from 25 min to 14 hours, were performed.

The field moisture contents of the soils in this study ranged from 30 to 50 percent saturation; because of this and the long duration of the test, the role of pore pressure was considered negligible. The 2 soils tested are on an observably creeping slope on glacial till. The textures were sandy clay loam and silt loam with dry densities of 71 and 68 lb/ft^3 respectively.

Figure 3 shows time-deformation curves resulting from bore-hole creep tests. On this and all subsequent figures, σ_n is the normal stress, τ is the shear stress, and w is the moisture content. During the first few minutes, deformation increases rapidly, but as time passes the deformation continues at a decreasing rate and becomes nearly linear to produce primary and secondary creep curves. This general type of curve has been obtained from various laboratory tests (3, 4). If the shear stress is applied at a level close to the shear strength, an inflection point is reached and is followed by an accelerated deformation rate to produce a tertiary creep curve. Some authors have found that the creep rate becomes essentially constant after a certain time giving a linear relation between shear stress and creep rate. They conclude that, for large values of time, the creep behavior of soils corresponds to the rheological model known as the Bingham body (5-8). This model contains a yield stress or minimum shear stress below which the soil will not exhibit viscous behavior. The reciprocal of the slope of the Bingham line is the differential or plastic viscosity.

Even though the bore-hole creep tests shown in Figure 3 do not become perfectly linear, at any time after 20 min a linear relation exists between creep rate and shear stress. That is, creep rates were measured on the time-deformation curves at various times between 10 and 50 min, and the creep rate of each time was correlated with shear stress by using least squares fit. Table 1 gives the results of these correlations for several normal stresses and moisture contents. Yield stresses are determined by extrapolating the line to 0 creep rate. For a time greater than 20 min, the yield stress is constant within ±0.1 psi and independent of time at which the slopes of the time-deformation curves were measured. A representative graph of these results is shown in Figure 4. Tests at stresses below the yield stress produced time-deformation curves that became horizontal after the initial deformation. Since the thickness of the shear zone is unknown, the shear deformation measurements are not strains and the reciprocal slope of the line is a pseudo-differential viscosity that increases as the test duration increases.

In general, the variations in creep rates obtained under identical test conditions are less than 15 percent. This variation appears reasonable when compared with laboratory experiments in which soil samples can be more rigidly controlled. Saito and Uezawa (9) have noted that, even with the same samples and loading conditions, creep rupture curves do not always coincide.

Variables Affecting Creep Behavior

We attempted to hold moisture content constant by completing as many tests as possible on the same soil in the shortest possible time. However, because of seasonal climatic variations, the field moisture content varied from 14.8 to 22.5 percent. It was found that, for a given stress, greater moisture contents resulted in greater deformations; and that finding agrees with those of Sherif (10).

However, for the limited range of moisture contents studied, there was no significant influence of moisture content on yield stress, as evidenced by the lack of a consistent trend and a variation of less than 10 percent.

Figure 1. Bore-hole shear device.

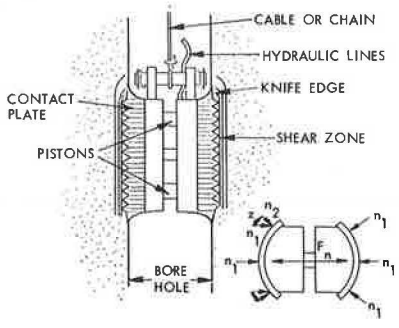

Figure 2. Pulling tripod and dial strain gauge.

Figure 3. Deformation versus time behavior for different shear stresses.

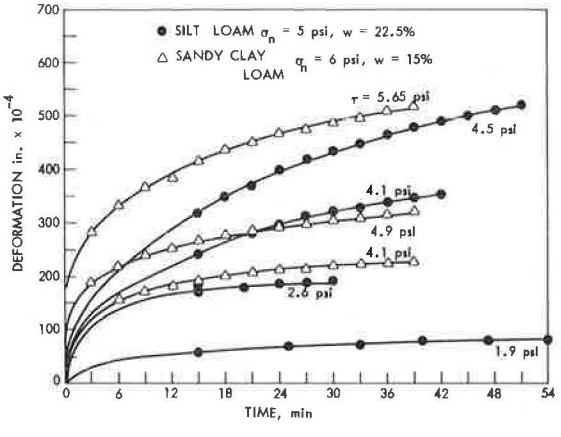

Figure 4. Slope of deformation versus time for sandy clay loam.

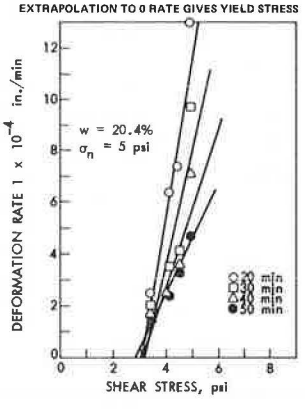

Table 1. Yield stress independence of time.

Type of Soil	Moisture Content (percent)	Normal Stress (psi)	Time (min)	Yield Stress (psi)	Apparent Viscosity Coefficient (lb-min/in.^{3})
Sandy clay loam	20.4	5	10	3.50	0.07
			20	3.10	0.15
			30	3.20	0.22
			40	3.10	0.32
			50	2.90	0.47
Sandy clay loam	18.2	5	10	3.45	0.14
			20	3.05	0.39
			30	3.10	0.70
			36	2.90	0.94
			42	3.30	1.08
			48	3.00	1.13
			52	3.10	1.14
Sandy clay loam	15.5	7	20	4.56	1.74
			25	4.67	2.20
			30	4.62	1.98
Sandy clay loam	17.5	8	15	5.19	0.30
			20	5.38	0.35
			25	5.30	0.44
			30	5.21	0.51
			35	5.22	0.55
			40	5.47	0.55
Silt loam	16.4	7	20	3.35	0.42
			30	3.44	0.56
Silt loam	17.8	7	25	3.39	0.79
			30	3.37	1.02
			40	3.16	1.21

The amount of consolidation time preceding application of shear stress was found to affect the creep behavior of the soil. In general, the deformation rate decreased as consolidation time increased. Creep tests with a consolidation time of 5 min exhibited a deformation rate 2.5 times greater than rates obtained for 20 min. However, a ratio of 1.14 was obtained when a consolidation time of 20 min was compared to one of 40 min, which is within the limits of error for nearly identical tests and is evidence that varying consolidation times in excess of 20 min do not significantly influence creep rates. The early, curved portion of the curves shown in Figure 3 probably reflect the effect of consolidation due to the increase in principal stresses following application of a shearing stress.

Creep Envelope

Tests were repeated at various normal stresses to obtain yield stresses given in Table 1. In general, the yield stress increases as a linear function of normal stress.

The linear relations between yield stress and normal stress may be thought of as a creep envelope analogous to the Mohr-Coulomb envelope shown in Figures 5 and 6. The shear strength envelope as determined with the bore-hole shear device is shown in the same figures. The least squares fit resulted in creep envelope intercepts of -0.22 and +0.35 psi on the shear stress axis or about 0 within the limits of experimental error. From these results, it is concluded that the creep envelope has essentially the same friction angle as the Mohr-Coulomb envelope and that cohesion is reduced to 0.

Several workers have commented on strength envelopes that result from soil creep. Haefeli (8) concluded that the effect of creep removes the cohesion and results in "residual shear strength" depending mostly on friction. Skempton (11) used a similar approach to arrive at a strength envelope in which cohesion is 0 and the internal friction angle is slightly reduced. Ter-Stepanian (6) hypothesized a creep envelope that passes through the intrinsic pressure intercept of the Mohr-Coulomb envelope, and, although the internal friction angle and cohesion were thereby reduced, some cohesion still contributed to the creep strength. Sherif and Wu (12) concluded that the creep limit and residual strength of soils in general are equal. The results of the bore-hole creep test agree with the conclusions of Skempton and Haefeli; i.e., cohesion is time-dependent, but internal friction remains essentially constant. It should be emphasized that tests in this phase of the study involved low-density, actively creeping soils.

COMPARATIVE LABORATORY TESTS

Tests on Loam Soils

Laboratory tests with a Geonor simple shear apparatus were performed to ascertain whether the observed creep behavior was the result of the peculiarities of the bore-hole shear creep test rather than of the true time-deformation characteristics of the soil.

The simple shear machine was selected for the laboratory phase of the investigation because of its simple operation when compared with triaxial apparatus. It also allows shearing strain measurements that are impossible with a direct shear machine. This direct application of shear stress is similar to the stresses applied in the bore-hole shear test, whereas triaxial shear results from compressive stresses.

A direct comparison of the bore-hole test and laboratory tests was attempted by collecting undisturbed samples of the same sandy clay loam and silt loam that were tested with the bore-hole device. These 2 soils are very friable, and, when extruded from thin-walled tubes, only 20 of the 35 samples collected were suitable for testing. The moisture contents of the laboratory samples ranged from 7.8 to 22.7 percent as compared with 14.8 to 22.5 percent for the moisture range of the bore-hole tests.

Each test was conducted on a separate sample about 2.2 cm thick at constant normal and shear stress. The time-deformation curves on these samples exhibit the same primary creep curves obtained from the bore-hole creep test; i.e., the curves show a large initial deformation followed by continuous creep at a decreasing rate. However, when deformation rates at a given time are compared at different stress levels and moisture contents, the results are somewhat erratic.

From the bore-hole data, for the range of moisture contents studied, the moisture content did not appear to affect yield stress; however, increasing moisture contents produced faster creep rates. Higher moisture contents in the laboratory tests at the same stress level resulted in both faster and slower creep rates. Often an increased shear stress resulted in slower creep rates.

There were only 2 or 3 samples at nearly constant moisture contents. In 2 of these cases the linear relation between deformation rate and shear stress was assumed, and a yield stress was extrapolated from only 2 points. These points gave yield stresses of about 2 psi for a normal stress of 3.5 psi, which fit the creep envelope determined from the bore-hole creep tests on those soils.

The presence of roots, pebbles, and unusually large cavities probably caused the erratic results of the laboratory tests. Because of the difficulty in handling the laboratory samples, the wide range of moisture contents, and the erratic results caused by pebbles and cavities, no further tests on the till-derived soils from the bore-hole test sites were attempted.

It has been inferred that in the bore-hole test the shear plane moves outward with each increase in normal stress (1). In the creep test, normal stress is held constant while the shearing stress is increased from levels causing no deformation up through the yield stress to stresses where shear failure occurs. In the bore-hole creep test, where several shearing stresses are applied at the same normal stress, it is questionable that the shear planes move outward with an increase in shear stress. Therefore, the bore-hole creep test may be more like laboratory tests in which a single sample is subjected to a shearing stress until the time-deformation curve equilibrates; then the stress is increased until a new time-deformation curve is established and another shear stress is applied. In this way the same sample is subjected to several different shearing stresses, and a step type of creep curve is produced. The alternative approach is to use a separate sample for each stress level as was done with the sandy clay loam and the silt loam. The soil behavior under these different types of stress applications was explored in "step types" of tests that were also run with the simple shear machine.

Tests on Undisturbed Loess

This second set of tests used undisturbed loess samples that classify as CL with liquid limits averaging 35 and plasticity indexes averaging 23. The in situ wet densities ranged from 92 to 105 pcf. The moisture ranged from 27 to 30 percent. The strength envelopes from bore-hole shear and bore-hole creep tests are shown in Figure 7.

Figure 8 shows 3 sets of step creep curves from simple shear tests. Creep rate, measured about 20 min after each load application, versus shearing stress is shown for the same tests in Figure 9. The tests give a good linear relation between shear stress and creep rate; however, the yield stress appears to be a function of the initial stress applied in each series.

The yield stresses from simple shear tests are also shown in Figure 7. Although the yield stress from test 23 falls on the creep envelope from the bore-hole test, the results of the other tests in which the initial stresses were higher gave yield stresses closer to the Mohr-Coulomb strength than to the creep strength. In general, the yield stress increases as the initial stress increases. Therefore, starting a creep test at higher shearing stresses has the effect of strengthening the soil. When attempts are made to evaluate a yield stress from the bore-hole test, the shear head would be repositioned in the bore hole between successive applications of shear stress so that a soil mass that has not been subjected to previous shear stress will be evaluated.

Tests on Remolded Loess

A series of simple shear creep tests was conducted on loess remolded to field density and moisture content (Figs. 10 and 11). These tests supported the conclusions of the tests on the undisturbed samples since higher initial shear stress resulted in higher yield stress. It was also shown that the linear relation between shear stress and strain rate is not the best to describe the behavior of this material. The pseudo-Bingham behavior observed in both bore-hole and simple shear tests is probably a

Figure 5. Failure envelopes for silt loam.

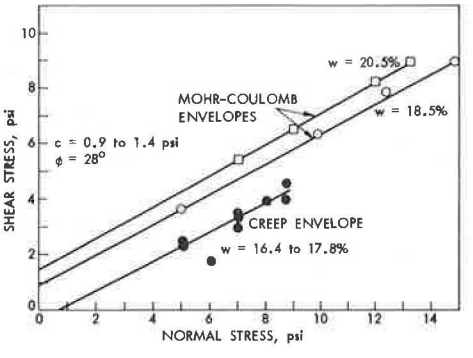

Figure 6. Failure envelopes for sandy clay loam.

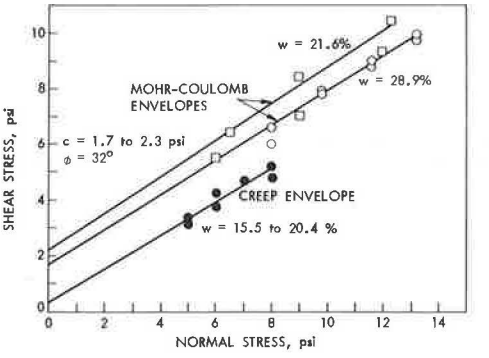

Figure 7. Mohr-Coulomb and creep envelopes from bore-hole data on loess.

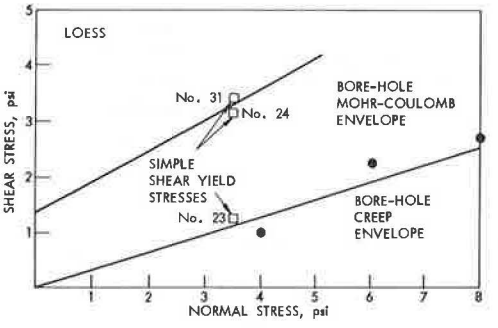

Figure 8. Creep curves from simple shear tests on undisturbed loess.

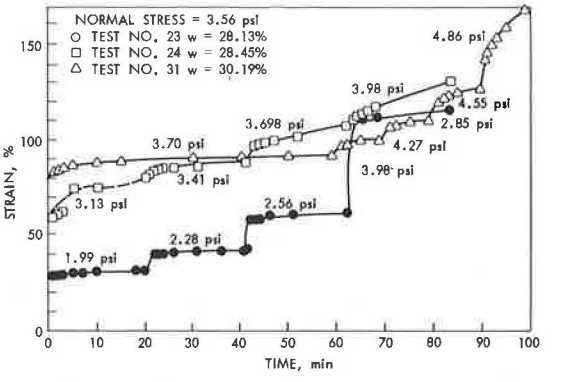

Figure 9. Shear stress versus creep rate for simple shear and bore-hole tests on undisturbed loess.

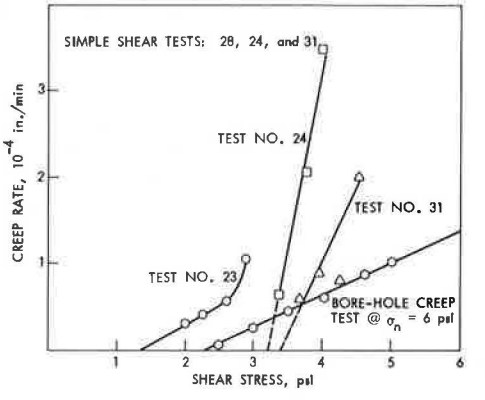

linear approximation of a relation that is better described by an exponential equation. This behavior of soils has been observed by many researchers, and a theoretical basis exists for these observations in rate process theory (13, 14, 15). This relation further suggests that a yield stress does not exist.

Laboratory tests have shown that stress history and the remolding effects during a single shear application change the structure and therefore the time-deformation characteristics of soil (22). Since the soil structure is constantly changed by application of the stresses, it appears more study is needed to evaluate how the soil structure is altered by the stresses.

The other conclusion is that within the stress range at which the soils exhibit primary or terminal creep behavior there is no true yield stress and that the behavior of these soils might best be approached through rate process theory.

SPECULATIONS ON YIELD STRESS

The time-deformation curves obtained from creep tests are generally divided into primary, secondary, and tertiary creep regions, where the strain rates either decrease with time, remain constant, or accelerate with time respectively. All of these regions, however, do not appear in every test. Some, for example, may only show decelerating primary creep behavior terminating at some strain (terminal creep). Figure 12 shows 3 types of curves commonly obtained in laboratory tests: primary, secondary, and tertiary creep behaviors. All 3 types of curves may be exhibited by a soil if a series of tests is conducted in which the stress level is increased from one successive sample to the next or if one sample is subjected to incrementally increasing stresses. At very low stresses the curves are of the terminal type and show only primary creep; as the stress level approaches the conventionally determined strength, the curves show tertiary creep. Although some authors have stated that the steady-state curves are characteristics of soils (8, 16), others note curves of the primary type (3, 4, 17, 18).

This study revealed that a bore-hole shear device can be used to generate primary and tertiary creep curves. However, the analyses applied to the bore-hole data emphasized steady-state and primary creep curves since the tertiary curves were observed to occur over a very narrow range of stresses close to the shear strength. The results of these analyses led to the conclusion that the creep behavior of the soils is similar to the rheological model known as the Bingham body. The yield stress that has resulted from this analysis can be called "pseudo-Bingham" yield stress.

An alternative means of analysis is the use of rate process theory. Although this approach has a theoretical basis, there are many aspects of the theory that need verification or modification. Further, there has been no suggestion for a practical application of this theory.

Noble and Demirel (19) applied rate process theory to the study of creep behavior but expanded the theoretical equation to account for soil structure. An important difference from previous work is their thesis that the inflection point on tertiary creep curves represents a unique, critical structure that is the same from one stress level to the next. Earlier Schmid (20), recognizing that structure is continually changing during the deformational history, suggested that the inflection point on the time-strain curve was the point in time at which a critical structure is attained; but he did not expand on that idea.

Our interpretation of the relation among the different types of curves is as follows. At stress levels where only primary curves are produced the critical structure is never reached, and stress has only the beneficial effect of strengthening the soil as it deforms. At stress levels that produce tertiary curves, failure will occur some time after initial application of the stress; larger stresses will produce failures in shorter times. The steady-state or secondary curves can be thought of as ones where the critical structure is reached and the deformation continues at a constant rate, neither accelerating nor decelerating. The stress that produces the steady-state curve is a true yield stress below which failure will not occur. A similar definition of yield stress has been suggested by Sherif and Wu (12) but without the rationale provided here.

Figure 13 shows a graph using data from Noble and Demirel's direct shear tests of deformation rate versus shear stress where the deformation rate is measured at the

Figure 10. Shear stress versus strain rate for remolded loess (applied stress is expressed as a percentage of shearing strength).

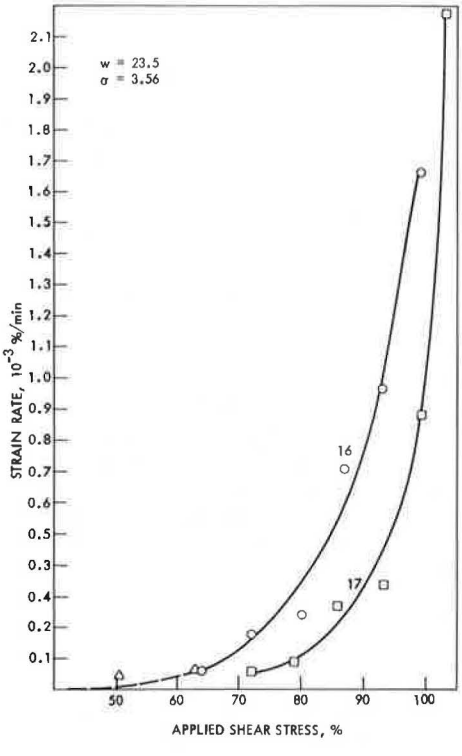

Figure 11. Shear stress-strain rate data for remolded loess plotted on semilog paper (applied shear stress is expressed as a percentage of shearing strength).

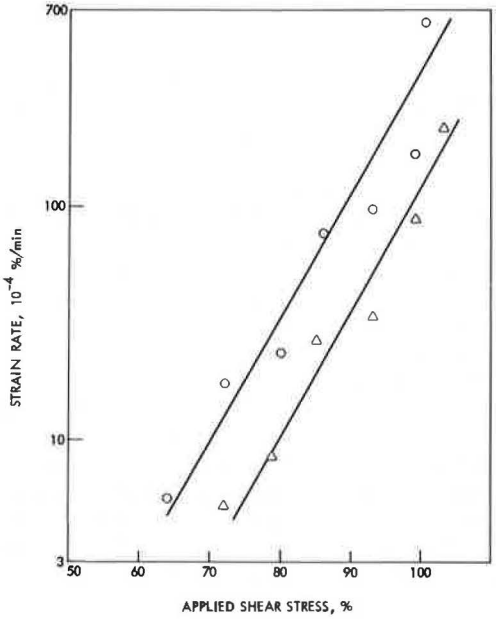

Figure 12. Primary, secondary, and tertiary creep behavior.

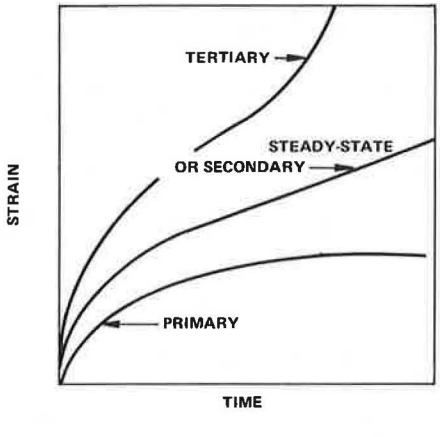

Figure 13. Deformation rate measured at the inflection point.

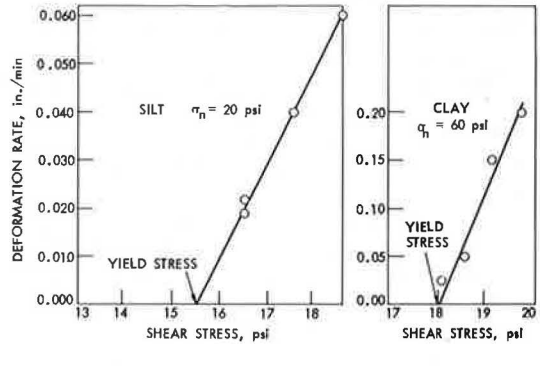

inflection point. As can be seen, this approach also produces a linear relation with a yield stress at 0 deformation rate. The concept of using the strain rate as measured at the inflection point or point of critical structure is intuitively more pleasing than making measurements on the primary curves at some arbitrary time after starting the test.

This interpretation leads to the conclusion that, if the steady-state or tertiary creep curves are not obtained at stresses appreciably below the shear strength as defined by the Mohr-Coulomb envelope, then shear strength and yield strength are essentially the same. However, if the tertiary curves occur over a wide range of stresses below the Mohr-Coulomb strength, the yield stress will be the one that produces a secondary creep curve that is the transition between primary and tertiary creep. This yield stress may be appreciably below the Mohr-Coulomb strength. Since all field and laboratory tests of this project produced the tertiary curves only at or near the Mohr-Coulomb strengths, a series of tests was conducted on remolded loess samples at various moisture contents up to 30 percent tertiary creep curves. None was successful. It may then be concluded that loess, at field density, does not have a yield strength below the shear strength.

It was noted that the bore-hole creep tests on the 2 loam soils became nearly linear after 20 min. Perhaps those soils do exhibit creep behavior, and the curves observed were very close to secondary creep curves; thus, the critical structure was attained, and the pseudo-Bingham yield stress is in fact close to the yield stress of this latest interpretation. It appears that empirical creep curves can be produced by the bore-hole shear device, and that leads to 2 possible analyses of data. However, we feel that selection of the proper method of analysis for the field test can be made only after a fundamental study on pure clay systems under controlled laboratory conditions.

CONCLUSIONS

This study has led to the following conclusions:

1. The bore-hole shear test device can be used on soils in the field to produce primary types of creep curves that become nearly linear about 20 min after application of a constant shear stress;
2. A graph of creep rate versus shear stress produces a curve with an apparently linear segment that can be extrapolated to 0 creep rate (the intercept is then referred to as pseudo-Bingham yield stress);
3. The pseudo-Bingham yield stress, when plotted as a function of normal stress, results in a linear relation called a creep envelope that goes through the origin and is essentially parallel to the Mohr-Coulomb envelope;
4. Laboratory tests with a simple shear machine on soil samples from field test sites produced primary creep curves similar to the bore-hole curves within the same range of shear stresses;
5. Pseudo-Bingham yield stresses from bore-hole and simple shear tests are comparable;
6. It is inferred that in the bore-hole creep test the same shear zone within the soil is subjected to a series of successively higher shear stress and the yield stress increases with a higher initial stress in sequence (to avoid effects of stress history, one should reposition the bore-hole shear head between each application of shear stress so that fresh soil is tested);
7. Soils that exhibit only primary creep up to shear stresses approximating Mohr-Coulomb shear strength do not have a true yield stress;
8. True yield stress is the stress that produces a secondary or linear creep curve and can be found by extrapolating the relation between creep rate measured at the inflection point of tertiary creep curves and shear stress back to the 0 creep rate line;
9. The creep rate from the bore-hole creep tests on the 2 loam soils becomes so nearly linear that the pseudo-Bingham yield stress is close to a true yield stress; and
10. Before more field work is attempted on bore-hole creep tests, controlled laboratory creep experiments should be run to verify the existence of yield stress and to establish a practical application of rate process theory (this work should verify, modify, or reject the conclusions given immediately above).

ACKNOWLEDGMENT

The authors wish to thank Stein Salomonsen, John Johnson, Bill Badger, and John Hartwell for their aid in running laboratory tests. This work was supported by the Engineering Research Insitutute at Iowa State University through funds provided by the National Science Foundation.

REFERENCES

1. Handy, R. L., and Fox, N. W. A Soil Bore-Hole Direct-Shear Test Device. Highway Research News, No. 27, 1967, pp. 42-51.
2. Millan, A. Field Test for Measuring Creep Susceptibility of Soils. Iowa State Univ., Ames, MS thesis, 1969.
3. Tan, T. K. Discussion. Proc. Fifth Internat. Conf. on Soil Mech. and Found. Eng., Paris, Vol. 3, 1961, pp. 141-142.
4. Kondner, R. L., and Krizek, R. J. Correlation of Creep and Dynamic Response of a Cohesive Soil. In Rheology and Soil Mechanics: Symposium of the International Union of Theoretical and Applied Mechanics (Kravtchenko, J., and Sirieys, P. M., eds.), Springer-Verlag, Berlin, 1966, pp. 33-41.
5. Vialov, S. S., and Skibitsky, A. M. Problems of the Rheology of Soils. Proc. Fifth Internat. Conf. on Soil Mech. and Found. Eng., Paris, Vol. 1, 1961, pp. 387-390.
6. Ter-Stepanian, G. On the Long-Term Stability of Slopes. Norwegian Geotechnical Institute, Pub. 52, 1963.
7. Finn, W. D. L. Earthquake Stability of Cohesive Slopes. Jour. Soil Mech. and Found. Div., Proc. ASCE, Vol. 90, 1966, pp. 29-61.
8. Haefeli, R. Creep and Progressive Failure in Snow, Soil, Rock, and Ice. Proc. Sixth Internat. Conf. on Soil Mech. and Found. Eng., Vol. 3, 1965, pp. 134-147.
9. Saito, M., and Uezawa, H. Failure of Soil Due to Creep. Proc. Fifth Internat. Conf. on Soil Mech. and Found. Eng., Paris, Vol. 1, 1961, pp. 315-318.
10. Sherif, M. A. Deformation and Flow Properties of Clay Soils From The Viewpoint of Modern Material Sciences. Highway Research Record 119, 1966, pp. 24-49.
11. Skempton, A. W. Long-Term Stability of Clay Slopes. Geotechnique, Vol. 14, 1964, p. 77.
12. Sherif, M. A., and Wu, M. J. Creep Limit and Residual Strength Relationship. College of Eng., Univ. of Washington, Seattle, Soil Eng. Rept. 5, 1969.
13. Murayama, S., and Shibata, T. On the Rheological Characters of Clay—Part I. Disaster Prevention Research Institute, Kyoto Univ. of Japan, Bull. 26, 1958, pp. 1-43.
14. Singh, A., and Mitchell J. General Stress-Strain-Time Functions for Soils. Proc. ASCE, Vol. 94, No. SM1, 1968, pp. 21-46.
15. Andersland, O. B., and Douglas, A. G. Soil Deformation Rates and Activation Energies. Geotechnique, Vol. 20, 1970, pp. 1-16.
16. Christensen, R. W., and Wu, T. H. Analysis of Clay Deformation as a Rate Process. Jour. Soil Mech. and Found. Div., Proc. ASCE, Vol. 90, No. SM6, 1964, pp. 125-153.
17. Goldstein, M., Ladipus, L., and Misumsky, V. Rheological Investigations of Clays and Slope Stability. Proc. Sixth Internat. Conf. on Soil Mech. and Found. Eng., Vol. 2, 1965, pp. 482-485.
18. Mitchell, J. D. Shearing Resistance of Soils as a Rate Process. Jour. Soil Mech. and Found. Div., Proc. ASCE, Vol. 90, 1964, pp. 29-61.
19. Noble, C. A., and Demirel, T. Effect of Temperature on Strength Behavior of Cohesive Soil. HRB Spec. Rept. 103, 1969, pp. 204-219.
20. Schmid, W. A Rheological Failure Theory for Clay Soils. ONR Progress Report, Proj. NR-981-177, 1960.

BEHAVIOR OF NEGATIVE SKIN FRICTION ON MODEL PILES IN MEDIUM-PLASTICITY SILT

Robert M. Koerner and Chirantan Mukhopadhyay, Drexel University

The mobilization of negative skin friction (downdrag) on deep foundations can be so large that either failure or excessive deformation of the structure founded thereon can occur. Yet little information regarding the behavior of the downdrag phenomenon is known. Since full-scale testing of the influence of the large number of variables involved is economically prohibitive, a simulated laboratory experiment has been developed. Results of negative skin friction distribution with increasing soil deformation confirm the validity of the experimental setup. The influence of pile batter, pile group spacing, soil-water content, and pile material on average negative skin friction is investigated. From these test sequences, generalized conclusions are drawn. Various means of preventing negative skin friction from occurring have also been examined, and the use of asphalt coatings on the pile is shown to be quite successful. The influence of asphalt coating viscosity and thickness on average negative skin friction is presented. These curves form the basis for a design method to eliminate the major portion of downdrag on pile foundations.

•THE MAGNITUDE of negative skin friction (downdrag) on deep foundations can be greater than the ultimate capacity of the foundation itself. Even when the capacity of the foundation is not approached, negative skin friction can result in excessive settlement of the foundation and the structure founded on it. Investigation into the behavior of the phenomenon has made relatively little progress and is typified by a wide variety of approaches toward a predictive technique. The Seventh International Conference on Soil Mechanics and Foundation Engineering brought the problem to the attention of many through a specialty session (18) and a state-of-the-art report (6). Verification of any proposed technique to evaluate downdrag magnitude requires test results that are most difficult to obtain in the field because of the extremely long time and expense involved for instrumentation. The alternate to full-scale field testing is scaled-down model tests that can be conducted in the laboratory under controlled conditions. It then becomes possible to experiment with the variables that affect the process.

This paper concerns itself with a laboratory study on the behavior of negative skin friction on model piles. The literature is reviewed, the approach taken is described, and a number of separate aspects of the problem are investigated. These are the fundamental behavior of downdrag, the effect of pile batter, the effect of pile group spacing, the effect of varying the soil-water content, and the effect of different pile materials.

Whenever the magnitude of downdrag force becomes excessively large, the foundation designer is often hard pressed for an alternate scheme. Quite often there is no alternate, so that a method whereby downdrag is significantly reduced, or even eliminated, is desirable. Thus, the use of pile coatings as a preventive measure against downdrag has also been investigated. Asphalt coating viscosity and thickness have been varied and are presented. Generalized conclusions are presented in the summary.

BASIC PROBLEM OF DOWNDRAG IN DEEP FOUNDATIONS

In the design of a deep foundation (e.g., a pile foundation), the ultimate carrying capacity consists of 2 components: the point capacity and the capacity along the shaft.

Sponsored by Committee on Foundations of Bridges and Other Structures.

This is shown in Figure 1 for both the standard case and the downdrag case. There it is shown that

$$Q_o = Q_p \pm Q_s \tag{1}$$

$$Q_o = A_p p_o \pm A_s s_o \tag{2}$$

where

Q_o = ultimate pile capacity,
A_p = area of pile point,
p_o = unit point resistance,
A_s = surface area of pile shaft,
$+s_o$ = positive skin friction,
$-s_o$ = negative skin friction, and
$-Q_s = -A_s s_o$ = downdrag force.

In the downdrag case (Fig. 1b), the problem becomes one of estimating the magnitude and behavior of the term $-s_o$ in Eq. 2. When this value is obtained, the downdrag force, $-A_s s_o$, can be easily obtained. This situation occurs with point-bearing piles where settlements of the pile point are either nonexistent or small.

The physical situations that bring about negative skin friction are well established and are as follows.

1. Remolding of the soil due to pile driving—When piles are driven in clay soils, there is an immediate loss of strength in the soil adjacent to the pile. With time there is a regain in strength (thixotropy) with the possibility of some negative skin friction. This situation probably gives the least amount of downdrag when compared with other situations. An estimate of its magnitude is given by Johnson and Kavanagh (13).
2. Soils undergoing consolidation—Compressible soils that are undergoing active consolidation when the deep foundation is placed will produce downdrag. This consolidation settlement occurs by the usual mechanism of dissipation of excess pore-water pressure but is prevented from occurring adjacent to the pile because of the adhesion and friction of the soil to the pile.
3. Surcharge-loaded soils—This situation occurs when a surcharge load is placed on the ground surface around a previously installed pile in which the foundation soil was in equilibrium or when a lowering of the groundwater table occurs. The surcharge load will cause settlement that is prevented by the previously installed piles, thereby mobilizing negative skin friction. Depending on the magnitude of the surcharge load, and the nature of the compressible soil, this situation is likely to cause the maximum amount of downdrag force on deep foundations.

NEGATIVE SKIN FRICTION COMPUTATIONAL METHODS

There are numerous methods available for predicting the magnitude of negative skin friction or the downdrag force resulting therefrom or both. Many methods assume that negative skin friction is directly analogous to the Mohr-Coulomb failure criterion when expressed as follows:

$$-s_o = c_a + \bar{\sigma}_h \tan \delta \tag{3}$$

$$-s_o = c_a + K\bar{\sigma}_v \tan \delta \tag{4}$$

$$-s_o = c_a + K\gamma' z \tan \delta \tag{5}$$

where

$-s_o$ = negative skin friction,
c_a = adhesion of soil to pile ($0 \le c_a \le \bar{c}$),
$\bar{c}$ = effective cohesion,

$\overline{\sigma}_h$ = average effective horizontal pressure,
$\overline{\sigma}_v$ = average effective vertical pressure,
K = coefficient of earth pressure ($K_A \leq K \leq K_p$),
K_A = coefficient of active earth pressure,
K_p = coefficient of passive earth pressure,
γ' = effective soil unit weight,
z = depth beneath ground surface,
δ = angle of shearing resistance soil to pile ($0 \leq \delta \leq \overline{\phi}$), and
$\overline{\phi}$ = effective angle of shearing resistance of soil.

Table 1 gives a chronological ordering of the various methods and a brief comment concerning each. In the 21 years represented in this table, we have gone full circle from the Terzaghi and Peck (21) suggestion to the Endo et al. (8) solution to the problem. Most investigations utilized Mohr-Coulomb shear strength with major differences in the methods of evaluating c_a, K, and δ. Others feel the problem to be more analogous to consolidation, in that the forces causing consolidation are related to or are equal to the downdrag force.

FULL-SCALE FIELD TESTS

Some of the previous methods for the computation of negative skin friction are based on the experience and intuition of the authors, and others are based on full-scale field tests. As mentioned previously, field testing is much more difficult than standard load transfer problems because of the long measurement periods involved. It is impractical to force consolidation settlements when one is dealing with low permeability soils since the time involved can be decades. Nevertheless, there have been field tests conducted (Table 2) involving different pile lengths, types, soils, and measurement techniques. As admirable as these tests have been, they also bring out the basic difficulty in drawing firm conclusions since so many different variables are involved.

Significant among these tests, however, is the work of Johannessen and Bjerrum (12), who measured negative skin friction on 15-in. diameter pipe piles in a soft to medium-soft marine clay. The negative skin friction was mobilized by 30 ft of surcharge load. This resulted in an average skin friction of 900 tsf in the lower section of the pile and at the pile point a maximum value of 2,000 tsf. Thus, an approximate downdrag force of 250 tons was at the pile point. This resulted in penetration of the pile point into the rock underlying the clay and exceeded the pile's ultimate capacity.

MODEL TESTING FACILITY

Because of the serious nature of the problem and the expense involved in full-scale field testing, a laboratory setup that could simulate the downdrag phenomenon on model piles was constructed. Model tests have been previously conducted by Whitaker (23) on pile groups and by Mazurkiewicz (16) on skin friction in sands. As shown Figure 2, the soil is placed in a 3-ft diameter and 3-ft high tank with a reaction frame on top. The ½-in. thick surcharge load plate has a 1½-in. diameter hole in the center and ¼-in. clearance around the outside. Load is applied to the plate and held constant by means of hydraulic jacks fastened to the reaction frame. Dial gauges are placed on the load plate to ensure uniformity of settlement and to measure surface deflections. The 1-in. diameter model pile is placed through the center hole in the surcharge plate and is fixed to a proving ring and then to the reaction frame. The pile being fixed in position simulates a point-bearing pile in the field. The proving ring records the total downdrag force from which average negative skin friction values can be computed.

The soil used throughout the tests to follow is a slightly organic clayey silt of medium plasticity (OH-OL by Unified Soil Classification System). Its in situ water content is near the liquid limit of 55 percent. The plasticity index is 20 percent, and the shrinkage limit is 27 percent. The particle size distribution curve is shown in Figure 3. All tests were conducted with the soil near its in situ water content except for the sequence that evaluated the effects of varying water content.

Figure 1. Basic phenomenon involved.

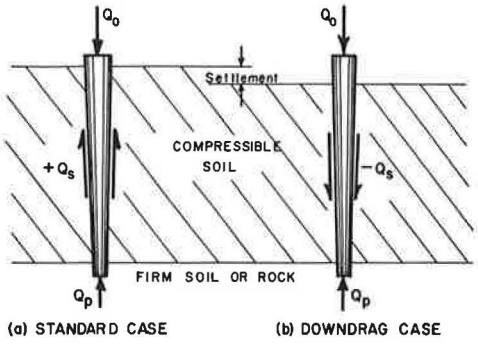

Figure 2. Experimental setup.

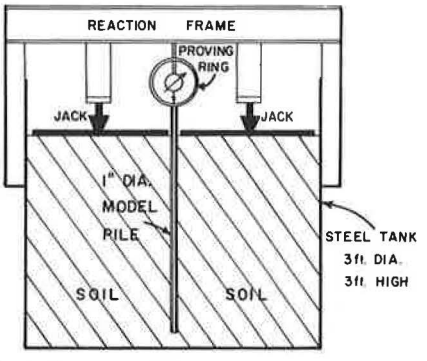

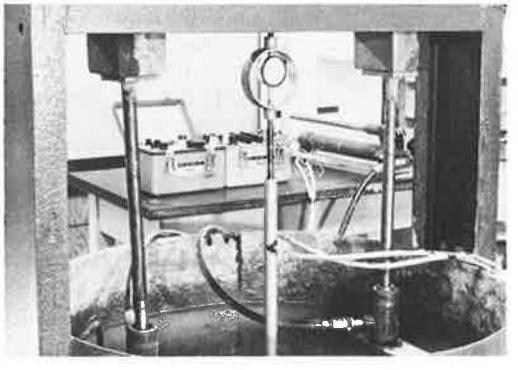

Figure 3. Particle size distribution of soil.

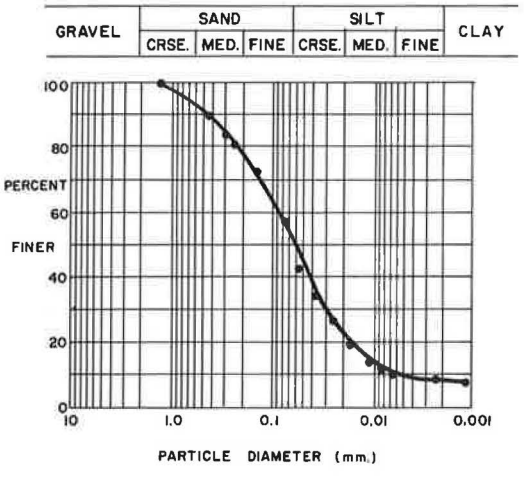

Table 1. Methods for computing negative skin friction.

Author	Reference	Year	Comment
Terzaghi and Peck	21	1948	$0 \leq -s_o \leq \tau$
Moore	17	1949	$-s_o = (\pi\tau + \bar{\sigma}_v) \tan \delta$
Zeevaert	24	1959	Analytic expression utilizing K_o
Buisson, Ahu, and Habib	5	1960	Analytic/graphic procedure requiring soil and pile characteristics
Elmasry	7	1963	Empirical equation based on statistical theory (15)
Weele	22	1964	Similar to tension piles
Johannessen and Bjerrum	12	1965	$-s_o = 0.20\ \bar{\sigma}_v$
Johnson and Kavanagh	13	1968	Analogous to solution of consolidation problem
Bowles	2	1968	$K_A \leq K \leq K_p$
Hansen	11	1968	Analytic expressions predicting upper limits
Poulos and Mattes	20	1969	c_a, K_o, δ from Broms (4)
Endo et al.	8	1969	$-s_o = \tau$ where τ is obtained from an unconfined compression test

Table 2. Full-scale downdrag tests.

Author	Reference	Year	Pile Length (ft)	Pile Material	Soil	Measurement Method
Weele	22	1964	45	Timber	Soft clay	Extensometer
Locher	15	1965	40	Concrete	Soft clayey silt	Extensometer
Johannessen and Bjerrum	12	1965	140	Steel pipe	Soft to medium-soft marine clay	Extensometer
Bozozuk and Labrecque	3	1968	270	Composite	Marine clay	Strain gauges
Bjerrum, Johannessen, and Eide	1	1969	100 to 190	Steel pipe	Marine clays	Extensometer
Endo et al.	8	1969	100 to 140	Steel pipe	Soft alluvial silt	Technique varied
Fellenius and Broms	9	1969	225	Concrete	Normally consolidated clay	Strain gauges

MODEL TESTING RESULTS

Negative Skin Friction Behavior

To verify the experimental setup just described and to obtain a better understanding of negative skin friction behavior require the downdrag distribution along the pile's length. The following technique was developed for this purpose (14).

A 1-in. OD by $\frac{7}{8}$-in. ID steel pipe was split along its axis and instrumented with 10 strain gauges (5 on each half) at 5-in. spaces. The strain gauge leads were brought up in the center of the pipe and out through its sides above the soil surface and then attached to standard instrumentation equipment. The pile halves were joined by a waterproof epoxy cement. The bottom of the pile was sealed and the top fixed to a proving ring as previously described.

The results of this phase of the study are shown in Figure 4. At low surcharge, hence low surface deflection, the entire downdrag force is carried in the upper portion of the pile. As surcharge increases, this force descends deeper along the pile until it reaches the bottom. Still further increase in surcharge load causes the slope of the force distribution to decrease until the ultimate negative skin friction value is reached. This behavior appears to be reasonable, and its total force agreed with the proving ring affixed to the top of the pile. In the remaining tests only the proving ring was used for measurements. However, for longer piles than those used here, the location of a neutral point (8), where the skin friction goes from negative to positive, becomes significant and must be determined in this manner.

Effect of Pile Batter

For anticipated horizontal loads and for greater stability, piles are often driven off vertically, i.e., batter piles. The amount of batter varies considerably, and the effect of negative skin friction on such piles is of interest. The experimental setup easily accommodated the inserting of piles on an angle to simulate this condition. To have a valid comparison, we tested 3 steel piles simultaneously, the center one always being vertical, and the valves compared well with the previously obtained values. The time between load increments was varied and found to have negligible effect on the maximum value of negative skin friction. There was approximately a 1-week interval between tests so that equilibrium could be established after the piles were inserted.

Figure 5 shows the study of this sequence of tests. Clearly, an increase in the amount of batter increases the average negative skin friction. The apparent reason is that one has not only the adhesion of the soil to the pile, which is independent of positioning, but also a direct contribution of the pressure from the soil above. As batter increases, this vertical pressure also increases in the proportion as shown. This response is contrary to the only known comparison made in the field. Endo et al. (8) have compared a vertical pile to one placed at a 1:7 batter, and the result was a 16 percent reduction in negative skin friction in the case of the battered pile. No discussion as to the reason for this response was offered.

Effect of Pile Group Spacing

Since piles are usually placed in a group configuration, a study of the effect of pile group spacing was undertaken. Nine concrete piles were placed in a 3 by 3 group and fixed to a single steel plate at their tops. This, in turn, was fixed to a single proving ring as shown in Figure 6. The spacing to diameter (S/D) ratio was varied at 1.0, 1.5, 2.0, 3.0, and 5.0. Individual holes for each of the piles were cut in the surcharge plate for each different spacing, and testing proceeded as before.

The results shown in Figure 7 are for average negative skin friction at maximum, $\frac{1}{2}$ maximum, and $\frac{1}{4}$ maximum surface deflections. A distinct break in the curves at about S/D = 2.5 is noted. For smaller S/D ratios, the negative skin friction values rapidly decrease. This is completely analogous to positive skin friction studies (23) in that a block failure will occur only at very close S/D ratios. The purpose of presenting 3 curves is to show that this trend is consistent over the entire range of average negative skin friction values and does not occur only at the limiting value. This value of S/D =

Figure 4. Distribution of downdrag force.

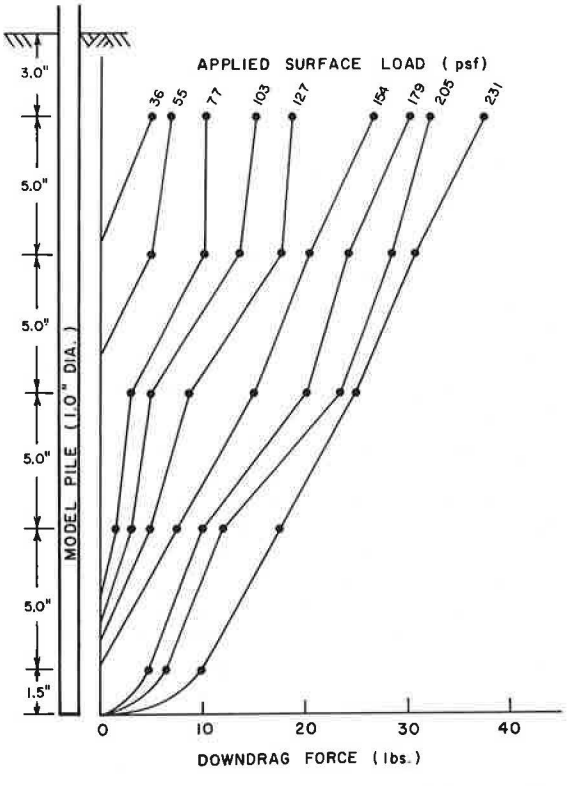

Figure 5. Effect of pile batter on average negative skin friction.

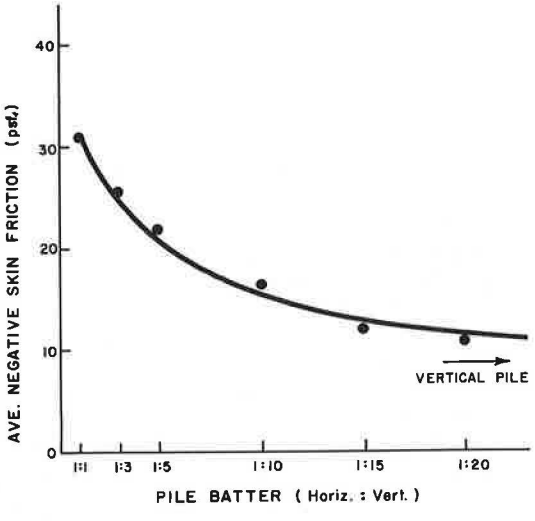

Figure 6. Experimental setup for group testing.

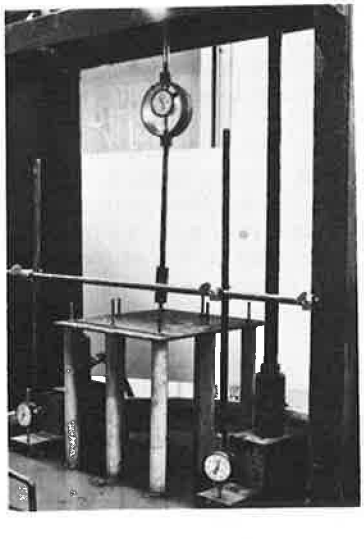

Figure 7. Effect of pile group spacing on average negative skin friction.

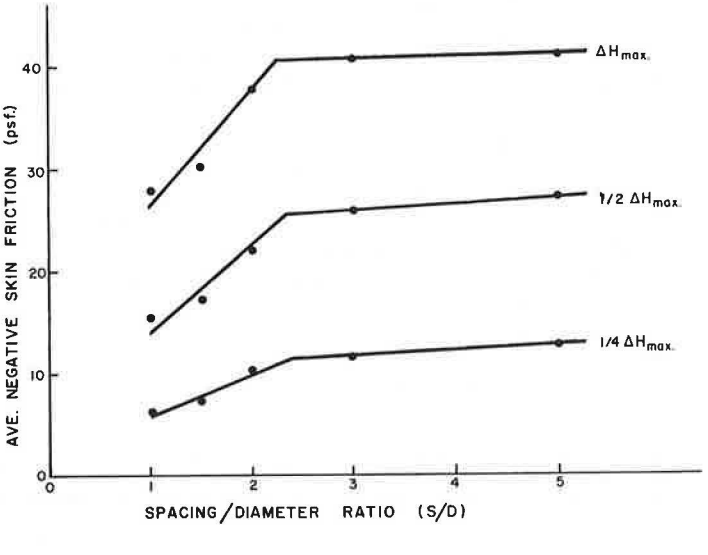

2.5 was suggested by Terzaghi and Peck (21) as being the recommended pile group spacing that is practical and yet minimizes negative skin friction.

Effect of Water Content and Pile Material

Piles made of the 3 common pile-forming materials (wood, concrete, and steel) were installed and tested simultaneously. Each was attached to a separate proving ring as shown in Figure 8. After this sequence of tests the assembly was dismantled and the soil was removed, dried, and replaced in the tank at a lower water content. This sequence was continued until the water content was below the shrinkage limit.

The combined results of the effect of water content and the effect of pile material is shown in Figure 9. Superimposed on this curve (dashed line) is the shear strength of the soil as determined from the unconsolidated-undrained triaxial tests below the plastic limit and from the laboratory vane shear tests for the soils above the plastic limit. All pile materials show increased average negative skin friction with decreasing water content. This is as expected since the shear strength of the soil is also increasing with decreasing water content. Of concern, however, is the relative positioning of the curves of different pile materials. At the liquid limit the wood pile develops full shear strength, the concrete pile develops 50 percent of the shear strength, and the steel pile develops 40 percent of the shear strength. This agrees reasonably with the published values of adhesion by Potondyi (19). At lower water content the steel pile maintains an approximate relation with strength, but the concrete and wood piles develop a much lower proportion of the total available shear strength. The tests were repeated several times at varying load rates and time intervals between tests with the same outcome for each sequence. The reason for this behavior is not clearly understood. It is possible that the soil, being below the shrinkage limit, may not have been completely bonded to the pile surface. Thus computation of average negative skin friction based on the total surface area of the pile may have resulted in values that are too low.

Effect of Asphalt Viscosity

The physical situations where negative skin friction is likely to occur have been previously described. If there is no other foundation scheme available to the designer, it may be proper to partially eliminate downdrag from occurring. The logical technique is to coat the pile's surface with a material that will not allow load transfer to pass onto the pile. Because of the large quantities involved and the cost thereof, the use of asphalt coatings seems reasonable and has been used in the field (10). Asphalts of different viscosities were tested, wherein the viscosity was indicated by its penetration grade and varied from very soft (600 to 800 penetration) to very stiff (60 to 70 penetration). The piles were coated with a $\frac{1}{8}$-in. thick layer of asphalt in this sequence of tests.

The results are shown in Figure 10 for the 5 asphalts tested. Most significant in such tests is the rate of surcharge load application. The slower load is applied, the lower is the developed average negative skin friction. Load increment time was extended until the curves became approximately constant. This load rate appears to be related to the coefficient of consolidation of the soil, c_v. As anticipated, the stiffer the asphalt is, the higher the average negative skin friction is. All curves represent a significant reduction in average negative skin friction from the untreated piles that were previously tested.

Effect of Asphalt Thickness

The previous set of tests utilized different viscosity asphalts but all were coated on the piles in $\frac{1}{8}$-in. thickness. This series varies the thickness from $\frac{1}{16}$ to $\frac{1}{4}$ in. These thickness tests were performed on the stiffest asphalt (60 to 70 penetration), the medium asphalt (150 to 200 penetration), and the softest asphalt (600 to 800 penetration).

The results are shown in Figure 11, which is plotted similar to Figure 10. The medium viscosity asphalt curves are shown as dashed lines. All curves show decreasing negative skin friction with increasing load time increments. Average negative skin friction decreases with increasing asphalt thickness. This is as anticipated since the

Figure 8. Experimental setup for pile material study.

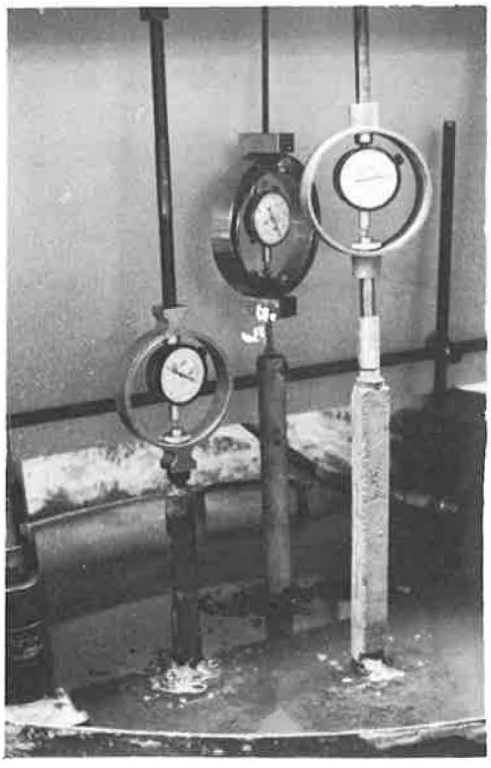

Figure 9. Effect of water content and pile material on average negative skin friction.

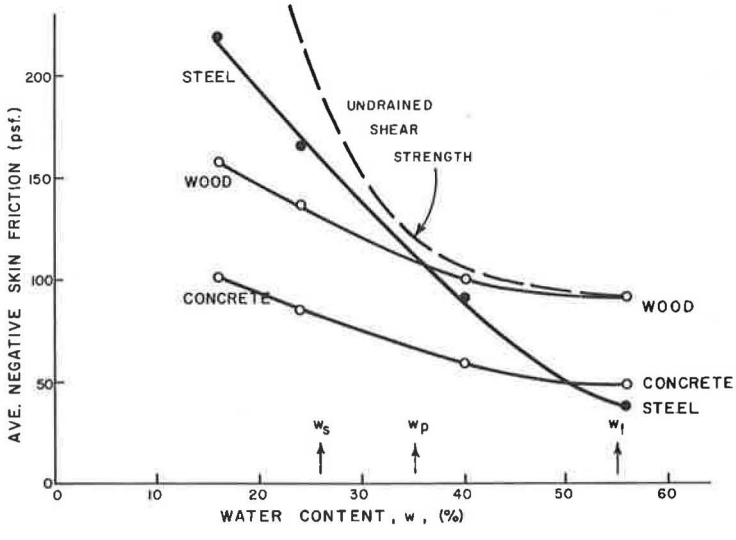

Figure 10. Effect of viscosity of asphalt coating on average negative skin friction.

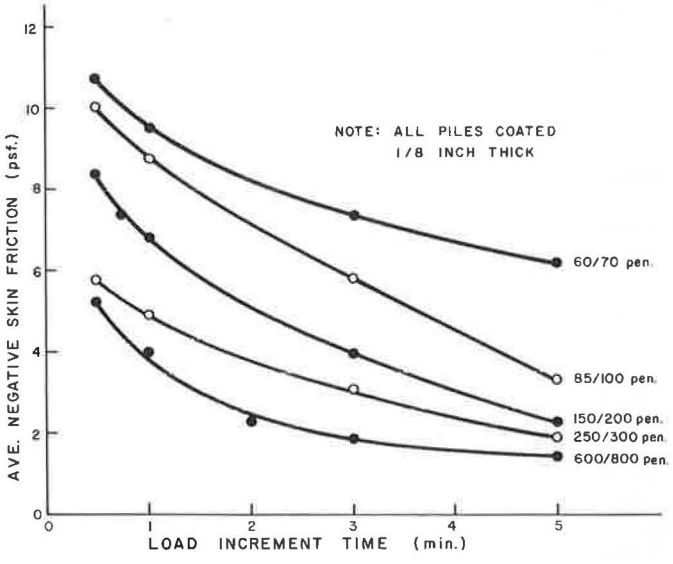

Figure 11. Effect of thickness of asphalt coating on average negative skin friction.

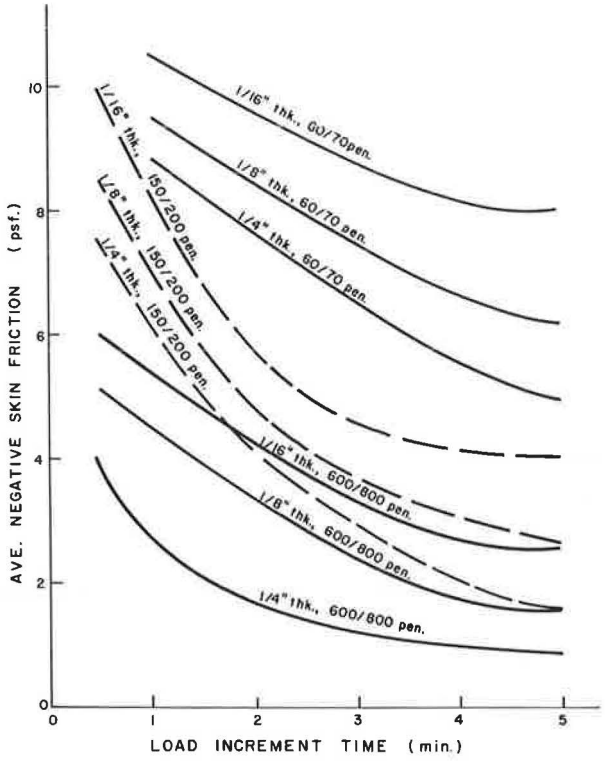

load transfer through the asphalt cannot be achieved with a thicker layer; thus, the asphalt absorbs a larger proportionate amount of the soil displacement and less is transferred onto the pile.

SUMMARY

Although the exact technique of computing downdrag force in a generalized form is still not available, a number of aspects of its behavior have been investigated. Some definite conclusions can be drawn therefrom.

1. As surface deformation proceeds, negative skin friction effects are felt on the pile at its top and proceed down from the pile to the bottom. Continued soil deformation causes equal increments of negative skin friction to be absorbed by the pile until the maximum value is mobilized over the entire length of the pile.
2. Batter piles develop larger downdrag forces than vertical piles. For pile batters greater than 1:10, average negative skin friction increases rapidly. These model test results are in disagreement with the only known field test on the effect of batter on negative skin friction.
3. Pile group spacings should be kept as low as possible to minimize negative skin friction. However, only with spacing-diameter ratios less than 2.5 is a significant reduction in average negative skin friction noticed, and such close spacings are often not practical.
4. As the water content of the soil decreases, the average negative skin friction increases. Since the shear strength of the soil is also increasing, there may be some relation available.
5. Tests on the effects of pile material on negative skin friction are not conclusive. This finding may indicate that the adoption of Mohr-Coulomb failure criterion to the prediction of negative skin friction will be difficult.
6. Use of asphalt coatings on deep foundations to reduce negative skin friction shows definite promise. It has been shown that the softer and thicker the asphalt coating is, the lower is the negative skin friction that is transferred to the pile.

ACKNOWLEDGMENTS

Support for this research project by the National Science Foundation is gratefully acknowledged. Preliminary tests were made by W. Lippincott and E. Trojan. The technical assistance of K. Whitlock and A. Yerger is greatly appreciated. F. Gzemski of the Atlantic Richfield Company supplied the asphalts used in this study.

REFERENCES

1. Bjerrum, L., Johannessen, I. J., and Eide, O. Reduction of Negative Skin Friction on Steel Piles to Rock. Seventh Internat. Conf. on Soil Mech. and Found Eng., Vol. 2, Mexico, 1969, pp. 27-34.
2. Bowles, E. Foundation Analysis and Design. McGraw-Hill, New York, 1968.
3. Bozozuk, M., and Labrecque, S. Downdrag Measurements on 270-Ft. Composite Piles. ASTM, Spec. Tech. Pub. 444, 1968, pp. 15-40.
4. Broms, B. B. Methods of Calculating the Ultimate Bearing Capacity of Piles—A Summary. Soils, No. 18-19, pp. 21-32.
5. Buisson, M., Ahu, J., and Habib, P. Le Frottement Negatif. Annales de l'Institute Technique de Batiment et des Travaux Publics, No. 145, Jan. 1960, pp. 29-46.
6. de Mello, V. F. B. Foundations of Buildings in Clays. Seventh Internat. Conf. on Soil Mech. and Found Eng., Mexico, 1969, State-of-the-Art Vol., pp. 49-136.
7. Elmasry, M. A. The Negative Skin Friction of Bearing Piles. Swiss Fed. Inst. of Tech., Zurich, thesis, 1963.
8. Endo, M., Minou, A., Kawasaki, T., and Shibata, T. Negative Skin Friction Acting on Steel Pipe Pile in Clay. Seventh Internat. Conf. on Soil Mech. and Found. Eng., Vol. 2, Mexico, 1969, pp. 85-92.
9. Fellenius, B. H., and Broms, B. B. Negative Skin Friction for Long Piles Driven in Clay. Seventh Internat. Conf. on Soil Mech. and Found. Eng., Vol. 2, Mexico, 1969, pp. 93-98.

10. Golder, H. Q., and Willeumier, G. C. Design of the Main Foundation of the Port Mann Bridge. Engineering Jour., Aug. 1964, pp. 22-29.
11. Hansen, J. B. A Theory for Skin Friction on Piles. Danish Geotechnical Institute, Copenhagen, Bull. 25, 1968, pp. 5-12.
12. Johannessen, I. J., and Bjerrum, L. Measurement of the Compression of a Steel Pile to Rock Due to Settlement of the Surrounding Clay. Sixth Internat. Conf. on Soil Mech. and Found. Eng., Vol. 2, Montreal, 1965, pp. 261-264.
13. Johnson, S. M., and Kavanagh, T. C. The Design of Foundations for Buildings, McGraw-Hill, New York, 1968.
14. Koerner, R. M. Experimental Behavior of Downdrag in Deep Foundations. Jour. Soil Mech. and Found. Div., Proc. ASCE, Tech. Note, Feb. 1971, pp. 515-519.
15. Locher, H. G. Combined Cast-In-Place and Precast Piles for the Reduction of Negative Friction Caused by Embankment Fill. Sixth Internat. Conf. on Soil Mech. and Found. Eng., Vol. 2, Montreal, 1965, pp. 290-294.
16. Mazurkiewicz, B. K. Skin Friction on Model Piles in Sand. Danish Geotechnical Institute, Copenhagen, Bull. 25, 1968, pp. 13-48.
17. Moore, W. W. Experiences With Predetermining Pile Lengths. Trans. ASCE, Vol. 114, 1949, pp. 351-393.
18. Nunez, E., and Varde, O. Negative Skin Friction and Settlements of Piled Foundations. Seventh Internat. Conf. on Soil Mech. and Found. Eng., Vol. 3, Mexico, 1969, pp. 473-478.
19. Potyondy, J. G. Skin Friction Between Various Soils and Construction Materials. Geotechnique, Vol. 2, 1961, pp. 339-353.
20. Poulos, H. G., and Mattes, N. S. The Analysis of Downdrag in End-Bearing Piles. Seventh Internat. Conf. on Soil Mech. and Found. Eng., Vol. 2, Mexico, 1969, pp. 203-209.
21. Terzaghi, K., and Peck, R. B. Soil Mechanics in Engineering Practice. John Wiley and Sons, New York, 1948.
22. van Weele, A. F. Negative Skin Friction on Pile Foundation in Holland. Proc., Symposium on Bearing Capacity of Piles, Roorkee, India, 1964, pp. 1-10.
23. Whitaker, T. Experiments With Model Piles in Groups. Geotechnique, Vol. 7, No. 4, London, 1957, pp. 147-167.
24. Zeevaert, L. Reduction of Point Bearing Capacity of Piles Because of Negative Skin Friction. Proc., First Pan-American Conf. on Soil Mech. and Found. Eng., Vol. 3, Mexico, 1959, pp. 1,145-1,152.

INFLUENCE VALUE GRAPHS FOR CIRCULAR BEARING AREAS

Alfreds R. Jumikis, College of Engineering, Rutgers University,
The State University of New Jersey, New Brunswick

ABRIDGMENT

Based on the extended use of Boussinesq's theory of elasticity pertaining to vertical stress distribution in a semi-infinite, homogeneous, isotropic, elastic hemispatial medium by surface loading, the author presents for the engineering profession systematic 3-dimensional influence values in graph form for determining vertical, normal stresses at any point in an elastic medium from a uniformly loaded circular bearing area. The influence value graphs are easy to use. Influence values can be picked out directly, and they facilitate a quick determination of vertical stress fields in soil. Thus, these influence values rationalize and expedite effectively the work of soil and foundation design engineers.

•TO MEET the great need for vertical stress distribution influence values in soil from uniformly loaded circular bearing areas and to rationalize and expedite further the work of foundation engineers, the author planned and opened up the necessary analytical material for computer programming and, within the course of his academic activities, prepared and is submitting herewith to the engineering profession corresponding systematic vertical stress distribution influence value graphs shown in Figure 1. A family of isobars is shown underneath the circle in percentage of the contact pressure intensity σ_o (Fig. 2).

These systematically arranged vertical normal stress influence values permit one to determine directly, quickly, and effectively vertical (σ_z) stresses in soil and their distribution and to ascertain stress fields at any point in the soil from uniformly loaded circular bearing areas.

The derivation of the spatial σ_z stress, viz., influence values, is based on extending integration of Boussinesq's basic vertical, spatial stress component equation at any point in the elastic medium for a single, concentrated load (10) to a circular bearing area for a given uniform, nonrigid surface loading distribution σ_o.

EARLY SOLUTIONS

An analytical solution for stress distribution in an elastic, semi-infinite medium from a uniformly loaded circular bearing area on the horizontal boundary surface of the hemispace has been worked out by Lamb (13) and Terzawa (18) by means of Bessel functions. Other authors on this subject are Carothers (2), Jürgenson (12), Love (15; 9, p. 155), Palmer (17), Fröhlich (6; 9, p. 151), Newmark (16), and Fadum (4).

SOME RECENT SOLUTIONS

In 1953, Lorenz and Neumeuer (14) put forward their method of vertical, normal stress calculations from a uniformly loaded circular bearing area for any point inside and outside the circle. Because of the mathematical difficulties involved in solving for the σ_z stress, these authors evaluated the corresponding influence values by means of numerical methods. Their influence values, however, are given for $\nu = 3$ and for the following distances from (0; 0; 0):

Sponsored by Committee on Mechanics of Earth Masses and Layered Systems.

Figure 1. Influence values for vertical, normal σ_z stress at any point in elastic medium from a uniformly loaded circular bearing area.

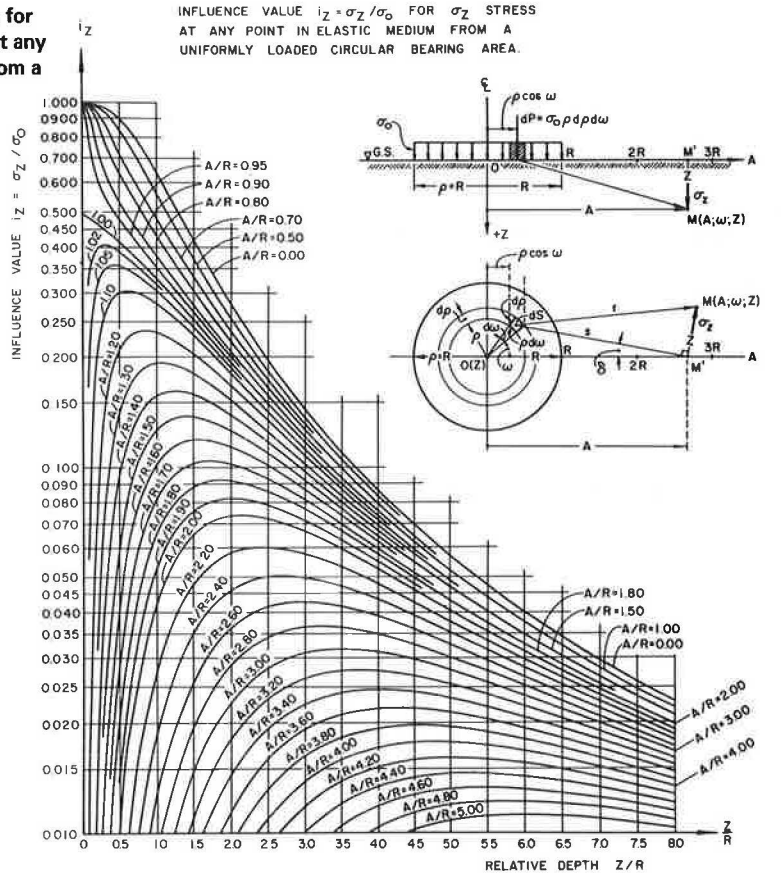

Figure 2. Isobars from a uniformly loaded circular bearing area.

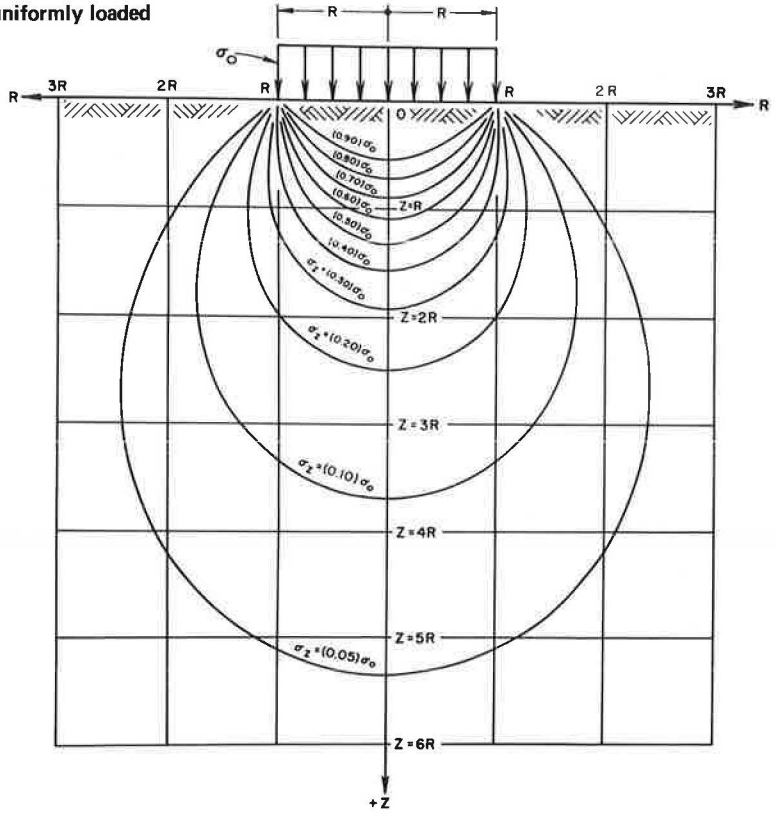

1. For one-half of the radius (r/2);
2. For the periphery of a circle with radius r; and
3. For a point at a distance of 2 radii away from the center of the uniformly loaded circle (9, pp. 153-155). Hence, also, these influence values are for limited use only.

In 1954, Foster and Ahlvin also published charts for stresses from a uniform circular load (5). In this paper, no theoretical basis underlying the preparation of the charts is given.

BASIS FOR PREPARING INFLUENCE VALUES

Derivation

The basis used by this author for calculating the vertical, normal stress σ_z at any point in the elastic medium [say, point M (Fig. 1), whose coordinates are A, $\omega = 0$, and z], brought about by a uniformly loaded circular bearing area S, is the summation of Boussinesq's single, elementary, concentrated loads $dP = \sigma_o \rho \, d\omega \, d\rho$ over the entire circular bearing area S (9, p. 155).

$$d\sigma_z = (3/2)(dP/\pi)(z^3/r^5) = (3/2)(\sigma_o/\pi)\left[z^3/\sqrt{(s^2 + z^2)^5}\right]\rho \, d\rho \, d\omega \qquad (1)$$

where

σ_o = intensity of uniformly distributed pressure over circle;
z = depth coordinate of point M below base level of circular bearing area;
$r = \sqrt{s^2 + z^2}$; (2)
= radius-vector from dS (viz., dP) to point M (Fig. 1);
$s = \sqrt{A^2 + \rho^2 - 2 A \rho \cos \omega}$; (3)
= horizontal distance from dP (dS) to point M′ (trigonometric cosine law);
A = horizontal, radial distance of point M, viz., point M′, from z-axis;
ω = amplitude for ρ; and
ρ = variable radius for elementary load dP over elementary surface area dS of circle.

Substituting Eq. 3 into Eq. 1 and indicating integration of Eq. 1 over the entire circular area, we obtain an expression for the σ_z stress sought for any point in the elastic medium as

$$\sigma_z = (3/2)(\sigma_o/\pi)z^3 \int_0^R \int_0^{2\pi} (\rho \, d\rho \, d\omega)/[(A^2 + z^2 + \rho^2 - 2 A \rho \cos \omega)^{5/2}] \qquad (4)$$

where R = radius of circle.

Solution

The integral from $\omega = 0$ to $\omega = 2\pi$ has been indicated already by Love (15) and by Lorenz and Neumeuer (14; 9, pp. 156-159)

Although the problem of finding the σ_z from a loaded circular area involves a uniformly distributed load σ_o, the computation of the σ_z stress is quite involved. The integral as given by Eq. 4 cannot be solved in a closed form. Its complete solution goes through elliptic integrals (15) or by numerical evaluation (14). The analysis necessary for evaluating the integral in Eq. 4 is rather long and involved. However, an analytical solution to Eq. 4 (due to Egorov, 3) for calculating the σ_z stress at any point in the hemispatial, elastic medium from uniformly loaded circular bearing areas involving elliptic integrals, as cited by Harr and Lovell (7) and by Harr (8), is given here by the author in terms of dimensionless parameters A/R and Z/R (Fig. 1) as

$$\sigma_z = \sigma_o \left(N - \frac{(Z/R)}{\pi\sqrt{(Z/R)^2\,[1 + (A/R)]^2}} \left\{ \frac{(Z/R)^2 - 1 + (A/R)^2}{(Z/R)^2 + [1 - (A/R)]^2}\, E(k) + \frac{1 - (A/R)}{1 + (A/R)}\, \Pi_o(k, p) \right\} \right) \tag{5}$$

where

A/R and Z/R = dimensionless parameters for relative distance and relative depth respectively;

E(k) and $\Pi_o(k, p)$ = Legendre's complete elliptic integrals of the second and third kind respectively (1);

$k = \sqrt{[4(A/R)]/\{(Z/R)^2 + [1 + (A/R)]^2\}}$ = modulus of elliptic integral; and

$p = -[4(A/R)]/[1 + (A/R)]^2$ = parameter of elliptic integral.

Equation 5 comprehends a general solution in general terms in 1 equation for 3 special cases characterized by the quantity N, namely:

Point M	A/R	N
On central Z-axis	0 or < 1	1.0
Inside of circle	< 1	1.0
Periphery of circle	1	0.5
Outside of circle	>1	0.0

These 3 N-values (1.0, 0.5, and 0.0) result after the first integration of Eq. 4 with respect to ρ.

The nature of the computer printout (in capital letters) necessitates the use of capital letters in this development for programming of the influence values $i_z = \sigma_z/\sigma_o$.

INFLUENCE VALUE GRAPHS

Use of Graphs

The influence value curves $i_z = \sigma_z/\sigma_o$ resulting from Eq. 5 are shown in Figure 1. The numerical value of the vertical σ_z stress is obtained by simply multiplying the corresponding influence value i_z with the given uniformly distributed surface loading σ_o over a circular bearing area as

$$\sigma = i_z\, \sigma_o \tag{6}$$

For example, if A/R = 2.2, Z/R = 2.5, and σ_o = 2.0 kg/cm^2, the influence value (Fig. 1) is i_z = 0.050, and the vertical stress σ_z is $\sigma = i_z\, \sigma_o$ = (0.050) (2.0) = 0.10 (kg/cm^2). Figure 2 shows isobars from a uniformly loaded circular bearing area.

Checking of Influence Values

These influence values were checked by comparing them with those already available in the technical literature. For example, the influence values along the vertical centerline (Z-axis) of the circle presented here were compared with those as published by Fadum (4). The comparison revealed a complete agreement in the $i_z = \sigma_z/\sigma_o$ values.

Further, a comparison was made of the author's and some of the few influence values given by Love (15). Again, a good agreement with the author's i_z-values was observed. The results independently arrived at by Love (15) and Carothers (2) are also in general in good agreement according to Palmer (17), thus, in a way, giving a tie-in check with Carothers' information. Also, the author's values [obtained by rigorous mathematical analysis (Eqs. 4 and 5)] are in reasonably good agreement with those determined by Lorenz and Neumeuer (14), obtained by the approximate method of numerical analysis

using Simpson's rule (11). Thus, there is fairly good reason to believe that the influence values as prepared and presented here by the author are plausible ones to use.

CONCLUSION

The essential feature of these tables and graphs is that they give influence values directly and immediately for the vertical σ_z stress for any size of circular bearing area, for any depth, at any point in the hemispace of the elastic medium, and for any contact pressure σ_o —not merely along the centerline under the center of the circle or half-radius, along the periphery of the circle, or at points distant 2r from the vertical z-axis of the uniformly loaded circular bearing area.

The reader will surely appreciate the analytical effort that went into the opening up of Eq. 5 for computation and preparation of these influence value tables and graphs now so easy to use.

ACKNOWLEDGMENTS

The author expresses his appreciation to the following persons who provided means for programming of these influence value tables and for processing of this paper: E. C. Easton, College of Engineering and Bureau of Engineering Research; R. C. Ahlert, Bureau of Engineering Research; M. L. Granstrom, Department of Civil and Environmental Engineering; and J. Wiesenfeld, Department of Civil and Environmental Engineering, all of Rutgers University. P. B. Singh, a graduate student in civil engineering, programmed the influence values.

REFERENCES

1. Byrd, P. F., and Fredman, M. D. Handbook of Elliptic Integrals for Engineers and Physicists. Springer, Berlin, 1954, p. 227.
2. Carothers, S. D. The Test Loads on Foundations as Affected by Scale of Tested Area. Proc. 1924 Internat. Mathematical Congress, Univ. of Toronto Press, Canada, Vol. 2, 1928, pp. 527-549.
3. Egorov, K. E. Concerning the Question of Calculating Stresses Under Ring-Shaped Foundation Footings. Mekhanika Gruntov, Sbornik Trodov 34, Gosstroiizdat, Moscow, 1958 (in Russian).
4. Fadum, R. E. Influence Values for Estimating Stresses in Elastic Foundations. Proc. Second Internat. Conf. on Soil Mech. and Found. Eng., Rotterdam, Vol. 3, 1948, p. 77.
5. Foster, C. R., and Ahlvin, R. G. Stresses and Deflections Induced by a Uniform Circular Load. HRB Proc., Vol. 33, 1954, pp. 467-470.
6. Fröhlich, O. K. Druckverteilung im Baugrunde. Springer, Vienna, 1934, p. 49.
7. Harr, M. E., and Lovell, C. W., Jr. Vertical Stresses Under Certain Axisymmetrical Loadings. Highway Research Record 39, 1963, pp. 68-77.
8. Harr, M. E. Foundations of Theoretical Soil Mechanics. McGraw-Hill, New York, 1966, p. 86.
9. Jumikis, A. R. Theoretical Soil Mechanics. Van Nostrand Reinhold, New York, 1969, pp. 151, 155, 156-159.
10. Jumikis, A. R. Stress Distribution Tables for Soil Under Concentrated Loads. College of Engineering, Rutgers University, State University of New Jersey, New Brunswick, Eng. Res. Pub. 48, 1969, pp. 7, 177-225.
11. Jumikis, A. R. Vertical Stress Distribution Influence Value Tables for Any Point in Soil Under Uniformly Distributed Loads. College of Engineering, Rutgers University, State University of New Jersey, New Brunswick, Eng. Res. Pub. 52, 1971.
12. Jürgenson, L. The Application of Theories of Elasticity and Plasticity to Foundation Engineering Problems. Jour. of Boston Society of Civil Engineers, Vol. 21, No. 30, July 1934.
13. Lamb, H. On Boussinesq's Problem. Proc., London Mathematical Society, Vol. 34, 1902, p. 276.

14. Lorenz, H., and Neumeuer, H. Spannungsberechnung infolge Kreislasten unter beliebigen Punkten innerhalb und ausserhalb der Kreisfläche. Die Bautechnik.
15. Love, A. E. H. Stress Produced in a Semi-Infinite Solid by Pressure on Part of the Boundary. Philosophical Trans., Royal Soc., London, Series A, Vol. 228, 1929, pp. 377-420.
16. Newmark, N. M. Influence Charts for Computation of Stresses in Elastic Foundations. Univ. of Illinois Bull., Series 338, Vol. 40, Nov. 10, 1942.
17. Palmer, L. A. Stress Under Circular Loaded Areas. HRB Proc., Vol. 19, 1939, pp. 397-408.
18. Terzawa, K. On the Elastic Equilibrium of a Semi-Infinite Solid. Jour. of Colloid Science, Art. 7, Vol. 37, 1916.

EFFECT OF CONE ANGLE ON PENETRATION RESISTANCE

Edward A. Nowatzki and Leslie L. Karafiath, Grumman Aerospace Corporation, Bethpage, New York

A theoretically correct 3-dimensional analysis of cone penetration using plasticity theory and the Coulomb failure criterion is presented. The differential equations of plastic equilibrium are solved numerically for an ideal uniform dry sand to show the variation of slip-line field geometry with changes in the apex angle of the cone. The results indicate that, with increasing apex angle, less soil volume is affected. The results of a series of laboratory tests are plotted to show how the value of cone index increases with increasing apex angle. The differential equations of plastic equilibrium are again solved numerically for soil and boundary conditions that correspond to those of the experiments. The results support the validity of the theory in dense sands and also demonstrate that soil compressibility affects the cone index to the extent that it no longer serves as a measure of frictional strength. For loose soils, differences in cone angles have little effect on cone index, all other conditions being equal. This condition can be identified by the use of 2 cones, one having an obtuse apex angle and the other an acute apex angle. The theoretical and experimental results are correlated to show how the theory may be used for any soil to predict the angle of internal friction.

•THE MERITS of using penetrometer data for determining soil properties have been discussed extensively (6, 9, 13). In many of these reports empirical expressions are derived purporting to relate penetration test parameters to soil properties, for example, blow count data of the standard penetration test (SPT) to the relative density of the soil being penetrated. Although most of the effort has been directed toward dynamic tests such as the SPT, some consideration has also been given to relating soil parameters to static cone penetration characteristics (18). Very little attention has been paid to a theoretical analysis of the interaction between a cone penetrometer and the failing soil during the penetration process, although there exists in the literature a well-established basis for such a study. The following paragraph presents a brief review of the pertinent contributions in the area of plasticity analysis of soil problems.

The theory of static equilibrium has been combined with the Coulomb failure criterion and applied to studies of soil bearing capacity. Prandtl (12) solved the resulting differential equation of plastic equilibrium for a strip footing on weightless soil (plane strain condition). Cox, Eason, and Hopkins (4) developed a general theory of axially symmetric plastic deformations in ideal soils and applied it to the problem of the penetration of a smooth, rigid, flat-ended circular cylinder into a semi-infinite mass of weightless soil. Drucker and Prager (5) and more recently Spencer (16) extended the theory for the plane strain case to include body forces such as soil weight and cohesion; Cox (3) and more recently Larkin (8) did the same for the axially symmetric case. In cases where the characteristic relations for the governing differential equations cannot be integrated explicitly, numerical methods are used. Sokolovskii (15) presented the most widely used procedure of numerical integration, a finite difference approximation based on the method of characteristics.

Sponsored by Committee on Foundations of Bridges and Other Structures.

Studies relating specifically to cone indentation problems are less numerous. Sneddon (14) derived a solution to the cone indentation problem within the framework of the classical theory of elasticity. Meyerhof (10) and Berezantzev (1) offered approximate solutions of the axially symmetric problem. The former applied the solution to a study of the effect of surface roughness on cone penetration; the latter investigated the use of penetrometer data to determine friction angle.

OBJECTIVE

An analysis is presented of the penetration of a perfectly rigid cone into an ideal granular soil whose strength properties are defined by the Coulomb failure criterion. Plastic stress states are considered to be symmetric with the central axis of a right circular cone. A purely frictional soil is assumed so that local pore-pressure buildup may be neglected. This ensures that failure occurs in shear zones rather than along a single failure surface. In the model used in the analysis, the limit load, obtained from a solution that satisfies the basic differential equations of plasticity and the boundary stress condition, is considered a lower bound (5).

SCOPE

This study is arranged in the following order: The variables are identified and defined, the governing equations of plastic equilibrium for the axially symmetric case are given, and the limitations of the present investigation are discussed. The major results obtained from the theory within those limitations are presented and discussed with reference to experimental data. Conclusions are drawn at this point in the analysis. Finally, the results of this study are summarized, and remarks are made concerning them and their relation to future research in this area.

NOTATION

The quantities defining the geometry of the problem are shown in Figure 1. The notation is as follows:

- A_o = area of cone base;
- c = cohesion;
- G = slip-line geometry similitude factor;
- CI = cone index, defined (in psi) as the penetration resistance/A_o where, in this study, the resistance at 6-in. penetration is used as a reference;
- R_o = radius of cone base;
- w = surcharge;
- r, z = coordinates;
- z_o = depth to which base of cone has penetrated;
- α = apex angle of cone or cone angle;
- β = complement to apex semiangle;
- γ = unit weight of soil;
- δ = friction angle between cone and soil;
- θ = angle between r-axis and major principal stress;
- φ = angle of internal friction of soil;
- ψ = $c \cot \varphi$;
- μ = $\pi/4 - \varphi/2$; and
- σ = $(\sigma_1 + \sigma_3)/2 + \psi$ (in general).

FORMULATION

The following set of differential equations represents the theoretically rigorous formulation to the problem of determining axially symmetric plastic stress states and slip-line fields:

$$d\sigma \pm 2\sigma \tan \phi d\theta - (\gamma/\cos \phi) [\sin(\pm\phi)dr + \cos(\pm\varphi)dz] + (\sigma/r) [\sin \phi dr \pm \tan \phi(1 - \sin \phi)dz] = 0$$

$$dz = dr \tan(\theta \pm \mu) \tag{1}$$

This set of equations is obtained by combining the equations of equilibrium derived from plasticity theory with the Coulomb failure criterion. The circumferential stress is assumed to be the intermediate principal stress and to be equal to the minor principal stress σ_3. The r-axis of the coordinate system is parallel to the ground surface, and the positive z-axis is perpendicular to it into the soil mass (Fig. 1). The upper sign refers to the family of slip lines corresponding to the first characteristics of the differential equations (i-lines), and the lower sign refers to the second (j-lines).

No closed-form solution to these equations exists. Several numerical solutions have been presented; however, these are restricted to the axially symmetric surface loading of the semi-infinite half space. The equations given below are the numerical form of Eq. 1 and are used to study the effect of soil properties and cone parameters on the penetration characteristics of a right circular cone penetrating soil. So that the problem can be kept perfectly general, soil body forces have been included in the formulation. For a given set of loading conditions w over the horizontal soil surface, the values of $r_{i,j}$, $z_{i,j}$, $\sigma_{i,j}$, and $\theta_{i,j}$ are computed for an adjacent nodal point (slip-line intersection point, Fig. 1) by use of the set of recurrence relations.

$$r_{i,j} = (z_{i-1,j} - z_{i,j-1} + \epsilon_1 r_{i,j-1} - \epsilon_2 r_{i-1,j})/(\epsilon_1 - \epsilon_2) \tag{2}$$

$$z_{i,j} = z_{i-1,j} + (r_{i,j} - r_{i-1,j})\epsilon_2 \tag{3}$$

where $r_{i,j}$ and $z_{i,j}$ are the coordinates of the adjacent nodal point, $\epsilon_1 = \tan(\theta_{i,j-1} + \mu)$, and $\epsilon_2 = \tan(\theta_{i-1,j} - \mu)$. With these values of $r_{i,j}$ and $z_{i,j}$, the computation is continued.

$$\sigma_{i,j} = \{2\sigma_{i-1,j}\sigma_{i,j-1}[1 + \tan\varphi(\theta_{i,j-1} - \theta_{i-1,j})] + \sigma_{i-1,j}D + \sigma_{i,j-1}C - \sigma_{i,j-1}\sigma_{i-1,j}(B/r_{i,j-1} + A/r_{i-1,j})\}/(\sigma_{i,j-1} + \sigma_{i-1,j}) \tag{4}$$

$$\theta_{i,j} = [\sigma_{i,j-1} - \sigma_{i-1,j} + 2\tan\varphi(\sigma_{i,j-1}\theta_{i,j-1} + \sigma_{i-1,j}\theta_{i-1,j}) + D - C + \sigma_{i-1,j}A/r_{i-1,j} - \sigma_{i,j-1}B/r_{i,j-1}]/2\tan\varphi(\sigma_{i,j-1} + \sigma_{i-1,j}) \tag{5}$$

where

$A = \sin\varphi(r_{i,j} - r_{i-1,j}) - \tan\varphi(1 - \sin\varphi)(z_{i,j} - z_{i-1,j})$;
$B = \sin\varphi(r_{i,j} - r_{i,j-1}) + \tan\varphi(1 - \sin\varphi)(z_{i,j} - z_{i,j-1})$;
$C = \gamma[z_{i,j} - z_{i-1,j} - \tan\varphi(r_{i,j} - r_{i-1,j})]$; and
$D = \gamma[z_{i,j} - z_{i,j-1} + \tan\varphi(r_{i,j} - r_{i,j-1})]$.

To apply these recurrence relations to the problem of cone indentation required that the geometric boundary conditions as well as the stress boundary conditions be formulated appropriately and included in the computer program. The geometric boundary conditions are simply mathematical descriptions of the cone geometry and its position at depth in terms of r, z, α, and R_o. The stress boundary conditions and the method of computation are essentially the same as those described by the authors elsewhere for 2-dimensional conditions (1).

Briefly, the stress boundary condition on the horizontal plane through the base of the cone is given by the surcharge w and the overburden soil pressure (Fig. 1). Overburden shear is disregarded. The slip-line field in the passive zones is computed by Eq. 1 starting with these boundary values and an assumed value for the horizontal extent of the passive zone. In the radial shear zone, the same equations are used, but special consideration is given to the central point where the j-lines converge (point Q, Fig. 1). This point is a degenerated slip line, where θ changes from the value at the passive zone boundary to that specified at the active zone boundary. The total change in θ is divided by the number of slip lines converging at this point to obtain an equal $\Delta\theta$ increment between 2 adjacent slip lines. The σ values for each increment are computed

from the equation $\sigma = \sigma_o e^{2(\theta-\theta_o)\tan\phi}$, which is the solution to Eq. 1 if both dr and dz vanish. Allowance must be made for the angle β as well as δ when transition values of θ and σ are assigned between the active and passive zones. These values of θ and σ for each slip line at this point permit the coordinates as well as the σ and θ values for all other points in the radial shear zone to be computed by Eq. 1. In the active zone, the same equations are used, except for the points at the loaded surface of the cone itself, where $\theta_{1,j}$ is assigned and $z_{1,j} = z_o + (R_o - r_{1,j}) \tan \alpha$. Here,

$$r_{1,j} = \{r_{1-1,j} \tan[(\theta_{1,j} + \theta_{1-1,j})/2 - \mu] - z_{1-1,j} + R_o \tan \alpha + z_o\}/$$
$$\{\tan[(\theta_{1,j} + \theta_{1-1,j})/2 - \mu] + \tan \alpha\} \quad (6)$$

and

$$\sigma_{1,j} = \sigma_{1-1,j} + \sigma_{1-1,j}(\theta_{1,j} - \theta_{1-1,j}) \tan \varphi + C - [(\sigma_{1-1,j}A)/(r_{1-1,j})] \quad (7)$$

The numerical computation is performed and adjustments are made, if necessary, to the value assumed for the horizontal extent of the passive zone until the slip-line field "closes" on the axis of symmetry at the apex of the cone.

RESULTS AND CONCLUSIONS

Theoretical Results

The numerical computation of the slip-line field geometries and associated stresses by the recurrence relations (Eqs. 2 through 5) was performed on an Adage, Inc., time-sharing computer system. This system is based on Digital Equipment Corporation PDP-10 processors. To show specifically the effect of cone angle on the slip-line field geometry, we solved the governing differential equations for a set of ideal soil conditions that describe a homogeneous, dry, and purely frictional sand. These conditions are $c = 0$, $\varphi = 37$ deg, $\gamma = 100$ pcf, $w = 1$ psf, and $\delta = 20$ deg. The numerical results were plotted automatically and electronically on the display tube of a Computer Displays, Inc., advanced remote display system. The slip-line fields for $R_o = 0.034$ ft (radius of the Waterways Experiment Station cone) and $\alpha = 15.5$, 30, 60, 90, 120, and 150 deg have been reproduced and are shown in Figure 2. Because the problem is axially symmetric, only half of the total field has been shown; the dashed line indicates the central axis of the cone. The geometric scale may be obtained for each figure from the knowledge that the base radius of the cone is 0.4 in. The scale shown in Figure 2a is 4 times that shown in Figure 2b.

For given soil strength parameters c and φ, the slip-line fields representing the solution of the differential equations are geometrically similar only if the ratio $G = \gamma\ell/(c + w \tan \varphi)$ is the same (3), where ℓ is a characteristic length usually taken equal to R_o. Although the slip-line geometry similitude factor G, as defined by Cox for the case of bearing capacity, is the same (4.512) in all of the cases shown in Figure 2, it is obvious that the slip-line geometries differ—an indication that the G-equality is a necessary but not sufficient condition for slip-line field similitude. In addition to G, there must also be equality in δ and a similitude in the geometric condition at both the free and loaded boundaries to obtain complete geometric similitude of the slip-line field.

Figure 2 distinctly shows a contraction of the radial shear zone with decrease in cone angle. The contraction is so pronounced (Fig. 2b) that the individual i- and j-lines are hardly discernible with the scale used. The active, passive, and radial shear zones all have curvilinear boundaries because of the 3-dimensional nature of the problem, an indication that the geometries obtained from the solution of the theoretically correct differential equations differ from those obtained by using the Prandtl solution for weightless soil and the log-spiral approximation in the radial zone.

Figure 2 also shows that, with decreasing cone angle, the affected volume of soil increases. For the soil and cones used, the volume of the body of revolution formed by the slip-line field for $\alpha = 30$ deg is about 10 times greater than that for $\alpha = 150$ deg.

For compressible soils, the size of the affected mass directly influences the load-penetration relation. The material must be compressed to a state in which friction is fully mobilized before shear failure along slip lines can take place. The load necessary to accomplish this compression is usually less than the load needed to fail the soil in shear. It follows that the larger the volume of the slip-line field is, the more the soil mass must be compressed to mobilize the friction fully. Therefore, cone indexes obtained with cone shapes that result in large-volume slip-line fields are likely to be less representative of the Coulombic strength than of the compressibility of the material.

Experimental Results

A series of penetration tests was conducted on Jones Beach sand by using aluminum cones. The friction angle between the aluminum surface of the cone and the sand was assumed to be uniform and equal to 15 deg on the basis of experiments performed by Mohr and Karafiath (16). The purpose of the tests was to determine the effect of cone angle α on the value of the cone index CI. The base area of cones having apex angles of 150, 90, and 30 deg was 0.5 in.^{2}. The 30-deg cone corresponds to the Waterways Experiment Station cone. Also used was a cone having a base area of 1.04 in.^{2} and an apex angle of 15.5 deg. This cone corresponds to that used until 1956 by the North Dakota State Highway Department for flexible pavement design. The ranges of φ over normal stress levels of interest for ranges of γ obtained from triaxial tests on Jones Beach sand were as follows:

γ (pcf)	φ (deg)
103.5 to 105.5	41 to 37
95.5 to 97.5	38 to 30

Uniform soil beds were prepared to a narrow range of desired densities in a facility specially designed for this purpose.

The cones were attached interchangeably to a 12-in. rod, and the entire assembly was mounted on the loading frame of an Instron testing instrument model TM-M (Fig. 3). The rate of penetration was set at 10 cm/min. Load-penetration curves were obtained automatically on a synchronized strip-chart recorder. Values of CI as defined for this study were determined directly from the load-penetration curves. The results of the penetration test series are shown in Figures 4 and 5.

Figure 4 shows the variation of cone index with change in cone angle for Jones Beach sand at various relative densities, as follows:

Density	Dγ	γ (pcf)
Dense	67 to 100	100 to 107
Medium	34 to 66	94 to 100
Loose	<34	88 to 94

It is clear from the figure that when the material is loose the cone angle has very little effect on the cone index (all values of CI are less than approximately 9 regardless of the size of the cone angle). On the other hand, for dense materials, CI varies from approximately 19 for the 15.5-deg cone to between 44 and 60 for the 150-deg cone. These results seem to verify the previously discussed effect of compressibility on the value of cone index. Apparently the frictional strength of the loose material cannot be fully mobilized until the material is sufficiently compressed to allow for complete shear failure. Calculations made on the basis of volume-change properties of the Jones Beach sand indicated that the average percentage of volume change of the soil mass within the slip-line field was virtually independent of the apex angle of cones having the same base area. Consequently, the displacement necessary to mobilize the full friction is roughly proportional to the volume of the slip-line field. These results suggest that, in order for the cone index to be used as a valid measure of the frictional strength of a soil, 2 cones should be used, both having the same base area but one having an obtuse apex angle and the other an acute apex angle. If the values of CI obtained from these 2 cones are similar, then the penetration resistance is governed by the

Figure 1. Geometry for cone indentation problem (boundary conditions and slip lines are symmetric with z-axis).

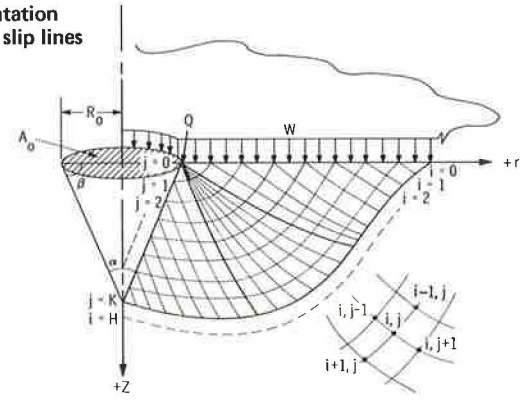

Figure 2. Slip-line fields for cones penetrating ideal soil.

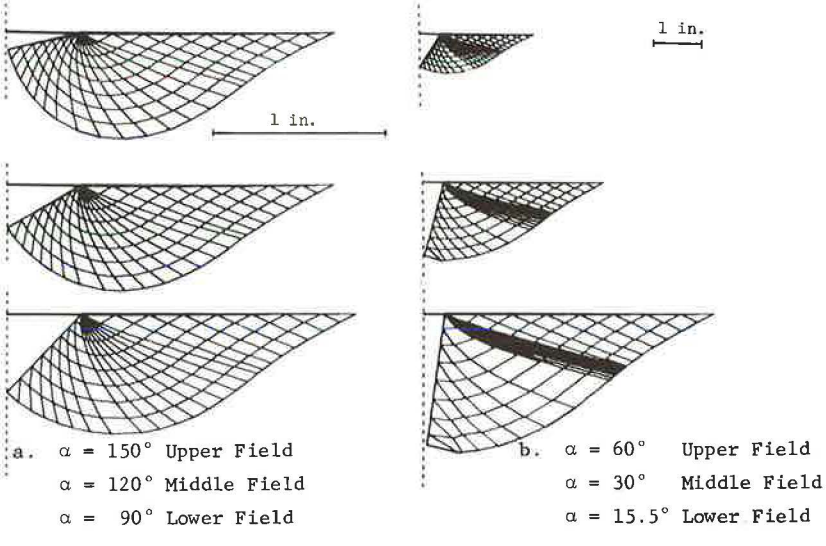

Figure 3. Loading and recording equipment for cone penetrometer test.

Figure 4. Cone index at 6-in. penetration versus cone angle for Jones Beach sand at various relative densities.

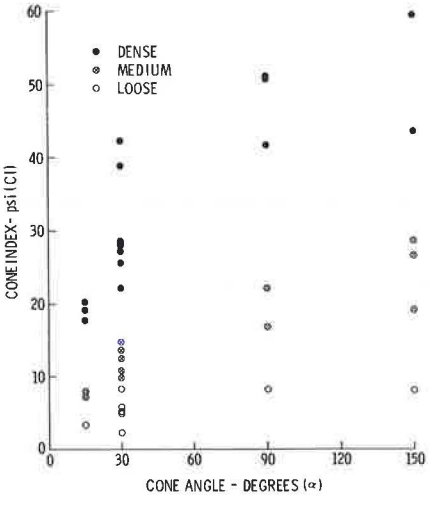

Figure 5. Cone index at 6-in. penetration versus unit weight for cones having different apex angles.

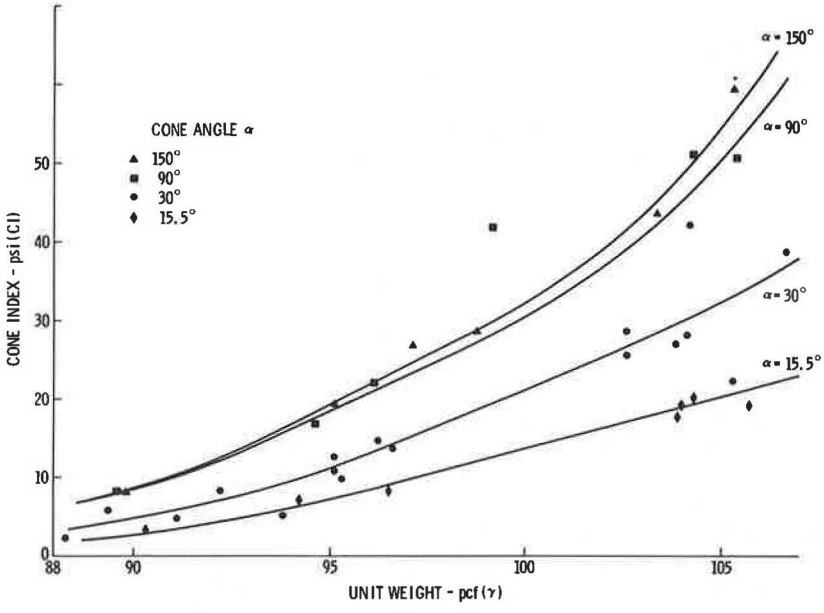

Figure 6. Cone index at 6-in. penetration versus unit weight for 150 deg.

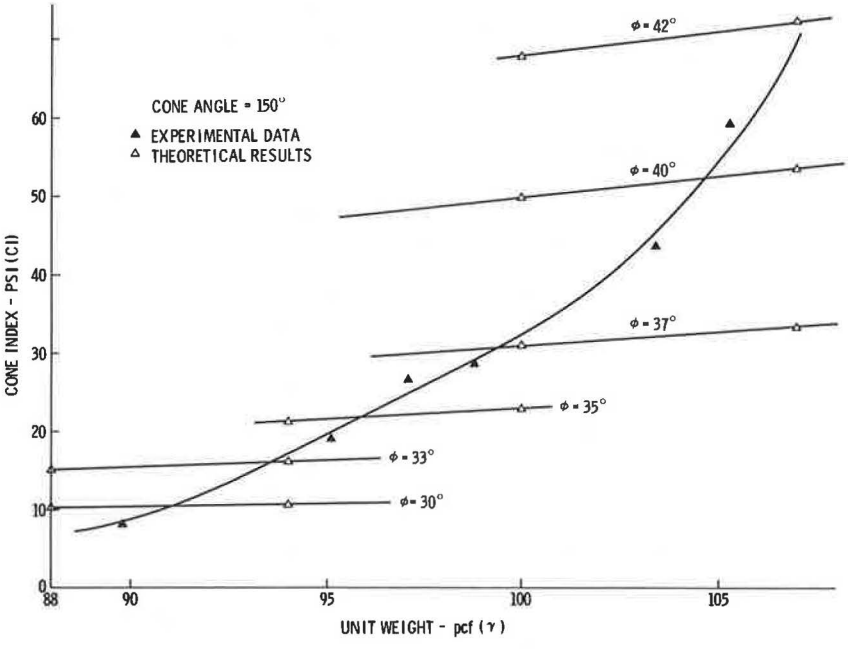

compressibility of the soil. If, on the other hand, the 2 values are markedly different, then a relation may properly be sought between CI and the strength parameters of the material.

Of course, the problem is not entirely that simple. In addition to the compressibility effect at lower relative densities, there is the effect of the variation of φ with γ. Figure 5 shows for each of the cones investigated the change in cone index with variation of unit weight. It is impossible from such a plot to distinguish which of the 2 effects has the greater influence. However, it seems reasonable to assume that, in the range of unit weights over which the material may be considered relatively dense, the compressional effect is negligible.

Comparison of Experimental and Theoretical Results

Figure 6 shows a comparison of the experimentally obtained values of CI over a wide range of unit weights with the values determined theoretically by the solution of the differential equations of plastic equilibrium. For clarity, only the results for the 150-deg cone are presented. The theoretical curves suggest that for φ constant there is little change in CI with variation in γ. The theoretical curves also show that for a given unit weight the value of CI is very sensitive to changes in φ. The experimental curve, which shows a pronounced decrease of CI with decrease in γ, not only reflects the change in φ with unit weight and stress level but also includes the effect of soil compressibility discussed above. Unfortunately, the experimental curve itself does not distinguish between these effects; however, for reasons cited above, it seems that the compressibility has the least influence on tests performed with dense material. For example, a cone index of 43 for Jones Beach sand at 103 pcf indicates a φ-angle of approximately 38 to 39 degrees (Fig. 6). For the stress level involved, this value of φ determined from cone penetrometer data agrees quite well with the values obtained from triaxial tests on Jones Beach sand.

Therefore, although the theory of plastic equilibrium has not been modified in this study to include in the computation of CI the effects of a curvilinear Mohr envelope (2, 17) or the contribution of soil compressibility, we believe that curves such as those shown in Figure 6 can be used to estimate an average value of φ from cone penetrometer data.

SUMMARY AND DISCUSSION

1. For the axially symmetric case, the slip-line field geometry derived from the theory of plastic equilibrium for a dry, uniform sand being penetrated by a cone differs markedly from that obtained by the Prandtl solution for weightless soil and the log-spiral approximation.
2. For materials at high relative densities, the cone index varies significantly with the size of the penetrometer apex angle, all other conditions being equal. This is not observed for loose materials. Soil compressibility, the variation of φ with γ, and the curvilinear nature of the Mohr failure envelope can account for this difference in performance.
3. Solutions derived from the theory of plastic equilibrium agree well with experimentally obtained cone penetrometer data and can be used, under certain conditions, to estimate the strength parameter φ for a dense dry sand. In all penetrometer investigations, the use of 2 cones is recommended to avoid misinterpretation of the cone index. One cone should have an obtuse apex angle, the other an acute angle.

Further investigations are needed to enhance the theory presented in this study. For example, it would be very desirable to incorporate into the computer program the curvilinearity of the Mohr envelope and the dependence of φ on unit weight. Similarly, the effect of compressibility on the penetration resistance of a material should be expressed quantitatively, and criteria for the mobilization of friction in the slip-line field should be established.

REFERENCES

1. Berezantzev, V. G. Certain Results of Investigation on the Shear Strength of Sands. Proc., Geotechnical Conf., Oslo, Vol. 1, 1967, pp. 167-169.
2. Berezantzev, V. G., and Kovalev, I. V. Consideration of the Curvilinearity of the Shear Graph When Conducting Tests on Model Foundations. Osnovaniya, Fundamenty i Mekhanika Gruntov, No. 1, 1968, pp. 1-4 (trans.).
3. Cox, A. D. Axially-Symmetric Plastic Deformation in Soils—II: Indentation of Ponderable Soils. Internat. Jour. of Mechanical Sciences, Vol. 4, 1962, pp. 371-380.
4. Cox, A. D., Eason, G., and Hopkins, H. G. Axially-Symmetric Plastic Deformation in Soils. Trans., Royal Soc., London, Series A, Vol. 254, 1961, pp. 1-45.
5. Drucker, D. C., and Prager, W. Soil Mechanics and Plastic Analysis or Limit Design. Quarterly of Applied Mathematics, Vol. 10, No. 2, 1952, pp. 157-165.
6. Fletcher, G. The Standard Penetration Test: Its Uses and Abuses. Jour. Soil Mech. and Found. Div., Proc. ASCE, Vol. 91, No. SM4, 1965, pp. 67-76.
7. Karafiath, L. L., and Nowatzki, E. A. Stability of Slopes Loaded Over a Finite Area. Highway Research Record 323, 1970, pp. 14-25.
8. Larkin, L. A. Theoretical Bearing Capacity of Very Shallow Footings. Jour. Soil Mech. and Found. Div., Proc. ASCE, Vol. 94, No. SM6, 1968, pp. 1347-1357.
9. Meyerhof, G. G. Penetration Tests and Bearing Capacity of Cohesionless Soils. Jour. Soil Mech. and Found. Div., Proc. ASCE, Vol. 82, No. SM1, 1956, pp. 1-19.
10. Meyerhof, G. G. The Ultimate Bearing Capacity of Wedge-Shaped Foundations. Proc., Fifth Internat. Conf. on Soil Mech. and Found. Eng., Paris, Vol. 2, 1961, pp. 105-109.
11. Mohr, G., and Karafiath, L. L. Determination of the Coefficient of Friction Between Metals and Nonmetals in Ultrahigh Vacuum. Research Department, Grumman Aerospace Corp., Rept. RE-311, Dec. 1967.
12. Prandtl, L. Ueber die Harte plastischer Korper. Gottingen Nachr., Math Phys. Kl., 1920, p. 74.
13. Schultz, E., and Knausenberger, H. Experiences With Penetrometers. Proc., Fourth Internat. Conf. on Soil Mech. and Found. Eng., Vol. 1, 1957, pp. 249-255.
14. Sneddon, I. N. The Relation Between Load and Penetration in the Axisymmetric Boussinesq Problem for a Punch of Arbitrary Profile. Internat. Jour. of Engineering Science, Vol. 3, 1965, pp. 47-57.
15. Sokolovskii, V. V. Statics of Granular Media. Pergamon Press, 1965.
16. Spencer, A. J. M. Perturbation Methods in Plasticity—III: Plane Strain of Ideal Soils and Plastic Solids With Body Forces. Jour. of Mechanics and Physics of Solids, Vol. 10, 1962, pp. 165-177.
17. Szymanski, C. Some Plane Problems of the Theory of Limiting Equilibrium of Loose and Cohesive, Non-Homogeneous Isotropic Media in the Case of a Non-Linear Limit Curve. In Non-Homogeneity in Elasticity and Plasticity (Olszak, W., ed.), Pergamon Press, 1958.
18. Soil Properties in Vehicle Mobility Research: Measuring Strength-Density Relations of an Air-Dry Sand. U. S. Army Engineer Waterways Experiment Station, Corps of Engineers, Vicksburg, Miss., Tech. Rept. 3-652, Aug. 1964.

EMBANKMENT TEST SECTIONS TO EVALUATE FIELD PERFORMANCE OF VERTICAL SAND DRAINS FOR INTERSTATE 295 IN PORTLAND, MAINE

Harl P. Aldrich, Jr., and Edmund G. Johnson, Haley and Aldrich, Inc., Cambridge, Massachusetts

A field test program was conducted in 1967-69 to evaluate the in situ performance of vertical sand drains. The work was sponsored by the Maine State Highway Commission in order to provide pertinent design data for the highway embankment of Interstate 295 in Portland, Maine. Test drains were installed to average depths of 60 to 70 ft at one location and 30 to 40 ft at another. The main objectives were to evaluate the relative effects of drain installation method (driven, jetted, and augered), drain spacing, and influence of soil type. Each drain type was installed at 10- and 14-ft spacing in a triangular pattern, and the test areas were surcharged with at least 20 ft of embankment fill above original grade. Backfigured values of the coefficient of consolidation for horizontal drainage, c_h, were compared with values interpreted from laboratory tests, assuming that there was no disturbance. The ratio was approximately one-half for the augered and jetted drains and considerably less for the driven drains. There was less evidence of disturbance for the augered and jetted drains; the driven drains indicated a significant reduction in c_h at the closer spacing. The test program illustrates that the method of installation is indeed important and that there is a need for development of improved methods of drain installation to further reduce the effects of remolding in sensitive clay soils.

•THE ALIGNMENT of Interstate 295, referred to as the Portland Loop, consists of a complex of expressways and feeder routes connecting with the Maine Turnpike in south Portland and terminating at Tukey Bridge located north of Portland. The selected route traverses 2 separate tidal-flat areas, each approximately 1 mile in length, at the Fore River crossing and along the easterly edge of the Back Cove area.

Initial studies by the Maine State Highway Commission (MSHC) and its consultants reached the conclusion that the most feasible highway design in these areas would be earth embankments, rather than viaduct structures, with the exception of required bridge crossings at the Fore River channel and at the interchanges.

The design pavement grades range from 15 to 50 ft above the existing tidal mud flats. Underlying each of the areas are extensive deposits of soft to medium consistency, sensitive, gray silty clays to depths of 100 ft or more. Overlying the clay in tidal areas are soft, weak organic clays, with depths from 10 to 40 ft.

Embankment settlements of up to approximately 7 ft were predicted, which would normally require several years to complete. Also there were serious embankment stability problems. Therefore, it was decided that the installation of vertical sand drains would be appropriate to increase the rate of consolidation and the gain in shear strength of the soft foundation soils. The magnitude of the project indicated that ap-

Sponsored by Committee on Embankments and Earth Slopes.

proximately 2 to 3 million linear feet of sand drains would be needed to achieve the desired results.

In view of the many unknown factors and variables associated with the design of sand-drain stabilization systems and the prediction of their performance, realistic cost estimates and construction scheduling were highly indeterminate. A number of reports (1, 5) discuss the many complexities involved with the design and installation of vertical sand-drain projects. The MSHC decided that an extensive field test program to evaluate at least some of the unknowns was warranted and would provide a much more realistic basis for final project design. Because of the differences in soil profiles, 2 separate test areas at the Back Cove and the Fore River crossings were necessary to provide criteria for final design of sand drains based on in situ performance records. For this purpose, 3 methods of sand-drain installation, which had been used in construction elsewhere, were selected. The standard driven-drain method, with closed-end mandrel, was included in order to measure the probable adverse effects of soil displacement, as compared to 2 other available installation methods that had been developed to minimize displacement in soft cohesive soils. The relative effects of drain spacing were evaluated by installing each drain type at 2 different center-to-center spacings on a triangular pattern.

In addition, the MSHC gained considerable experience with respect to design and construction of embankments placed on soft organic clay soils in the presence of a tidal range of approximately 9 ft.

SITE AND SUBSURFACE SOIL CONDITIONS

The Long Creek-Fore River area is a transverse river crossing of approximately 4,200 ft between shorelines, of which all but approximately 300 ft is exposed mud flats at periods of low tide. Access for embankment construction equipment in this vicinity could be gained from either shoreline only by advancing out over completed fills.

The Back Cove area covers a distance of approximately 4,500 ft along the easterly edge of a broad tidal cove, most of which is exposed at periods of low tide. Access for embankment construction was available at several points along the shoreline from the existing parallel roadway, Marginal Way. Outboard of the proposed embankment, an existing dredged channel had to be maintained.

At each of these areas, the tidal range is approximately 4.5 ft above and below USCGS mean sea level, which is referenced here as el. 100.

The soil conditions throughout the project limits are described in MSHC reports (6, 7) based on borings and laboratory tests performed by the MSHC prior to 1967. Subsequently, additional borings were made in connection with the Back Cove test (BCT) site and the Fore River test (FRT) site and with final design.

An earlier report (8) contains a complete summary and interpretation of soil data and analyses of soil engineering properties, based on MSHC laboratory data, as well as additional testing performed by Haley and Aldrich, Inc., and at the Massachusetts Institute of Technology.

The major subsoils encountered in the project areas are given in Table 1. For convenience in referencing, they are designated as layers A, B, C, and D, with subdivisions as noted.

A general soil profile across the BCT site is shown in Figure 1. Depth profiles at each of the 6 test areas within the BCT site are shown in Figure 2. Underlying the clay, layer D is considered to be a free-draining sand and gravel generally 10 to 20 ft thick, extending to the bedrock surface. During the original borings in the vicinity, artesian pressures on the order of 5 ft were encountered in this sand layer.

Typical properties of the cohesive materials at the site are given in Table 2, including the approximate compressibility factors based on a very thorough evaluation of all available test data. For layer C, the silty clay is medium to soft in consistency, only slightly precompressed, with an average liquidity index of about 1.2. The sensitivity of this material is estimated to range from 10 to 20.

General soil profiles at the FRT site are shown in Figure 3; detailed depth profiles at each of the 4 test areas within the FRT site are shown in Figure 2. At this site the

Table 1. Foundation soil types.

Layer	Soil	Description	Remarks
A	Organic clay	Medium to soft slightly organic gray silty clay with many broken shells, bits of wood chips, frequent sandy zones, and occasional peaty zones	Usually the surface layer in tidal mud-flat areas
A_s	Organic sand	Loose, slightly organic, gray silty sand with broken shells	Generally encountered at bottom of layer A at Fore River
B	Stiff clay crust	Medium to very stiff, weathered, gray or brown silty clay with occasional sand layers	Often forms the crust of layer C
C	Gray silty clay with black specks	Gray silty clay with black specks or bands and occasional shells; medium to soft and very sensitive at Back Cove, and medium to stiff at Fore River	Illitic marine clay that has been leached
C′ or C″	Varved clay with black bands	Same as above, with lenses to alternate layers of silt or sand or both; soil frequently becomes more varved or more sandy or both with depth	Frequently forms the lower portion of layer C
C_s	Silty sand	Loose to dense gray silty sand (usually poorly defined)	Sometimes encountered at top of layer C at Fore River
D	Silty sand and gravel	Medium to loose gray silty sand and gravel, with artesian water pressure	Generally overlies bedrock; free draining

Figure 1. Back Cove test section.

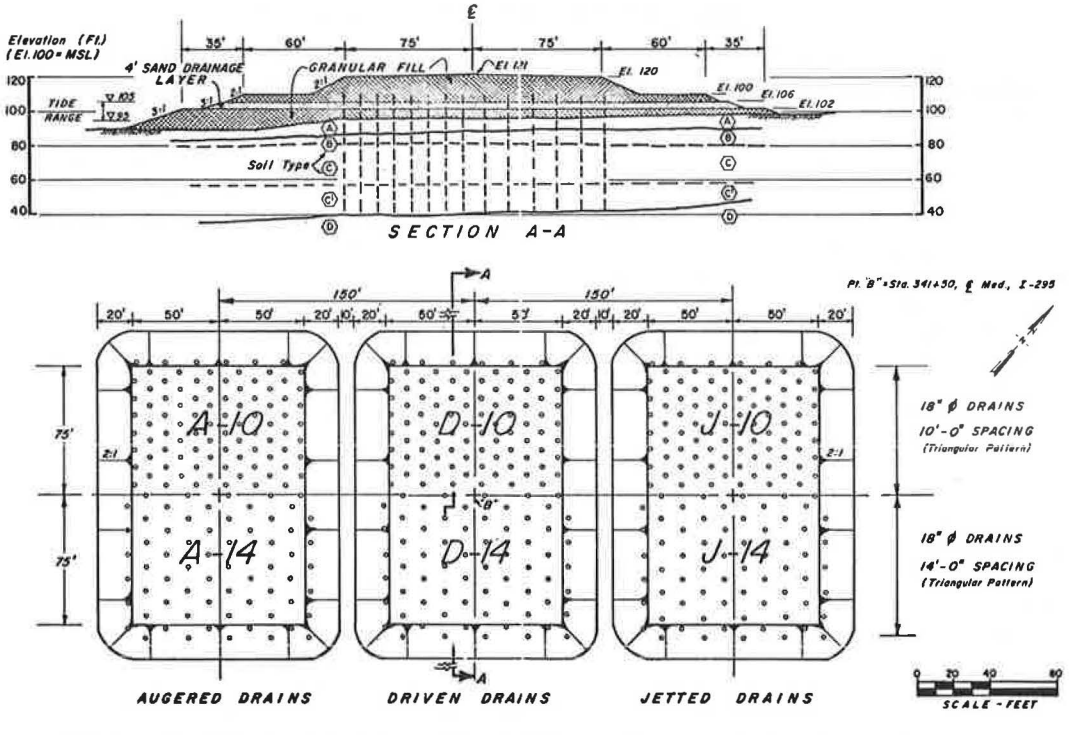

organic clay is underlain by granular soil (layer D) approximately 20 ft in thickness, extending to probable bedrock surface at approximately el. 50.

Summarized soil properties and compressibility values are given in Table 2. The organic clay (layer A) is slightly precompressed. The Atterberg limits fall close to the A-line on the plasticity chart, with the plasticity index averaging about 34 percent; the liquidity index is usually very near unity. The sensitivity of this material is on the order of 5 to 10. Ladd, Aldrich, and Johnson (10) give further information on the strength and stress history characteristics of this soil.

DESIGN OF TEST SECTIONS

The selection of suitable sites for the 2 test sections included the following general considerations: (a) They should be within the limits of future highway construction in order to salvage the fills and sand drains after completion of the tests; (b) the subsoil conditions should be representative of a major portion of each project area; (c) the subsoil conditions within the test areas must be reasonably uniform for purposes of the controlled tests; and (d) the sites must be readily accessible from the shore and be within property limits that the MSHC could gain rights to at the time.

Specific considerations at each site selected were as follows:

1. At the BCT site, the outer limits of fill were restricted in part by the existing channel, the inboard side was designed to maintain an existing storm sewer discharge, and the center of the fill area was located to coincide with the centerline of the I-295 median; and
2. At the FRT site, it would have been too costly to place the fill in the river proper, and, therefore, it was necessary to locate within the Long Creek area where space was limited by the presence of an important pipeline crossing, which could have been damaged by the fill construction (the test area was subdivided into 4 sections rather than 6 as at BCT).

A supplementary benefit realized from the test project was to be gained in the selection of suitable earthwork materials for the embankments and development of feasible methods of placement. There was a degree of uncertainty regarding difficulties that might be encountered in the placement of fills out over the existing soft organic clay (mud flats)—coping with a tidal range of approximately 9 ft, losses of material due to erosion, fill stability, trafficability of construction equipment, and other related problems.

Granular borrow for underwater fill and for embankment fill were specified in accordance with general MSHC standards for such materials, for which a wide gradation range is acceptable.

A uniform, 4-ft thick sand-drainage layer was specified to be placed above el. 102. to provide unrestricted drainage. Material of the same gradation was also specified for the sand-drain backfill (free-draining sand with less than 2 percent passing a No. 200 sieve).

The horizontal drainage layer was placed at the lowest practical level for efficiency. Therefore, it was necessary to penetrate this layer completely with the drains, which were installed from a stable working level at el. 110 (BCT) and el. 108 (FRT).

Back Cove Test Site

The 3-section fill area, as shown in Figure 1, was designed to provide for testing of 3 types of drains. Alternate layouts that might have achieved better symmetry were considered but ruled out because of variations in subsoil conditions, existing channel, property limits, and budget. Although there are some variations in soil profiles beneath each area, they were carefully observed and accounted for in the analyses. The theoretical stress distribution below each surcharge fill is such that the overlapping effects are minimal, and reasonably uniform stress conditions apply for each of the 6 areas.

The dimensions of the initial stage of fill, which was placed to el. 110, is 520 by 270 ft. At this level the sand drains were installed. Each sand-drain area was subse-

Figure 2. Soil profiles and instrument locations at test sections.

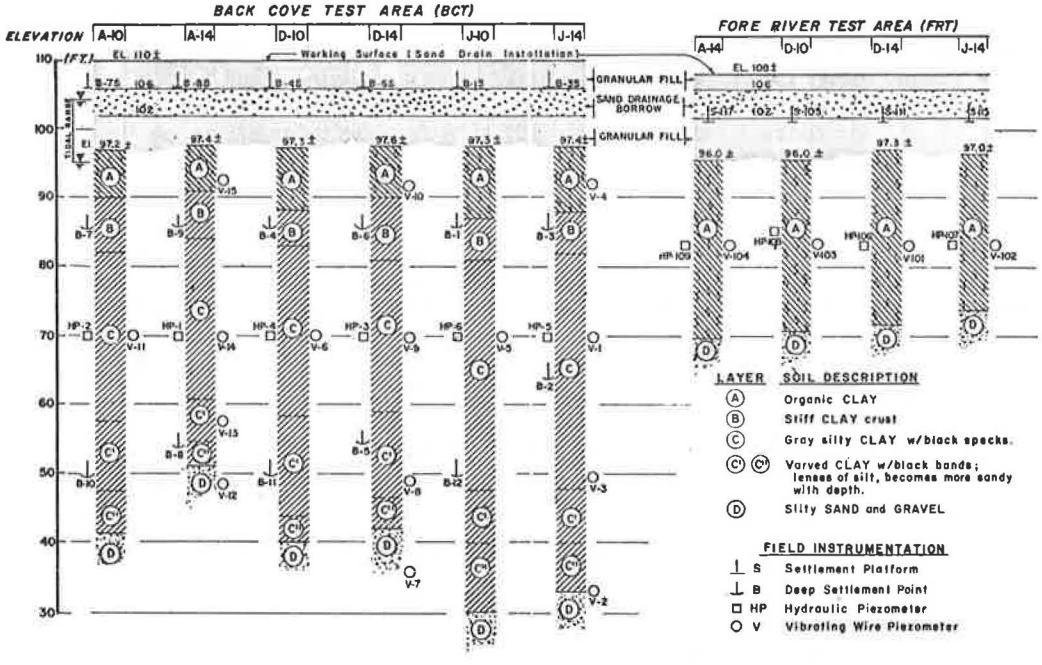

Table 2. Properties of cohesive foundation soils.

Layer	Site	Natural Water Content (percent)	Atterberg Limits W_L	Atterberg Limits PI	Specific Gravity	Total Unit Weight (pcf)	Average Field Vane Strength (psf)	Approximate Sensitivity	One-Dimensional Consolidation CR[a]	One-Dimensional Consolidation CR[b]	One-Dimensional Consolidation RR[c]	Stress History
A	BCT	—	—	—	2.66	102.5	400 ± 100	5 to 10	0.22	0.25	0.022	Slightly precompressed
	FRT	65 ± 15	65 ± 15	34 ± 12	2.66	101	600 ± 100	5 to 10	0.24	0.25	0.022	Slightly precompressed
B	BCT and FRT	—	45 ± 5	22 ± 3	2.78	118	Over 2,000	—	—	—	0.020	Very highly precompressed
C and C′	BCT	47 ± 7	44 ± 5	20 ± 4	2.78	111	650 ± 150	10 to 20	0.24	0.28	0.020	Slightly precompressed
	FRT	40 ± 15	42 ± 7	20 ± 4	2.78	115	1,500 ± 500	10 to 20	0.21	0.25	0.022	Moderately precompressed
C″	BCT	—	—	—	2.78	115	—	—	0.20	0.20	0.020	Slightly precompressed

[a]Virgin compression ratio = $C_c/1 + e_o$ measured from odometer tests.
[b]Virgin compression ratio value, modified for use in analyses, to account for sample disturbance or 3-dimensional effects or both.
[c]Recompression ratio = $C_r/1 + e_o$, taken along the rebound curve; this may be low, and values of RR as high as 0.05 ± 0.02 should be considered.

quently surcharged by 10 ft of additional fill, placed in 3 separate pads measuring 100 by 150 ft each. The center of each pad was crowned to 1 ft higher for purposes of drainage and to allow for "dishing" with settlement. A 60-ft wide berm extends in all directions beyond the sand-drain test areas for stability and vehicle access.

Fore River Test Site

At the FRT site, space and budget limitations restricted the size of the test area. Figure 3 shows that a square fill area permitted the installation of drains in 4 quadrants for symmetry. The location was further restricted by the presence of existing 12- and 18-in. oil pipelines buried in the soft tidal flats. These could not be disturbed until such time as a stabilized alternate crossing route was prepared.

The design dimensions of the initial fill to el. 110 were approximately 240 by 240 ft, and the limits of an additional 10-ft surcharge fill were 120 by 120 ft, which was subdivided equally into 4 test sections. A 40-ft wide level berm extends around the perimeter for stability and access.

VERTICAL SAND DRAINS

In view of budget limitations, the scope of this program included only those factors that could be more readily observed and be of most direct benefit to this particular project. The test program included the following considerations:

1. A comparison of various drain diameters was not attempted (in this case, all drains were to be 18 in., a size that is commonly used in the United States);
2. A triangular pattern of drain layout was assumed to be most efficient, based on theoretical considerations (3);
3. Maximum and minimum center-to-center drain spacings of 14 and 10 ft respectively were selected to "bracket" the probable range in final design, with the anticipation that performance for intermediate spacings could be interpolated from the field results;
4. Methods of installation were limited to 3 types, each type to utilize equipment and procedures generally accepted and used elsewhere on previous work;
5. Generally accepted gradation requirements for sand backfill materials were adopted; and
6. Rate and magnitude of consolidation of the compressible soils and pore pressure dissipation were observed by field instrumentation (as necessary).

Selection of the 3 drain types was based on several considerations.

The driven with closed-end mandrel method was included because it was the most commonly used in the past (2) and was generally found to be the least expensive to install. However, there was serious doubt as to the effectiveness of this method in soft, sensitive soils, for the disturbance associated with installation would probably increase total settlements and reduce in situ shear strengths where potential stability problems exist (1). This method was included, therefore, to provide a measure of comparison.

Of the several methods utilizing jetting procedures available in 1967, the jetted with open-end mandrel method, which had been in use for several years, deserved consideration. It was believed that there would be essentially no lateral displacement of in situ soils during installation because all soil is theoretically cut and removed by internal jetting action within the casing.

The augered with continuous hollow shaft auger method, which had been developed and patented in recent years (11), was considered by many to satisfy the requirements of a "nondisplacement" installation method. There were specific problems at this site to be evaluated such as the difficulties in augering through 10 to 15 ft of granular fill, the penetration of a stiff clay crust at Back Cove, and possible equipment limitations when advancing to depths of approximately 80 ft.

CONSTRUCTION OF TEST SECTIONS

A contract for construction of the embankment stabilization test project was awarded by the MSHC in April 1967. The placement of underwater fill started initially at the BCT site during April and at the FRT site in May. The fill was brought up to working

level for installation of sand drains by July 1967. The settlement platforms, deep settlement points, and piezometers (vibrating wire type) were installed as soon as possible. The platforms were placed by the contractor, and observation readings were taken by MSHC personnel. All other instrumentation was installed and observed by commission personnel. The vertical sand drains were installed after filling had been brought to a stable working level (el. 110 at BCT and el. 108 at FRT). The augered and jetted drains were installed in both areas during July and August, and the driven drains were placed during September and October 1967. The placement of the remainder of the test embankment fills proceeded thereafter and was essentially completed by late November 1967.

Augered Drains

A design total of 183 augered sand drains were installed by the contractor (11). The 18-in. diameter hollow-stem auger was advanced to the required depths by lowering the assembly under its own weight while being rotated by the electric drive motor through the assembly at the top of the shaft. A guide, close to the base of the leads, controlled plumbness. In general, the rate of advance was controlled at approximately 1 pitch length per revolution. However, at the BCT site, the auger often met high resistance in the stiff clay crust, resulting in slower penetration rates; at the FRT site, faster rates occurred in the soft organic clay soils. When the maximum depth was reached, the shaft was given one complete revolution in the reverse direction. The specified sand backfill was placed from a loading skip, filling the 8-in. inside diameter hollow stem and the feed tank at the top. With air pressure (up to 75 psi) applied to the internal system, the unit was pulled out of the ground without further rotation. Sand was expelled through the bottom of the shaft as the steel cover plate fell free of the end.

Driven Drains

A design total of 235 driven drains were installed by the contractor. The 16-in. OD mandrel, with an 18-in. built-up end section, was driven by means of an air-operated McKiernan-Terry Model 11-B-3 hammer (rated energy = 19,000 ft-lb). Plumbness was maintained by guides attached to fixed leads. The initial penetration through the sand fill proved to be very difficult. At the BCT site, it was found necessary to assist the penetration of the mandrel by means of portable jet pipes. Also, the contractor experimented by using a vibratory hammer for the last 12 drains but with limited success. Upon advancing to maximum depth, the mandrel was filled with specified sand by means of a skip that traveled up the leads. Air pressure, up to 100 psi, was applied, and the mandrel was extracted. By trial, the most suitable air pressures for various depths were determined.

Jetted Drains

A design total of 183 jetted sand drains were installed by a subcontractor. The top of the 18-in. OD casing was suspended from a bridle and cable arrangement attached to the crane rig (without guides near the bottom). The "holepuncher" consisted of a 12-in. OD internal jetting pipe, fitted with connections for water hoses at the upper end, which could be lifted independently within the outer casing. Its travel with respect to the casing was limited by a built-up flange that would stop against the built-up driving head at the top of the casing. Thus, the length of the internal pipe determined the penetration depth of the holepuncher with respect to the outer casing. Generally, the pipe was maintained approximately 12 in. short of the casing tip. The holepuncher was raised and lowered such that the whole assembly penetrated the soil by the combined washing and chopping action. When the holepuncher had advanced to full depth, the flow of water continued until solid materials within the casing were removed and the amount of suspended solids in the wash water was acceptable (2 percent specified). The holepuncher assembly was then removed, and the casing was backfilled with specified sand, through the water, whereupon the casing was pulled and the drain was completed.

INSTRUMENTS AND FIELD MEASUREMENTS

A major design objective had been the creation of essentially similar soil stress conditions below the interior portions of the surcharge fill at each of the 6 sand-drain test areas at the BCT site and at each of the 4 quadrants at the FRT site so that drain performance could be evaluated. Therefore, the major concentration of instrumentation was within and below the central portion of each of these areas. Figure 2 shows the location and identification of instrumentation.

Settlement measurements were obtained at original ground surface by means of standard settlement platforms (SP) and at intermediate depths (to obtain relative consolidation within layers A and C) by means of deep settlement points (DSP). For the latter, Borros points were used (modification of anchor posts, manufactured by the Borros Company, Ltd., Sweden). All piezometers (vibrating wire type supplied by Geonor, Ltd.) were located as closely as possible to the midpoint of the equilateral triangle formed by 3 adjacent sand drains. Observations at the BCT site were made at middepth in soils of layers A, C, and D, whereas at the FRT site they were required only within layer A. For purposes of comparison and supplementary data, a number of porous-tube hydraulic piezometers were also installed.

All measurements were made and recorded by MSHC field personnel.

EVALUATION OF PERFORMANCE OF TEST SECTIONS

Analysis of Field Data

To evaluate the field results, we realized that direct comparative plots of settlement versus time for each test group would not be sufficient because the depth of compressible soils varied at each section, and the method of drain installation might have affected the rate and amount of consolidation settlement. Therefore, the following approach was adopted.

1. After the observed settlement curves were adjusted for possible instrument errors, for movements due to soil heave, and for initial settlements due to undrained shear, semilog plots of consolidation settlement versus time were prepared. Because the soil thicknesses for each area varied, the data were then replotted in terms of percentage of vertical strain versus time. However, these plots indicated that primary settlement was not complete (as of November 1969); therefore, it was necessary to predict the magnitudes of final consolidation settlements, from which the estimated average degree of consolidation, U percent, was plotted for each test area. Also, semilog plots of the excess pore-pressure ratio, u/u_o, versus time were prepared. From either of these 2 plots, backfigured values of c_h were computed.
2. The cost of a sand-drain installation is strongly influenced by the adopted design value of the coefficient of consolidation, c_h. Therefore, relative "efficiencies" of the sand-drain test groups at the BCT and FRT sites were compared on the basis of the resultant backfigured values of c_h. These values serve as a basis for determining expected rates of settlement for each group, whereas the ratios of the backfigured field values to the laboratory values, determined for relatively undisturbed soil samples, serve as a basis for evaluating the apparent degree of disturbance that might have taken place in the field.
3. Another important consideration is the effect of the particular type of drain installation on the final total amount of consolidation settlement, for soils that are disturbed or remolded in situ become more compressible.
4. To arrive at meaningful conclusions with respect to the relative or absolute performance of the sand drains required that a considerable amount of judgment be applied to the analysis of the field data. This was largely attributed to the following: (a) The primary consolidation of the compressible soils (layer C at the BCT site and layer A at the FRT site) was not complete as of November 1969 (approximately 2 years after completion of surcharging), and (b) the observed pore-pressure readings were quite erratic, especially at the BCT site. Therefore, the conclusions presented here were not based entirely on factual observations inasmuch as it was necessary to adopt

Figure 3. Fore River test section.

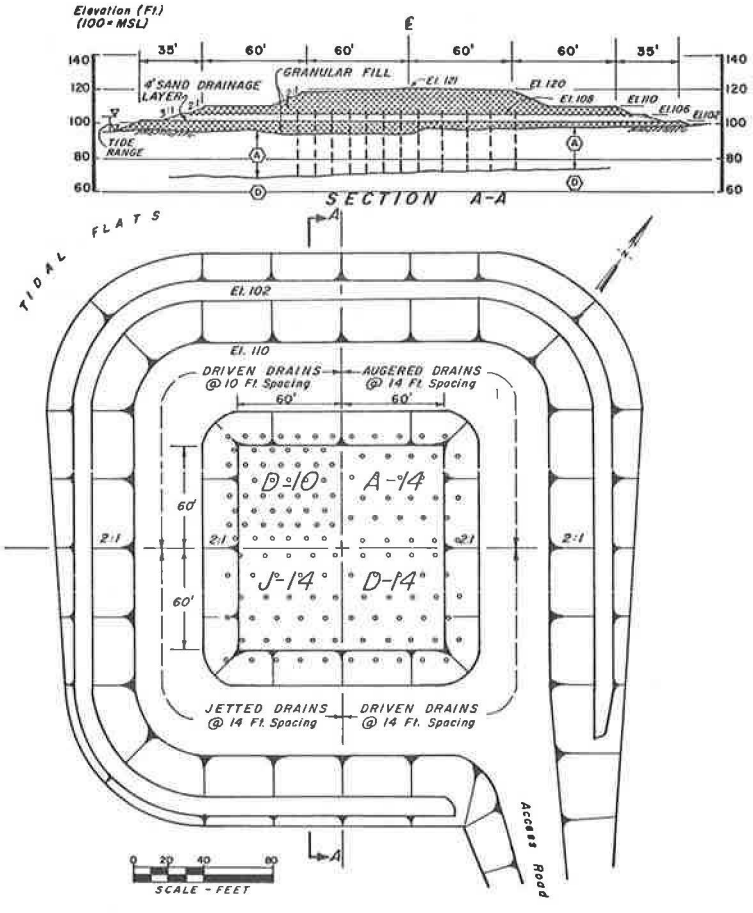

Table 3. Summary of results.

Site	Sand-Drain Installation Method	Sand-Drain Spacing (ft)	Coefficient of Consolidation: Backfigured From Field Tests (ft^2/day)	Coefficient of Consolidation: Field: Laboratory	Predicted Total Primary Consolidation: Laboratory Tests (ft)	Predicted Total Primary Consolidation: Field Data[a] (ft)	Predicted Total Primary Consolidation: Field: Laboratory
BCT	Driven	10	0.040	0.27[b]	1.89[c]	2.95[c]	1.56
		14	0.040	0.27	1.58	3.53	2.23
	Augered	10	0.080	0.53	1.86	1.70	0.91
		14	0.100	0.67	1.63	1.86	1.14
	Jetted	10	0.065	0.43	1.84	2.84	1.54
		14	0.085	0.57	0.97	1.97	2.03
FRT	Driven	10	0.030	0.38[d]	3.0	4.0	1.33
		14	0.055	0.69	3.0	4.0	1.33
	Augered	14	0.065	0.81	3.2	3.7	1.15
	Jetted	14	0.065	0.81	2.7	3.2	1.18

[a]Predicted from field data as of Nov. 1969 (primary settlement not complete).
[b]Average value adopted from laboratory odometer tests, $c_h = 0.15 \pm 0.07$ ft^2/day.
[c]For layer C, between shallow and deep settlement points.
[d]Average value adopted from laboratory odometer tests, $c_h = 0.08 \pm 0.04$ ft^2/day.

many assumptions during the course of these analyses. Where feasible, averaging methods were employed to minimize the effect of any erroneous assumptions. A complete report on the test project is contained in another publication (9).

Principal Field Results

The predicted and field-measured results of major significance for each test area are given in Table 3.

For the BCT section, the principal results are as follows.

1. All 3 drain types caused a significant reduction in the effective values of c_h. The augered and jetted types were, however, relatively more efficient than the driven type by a factor of 1.5 to 2.5.
2. For the augered and jetted drains, the closer spacing (10 ft on center) resulted in 20 to 25 percent lower values of c_h than the larger spacing (14 ft); for the driven drains, no appreciable difference was indicated.
3. The magnitudes of the predicted total final field consolidation settlements for the areas of driven drains were 1.5 to 2.2 times greater than values predicted from laboratory tests. The jetted areas also showed a considerable increase, whereas the augered areas agreed within approximately 15 percent.

For the FRT section, the principal results are as follows.

1. All 3 drain types caused a reduction of the effective values of c_h but not so large as for the soils at the BCT site. The driven type was definitely less efficient than the other types at equivalent 14-ft spacing.
2. For the driven drains, the closer spacing (10 ft) resulted in a further reduction of c_h of approximately 45 percent. (The spacing effect was not tested for the other 2 drain types.)
3. The magnitudes of the predicted total final field consolidation settlements for driven drains were 1.3 times greater than values predicted from laboratory tests. The augered and jetted types had closer agreement, within 15 to 20 percent.

PRINCIPAL CONCLUSIONS

1. The method of installation is very important in the very sensitive (S_t = 10 to 20), slightly layered, inorganic clay (layer C, BCT site). In spite of the relatively smaller soil displacements associated with the augered and jetted methods of installation used here, the effective backfigured in situ coefficient of consolidation for radial drainage, c_h, was only 45 to 65 percent of the value based on laboratory tests. An even further reduction was observed for driven drains.
2. The method of installation is not quite so important for the soft, less sensitive (S_t = 5 to 10), slightly organic clay (layer A, FRT site). The driven drains did show, however, that there are significant reductions in c_h with closer drain spacing.
3. These tests clearly indicate that further improvements in the methods of sand-drain installation are needed to increase the relative efficiencies in sand-drain performance. Some of the anticipated advantages or benefits would be in terms of (a) further reduction in sand-drain footage requirements, (b) reduction in time required to achieve desired consolidation, and (c) reduction in the magnitude of total vertical settlement in treated areas.

RECOMMENDED GUIDELINES FOR FUTURE FIELD TEST PROGRAMS

There are many obvious benefits in the performance of a full-scale field test and evaluation program. In this way, realistic design parameters can be observed and measured. Based on the experiences gained from this project, the following comments and guidelines are offered:

1. Select test locations at which subsoil conditions are known to be typical of the major portions of the anticipated project;
2. Make very detailed studies of the soils directly below the test area (include a number of laboratory tests to determine compressibility, stress history, permeability,

and sensitivity and to determine by an adequate number of borings and field tests the limits and possible variations in soil strata, field vane shear strength, field permeability, and existing hydrostatic conditions);

3. Make conservative estimates of time required to achieve primary consolidation and establish a time schedule to permit this and to allow for contingencies (it is extremely difficult to evaluate results unless primary consolidation is completed in the field);

4. Select a drain type or types that appear to promise a minimum of soil disturbance if the soils are sensitive (in any event, include, for comparison, an area of driven drains and also include, if possible, a fully instrumented nondrain area for comparison of pore pressure and strain settlement behavior under similar loading conditions);

5. Include sufficient field instrumentation to provide reliable piezometric and settlement data throughout the anticipated time period (careful attention must be given to accurate location of instruments with respect to drain locations, installation of instruments at several depths within the compressible layer, and provision of an adequate number of duplicate instruments, particularly piezometers, to serve as backup units in case of malfunction);

6. Install sufficient settlement units at an early stage of filling to record initial strain and early consolidation movements prior to, and immediately after, drain installation; and

7. Install the various types of sand drains within as short a time period as possible and apply the surcharge load as uniformly and rapidly as possible thereafter to minimize the effects of time delays and to provide a reasonable basis for comparative performance of drain types.

ACKNOWLEDGMENTS

The authors wish to commend the Maine State Highway Commission and the Federal Highway Administration for their foresightedness in planning and sponsoring the project described here. We gratefully acknowledge and appreciate the outstanding cooperation and assistance provided by commission personnel throughout the many difficult phases of the project, especially the following: David Stevens, Martin Rissel, David Ober, William Harris, Walter Hendrickson, Frederick Boyce, Melvin Morgan, Kenneth Dinsmore, and John Hodgkins. We would also like to commend the general contractor, W. H. Hinman Company, and the subcontractors for their efforts and especially their willingness to seek improvements and modifications in sand-drain installation procedures for the benefit of the test project. A major portion of the analyses and interpretation of field data required for this work was performed by Charles Ladd, Massachusetts Institute of Technology, who served as a consultant to Haley and Aldrich, Inc.

REFERENCES

1. Casagrande, L., and Poulos, S. On the Effectiveness of Sand Drains. Canadian Geotechnical Jour., Vol. 6, No. 3, 1969.
2. Johnson, S. J. Foundation Precompression With Vertical Sand Drains. Jour. Soil Mech. and Found. Div., Proc. ASCE, Vol. 96, No. SM1, 1970.
3. Study of Deep Soil Stabilization by Vertical Sand Drains. Moran, Proctor, Mueser and Rutledge, 1958.
4. Moore, L. H. Summary of Treatments for Highway Embankments on Soft Foundations. Highway Research Record 133, 1966, pp. 45-59.
5. Weber, W. G., Jr. Experimental Sand Drain Fill at Napa River. Highway Research Record 133, 1966, pp. 23-44.
6. Subsurface Investigation for the Proposed Construction of I-295 in the Back Cove Area, Portland, Cumberland County. Maine State Highway Commission, Jan. 1967.
7. Subsurface Investigation for Proposed Construction of I-295, Long Creek Interchange and Fore River in the Cities of South Portland and Portland, Cumberland County. Maine State Highway Commission, June 1967.
8. Engineering Properties of Foundation Soils at Long Creek-Fore River Areas and Back Cove. Haley and Aldrich, Inc., Rept. 1, Oct. 1969.

9. Test Sections to Evaluate Field Performance of Vertical Sand Drains. Haley and Aldrich, Inc., Rept. 2, Jan. 1970.
10. Ladd, C. C., Aldrich, H. P., Jr., and Johnson, E. G. Embankment Failure on Organic Clay. Proc., 7th Internat. Conf. on Soil Mech. and Found. Eng., Mexico, Vol. 2, 1969, pp. 627-634.
11. Landau, R. E. Method of Installation as a Factor in Sand Drain Stabilization Design. Highway Research Record 133, 1966, pp. 75-97.

DISCUSSION

Richard E. Landau, West Hempstead, New York

As an interested party (consultant to Haley and Aldrich, Inc., for review of test section plans for Back Cove and holder of U. S. Patent 3096622 and others for sand-drain installation by means of augers) to the investigation of the performance of sand drains installed by the mandrel, jetting, and auger methods, the writer was disappointed at the inability of the authors to reach substantive conclusions.

It is the opinion of the writer that the inability of the authors to develop more cogent results relates to their questionable use of laboratory-derived c_h values, which have a range (Table 3) varying by 300 percent for each soil type involved, e.g., from 0.08 to 0.22 ft^2/day at Back Cove and from 0.04 to 0.12 ft^2/day at Fore River. The use of an "average" value of c_h in each instance as a common denominator for backfigured field values developed for each method of sand-drain installation (in order to produce a comparative measure of field performance of each method) results in numerical values having no significance. Considering that the mandrel method of installation has the characteristic of 100 percent displacement of the subsoil in the cavity formation process, the writer has developed data given in Table 4 to show the effectiveness of each method of sand-drain installation using the c_h values obtained from the mandrel-stabilized areas as the basis for comparison. It is evident from this presentation that the most effective method of sand-drain installation is consistently the auger method.

Inasmuch as subsoil disturbance results in altering the consolidation characteristics of subsoil in a manner that increases the magnitude of settlement as compared to that obtained for undisturbed soil, the ratio of field to theoretical settlement given by the authors in Table 3 is given again in Table 5.

A review of the settlement ratios given in Table 5 indicates that the auger method of sand-drain installation produces the least disturbance of the 3 methods tested. Fur-

Table 4. Sand-drain effectiveness.

Site	Soil	Sand-Drain Spacing (f)	Effectiveness Ratio of Method[a] ($c_h/c_{h,\ mandrel}$)		
			Mandrel	Jetting	Auger
BCT	Silty clay	10	1.0	1.6	2.0
BCT	Silty clay	14	1.0	2.1	2.5
FRT	Organic clay	14	1.0	1.2	1.2

[a]The greater the effectiveness ratio is, the greater is the efficiency of the sand-drain installation method. The increase in efficiency with an increase in sand-drain spacing is to be expected (11).

Table 5. Settlement ratio.

Site	Soil	Sand-Drain Spacing (ft)	Settlement Ratio of Method[a] (field value/theoretical)		
			Mandrel	Jetting	Auger
BCT	Silty clay	10	1.56	1.54	0.91
BCT	Silty clay	14	2.23	2.03	1.14
FRT	Organic clay	14	1.33	1.18	1.15

[a]The lower the settlement ratio is, the less is the disturbance induced by the sand-drain installation method (11, pp. 82ff).

thermore, the range of results in the field for the auger method varies from the theoretical by a consistent value of approximately 15 percent, while the settlement ratio results obtained by both the jetting and mandrel methods are inconsistent and range up to 100 percent or more in excess of theoretical. The indications that the mandrel method shows its best results when applied to the stabilization of organic clay at the FRT site cannot be taken as an indication that displacement methods are best applied in such soil types, for this is contrary to the results obtained for the mandrel method as applied to the organic clay of Flushing Meadows in New York (11, p. 85). In contrast to this, the relatively mediocre results obtained at the FRT site for the nondisplacement methods are believed to be related to the fact that the specifications applied for the test installations did not provide for close control of the axial deviation of the cavity-forming apparatus during the sand-drain installation process. Such control is considered essential, particularly when applied to soft soils, as was encountered at Fore River, which is in contrast to the stiffer soils encountered at Back Cove. Since the construction of the test section, the criterion evolved for such control requires that the axis of the cavity-forming apparatus be maintained within a tolerance of 1 in. in 15 ft at all times during the sand-drain installation process. More effective results can be expected by requiring that the apparatus be guided at its upper end and at a point within 10 ft of the ground surface during at least the first 25 ft of penetration of the apparatus into the subsoil.

Although the writer concurs with the authors that additional test sections would be desirable to establish sand-drain design criteria throughout the country, the guidelines for such work as presented by the authors are considered to be much too general for implementation by interested agencies. In this vein, it may be of interest to the reader to know that the HRB Committee on Embankments and Earth Slopes is sponsoring the development of a formal approach to the design and testing of sand-drain installations in an effort to fill this need.

AUTHORS' CLOSURE

Landau candidly admits that he is an "interested party" in view of his direct beneficial interest in promoting the use of the hollow-stem auger method of drain installation.

The authors emphasize that this test program was planned, executed, and evaluated on a strictly impartial basis. The objective of this work was to establish realistic performance data for specific application to the design of the planned sand-drain installation rather than to serve as a "proving ground" for the selection of the most superior type of drain. It was demonstrated that this field test program was fully justified, for the design criteria that probably would have been adopted on the basis of previously available laboratory odometer test data alone would not have been adequate (i.e., the desired soil stabilization would not have been achieved within the available construction time limits).

As stated in the paper, each of 3 types of sand drains were installed at 2 spacings, and their performances were observed in terms of the settlement achieved and the pore-pressure dissipation within the compressible soil layers. The observation and evaluation of these data might have been relatively straightforward, except that a number of complicating factors and conditions had to be considered in the analysis of the results. Some of these are discussed below.

1. The time available (2.5 years) was insufficient to achieve completion of "primary" consolidation for the drain spacings selected.
2. Therefore, the backfigured values of the coefficient of consolidation, c_h, based on settlement data, had to be based on estimated degrees of consolidation for each test area as best interpreted from available pore-pressure and settlement data.
3. The pore-pressure data were influenced by the initial pore pressures developed during drain installation (including the augered type, which produced excess heads up to 7 ft at the BCT site). It is difficult to handle this situation adequately from a theoretical viewpoint.

4. The pore-pressure data were, or could have been, influenced by the relative positions of piezometers with respect to the centerline between adjacent drains, inherent instrument errors, and potential long-term deterioration of instrument accuracy after several feet of settlement occurred.

5. The settlement data were generally considered to be reliable, but considerable judgment was required to take into account the influence of lateral movements due to shear deformations that occurred during initial fill placement and movements associated with the installation of the drains per se, such as the heave that occurred with the driven drains.

6. A major problem arose from the fact that in several instances the total measured settlements within given increments of soil depth actually exceeded the magnitudes anticipated from theoretical predictions based on laboratory data. Plots of percentage of strain versus log time generally yielded essentially straight lines, even after nearly 2.5 years since the middle of the loading period, which strongly suggested that primary consolidation was not yet completed. The piezometers also generally showed that significant excess pore pressure still existed after 2.5 years. Therefore, considerable judgment had to be used to develop "predictions" of the final consolidation settlements, especially at the BCT site because of the sensitive nature of the clay. At the BCT site, these predictions were made as follows: (a) Plots of percentage of strain versus the average effective stress (to a log scale) were developed based on the average degree of consolidation from measured piezometer data between the deep settlement points; and (b) these plots were then extrapolated, assuming a linear relation between strain and log effective stress, to the final computed effective stress that would exist after all excess pore pressures had dissipated (9, Appendix H). In many cases, these extrapolations yielded a final consolidation settlement that was 1.25 to 2.0 times the measured settlement after 2.5 years. Moreover, the shape of the "field" compression curves was sometimes contrary to that which would be expected (based on what is known about the effects of disturbance on the compression characteristics of sensitive clays). Consequently, the values of predicted total field consolidation settlements given in Table 3 are subject to considerable uncertainty in some cases.

Specific comments on Landau's statements are offered as follows.

1. The admittedly wide range of laboratory values of c_h reflected the extreme limits of all data collected. The odometer tests were performed by 3 different agencies, using samples obtained from various elevations and locations, with a variety of laboratory testing equipment and techniques. The selected values of c_h, however, took into account all of these factors, plus others such as the typical variation of c_h with applied load, to arrive at the "best" laboratory value.

2. The use of the best average laboratory value of c_h was believed to be the most logical basis for a common denominator for backfigured field values. We believe the resulting ratios do have numerical significance. They illustrate the relative degrees of efficiency among the 3 drain types (which Landau simply gives in a different format in Table 4), and, of more importance, they illustrate the relative efficiency of each drain type with respect to average laboratory values of c_h for these soils, which might have been adopted for design without the benefit of field observations. In addition, the effects of spacing can be observed for each drain type as well as the degree of disturbance for the 2 soil types.

3. It is readily agreed that the drains installed by the augered method do appear to have a somehwat higher relative efficiency than those installed by the jetted method as given in either Table 3 or Table 4. However, in view of the clearly inferior relative performance of the driven drains, the recommendation was given to the MSHC that this latter method be excluded from the specifications and the design value of c_h be based on the average field performance of the jetted and augered methods.

4. The footnote to Table 4 states that an increase in efficiency with an increase in sand-drain spacing is to be expected. This statement is contrary to theoretical relations that indicate that the "effective" c_h value for any compressible soil is independent of sand-drain spacing (if the effects of remolding in the immediate vicinity of individual drains are ignored). We believe that the increases in efficiency computed for the larger

drain spacings at the BCT site indicate that these methods did, in fact, cause some disturbance close to these drains and that the overall influence on the effective c_h value becomes less with larger spacings. Moreover, field data obtained from the Dutch "jet-bailer" method of drain installation in Portsmouth, New Hampshire, in a very sensitive clay, clearly showed no effect of drain spacing (for spacings varying from 9.0 to 16.2 ft on center with 12-in. diameter drains) on the computed in situ values of c_h (12).

5. The authors did not intend to give the impression that the driven method is given suitable than other methods in organic clay soils. The fact that the efficiency ratio was higher for all 3 drain types (at the 14-ft spacing) at the FRT site simply indicates that these organic clay soils are apparently less sensitive to the disturbance associated with drain installation at these drain spacings than the soils at the BCT site.

6. We judged the performance of the nondisplacement drains at the FRT site to be very good rather than "relatively mediocre," inasmuch as the efficiency ratio was 0.81 for both the augered and jetted methods.

7. No quantitative criteria for drain plumbness were given in the specifications for installation inasmuch as there is no practical, feasible way to measure the alignment of the in situ sand drain. It was specified, however, that the drains be located within a tolerance of 4 in. from design position at the ground surface and that the equipment be maintained in a plumb position to install "vertical" sand drains. The MSHC inspection personnel did, in fact, maintain very close checks on plumbness of the equipment during installation. The driven and augered drains were installed by using a crane with fixed leads, whereas the jetted type was not. The major reason for insisting on plumbness was, in this instance, the fact that subsequently piezometers were to be installed at locations that were supposed to be midway between adjacent drains.

8. The criterion for plumbness referred to by Landau (1 in. per 15 ft or 0.55 percent) is believed to be excessively strict and one that cannot be verified in a practical manner. Although it is certainly agreed that close tolerance with regard to plumbness is important, it is likely that there will always be an inherent random pattern of out-of-plumb drains within an overall area. That, we feel, is not nearly so important as the quality of installation of individual drains.

9. The guidelines and comments given at the end of the paper were obviously intended to be general in nature. Any specific test program would have to be developed with a great deal of study of the specific local conditions.

10. The authors are extremely pleased to learn that the HRB Committee on Embankments and Earth Slopes is sponsoring the development of a formal approach to the problem. We hope that the studies and comments presented here, plus other unpublished information that is available, will contribute in some way to such an undertaking.

Reference

12. Ladd, C. C., Rixner, J. J., and Gifford, D. G. Performance of Embankments With Sand Drains on Sensitive Clay. Jour. Soil Mech. and Found. Div., Proc. ASCE, 1972.

REVIEW OF PARTICLE-SIZE CLASSIFICATIONS OF SOILS

Gilbert L. Roderick, College of Applied Science and Engineering,
University of Wisconsin—Milwaukee

A review of particle-size classification systems for soils is made. Early systems and the evolution to systems now in use by agriculturalists, engineers, and geologists are presented. Thirty-two systems are given, and where possible the reasons for the various particle-size ranges and name designations are given. Factors considered in establishing particle-size limits include tillage properties, water retention, capillarity, root penetration, mineralogical and chemical composition, colloidal properties, specific soil usages, ease of presentation and data analysis, and method of testing. For systems commonly used at present, there is considerable variation in the size ranges assigned to the various descriptive names such as clay, silt, and sand. There is even more variation in subdivisions of major groups. Considerable compromising would be required to establish a common particle-size classification system for soils.

•SOILS consist of mineral particles that cover a wide range of sizes. It is advantageous to assign names to describe particles that lie between certain size limits. These names are convenient to use and give more information than does a mere statement that the particles lie between certain size limits.

Many systems for the particle-size limits of the various soil components have been proposed and used. However, many discrepancies exist among these systems. Thus, a certain term may designate very different materials depending on the system used.

All of the particle-size limit schemes are arbitrary because no clear-cut divisions can be made among members of a continuous series. The originators of the various systems were influenced by many factors when they made their selections. These include the field of study such as agriculture, engineering, or geology; the convenience of investigation; the methods and apparatus available for analysis; the ease of presenting data; the convenience for statistical analysis; and the previous work done and systems used.

Some of the investigators tried to place the limits to correspond with the various properties of the soil compenents; many were more interested in the ease and convenience of obtaining and presenting data.

The purpose of this paper is to review many of the systems that have been proposed and used and to present the reasons for the selection of particle-size limits, if possible. The systems are grouped according to the source of information, i.e., agricultural, engineering, or geological literature.

SYSTEMS REPORTED IN AGRICULTURAL LITERATURE

Figure 1 shows particle-size definitions reported in agricultural literature. The early European systems proposed by Wanschaffe (8), Wolf (55), Kuhn (14), and a German permanent committee for soil investigation (14) were apparently based on arbitrary selections.

In 1895 Williams (54), of Russia, presented the system, based on grain size and shape, used by Fadejeff in his lectures at the Agricultural Academic Petroffskaja. Wil-

Sponsored by Committee on Exploration and Classification of Earth Materials.

liams agreed with this system except for the earthy soil group, as shown. He called the last fraction clay because the soil owes almost all of its cohesion to this portion, the cohesion of the silts being due to organic matter present. In addition, the specific gravity of the clay fraction is less than that of the others. The transition from sand to silt results in a sudden strong increase in water retention, but the increase is even more significant when the transition is from silt to clay. The same trend is observed with permeability; sand is very permeable, silt is much less so, and clay sometimes is completely impermeable. The amount and rise of capillary water are also factors. All of the larger particles are products of physical reduction of quartz and other minerals, while clay is a product of chemical weathering.

One of the early investigators in the United States was Hilgard (23, 24, 25), who used an elutriating device to perform mechanical analyses. His particle size limits and hydraulic values are given in Table 1. The values for particle size refer to the diameters of the largest and most nearly rounded quartz grains in each sediment, the quartz grains being used as standard. Hilgard felt his hydraulic values gave a better definition. This value is the velocity of an upward current of water, in mm/sec, that will carry off a fraction of the soil, i.e., the buoyant power of an upward current of water moving under a constant and uniform velocity. With respect to the porosity of the soil on the one hand and its compactness and resistance to tillage on the other, he felt silt sediment with hydraulic value of 0.5 ($\frac{1}{36}$-mm diameter) was neutral. Therefore, portions $>\frac{1}{36}$ mm were designated as coarse materials that increase lightness and porosity of soil in proportion to percentage. The fine portion, $<\frac{1}{36}$ mm, modifies the plastic properties of the clay but also makes soil heavier in tillage than if it were absent.

In 1887 Osborne, of the Connecticut Agricultural Experiment Station (34), reported the results of a study of various mechanical analysis methods. He used purely arbitrary particle-size limits that could be conveniently determined with his optical micrometer. Sieves of 1, 0.5, and 0.25 mm were used, and elutriation and sedimentation were used for smaller particles. Other limits used for more detailed analyses were 1, 1 to 0.5, 0.5 to 0.25, 0.05 to 0.02, 0.02 to 0.01, 0.01 to 0.005, and <0.005 mm.

Early workers in the U. S. Department of Agriculture adopted most of Osborne's limits (16, 17, 31, 53). Whitney (53) placed a lower limit of 0.001 mm for clay because a soil suspension that has stood for several weeks will show particles of that size. Later the Bureau of Soils combined the 2 silt groups into 1 from 0.05 to 0.005 mm and designated clay as anything <0.005 mm (16).

In 1899 Hopkins, of the Bureau of Chemistry, U.S. Department of Agriculture (28), made a proposal for a more scientific division of soil particles. To illustrate the arbitrariness of the method being used by the Bureau of Soils, he quoted correspondence from Osborne:

> In working out the beaker method of soil analysis I employed the limits of the various grades with reference simply to convenience in using my eyepiece micrometer. I have always thought that the limits of the various grades should be determined by a careful consideration of the various conditions involved in the problem of proper mechanical analysis of a soil, and have been surprised to see that the arbitrarily chosen limits of the various grades employed by me have been followed by others in applying the method in practice.

Hopkins considered as a serious objection the fact that the ratio of the largest to the smallest particles of each division was not constant. The limits for silt were 2 times wider than those for fine sand and $2\frac{1}{2}$ times wider than those for other groups. The differences in the ratios of surfaces and volumes were even larger, yet capillarity and porosity are more closely related to these than to the diameters.

Hopkins' method assumes that there is a theoretical composition of a soil of uniform gradation within the limits of the system and that the end divisions contain the average percentage of material. He adopted a common factor of $\sqrt{10}$ (approximately 3.2) in passing from the smallest to the largest particle in all divisions of defined limits; therefore, the ratios are all constant. The system can be expanded by using $\sqrt[4]{10}$ (approximately 1.8); each of the divisions defined above will be divided into two.

Figure 1. Particle-size classifications from agricultural literature.

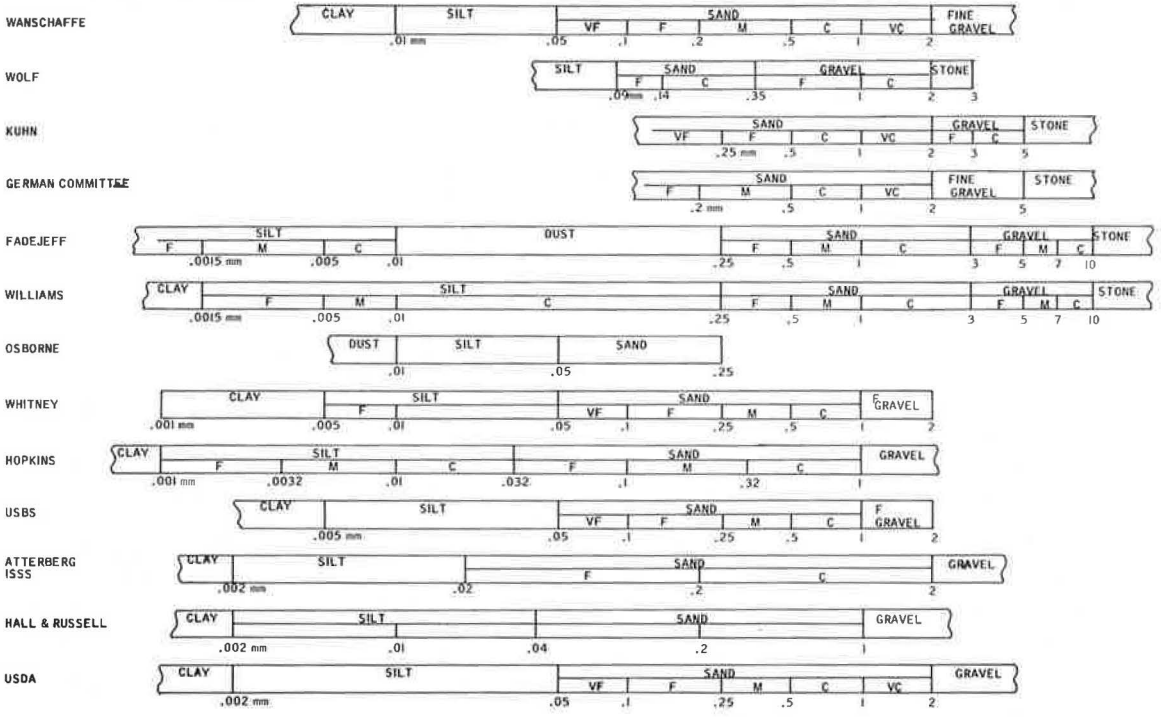

Table 1. Hilgard's hydraulic values and particle sizes for soil fractions.

Name	Hydraulic Value (mm/sec)	Size (mm)
Coarse grits	?	1 to 3
Fine grits	?	0.5 to 1
Coarse sand	64	(80 to 90) × $^{1}/_{180}$
Medium sand	32	(50 to 55) × $^{1}/_{180}$
Fine sand	16	(25 to 30) × $^{1}/_{180}$
Finest sand	8	(20 to 22) × $^{1}/_{180}$
Dust	4	(12 to 14) × $^{1}/_{180}$
Coarsest silt	2	(8 to 9 × $^{1}/_{180}$
Coarse silt	1	(6 to 7) × $^{1}/_{180}$
Medium silt	0.5	(4 to 5) × $^{1}/_{180}$
Fine silt	0.25	(2.5 to 3) × $^{1}/_{180}$
Finest silt	0.25	(0.1 to 2) × $^{1}/_{180}$
Clay	0.25	?

Extensive studies of soil properties were made in Sweden in the early part of this century by Atterberg (7, 8, 9, 10, 11, 12). He classified soil particles finer than 2 mm into 5 principal groups:

1. Large sand grains that form water-permeable sands;
2. Finer grains that form water-retaining sands;
3. Microscopic "silt" particles that form mud with rain and that display a certain cohesiveness on drying;
4. Fine particles, or semicolloids, that can be measured by a microscope and that in water show the molecular motion characteristic of colloids and are coagulated easily by acids and salt; and
5. Colloid particles that cannot be measured with a microscope.

Because the fourth and fifth groups cannot be quantitively separated, they are placed together in one group.

The particle-size limit between water-permeable and water-retaining sands is not sharp. Atterberg placed it at 0.2 mm. Sand from 0.5 to 0.2 mm diameter can retain only 30 mm of water, while sand from 0.2 to 0.1 mm can retain 110 mm of water above the capillary limit.

Atterberg placed the size limit between sand and silt at 0.02 mm for various reasons. Particles from 0.2 to 0.02 mm possess good capillarity and allow fast capillary movement of water. Materials finer than 0.02 mm show very high capillarity, but the movement of water in the capillaries is retarded. Also, 0.02 mm appears to be the upper bound for the strong coagulation of fine materials in water containing acids or salts. This particle size is also about the limiting size that can be distinguished by the naked eye. Also, the boundary for the penetration of the root hairs of grasses into interspaces between soil grains occurs at grain sizes of about 0.02 mm.

The limit between silts and clays was placed at 0.002 mm primarily because particles smaller than this exhibit strong Brownian motion when settling from a water suspension. Grains of 0.002 mm are only weakly affected; those of 0.003 mm not at all. Also, materials finer than 0.002 mm show very retarded movement of water in the capillaries.

Atterberg placed the limit between sand and gravel at 2 mm material larger than this possesses an insignificant capillarity. Stones of dimensions between 2 to 20 cm, which are moved about by wave action on beaches, he designated as pebbles. Larger stones, not rolled by waves, were called boulders.

Atterberg's main particle-size limits were, therefore, 20, 2, 0.2, 0.02, and 0.002 mm. Limits for subdivisions were set at 6 times powers of ten, for $2 \times \sqrt{10} = 6.32$ and $6.32 \times \sqrt{10} = 20$; 6.32 was rounded off to 6. These dimensions will plot as equal lengths on a logarithmic scale.

Later Atterberg felt it would be advantageous to change the limits between coarse sand and fine sand, fine sand and silt, and silt and clay from 0.2, 0.02, and 0.002 mm to 0.3, 0.03, and 0.003 mm (7, 9). The limit between water-permeable and water-retaining sands is not sharp but lies at about 0.3 or 0.2 mm. The limit between macroscopic and microscopic particles is somewhat sharper; particles of 0.04 mm can be clearly distinguished with a magnifying glass, whereas those of 0.03 can hardly be. The root hairs of plants such as peas and beans are too large to penetrate between soil particles finer than 0.03 mm, although grass root hairs are limited to 0.02 mm. He found that grains larger than 0.03 have the appearance of true sand grains and smaller ones appear as dust. Brownian movement is affected by temperature, and so the size limit is not constant but probably lies near 0.003 mm. The 0.003-mm limit is also of great physiological significance in that most bacteria cannot move between soil particles of small diameter.

The chief advantage to be found in changing the limits would be the length of time required to separate the fractions in a sediment analysis. When the fine clay was separated from silt in the sediment analysis then in use, a settling time of 8 hours was required. Changing the limit to 0.003 mm would shorten this to 4 hours. Likewise, the settling time for separation of silt from fine sand would be shortened from $7\frac{1}{2}$ to $3\frac{3}{4}$ min by changing the limits from 0.02 to 0.03 mm.

Although Atterberg was in favor of the changes, his originally defined limits gained wider usage. Later he expressed the opinion that the 0.02-mm limit was more correct than 0.03 mm for the upper limit of water-retaining sand (13).

Atterberg felt his system agreed fairly well with that proposed by Williams (54). In his opinion, the U.S. Bureau of Soils System placed too much emphasis on the macroscopic particles and not enough on the microscopic portion, the limits should go lower than 0.005 mm, and the system had far too many divisions.

In 1914 an international commission on mechanical and physical soil investigations discussed a proposal to accept Atterberg's scale as an international system (41). Hilgard felt Atterberg's limits of 2.0 to 0.2 mm for coarse sand was too extensive. He wanted coarse sand to be 2.0 to 0.5 mm, fine sand to be 0.2 to 0.02 mm, and coarse and fine silt to be <0.02 mm. In his opinion, clay has no specific diameter, but practically it must include the silts finer than 0.0016 mm. Whitney did not see how Atterberg's system was any better or worse then any other. He thought the U.S. Bureau of Soils System should be given consideration. However, most members of the commission were in favor of Atterberg's methods although a few wanted to use a different method for clay determination. Atterberg's scale was accepted as the International System.

In 1911, Hall and Russell (22) presented a system that was used in Great Britain for a number of years. The fractions, except for clay and part of the fine silt, do not represent distinct substances, so the limits are artificial, merely for convenience of discussion. Fine silt from 0.01 to 0.005 mm was considered to be of the same character as the coarser materials although the silica content is less. The finer fraction, 0.005 to 0.002 mm, has about 20 percent less silica while the alumina, ferric oxide, and potash contents increase. Clay, <0.002 mm, is a complex silicate, or a mixture of several, and is most important in determining soil fertility. It binds the soil and increases water-holding capacity, depending on the amount of clay content present. The clay possesses properties of colloids while the fine silt does not.

Atterberg's scale was adopted by the Great Britain Agricultural Education Association in 1927 (39) and was adopted as the official British method in 1928 (38); however, a modified velocity scale was used. In Atterberg's system, material with an equivalent diameter of 0.002 mm was considered to have settled from a 10-cm height of water at 20 C after a period of 8 hours; 0.02-mm equivalent diameter material settled out in 7½ min, and 0.2-mm material settled in 5 sec (40). For the modified scale, Atterberg's designation for 0.002 material was used as a base. A particle that settled 10 cm in 8 hours in water at 20 C was defined as 0.002-mm equivalent diameter, and the others were computed by Stoke's law on that basis. This gives 4 min 48 sec for 0.02 mm and 2.88 sec for 0.2 mm, although the last fraction is separated in practice by sieving. The new scale was adopted because, inasmuch as it was an international scale, it was widely used in the dominions and colonies, and uniformity in scale for the British Empire could be attained.

In the United States, conflicts in laboratory limits between silt and clay in the U.S. Bureau of Soils System and textures determined by soil surveyors in the field often occurred. In 1936, Shaw and Alexander (42) reported results of a study that they made. Soils were divided into silt 0.05 to 0.005, coarse clay 0.005 to 0.002, and fine clay or colloid <0.002 mm groups. They found that the coarse clay acted physically very like silt, and several soil surveyors classified it as silt. Chemical tests showed that the silica content of the 0.005- to 0.002-mm fraction was more closely related to the silt than to the fine clay. They recommended changing the lower limit of silt to 0.002 mm. Also, Troug, Taylor, Simonson, and Weeks (47, 48) in 1936 recommended changing the lower limit of silt from 0.005 to 0.002 mm. Clay with an upper particle-size limit of 0.002 mm is practically free of primary minerals, such as feldspars that weather easily. Certain minerals, such as quartz and muscovite, which are relatively resistant to chemical weathering, may be present in both primary and secondary form. Thus, clay less than 0.002 mm consists almost entirely of material that has great resistance to further decomposition. If separation is made at 0.005 mm, appreciable amounts of feldspar and other easily weathered minerals may be present.

In 1938, the U.S. Department of Agriculture System was adopted with the silt range from 0.05 to 0.002 mm and clay <0.002 mm (30). The other limits were the same as those in the older U.S. Bureau of Soils System. Later, in 1947, the size range from 2.0 to 1.0 mm was renamed "very coarse sand" rather than "fine gravel." Fine gravel is used for fragments from 2 mm to ½ in. in diameter (43).

SYSTEMS REPORTED IN ENGINEERING LITERATURE

Figure 2 shows particle-size definitions reported in engineering literature.

In 1925, Terzaghi (46) set forth the system that evolved to what is known as the Continental System. His system utilized part of Atterberg's and part of one presented by Ramann that was essentially the same as the one proposed by a German permanent committee (14) in 1894. Terzaghi used the latter for coarser material and Atterberg's for the finer portions. In the Continental System (19) the clay portion is reduced to one group of <0.002 mm, and particles larger than sand are defined.

In early studies of sand-clay and topsoil roads in the United States, the Bureau of Public Roads used the following definitions for various soil fractions (15, 20, 26).

Sand: That portion of the soil that passes the No. 10 sieve but is retained on the No. 200 sieve (2.0 to 0.07 mm) and that settles out of a 500-cc mixture of soil and water in 8 min. Coarse sand and fine sand were initially separated by the No. 60 sieve (0.25 mm); this was later changed to the No. 40 sieve (0.42 mm).

Silt: That portion that passes the No. 200 sieve (0.07 mm) and that settles out of the water suspension in 8 min.

Clay: That portion that passes the No. 200 sieve and remains in suspension after 8 min but that is thrown down by a centrifugal force equal to 500 g exerted for a period of ½ hour. This grain size is about 0.03 or 0.02 mm.

Suspension Clay: That portion that remains in suspension after centrifuging.

The limits given above were purely arbitrary and set because of convenience of separation by the method then being used. These early size ranges were later supplemented by the Bureau of Public Roads System as shown in Figure 2.

Hogentogler (26) gave several reasons for the system: (a) Use of the No. 40 sieve to separate coarse sand from fine sand eliminates one determination in the mechanical analysis because tests for properties of the finer portions are performed on the material that passes the No. 40 sieve; (b) with the exception of the division between coarse and fine sands, the limits correspond to those of the U.S. Bureau of Soils System, and this facilitates use of information in soil surveys made by that bureau, in which the mechanical analysis plays an important part; (c) grading by the sizes given above is accomplished as easily as grading by the former sizes was accomplished by earlier methods; and (d) each division represents a group of particles having a special significance.

The physical significance of the various size divisions were presented as follows.

Gravel is rock fragments that are usually rounded by water action and abrasion. Quartz is the principal constituent. Gravel that is only slightly worn, rough, and subangular commonly includes granite, schist, basalt, or limestone.

Coarse sand is likely to consist of the same minerals as the gravel. It is usually rounded like pebbles.

Fine sand is usually more angular than coarse sand.

Silt consists of bulky grains that are similar to fine sand except for size and have the same mineral composition. However, it may be largely a product of chemical decay rather than of rock grinding and, therefore, may consist of silicates of aluminum and alkaline earths and of oxides of iron. In other cases, the silt may be composed of foreign materials such as diatoms, pumice, or loess.

Clay is the coarser fractions that usually and mainly consist of original fragments such as quartz and feldspar. However, clay consists almost entirely of the secondary products of chemical weathering. It differs from the coarser fractions in that it is the chemically reactive portion of the soil; the coarser fractions are inert.

Colloids, in a strict sense, are only those finer clay particles that show pronounced Brownian movement when suspended in water. Some authorities place the upper limit at 0.002 mm. In tests of soils for highway purposes, colloids are considered as particles 0.001 mm in diameter and finer.

The American Society for Testing and Materials (4) and the American Association of State Highway Officials (1) originally used the same limits as used in the older Bureau of Public Roads System. Later both of these organizations (2, 5, 6) changed the limits of the coarser material to correspond to openings in standard sieves used. These include No. 4 (4.76 mm), No. 10 (2.00 mm), No. 40 (0.42 mm), and No. 200 (0.074 mm).

In 1930, Gilboy put forth a system that has gained wide engineering usage. It is commonly known as the M.I.T. System and has been adopted by the British as a standard system (33). This system was also recommended by Kopecky (18, 29) as early as 1914.

In 1947 the Civil Engineering Division of the American Society of Engineering Education presented its definitions of the various soil components (36, 45). From an engineering point of view, the primary difference between sand and gravel is the size of the grains. The primary differences between sand and silt are that particles of silt cannot be readily distinguished by the unaided eye and that silt exhibits considerable capillarity. The significant difference between silt and clay is that clay has plastic properties that silt does not. In fine-grained soils, the influence of grain size is dominated by the influence of mineralogical and chemical composition. Therefore, gravel and sand should be defined on the basis of grain size; sand and silt on the basis of grain size and capillarity; and silt and clay on the basis of plasticity.

In view of the general agreement of the systems in use, such as the International, the M.I.T., and the Public Roads, the size limit between gravel and sand was defined at the No. 10 sieve (2.0 mm). The maximum gravel size corresponds to the maximum size generally used in highway and airport engineering.

On the basis of practical engineering considerations, the limit between sand and silt was put at the No. 200 sieve (0.074 mm). The sand grains passing the No. 100 sieve and retained on the No. 200 are about the finest particles that can be easily distinguished by the unaided eye. Also, the No. 200 sieve is the practical limit of sieving in a mechanical analysis. Coarse sand has a harsh gritty feel; medium sand has a less pronounced gritty feel, but every grain can be felt; fine sand has a much softer and less gritty feel.

As the portion of silt exceeds about 10 percent of the total, capillarity becomes increasingly important. It is almost as significant in determining the properties and behavior of silts as plasticity is for clays or the lack of capillarity is for sands. Drainage and frost heaving properties of silts follow the same general patterns as capillarity. As little as 10 percent finer than the No. 200 sieve considerably impedes drainage; more than 20 percent silt makes the soil almost nondrainable.

Knowledge of a lower size limit for silt would be of great practical value because of the marked differences between silt and clay. These differences, however, are due not simply to grain size but to colloidal and other properties of clay. Silts are composed of fine mineral fragments that are altered very little from the parent material, while clay minerals are formed by chemical weathering and decomposition. There is no simple and satisfactory method for separating silt and clay because of an overlapping range of particles sizes that may or may not display properties of clay. Silt is defined as material passing the No. 200 sieve, being nonplastic, and having little or no strength when air dried. Clay-soil is material passing the No. 200 sieve, having plastic properties, and having considerable strength when air dried.

The U.S. Army Corps of Engineers and the U.S. Bureau of Reclamation use the Unified Soil Classification System based on a proposal by Casagrande (18). In this system, the grain-size limits (44) are essentially the same as those reported in ASTM Standard D422-63.

In 1957, the Highway Division Committee of ASCE (35) presented a system that corresponds closely with the old Bureau of Public Roads System. The only exception is that there are 3 rather than 2 sand subdivisions. These are defined by standard sieves, i.e., No. 10 (2 mm), No. 30 (0.6 mm), No. 80 (0.2 mm), and No. 270 (0.005 mm). Gravelly soils contain ≥15 percent gravel; sandy soils, ≥50 percent sand or gravel; silty soils, 40 to 100 percent silt size; and clays, 30 to 100 percent clay and colloids.

SYSTEMS REPORTED IN GEOLOGIC LITERATURE

Figure 3 shows particle-size definitions reported in geologic literature. Early systems were presented by Orth (52), Diller (51), Udden (50), and Keilhack (21, 52). Diller's system was later used by the New York City Aqueduct Commission with the exception that fine gravel was defined as being between 1 and 5 mm.

Udden's system (50) is a uniformly decreasing series in which each limit is $\frac{1}{2}$ the preceding one. They system was used for reporting data on wind deposits. Later, in a report on clastic sediments, Udden (49) expanded his scale upward and downward to include size ranges for coarse, medium, and fine clay; large, medium, small, and very small boulders; and very coarse gravel. In Udden's system all portions plot as equal lengths on a semilog plot.

Boswell's system (32) was used in Great Britain for studying materials used in glass industries.

In 1913, Grabau (21) took the systems of Diller and Keilhack and several variations of these to device a scale to serve as a standard for comparison.

Wentworth proposed a scale of grade and class terms for clastic sediments in 1922 (52). In fixing the limiting sizes, he was governed by 2 considerations. First, there was a growing acceptance among geologists and engineers of a series of sieves for classification in which openings of consecutive sizes were in the ratio of 2 of $\sqrt{2}$, starting with 1-mm standard. A geometrical series is ideal for the purpose, for a change of 1 in. is of the same significance and importance in the size of 10-in. cobbles as a change of $\frac{1}{10}$ in. in the size of 1-in. pebbles. The use of a geometric series makes the successive grades fall into equal units on a graph for easier reading and interpretation. Wentworth considered 2 as the most convenient ratio and 1 mm as the most convenient and logical starting point. More minute subdivisions could be obtained by using $\sqrt{2}$ or $\sqrt[4]{2}$; these fit with and form subdivisions for the fundamental power series of 2. His second consideration was to make the limits as close as possible to those commonly used by the majority of geologists. He presented the systems of Keilhack, Grabau, Orth, Diller, U.S. Bureau of Soils, Baker, Udden, and New York City Aqueduct Commission as those in common use.

Alling proposed a grade scale for sedimentary rocks in 1943 (3). He was looking for a convenient scale for use with thin sections and polished blocks; his scale is not meant for 3-dimensional studies. Alling believed a satisfactory scale should have 4 fundamental properties: (a) The grain sizes should constitute a continuous series; (b) any division of the series will be arbitrary; (c) convenience of use is a criterion; and (d) statistical analysis requires the use of a constant geometric ratio. He disagreed with Wentworth's contention that 2 was the most convenient constant ratio to use. Rather than 2, he preferred to use a constant ratio of 10. This places the limits for the major division at 0.0001, 0.001, 0.01, 0.1, 1, 10, 100, and 1,000 mm He used Hopkins' proposal of a factor of $\sqrt[4]{10}$ for expanding the system (28). This divides each major division into 4 minor ones (very fine, fine, medium, and coarse), all of which give sections of equal width when plotted on a logarithmic scale. His major divisions are colloid, clay, silt, sand, gravel, cobble, and boulder.

In 1947 a subcommittee on sediment terminology for the American Geophysical Union proposed a scale of grain sizes (37). This scale was made up after a survey of systems in use and recommendations of practicing geologists. Again, each portion plots as an equal length on a semilog plot.

NEED FOR A COMMON CLASSIFICATION SYSTEM

There are obvious advantages in having a standard particle-size limit system that would apply to all fields of endeavor. This would enable workers to use data from other sources without first translating them into their particular system.

In this author's opinion, the first step in establishing such a standard system should be to determine the basis on which the particle-size limits are to be selected. The most logical basis would be the natural properties of the soil, such as permeability, capillarity, plasticity, and mineralogical and chemical composition. The next step would be to define what is meant by the terms used to designate the various soil fractions.

Figure 2. Particle-size classifications from engineering literature.

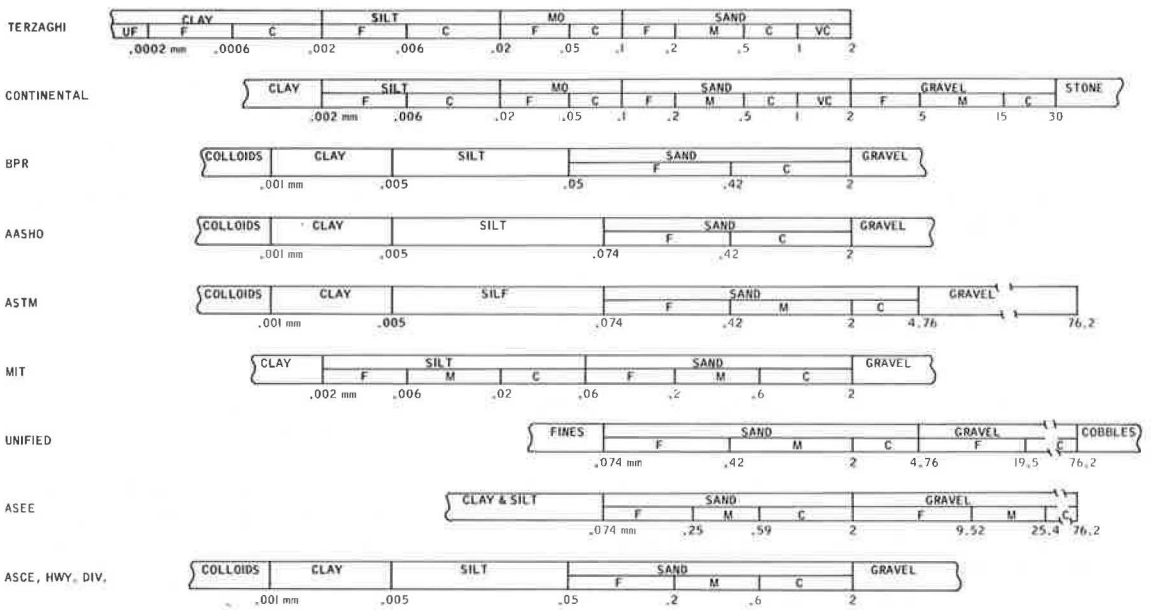

Figure 3. Particle-size classifications from geologic literature.

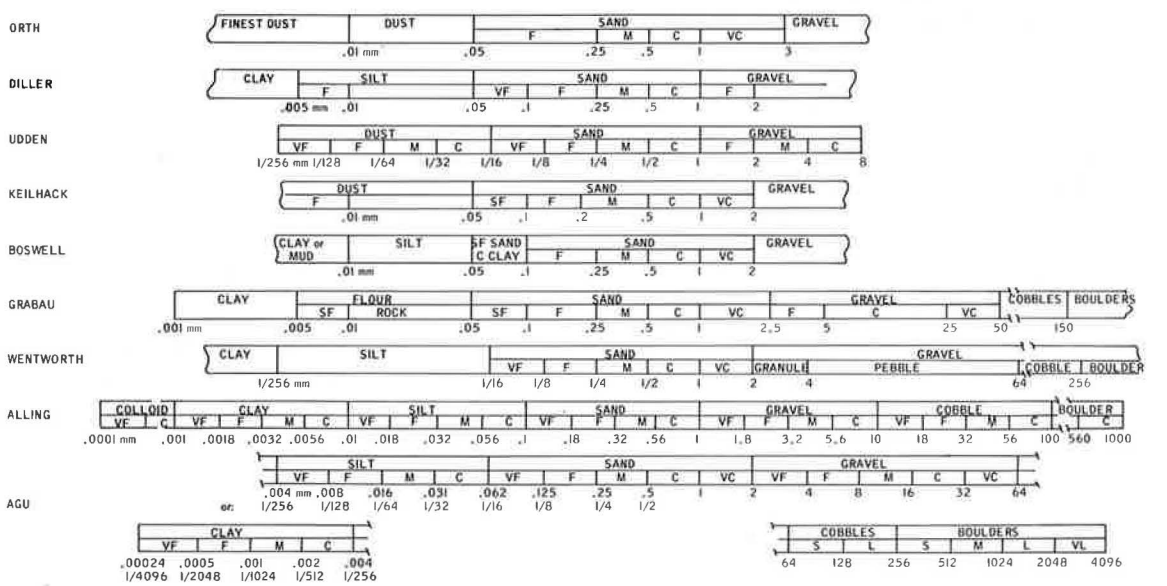

This is where the most difficulty would be encountered. First, the limits between the major soil components—gravel, sand, silt, and clay—should be defined and then the limits for subdivisions of the major components selected.

The difficulty would be in reaching agreement on what constitutes the "natural limits" of a soil. This would require compromise by all sides because what is considered an obvious limit by one group may be quite different from the views of others. If a system attempts to include all of the limits that may be desired by various groups, it will soon become unwieldy and defeat the purpose for which it is designed. The number of limits should be kept at a minimum, which will ensure ease of analysis and still present the desired information.

SUMMARY

All of the systems for designating particle-size limits are based on arbitrarily selected limits. Some investigators attempted to make their selections correspond with various properties of the soil fractions. Thus, in agricultural investigations things such as tillage properties, water retention, capillarity, penetration of plant roots, mineralogical and chemical composition, and colloidal properties were used as bases for various particle-size limits.

Early engineering systems were based on the agricultural limits then in use. Some of the newer systems have particle-size limits that roughly correspond to materials used for specific engineering purposes. Engineering systems tend to evolve to the use of certain standard sieves for the particle-size limits. The shape and slope of the particle-size distribution curve are considered to be of more importance than arbitrary grain-size limits. In some of the systems, no limit is placed between silt and clay; the classification is made on the basis of plasticity and cohesion, which are more direct functions of clay mineralogy.

Some of the systems reported in geological literature are quite similar to those proposed in agricultural literature. Geological systems tend to follow a geometric series of particle-size limits. The use of a constant geometric ratio (such as 2 or 10) makes the system more convenient to use and makes statistical analyses of data easier.

There is a general agreement among the systems commonly used at present on 2 mm as the lower limit for gravel. A few engineering systems (such as concrete technology) use the No. 4 sieve (4.76 mm) for this limit, 4.76 to 2.0 mm being designated "coarse sand." The limits between sand and silt are more varied. Common sizes are 0.02, 0.05, 0.06, 0.62, and 0.074 mm. The 0.02-mm limit, however, is not widely used in this country. Common limits between silt and clay are 0.002, 0.005, and 0.004 mm. Some engineering systems do not use a particle-size limit but base this division on plasticity and cohesion.

The limits commonly used for subdividing the major components are even more varied. Even here some of the limits are approximately the same, but different terms are used to describe the fractions thus separated. Some systems employ many more subdivisions than do others.

A common classification system, applicable to all of the disciplines concerned, would eliminate present contradictions and be of considerable value. However, compromises by all areas would be required to devise such a system.

REFERENCES

1. Standard Method of Mechanical Analysis of Soils. AASHO, Method T-88, 1935.
2. Standard Method of Mechanical Analysis of Soils. AASHO, Designation T-88-49, 1950.
3. Alling, H. L. A Metric Grade Scale for Semimentary Rocks. Jour. of Geology, Vol. 51, 1943, pp. 259-269.
4. Standard Method for Grain-Size Analysis of Soils. ASTM, Designation D 422-39, 1944.
5. Tentative Method for Grain-Size Analysis of Soils. ASTM, Designation D 422-54T, 1958.

6. Standard Method for Grain-Size Analysis of Soils. ASTM, Designation D 422-63, 1964.
7. Atterberg, A. Die Bestandteile der Mineralboden, die Analyse, Klassifikation und Haupteigenschaften der tonartigen Böden. Comptes Rendus de la Première Conference Internationale Agrogeologique, 1909, pp. 289-301.
8. Atterberg, A. Die Eigenschaften der Bodenkorner und die Plastizitat de Böden. Kolloidchemische Beihefte, Vol. 6, 1914, pp. 55-89.
9. Atterberg, A. Die mechanische Bodenanalyse. International Agrogeologenkonferenz, Stockholm, Vol. 2, 1910, pp. 5-11.
10. Atterberg, A. Die mechanische Bodenanalyse und die Klassifikation der Mineralboden Schruedens. Internationale Mitteilunge für Bodenkunde, Vol. 2, 1912, pp. 312-342.
11. Atterberg, A. Die rationelle Klassifikation der Sand und Kiese. Chemiker-Zietung, Vol. 29, 1905, pp. 195-199.
12. Atterberg, A. Studien auf dem Gebiete der Bodenkunde. Die Landwirtschaftlichen Versuchs-Stationen, Vol. 69, 1908, pp. 93-143.
13. Beam, W. The Mechanical Analysis of Arid Soils. Cairo Scientific Jour., Vol. 56, 1911, pp. 107-119.
14. Die Bodenanalyse. Die Landwirtschaftlichen Versuchs-Stationen, Vol. 43, 1894, pp. 335-343.
15. Boyd, J. R. Physical Properties of Subgrade Materials. Canadian Engineer, Vol. 43, 1922, pp. 362-364.
16. Briggs, L. J., Martin, F. O., and Pearce, J. R. The Centrifugal Method of Mechanical Soil Analysis. Bureau of Soils, U.S. Department of Agriculture, Bull. 24, 1904.
17. Briggs, L. J. Objects and Methods of Investigating Certain Physical Properties of Soils. U.S. Department of Agriculture Yearbook, 1900, pp. 397-410.
18. Casagrande, A. Classification and Identification of Soils. Proc. ASCE, Vol. 73, 1947, pp. 783-810.
19. Glossop, R., and Skempton, A. W. Particle-Size in Silts and Sands. Jour. of Institution of Civil Engineers, Vol. 25, 1945, pp. 81-105.
20. Goldbeck, A. T. Tests for Subgrade Soils. Public Roads, Vol. 4, 1921, pp. 15-20.
21. Grabau, A. W. Principles of Stratigraphy. A. G. Seiler, New York, 1913, pp. 286-288.
22. Hall, A. D., and Russell, E. J. Soil Surveys and Soil Analyses. Jour. of Agricultural Science, Vol. 4, 1911-12, pp. 182-223.
23. Hilgard, E. W. Methods of Physical and Chemical Soil Analysis. Agri. Exp. Station, Univ. of California, Circular 6, 1903.
24. Hilgard, E. W. On the Silt Analysis of Soils and Clays. American Jour. of Science and Arts, Vol. 6, 1873, pp. 288-296, 333-339.
25. Hilgard, E. W. Soil Investigation, Its Methods and Results. Agri. Exp. Station, Univ. of California, Annual Rept., 1890, pp. 158-159.
26. Hogentogler, C. A. Engineering Properties of Soil. McGraw-Hill, New York, 1937, pp. 20-23.
27. Hogentogler, C. A., Wintermeyer, A. M., and Willis, E. A. Subgrade Soil Constants, Their Significance, and Their Application in Practice. Public Roads, Vol. 12, 1931, pp. 89-108.
28. Hopkins, C. G. A Plea for a Scientific Basis for the Division of Soil Particles in Mechanical Analysis. Division of Chemistry, U.S. Department of Agriculture, Bull. 56, 1899, pp. 64-66.
29. Kopecky, J. Ein Beitrag zur Frage der neuen Einteilung der Kornungspordukte bei der mechanischen Analyse. Internationale Mitteilunge für Bodenkunde, Vol. 4, 1914, pp. 199-202.
30. Lyon, T. L., and Buckman, H. O. The Nature and Properties of Soils, 4th Ed. Macmillan Company, New York, 1943.
31. Methods of the Mechanical Analysis of Soils. Division of Agricultural Soils, U.S. Department of Agriculture, Bull. 4, 1896.

32. Milner, H. B. Sedimentary Petrography, 4th Ed. Macmillan Company, New York, 1962, pp. 178-193.
33. Morgan, E. An Outline of Particle Size Analysis and Some of Its Uses. Jour. of Institution of Municipal Engineers, Vol. 80, 1954, pp. 329-342.
34. Osborne, T. B. Annual Report of the Connecticut Agricultural Experiment Station for 1886. 1887, pp. 141-159.
35. Progress Report of the Committee on Significance of Tests for Highway Materials. Jour. of Highways Div., Proc. ASCE, Vol. 83, No. HW4, Paper 1385, 1957.
36. Report of Committee 7 on Foundation and Soil Mechanics. Civil Engineering Div., ASCE, Bull. 12, 1947.
37. Report of the Subcommittee on Sediment Terminology. Trans., American Geophysical Union, Vol. 28, 1947, pp. 936-938.
38. The Revised Official British Method for Mechanical Analysis. Jour. of Agricultural Science, Vol. 18, 1928, pp. 734-737.
39. Revised Official Method for the Mechanical Analysis of Soils. Agricultural Progress, Vol. 5, 1928, pp. 137-144.
40. Robinson, G. W. The Grouping of Fractions in Mechanical Analysis. First Internat. Congress of Soil Science, Vol. 1, 1927, pp. 359-365.
41. Schucht, E., reporter. Bericht über die Sitzung der internationalen Kommission für die mechanische and physikalische Bodenuntersuchung. Internationale Mitteilungen für Bodenkunde, Vol. 4, 1914, pp. 1-31.
42. Shaw, T. M., and Alexander, L. T. A Note of Mechanical Analysis and Soils Texture. Proc., Soil Science Society of America, Vol. 1, 1936, pp. 303-304.
43. Soil Survey Manual. Agricultural Research Administration, U.S. Department of Agriculture, 1951, p. 207.
44. Spangler, M. G. Engineering Characteristics of Soils and Soil Testing. In Highway Engineering Handbook (Woods, K. B., ed.), McGraw-Hill, New York, 1960, p. 8-7.
45. Symposium on the Identification and Classification of Soils. ASTM, Spec. Tech. Pub. 113, 1951.
46. Terzaghi, K. Erdbaumechanik auf bodenphysikalischer Grundlage. Franz Deuticke, Leipzig und Wien, 1925.
47. Troug, E., Taylor, J. R., Simonson, R. W., and Weeks, M. E. Mechanical and Mineralogical Subdivisions of the Clay Separate of Soils. Proc., Soil Science Society of America, Vol. 1, 1936, pp. 175-179.
48. Troug, E., Taylor, J. R., Simonson, R. W., and Weeks, M. E. Procedure for Special Type of Mechanical and Mineralogical Soil Analysis. Proc., Soil Science Society of America, Vol. 1, 1936, pp. 101-112.
49. Udden, J. A. Mechanical Composition of Clastic Sediments. Bull. of Geological Society of America, Vol. 25, 1914, pp. 655-744.
50. Udden, J. A. The Mechanical Composition of Wind Deposits. Augustana Library, Pub. 1, 1898.
51. U.S. Geological Survey Bull., Vol. 150, 1898, p. 380.
52. Wentworth, C. K. A Scale of Grade and Class Terms for Clastic Sediments. Jour. of Geology, Vol. 30, 1922, pp. 377-392.
53. Whitney, M. Some Physical Properties of Soils in Their Relation to Moisture and Crop Distribution. Weather Bureau, U.S. Department of Agriculture, Bull. 4, 1892.
54. Williams, W. R. Untersuchungen über die mechanische Bodenanalyse. Forschungen auf dem Geibiete der Agrikultur-Physik, Vol. 18, 1895, pp. 225-350.
55. Wolf, E. V. Die Bodenuntersuchung. Die Landwirtschaftlichen Versuch-Stationen, Vol. 38, 1891, pp. 290-295.

INFLUENCE OF GEOLOGY AND PHYSICAL PROPERTIES ON STRENGTH CHARACTERISTICS OF LATERITIC GRAVELS FOR ROAD PAVEMENTS

J. W. S. de Graft-Johnson, H. S. Bhatia, and S. L. Yeboa,
Building and Road Research Institute, Ghana

Lateritic gravels are the commonly available local material for road and airfield construction in the tropics and subtropics. Because of the wide variations in their nature and physical properties, the selection of an appropriate type of lateritic gravel presents some problems. In the present study the effect of geology, climate, and topography on the nature and formation of such gravels is studied. As a result of the investigations, the lateritic gravels are divided into 4 groups on the basis of geology and physical properties. The study indicates that the proposed groups have a distinct range of engineering properties that can be depicted from simple physical properties. The results obtained have been applied to road failure studies in Ghana, and some interesting observations on the performance of each group of samples are made. The study is considered useful for making a judicious choice of lateritic gravels for satisfactory performance and adequate stability of road pavements.

•LATERITIC gravels are the traditional road-building materials in many tropical countries, especially in Asia and Africa. The value of lateritic gravels as a material of construction has been studied in a good deal of detail by a large number of investigators in many parts of the world. On account of the physical vastness of the areas over which laterites are formed and the wide variations in climatic conditions and geological formations, it has not been possible to generalize the physical properties and engineering behavior of lateritic soils. In addition, no satisfactory classification system has so far been developed that is likely to divide laterites and lateritic soils into different groups, which would reflect the engineering properties and field behavior of such soils. A large number of researchers agree that, for studying the formation and physical properties of lateritic soils and gravels in a generalized way, the pedological grouping is of a considerable value, for it takes into consideration climate, geology, relief, and vegetation.

In Ghana, Gidigasu (14) has studied fine-grained lateritic soils over various geological formations in the 4 climatic zones of the country, namely, coastal savannah, forest, rain forest, and interior savannah. The 4 climatic zones have a distinct range of rainfall as shown in Figure 1, and the samples from each region show certain trends of physicochemical and index properties. For engineering use, such generalizations do provide guidelines on the mode of formation and physical properties of the soils, but for laterite gravels this is of a limited value in terms of assessing their engineering behavior.

On any road or airfield project, thousands of samples must be tested for the selection of appropriate materials for design and construction. A number of highway authorities have adopted physical tests such as particle-size distribution and Atterberg limits

Sponsored by Committee on Soil and Rock Properties.

for the preliminary selection of soil and gravel for road bases and subbases. The materials satisfying the grading and Atterberg limits must also be tested for strength before they are accepted for construction. On account of the very large variation of physical and engineering properties of lateritic gravels, it is considered desirable to have some system for their grouping based either on genetics or on simple physical tests that would reflect broadly the engineering characteristics of the materials. Such a grouping can assist in a better understanding of the behavior of laterites and in reducing the amount of detailed testing on a project. On the basis of such a grouping, only those materials likely to show strength characteristics within specified limits of base, subbase, and fill material are tested in much detail. de Graft-Johnson et al. (9) divided the lateritic gravels into 4 groups and studied the physical and engineering properties of each group. The study indicated that such a grouping, based mainly on the physical characteristics of gravels, could assist very effectively in providing useful guidelines on the strength characteristics. The present study is an extension of the earlier investigation and involves 490 samples of lateritic gravels from the various regions of Ghana. Any samples having more than 50 percent passing the No. 8 ASTM sieve were not included.

The groups established in the present study should not be confused with soil classification systems such as the Unified Soil Classification or classification systems of the U. S. Bureau of Public Roads or the American Association of State Highway Officials. According to the classification systems, most of the lateritic gravels fall broadly in 2 groups, and even these 2 groups cannot effectively be used for preliminary selection of materials for pavement structures. For example, in the Unified Soil Classification System, all lateritic gravels fall in the silty gravel and gravel-sand mixtures or the clay gravel and gravel-sand-clay mixtures. Similarly in the AASHO or BPR classifications, most of the gravels fall in groups A-1 and A-2.

OBJECTIVES OF STUDY

The objectives of the present study were the following:

1. To study the influence of geology, climate, and topography on the properties of laterite gravel;
2. To evolve a grouping system for lateritic gravels by using routine physical tests;
3. To establish whether the groupings evolved can assist in depicting the range of engineering properties for each group and thus facilitate the preliminary selection of materials on a project; and
4. To determine whether the proposed groupings have any bearing on the field behavior of lateritic gravels in road pavements.

FACTORS INFLUENCING PHYSICAL NATURE AND FORMATION OF LATERITES

The various factors influencing the formation of soils are parent materials (geological formation and age), climatic conditions, vegetation, and topography.

Geology

Figure 1 shows that in general Ghana is divided geologically into 4 groups:

1. Acid igneous, which includes rocks like granites, acid gneiss (Dahomeyan series) and quartzites (Togo and Tarkwaian series);
2. Basic igneous, which includes rocks like basalt, gabbro, dolerite (Dahomeyan series), and intrusives;
3. Metamorphic rocks such as shales, phyllites, and schists (Sekondian, Accraian, Voltaian, and Birrimian series);
4. Sedimentary rocks, such as sandstone and limestone (Cretaceous, Amisian, Accraian, Voltaian, and Buem series).

The study of typical soil profiles over various geological formations in Ghana revealed that the materials formed over granite and gneiss were generally coarse in

texture, and the kaolin clay mineral in such soils was formed because of the weathering of quartz, feldspar, and mica. The quartz and mica were very much resistant to weathering and remained unchanged except for leaching of iron from biotite. The materials formed on these rocks were generally sandy and silty in nature with a mottled zone near the surface and iron pan layers 1 to 3 ft thick between 3 and 10 ft from the surface.

Gravels on basic igneous rocks, such as basalt, gabbro, and dolerite, had a high concentration of calcium-rich feldspar and other minerals, which were likely to weather quickly to form amorphous hydrous oxide. The absence of quartz tended to produce plastic materials with fine gradings. Such soils had low permeability and high concentration of iron content, which was not readily removed by leaching.

The gravels on shales, phyllites, and schists, formed initially from clay and silt deposits including some secondary minerals such as mica and quartz from the micaceous quartz veins, were generally clayey in nature and had a reasonable concentration of iron oxide. Laterite hardpans generally developed over such formations near the crest of the slopes. The detrital hardpans mixed with residual soil were good gravels. The residual soils on lower slopes of such formations were poorly drained micaceous clays with varying proportions of quartz obtained as detrital material from quartz veins.

Gravels overlying sandstone and quartzites had a large proportion of quartz in their fine fractions in the form of cemented sand grains (sandstone) or secondary quartz (quartzite). The cementing materials in such rocks were iron and calcium salts that were leached out in the profiles, leaving behind quartz that was unaffected by weathering. The residual materials were generally well-drained sandy gravels. The iron hardpans in such profiles were often developed over high grounds. The effect of parent rock on the particle-size distribution of residual soils is shown in Figure 2.

Climate

The climatic factors influencing the formation of various soils are temperature and rainfall. For example, the coastal and interior savannah zones of Ghana are areas where there is intermediate rainfall and where total evaporation in a year exceeds rainfall; this initiates an upward capillary movement of the product of chemical weathering. The forest zone has a high rainfall, and the soils are covered with thick vegetation. This tends to produce deep chemical weathering and produces quick induration when the soils are exposed. The water table in this region is generally high, and erosion is low.

D'Hoore (11) in his pedologic map of Africa divided the lateritic soils into ferruginous, ferralitic, and ferrisol soils and showed a generalized distribution of those soils depending on climatic conditions alone. According to D'Hoore, the ferruginous soils generally occur in areas with 20 to 60 in. of rainfall per year. The ferralitic and ferrisol soils were formed in areas with rainfall of more than 60 in. per year. Lyon Associates (19) noted that most of the samples tested by them showed a good correlation between the index properties and the pedologic classification proposed by D'Hoore. The test results indicated that ferruginous soils had liquid and plastic limits of less than 50 and 25 respectively, whereas ferralitic and ferrisol soils had liquid and plastic limits of more than 50 and 20 respectively. These factors do form a basis for classifying fine-grained materials in a very generalized way, though this classification is not entirely satisfactory in the case of gravelly materials where a large number of additional variables affect the grain-size distribution and make the assessment of engineering characteristics very complex. The use of such classification systems was, therefore, considered of a limited value in the present study.

Topography

It had generally been noted that most of the borrow areas of good base and subbase gravel were located either on high grounds as primary residual laterite that was rich in sesquioxides of iron and aluminum or on midslopes as secondary laterite that had sesquioxides of iron and aluminum transported into the profile and deposited by groundwater movements. It was, therefore, inferred that laterites formed over high slopes

Figure 1. Geologic map of Ghana and sites of laterite gravel samples.

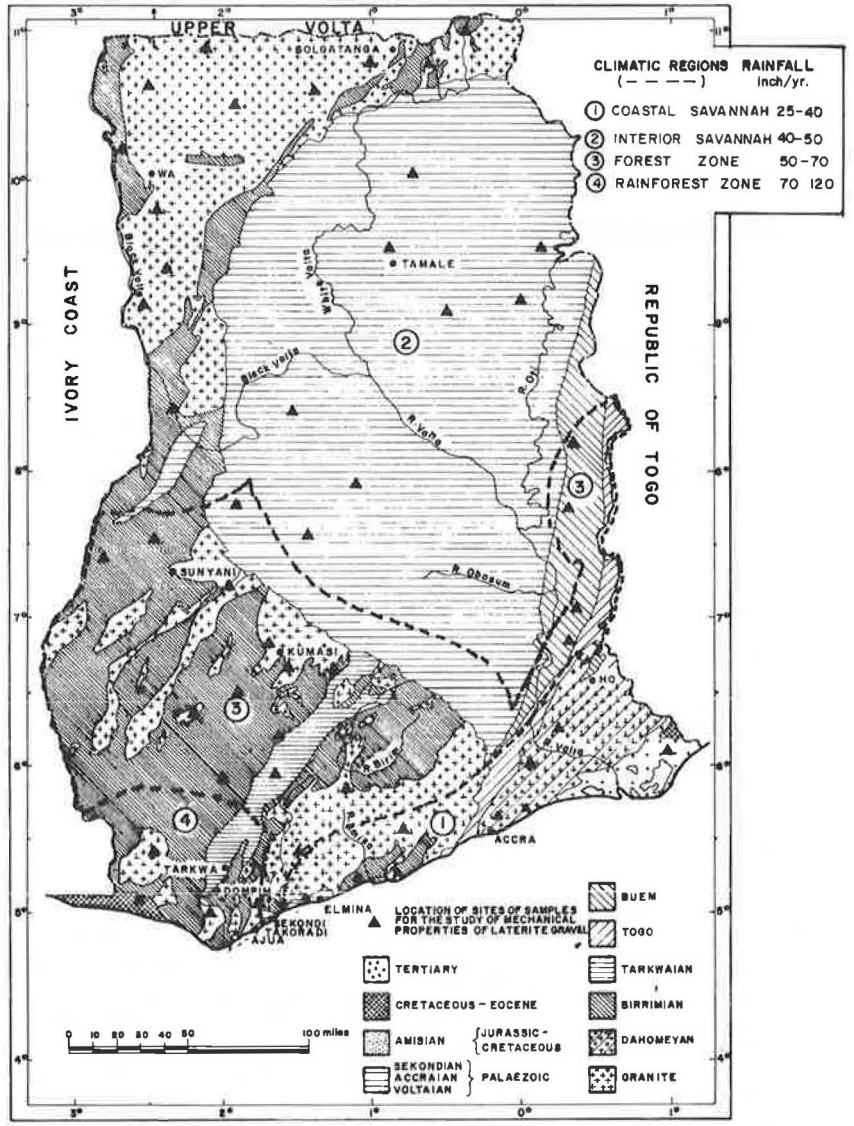

Figure 2. Grading curves of lateritic soil on various parent rocks.

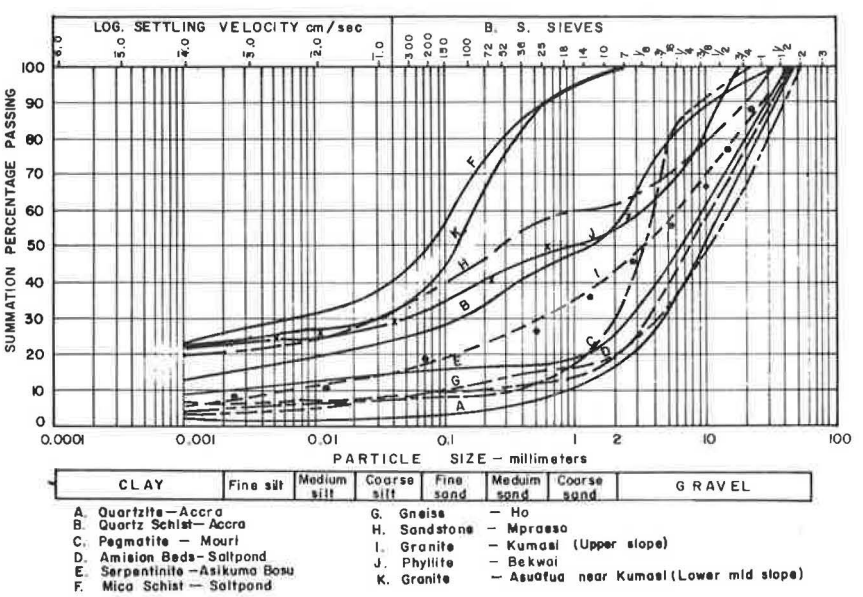

have relatively fewer fines and, therefore, are more suitable for road pavements than gravels found on lower slopes and in valleys.

In the present study, only 14 out of 490 samples were obtained from borrow areas on the lower slopes or in the valleys. All of the other samples were from the upper and middle slopes or from areas where the topography was plain. The samples collected from low slopes and valleys were very plastic and were an unpredictable mixture of clay and gravel.

SELECTION OF SAMPLES AND TESTING

The 490 samples were subjected to the following tests: particle-size distribution, Atterberg limits, moisture-density relations using Ghana compaction standard (compaction in a standard CBR mold in 5 layers with a 10-lb AASHO hammer from an 18-in. drop), and CBR (soaked and unsoaked). Triaxial tests were also conducted on few selected samples. These samples included the soils tested at the Building and Road Research Institute and by the Materials Branch of the Public Works Department of Ghana in connection with a number of road projects in the country. The inclusion of samples from the Materials Branch not only provided a broad basis for this study but also helped to assess the practical value and utility of the findings of this investigation. The distribution of various samples selected in the present study is shown in Figure 1.

Of the 490 samples selected for this study, 38 percent came from climatic regions having rainfall between 40 and 60 in. and 62 percent from regions having rainfall between 60 and 120 in. per year.

MECHANICAL STRENGTH OF COARSE GRAVEL

Several investigators, Ackroyd (2), Clare (8), de Graft-Johnson et al. (9), and Novais-Ferreira and Correia (17), have suggested the importance of mechanical strength of aggregates in relation to their mechanical breakdown and weathering under different environments in the field. A weak gravel is likely to break down because of chemical weathering or mechanical processes during and after construction. The breakdown of gravels in base and subbase layers tends to change the gradings and Atterberg limits of the material and to cause a considerable distress in road pavements. It is, therefore, important that a minimum value of mechanical strength for the coarse fractions be specified in addition to the specified values of Atterberg limits, particle-size distribution, and CBR test. These are the tests generally included in most of the standard specifications for road gravels. de Graft-Johnson et al. (9) have suggested that the aggregate impact test is a useful criterion for assessing the mechanical strength of laterite gravels, and this can form a reasonable basis for inclusion in future specifications. [In the aggregate impact test, BS-812, resistance to impact is measured on a 1½-in. deep bed of ½-in. chippings in a 4-in. diameter mold struck 15 blows by a 30-lb hammer falling from a height of 15 in. The percentage of fines passing No. 7 BSS (2 mm) as a result of the impact is known as aggregate impact value.] As a result of a recent study on the mechanical strength of lateritic gravels of Ghana (4), the following is recommended for rating gravels of different mechanical strength:

Aggregate Impact Value (percent)	Los Angeles Abrasion Value (percent)	Performance Rating
30	40	Excellent
31 to 40	41 to 50	Good
41 to 50	51 to 60	Average, generally unsuitable
>50	>60	Very poor

The study further suggests that any gravels having aggregate impact values of more than 40 percent and Los Angeles abrasion values of more than 50 percent should be avoided for base construction.

PHYSICAL PROPERTIES

Particle-Size Distribution

Besides the mechanical strength of a gravel, the most important factor influencing its value as a material of construction is grading. The particle-size distribution of the samples was examined to determine the limits within which the distribution varies in lateritic gravels. Although the total variations of different fractions in the samples studied were wide, there was some similarity in the grain-size distribution of samples obtained from the areas having similar climate and geology. Geologic and climatic factors did influence the gradings of the samples within reasonable limits, though these factors could not exclusively be used as a basis for grouping because the variations in about 13 percent of the samples from the same geologic and climatic region followed no distinct pattern of grading. This was attributed to the predominance of other factors over geology and climate in the formation of such soils.

Earlier de Graft-Johnson et al. (9) suggested 4 grading envelopes within which most of the lateritic gravels could be accommodated with ease. These grading limits for each group have been slightly modified as a result of further studies of a number of samples from the road pavements and also of considerations of the influence of geology on such gravels. The slightly modified grading envelopes as a result of the present study are shown in Figure 3.

In groups 1 and 2, 80 and 83 percent of the samples studied were formed over granite and gneiss, whereas 20 and 17 percent of the samples belonged to other geological formations. In groups 3 and 4, 83 and 92 percent of the samples were formed over phyllite, schist, shales, and limestone, whereas only 17 and 8 percent belonged to granite and gneiss. This tends to suggest a strong influence of geology on the particle-size distribution of the lateritic gravels. No definite conclusion could be drawn, however, on the effect of rainfall on the particle-size distribution of the gravels collected from different regions of Ghana.

To see the significance of the proposed grouping, we used a statistical method known as multiple measurements (12) to discriminate between 2 groups. The general problem was set up as a function of the form

$$Z = Y_1X_1 + Y_2X_2 + Y_3X_3 + \ldots + Y_nX_n$$

where X_1, X_2, X_3, and X_n are variables that in the present study are liquid limit, plasticity index, maximum density, optimum moisture content, and California bearing ratio; and Y_1, Y_2, Y_3, and Y_n are the corresponding weights or coefficients to give the discriminating power. If the 2 groups to be discriminated were 1 and 2 and there were n_1 sets of measurements for group 1 and n_2 sets of measurements for group 2, the ratio of the differences between group means Z_1 and Z_2 to the differences between the groups as represented by standard deviation was maximized as

$$G = (\overline{Z}_1 - \overline{Z}_2)^2 \Bigg/ \left[\sum_{i=1}^{n_1} (Z_i - Z_1)^2 \sum_{j=1}^{n_2} (Z_j - Z_2) \right]$$

By differentiation with respect to the individual coefficients, we calculated the differences among and within the groups and the mean square for each difference. The ratio of the mean square among groups to the mean square within the group, known as the F-ratio, was calculated. The comparison of the experimental F-ratio to the statistical F-ratio indicated that the 4 groups proposed were very highly significant in terms of their properties such as liquid limit, plasticity index, maximum density, optimum moisture content, and CBR values. The results of the discriminatory analysis for the 4 groups are given in Table 1.

Atterberg Limits

The Atterberg limits tests carried out on air-dried samples by using a standard procedure did not indicate a separate range of Atterberg limits for the proposed 4

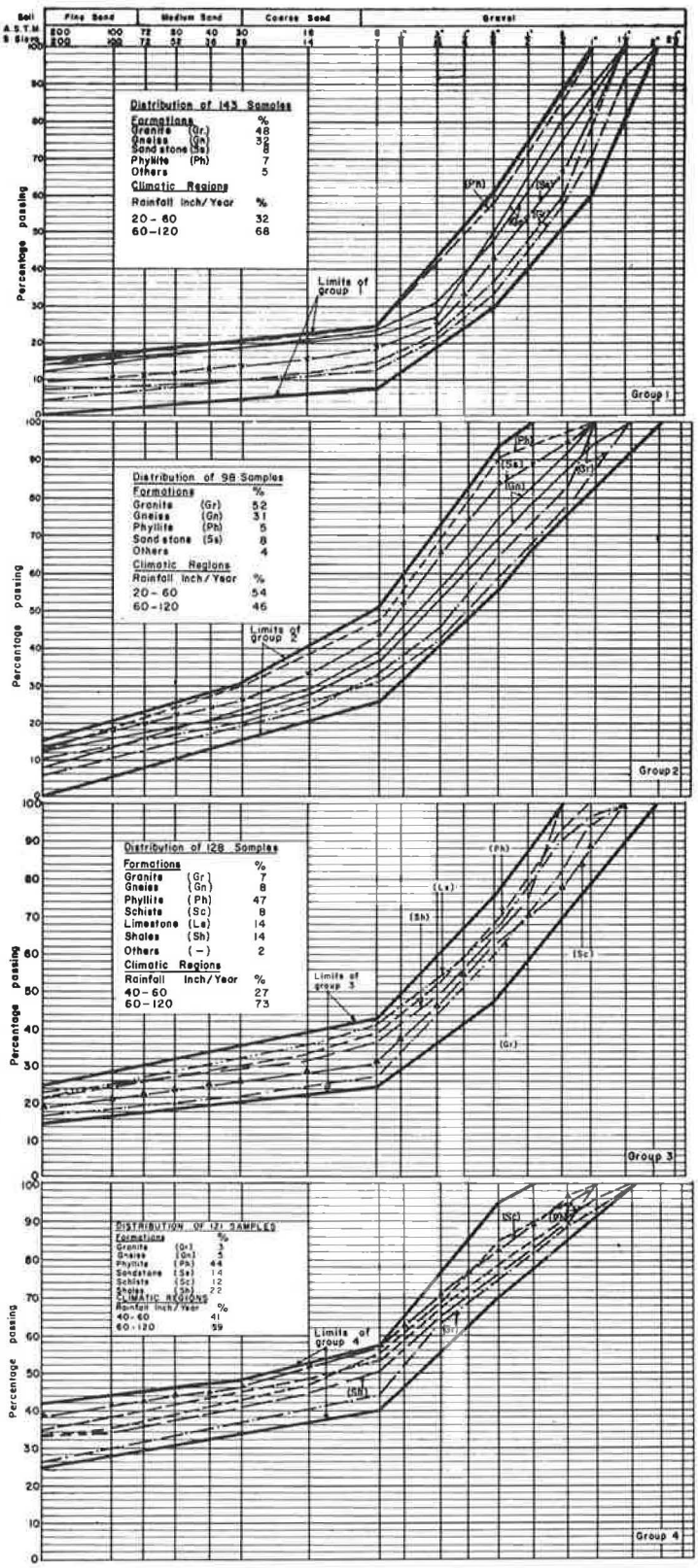

Figure 3. Typical grading curves of 4 sample groups on different geologic formations.

grading envelopes. There was considerable variation of these limits for samples falling in each grading envelope, though as a general rule the Atterberg limits increased progressively from group 1 to group 4. In view of a certain amount of overlapping in the Atterberg limits, no separate range of values could be given for each group. The histograms indicating the distribution of these values are shown in Figure 4. In addition, these values were plotted on Casagrande's plasticity chart as shown in Figure 5. Such variations of Atterberg limits were considered normal, for these limits depended on a large number of factors such as geology, relief, state of dehydration of iron, nature of clay minerals, and residual or nonresidual soil. The general variations of liquid limit, plastic limit, and plasticity index for all 4 groups are given in Table 2.

Moisture-Density Relations

The engineer is mainly interested in the suitability of a compacted soil when it is used as a material of construction. The assessment of suitability in the present study was made through the strength characteristics of compacted gravels under different conditions of moisture contents. The 3 modes of compaction generally adopted in Ghana are as follows:

Compaction Standard	Energy ($ft\text{-}lb/ft^3$)
Modified AASHO	56,750
Ghana	22,500
Proctor's	12,375

Ghana compaction is between the modified AASHO and the Proctor's compaction in terms of compactive energy. Ghana compaction standard is generally adopted on most of the road projects in Ghana; therefore, this standard was used for arriving at the moisture-density relations for most of the soils included in this study. Hammond (16) conducted a separate investigation on a few typical samples from each of the 4 groups to determine the effect of 3 levels of compaction on the strength characteristics of the soil; those results are reported elsewhere.

The moisture-density relations of some typical samples of gravels falling in the 4 grading envelopes are shown in Figure 6. The maximum densities and optimum moisture contents and their median values are shown in Figure 7. The maximum, minimum, and mean values in addition to standard deviation values are also given in Table 2. The range of optimum densities and optimum moisture contents for the Ghana compaction standard was relatively little different between sample groups 1 and 2, but this difference increased progressively in sample groups 3 and 4. Each group of gravels showed maximum densities in a rather narrow range, though the values overlap to some degree, and this was considered normal. The very fact that samples belonging to different groups showed their maximum optimum densities and optimum moisture contents in different ranges indicated that there was a strong influence of grading on the moisture-density relations of a gravel.

An attempt was, therefore, made to correlate grading with the maximum density. This was achieved by converting the grading into a single parameter known as the fineness index. This index is a modified form of the fineness modulus used in concrete aggregates and of the granulometric modulus used by Novais-Ferreira and Correia (17) for gravel studies. The set of sieves used in Ghana for particle-size distribution is slightly different from the set used by the researchers referred to above; therefore, the parameter in this study was called the fineness index (FI) to avoid confusion. The fineness index in the present study was the accumulative value of the percentage passing the $^3/_4$-in., $^3/_{16}$-in., No. 8, No. 30, and No. 300 ASTM or No. 7, No. 25, and No. 200 BS sieves divided by 6. The increasing values of FI reflected the finer nature of the materials.

An attempt was made to develop correlations between FI and maximum density for all 4 groups. The plotted points and their regression curves are shown in Figure 8. There is significant linear correlation between the fineness index and the maximum density for each group of lateritic gravels.

Table 1. Results of statistical discriminant analysis.

Group	Number of Samples	Mean Value: Liquid Limit	Plastic Limit	Maximum Density	Optimum Moisture Content	CBR	Experimental F-Value[a]	Statistical F-Values[b]	Remarks
1	143	35.56	14.96	133.95	9.06	64.22	3.7	3.130	Satisfactory
2	98	30.76	11.60	135.00	8.92	63.01	13.0	3.112	Highly significant
3	128	36.71	15.41	130.48	10.02	45.55	24.4	3.132	Very highly significant
4	121	42.31	19.74	129.22	11.00	30.93			
2	98	30.76	11.60	135.00	8.92	63.01	9.9	3.138	Highly significant
3	128	36.71	15.41	130.48	10.02	45.85	24.4		
4	121	42.31	19.74	129.22	11.00	30.93		3.170	Very highly significant
3	127	36.71	15.41	130.48	10.02	45.85	9.1		
4	121	42.31	19.74	129.22	11.00	30.93		3.130	Significant

[a]Ratio of mean square among groups to the mean square within the group; the higher the experimental F-value relative to the statistical F-value, the more significant is the difference among the groups.
[b]1 percent confidence.

Figure 4. Distribution of liquid limit and plasticity index of 4 sample groups.

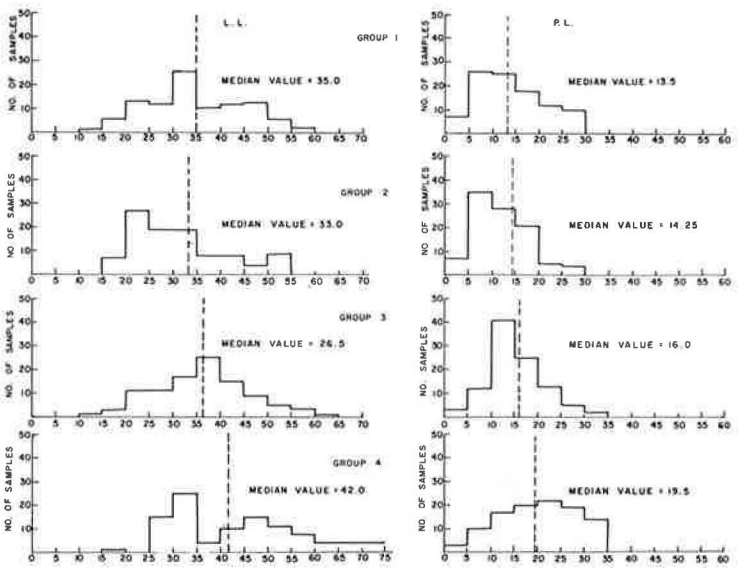

Figure 5. Casagrande's chart of limits of 4 sample groups.

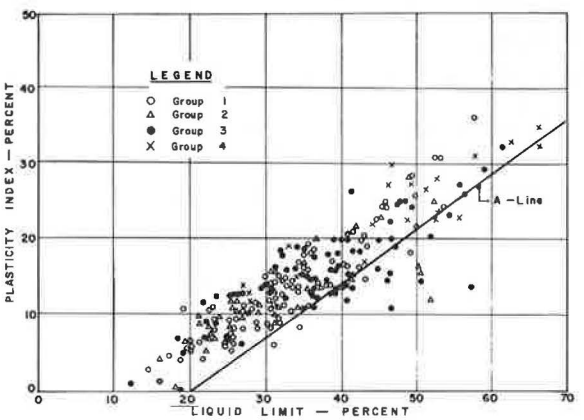

Table 2. Limits, density, and moisture content of 4 sample groups.

Group	Value	Liquid Limit	Plastic Limit	Plasticity Index	Maximum Dry Density	Optimum Moisture Content
1	Maximum	58.4	31.0	36.3	141.8	13.8
	Mean	34.4	19.9	14.4	139.0	9.2
	Minimum	14.5	8.01	1.6	123.2	6.1
	Standard deviation	10.3	4.5	7.3	17.3	1.5
2	Maximum	53	40.0	28.0	142.2	13.5
	Mean	31.4	18.9	12.5	139.1	8.9
	Minimum	16.7	1.0	4.0	130.8	5.6
	Standard deviation	9.21	6.32	5.48	3.36	2.36
3	Maximum	61.8	44.4	31.3	138.5	15.8
	Mean	37.2	24.7	15.3	130.0	9.92
	Minimum	12.9	10.0	0.9	110.0	2.07
	Standard deviation	9.84	7.66	5.36	4.52	2.07
4	Maximum	73	48.0	34.9	133.9	16.4
	Mean	43.4	23.3	20.6	126.6	11.4
	Minimum	18.4	10.2	3.2	120.6	8.9
	Standard deviation	13.74	8.1	7.29	3.82	1.89

Figure 6. Moisture-density relations of 4 sample groups.

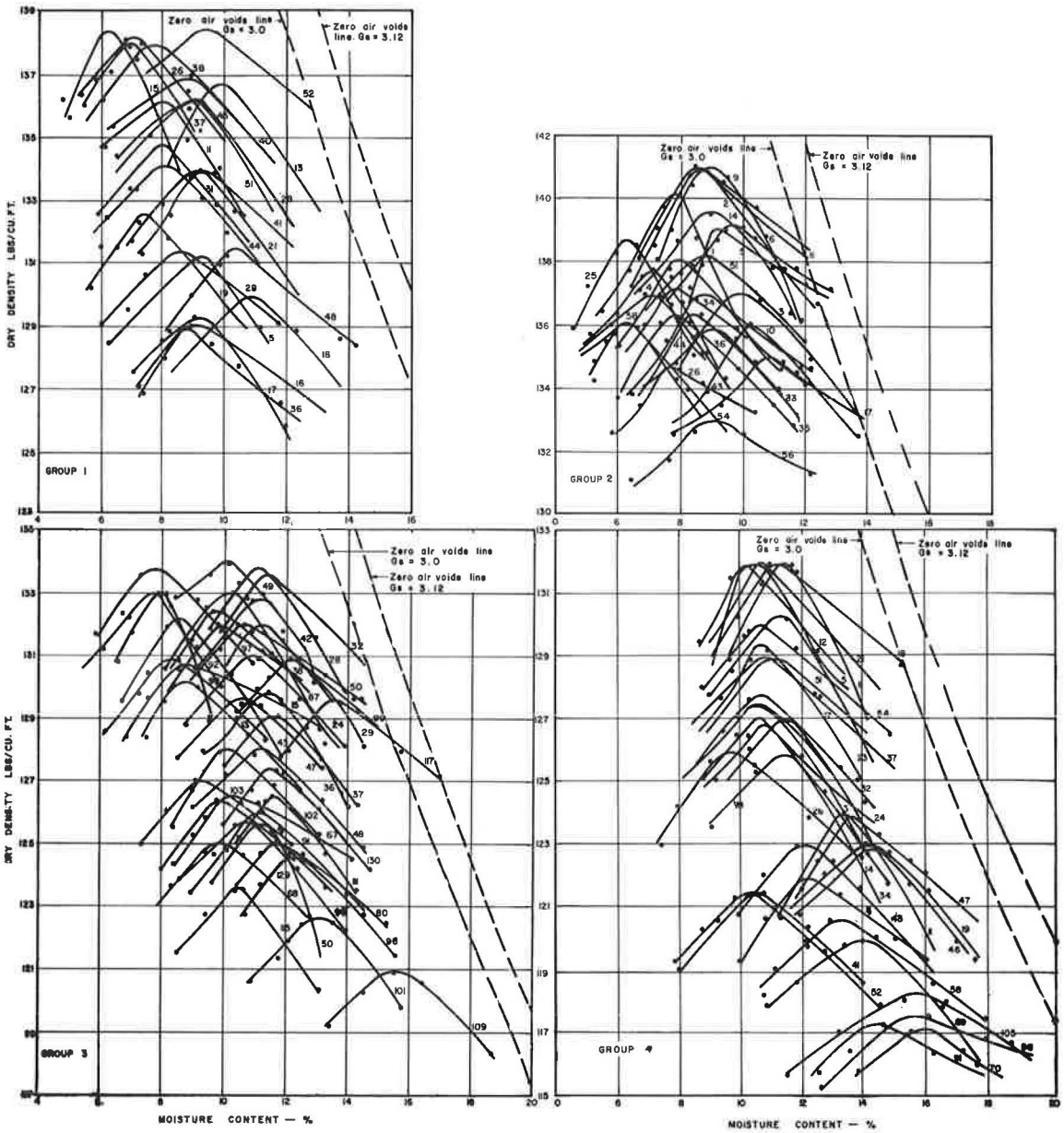

Figure 7. Distribution of maximum dry densities of 4 sample groups.

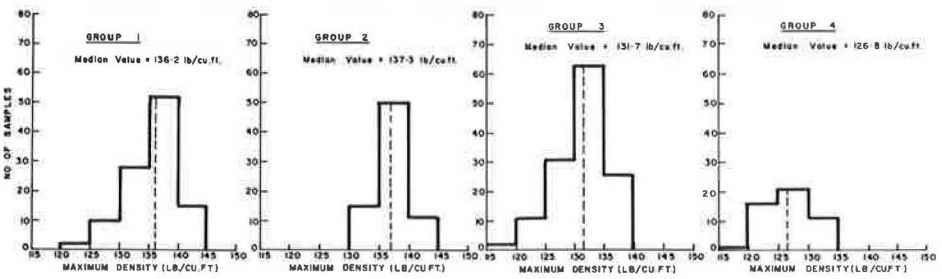

Figure 8. Relation of fineness index and maximum dry density of 4 sample groups.

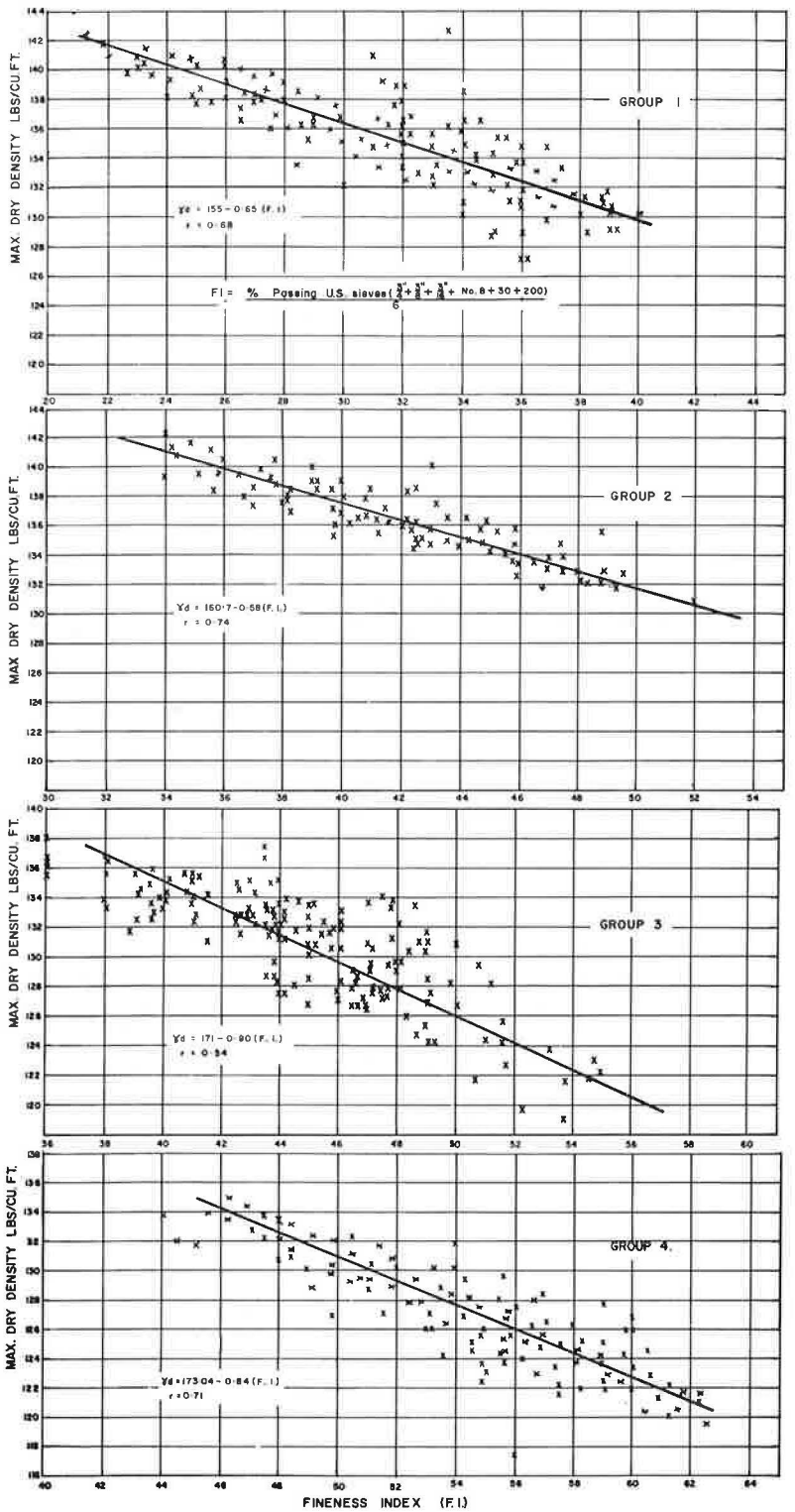

STRENGTH CHARACTERISTICS

The strength characteristics of gravels in the present investigations were studied by means of the CBR tests, and shear parameters were determined for a few selected samples in a triaxial cell. The CBR test was considered an indirect test for the evaluation of strength characteristics of pavement materials. The soaked CBR values were determined for each sample at optimum moisture content by using Ghana compaction standard. The histograms showing the distribution of CBR values for the 4 sample groups are shown in Figure 9.

The 2 important factors likely to influence the strength characteristics of a gravel under worst conditions of moisture are its maximum density and plasticity characteristics of its fines. In a previous study by de Graft-Johnson et al. (9), a parameter known as the suitability index (SI) was used to assess the CBR values of lateritic gravels; the index is based on the percentage of coarse gravel fractions in a soil, the liquid limit, and the plasticity index of its fines.

$$SI = A/B \log_{10} C$$

where

A = fraction retained on No. 8 ASTM or No. 7 BS sieve,
B = liquid limit, and
C = plasticity index.

The present study indicated that the SI was a useful parameter for assessing the strength characteristics of samples collected from the same climatic and geological areas. However, the results showed a certain amount of scattering when samples from different climatic and geologic regions were plotted together (Fig. 10).

The grading and plasticity characteristics have a considerable influence on the maximum density and the strength characteristics of a material. An attempt was, therefore, made to use maximum density and plasticity index as 2 parameters for assessing the strength characteristics of a compacted gravel. The maximum density at Ghana compaction and the fineness index obtained from grading had significant correlations. It was further seen that log of (maximum density/PI) had linear correlation with soaked CBR values, and the following general expression was established:

$$CBR = C_1 \log (\gamma d \text{ max}/PI) + C_2$$

where C_1 and C_2 are constants with different values for the 4 groups. The plotted values of (maximum density/PI) against CBR values on a semilog scale are shown for the 4 groups in Figure 11. The correlation coefficients in all the groups are very significant. Combining the 2 statistical relations between FI and maximum density and also between log (maximum density/PI) and CBR values made it possible to assess the CBR values of each sample group at a given compaction standard from simple physical tests, namely, the grading and the Atterberg limits. The statistical relation for the 4 groups of gravel are shown below.

Group	CBR	Correlation Coefficient
1	$42.6 \log [(146.4 - 0.335 \times FI)/PI] + 20.63$	0.62
2	$76.0 \log [(149 - 0.287 \times FI)/PI] - 23.89$	0.84
3	$50.0 \log [(144.4 - 0.296 \times FI)/PI] - 3.86$	0.64
4	$41.8 \log [(151.8 - 0.47 \times FI)/PI] - 4.34$	0.71

The regression lines for the actual CBR values and the statistical CBR values for all 4 groups are shown in Figure 12, and they show significant correlations.

Triaxial Testing

An attempt was made to study the shear parameters of a few typical gravels from each of the proposed groups of samples. The 3-stage triaxial consolidated undrained

Figure 9. Distribution of CBR values of 4 sample groups.

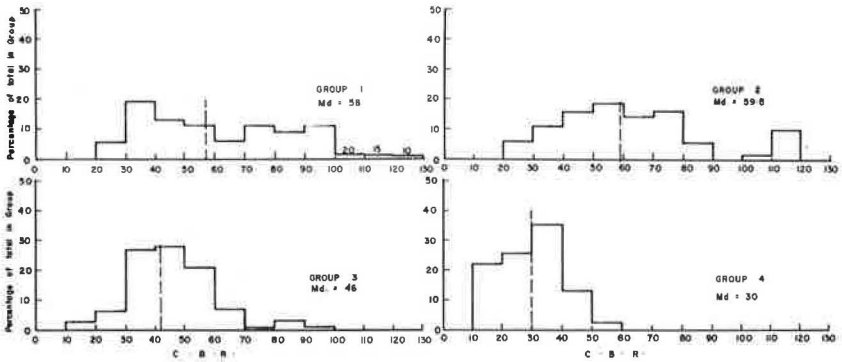

Figure 10. Relation of suitability index and soaked CBR values of 4 sample groups.

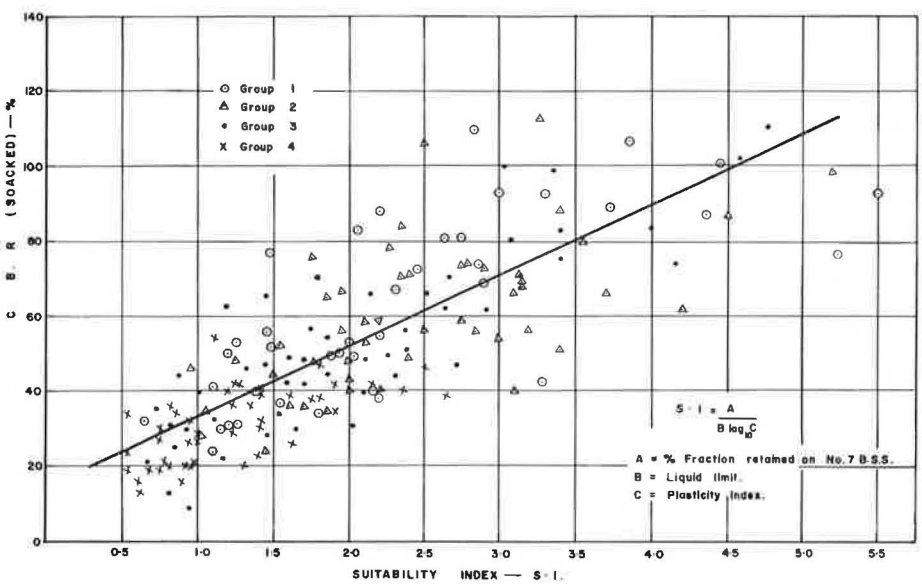

Figure 11. Relation of maximum dry density, plasticity index, and CBR values of 4 sample groups.

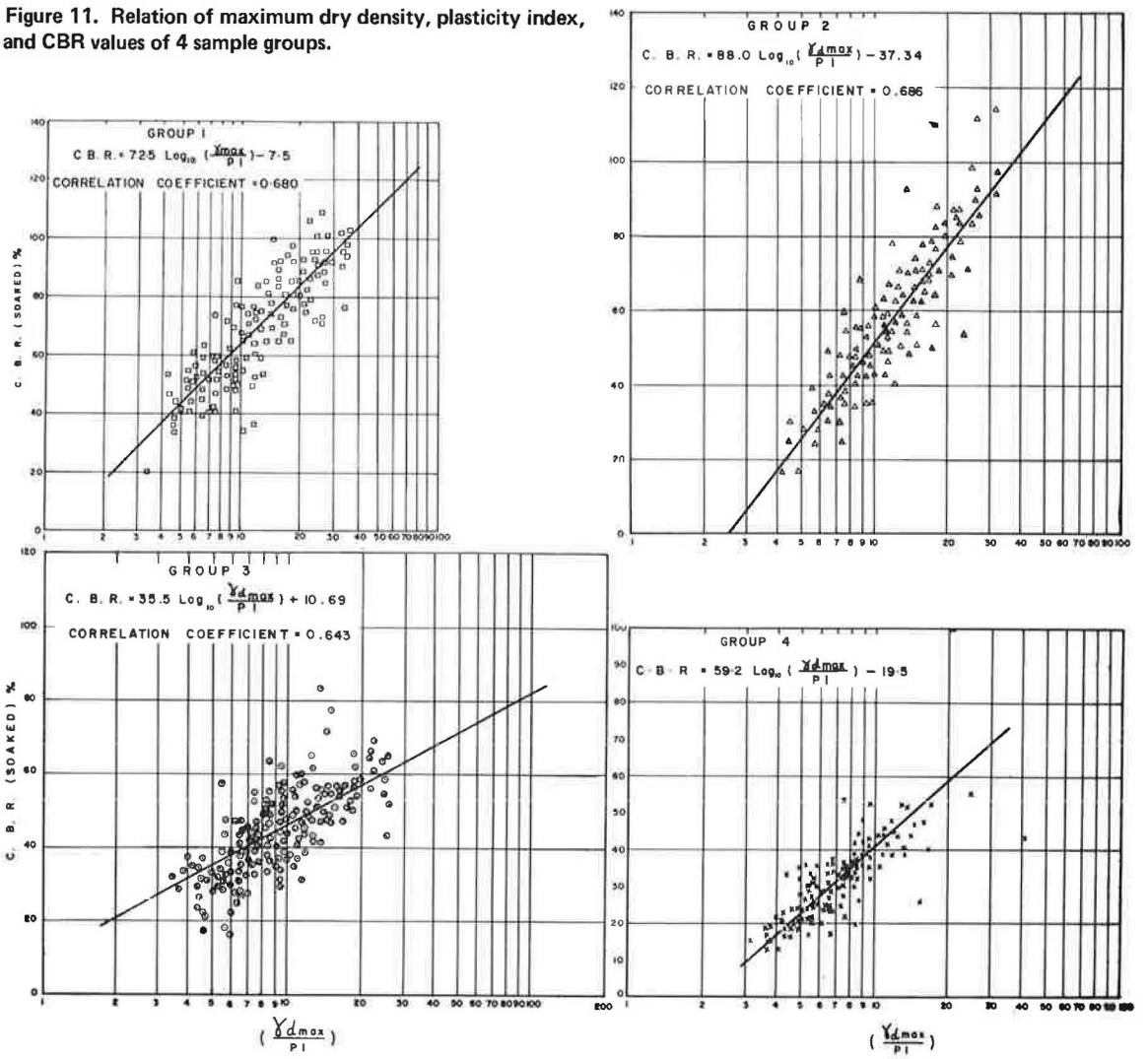

Figure 12. Experimental and statistical CBR values of 4 sample groups.

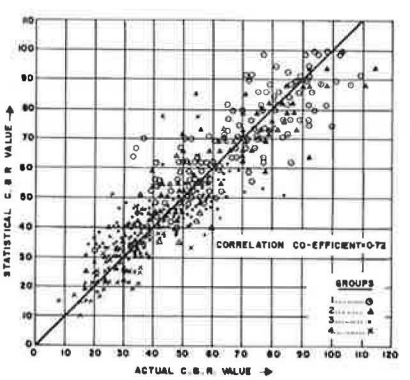

Figure 13. Typical triaxial test results of 4 sample groups.

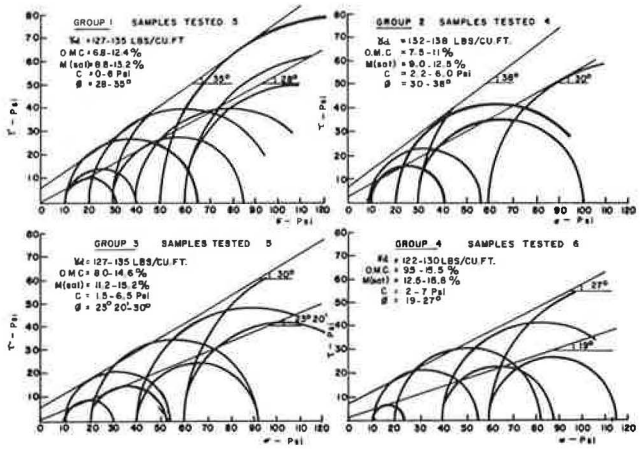

Figure 14. Actual and statistical CBR values of base gravels from trunk-road failure investigation.

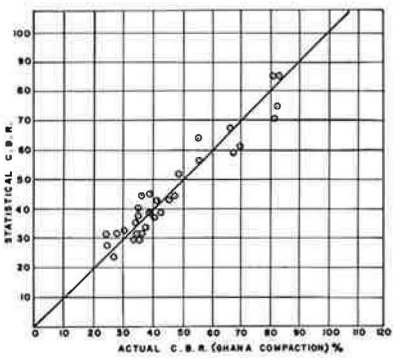

Table 3. Shear parameters in triaxial tests of 4 sample groups.

Group	Number of Tests	Maximum Dry Density (lb/ft^3)	Optimum Moisture Content (percent)	Final Moisture Content at Testing (percent)	Shear Parameters	
					C (psi)	ϕ (deg and min)
1	2	128 to 139	6.8 to 12.4	8.8 to 13.2	0.0 to 6.0	28 to 35
2	4	132 to 138	7.5 to 11.0	9.0 to 12.5	2.2 to 6.0	30 to 38
3	5	127 to 135	8.0 to 14.6	11.2 to 15.2	1.5 to 6.5	23 and 0.20 to 30
4	6	122 to 130	9.5 to 15.5	12.5 to 15.8	2.0 to 7.0	19 to 27

tests were performed on 4-in. wide and 8-in. high samples, compacted at optimum moisture content to maximum density by using Ghana compaction standard. The samples were saturated by using back pressures. The shear parameters obtained in the study are shown in Figure 13 and given in Table 3. Values of cohesion were rather low in sample groups 1 and 2 but showed an increase in sample groups 3 and 4. The angles of internal friction, on the other hand, were maximum in sample groups 1 and 2, but the values decreased progressively in sample groups 3 and 4. This confirmed the findings made in the CBR test that the relative strengths of sample groups 1 and 2 were in all the cases higher than those of sample groups 3 and 4.

FIELD INVESTIGATIONS

Failure investigations were carried out recently on trunk roads in Ghana to assess the causes of pavement failures. On the basis of visual observations of the condition of road surface, the pavements were divided into 4 groups: excellent, good, fair, and poor. Few sections having these ratings were selected for investigating the specific causes of road failures. For purposes of fair comparison and evaluation, sections were selected for the study that had similar physical conditions such as cut or embankment sections, with and without shoulders, or nature of surface drainage. Under similar conditions of road pavements, the following broad conclusions could be drawn on the performance of materials.

1. Most of the failed sections had the grading of their base gravels falling within the limits of groups 3 and 4. The sections showing least sign of distress had gradings conforming to groups 1 and 2. There were few exceptions where sections not showing any signs of failure had the gradings conforming to groups 3 and 4. Similarly, few exceptions were noted where the pavements having gravels belonging to groups 1 and 2 showed signs of distress. In all such cases, the surface drainage and the shoulders seem to have played the decisive role in their performance. For example, sections showing satisfactory behavior but having gravels of groups 3 and 4 had in all the cases shoulders 5 to 6 ft wide and surface drains provided on both sides of the traveled way. The complete absence of shoulders and inadequate drainage had in some cases affected the performance of gravels of groups 1 and 2 adversely.
2. No definite conclusions could be drawn on the range of Atterberg limits to be attributed to failed sections except that soils belonging to groups 3 and 4 had generally higher values. In a few cases, the base gravels having plasticity indexes as high as 10 or 15 showed reasonably satisfactory behavior, and this could again be due to favorable drainage conditions on the site.
3. The maximum densities obtained by using Ghana standard compaction were in all the cases in conformity with the ranges specified for different groups given in Table 2.
4. The actual and statistical CBR values using grading and the plasticity index of the samples gave significant correlation, and this is shown in Figure 14.
5. A number of failures in addition were noted to be the result of a combination of several factors such as inadequate thickness, poor drainage, or defective surfacing. These are not within the scope of this study and are discussed elsewhere.

SUMMARY AND CONCLUSION

1. The study is an extension of the work carried out earlier at the Building and Road Research Institute on the use of laterite gravels for road pavements. The present investigation was aimed at studying the factors responsible for the engineering properties of lateritic gravels. The factors studied were geology, climate, relief, and physical properties.
2. The present investigations revealed that there is a significant influence of geology and climate on the texture, the grading, and the physical and engineering properties of the material. Though the combination of all such factors produces a complex pattern of soil formations, these factors could be usefully employed as a general guide in depicting the physical properties of a material. The geology, climate, and topography had predominant influence on the physical properties in the sedentary profiles.

3. Texture, geology, and climate were used as guidelines grouping all lateritic gravels of Ghana into 4 distinct grading envelopes. The grading in turn had considerable influence on the maximum dry density achieved in the standard moisture-density test, provided the coarse gravel fractions had certain minimum strength to avoid easy breakdown of gravels.

4. Laboratory and field studies suggested the rating of the mechanical strength of the coarse fractions in laterites by using the standard aggregate impact test. Any gravels having aggregate impact values of more than 40 did not perform too well as road bases. The gravels with values of more than 40 generally are crushed and disintegrate during and after construction and tend to produce a material of fine texture likely to affect the performance of the road pavement.

5. The gravels falling in any one of the 4 grading envelopes showed a definite range of maximum densities, provided they conformed to the minimum mechanical strength values. A very significant correlation existed between the fineness index and the maximum dry density. The fineness index is the accumulative value of percentage passing the $^{3}/_{4}$-in., $^{3}/_{8}$-in., $^{3}/_{16}$-in., No. 8, No. 30, and No. 200 ASTM sieves divided by 6.

6. The strength characteristics of gravels at saturation were influenced by the density and the plasticity characteristics of the material. Significant correlations could, therefore, be established between log (maximum density/PI) and CBR values for samples of each group.

7. Field investigations had been carried out to check the effectiveness of the proposed grouping system. The investigations indicated that statistical assessment of CBR values at a given compaction standard could reasonably be made by using simple tests like gradings and Atterberg limits.

8. The field studies also pointed out that sections having base materials in groups 1 and 2 generally showed satisfactory behavior, whereas sections with gravels in groups 3 and 4 showed poor performance. It was also found that the mechanical strengths of the gravels in groups 3 and 4 were generally poor.

9. The present study gave a range of shear parameters for each group of gravels as determined at the maximum densities by using Ghana compaction standard. The shear parameters were obtained in consolidated undrained triaxial tests using samples 4 in. wide and 8 in. high.

10. It is considered that the study helps in understanding the nature and the properties of laterite gravels as affected by the various geologic processes. In addition, it provides a reasonable statistical method for assessing the strength characteristics of gravels from simple physical tests, such as grading and Atterberg limits. The method can assist in considerable reduction of the bulk testing of samples on a project and thus affect economy, choice of materials, and quality control.

ACKNOWLEDGMENTS

The present study is part of a 2-year research project on laterite and other problem soils of Africa. It was sponsored jointly by the U. S. Agency for International Development and the Ghana Building and Road Research Institute. The assistance rendered by the staff of the Lyons Associates, Inc., consultant for the U. S. Agency for International Development, is acknowledged. Thanks are due to R. B. Peck of the University of Illinois and James Eades of the University of Florida, who acted as consultants on this project, for their keen interest, guidance, and encouragement during the project. The authors also acknowledge with thanks the assistance rendered by C. M. Pant, and H. R. Agarwal of the Ghana Public Works Department in providing some of the data during the course of this study. Thanks are also due to J. P. Meyer, U.S. Peace Corps volunteer, who carried out the computer program. The study in the laboratory was handled by A. A. Hammond and S. K. Bani with the assistance of S. K. Afunyah, E. A. Quarcoo, and P. K. Y. Sarkodie.

REFERENCES

1. Ackroyd, L. W. The Correlation Between Engineering and Pedological Classification System in Western Nigeria and Its Implications. Proc., Third Reg. Conf. for

Africa on Soil Mech. and Found. Eng., Salisbury, Southern Rhodesia, Vol. 1, 1963, pp. 85-88.
2. Ackroyd, L. W. Formation and Properties of Concretionary and Non-Concretionary Soils in Western Nigeria. Fourth Reg. Conf. for Africa on Soil Mech. and Found. Eng., Cape Town, South Africa, 1967.
3. Bhatia, H. S., Gidigasu, M. D., and Hornsby-Odi, A. G. The Importance of Soil Profiles to the Engineering Studies of Laterite Soils in Ghana. Ghana Building and Road Research Institute, Kumasi, Proj. Rept. SM8, 1970.
4. Bhatia, H. S., and Hammond, A. A. Durability and Strength Properties of Lateritic Aggregates of Ghana. Ghana Building and Road Research Institute, Kumasi, Proj. Rept. SM9, 1970.
5. Methods of Sampling and Testing Mineral Aggregates, Sand and Fillers. British Standard Institution, 1960.
6. Bruckner, W. D. Laterite and Bauxite Profile of West Africa as an Index to Rhythmical Climatic Variations in the Tropical Belt. Eclogae Geologicae Helvetiae, Vol. 50, No. 2, 1955.
7. Proposed Programme of Research Project, Laterites and Other Problem Soils of Africa. Ghana Building and Road Research Institute, Kumasi, Proj. Rept. SM1, 1958.
8. Clare, K. E. Road Making Gravels and Soils in Central Africa. Gt. Brit. Road Research Laboratory, Overseas Bull. 12, England, 1960.
9. de Graft-Johnson, J. W. S., Bhatia, H. S., and Gidigasu, M. D. The Engineering Characteristics of Lateritic Gravels of Ghana. Proc., Seventh Internat. Conf. on Soil Mech. and Found. Eng., Mexico, Vol. 1, 1969.
10. de Graft-Johnson, J. W. S., and Bhatia, H. S. Engineering Properties of Lateritic Soils. Seventh Internat. Conf. on Soil Mech. and Found. Eng., Mexico, Vol. 2, 1969.
11. D'Hoore, J. L. Soil Map of Africa (scale 1:5,000,000) and Explanatory Monograph. Comm. for Tech. Co-op. in Africa, Pub. 93:205P, 1964.
12. Fisher, R. A. Statistical Methods for Research Workers, 8th Ed. Oliver and Boyd, London, 1964, pp. 249-289.
13. Gidigasu, M. D. Literature Review on the Formation and Morphological Characteristics and Lateritic Soils. Ghana Building and Road Research Institute, Kumasi, Proj. Rept. SM2, 1968.
14. Gidigasu, M. D. The Highway Geotechnical Properties of Ghana Soils. State Technical Univ., Warsaw, PhD thesis, 1969.
15. Gidigasu, M. D. Literature Review on the Engineering Characteristics of Laterite Soils. Ghana Building and Road Research Institute, Kumasi, Proj. Rept. SM7, 1970.
16. Hammond, A. A. A Study on the Engineering Properties of Some Lateritic Gravels From Kumasi District. Ghana Building and Road Research Institute, Kumasi, Proj. Rept. SM5, 1970.
17. Novais-Ferreira, H., and Correia, J. A. The Hardness of Lateritic Concretions and Its Influence in the Performance of Soil Mechanics Tests. Proc., Sixth Internat. Conf. on Soil Mech. and Found. Eng., Montreal, Vol. 1, 1965, pp. 82-86.
18. Engineering Study of Laterite and Lateritic Soils in Connection With Construction of Roads, Highways and Airfield. U. S. Agency for International Development, 1969.
19. Laterite Soil Study. Lyons Associates, Inc., Quarterly Rept. 1 to U. S. Agency for International Development, April 1969.
20. Laterite and Lateritic Soils and Other Problem Soils of Africa—An Engineering Study. U. S. Agency for International Development, 1971.

SIGNIFICANCE OF PRETESTING PREPARATIONS IN EVALUATING INDEX PROPERTIES OF LATERITE MATERIALS

M. D. Gidigasu and S. L. Yeboa, Building and Road Research Institute, Ghana

This study assessed the implications of the different degrees of dessication of the dry savannah zone and wet forest zone laterite minerals in Ghana in terms of the effect of pretesting preparations on some laboratory index test results. The study shows that wet forest zone materials and the deep-layer, dry savannah zone soils are more sensitive to drying than highly dessicated top soils from the dry savannah zone. The conclusions reached in the study have emphasized the danger inherent in writing specifications for field-compaction contracts based only on the laboratory tests carried out on air-dried samples. The study has also emphasized the usefulness of a method in which the final contract specification for field compaction is based on actual field trial compaction tests at the equilibrium moisture contents likely to exist during the life of the structure.

•STUDIES on the engineering properties and experiences of field performance of laterite materials have revealed a wide range of properties and have corrected the earlier misconception that all laterite materials have similar properties and are generally troublesome and undesirable highway and foundation materials. It has been amply demonstrated that the varied properties of laterite materials are due to their genesis, mineralogy, and environmental conditions.

Decomposition under temperate conditions of low-chemical and soil-forming activity does not continue past the clay-mineral forming stage, whereas under tropical rain forest conditions of high temperature and rainfall the clay minerals tend to decompose into various forms of oxides in relation to the nature of the weathering system. The climate, topography, and vegetation influence the weathering through their control of the character and direction of movement of water through the alternation zone and determine whether the weathering system and drainage conditions are productive of kaolinite, halloysite, illite, or montmorillonite type of mineral or some less known secondary minerals (20).

The anomalous engineering behavior, including sensitivity to drying, of some laterite materials has been shown to depend on the predominant clay mineral composing the clay fraction and the unique granular structure of these materials (14, 22, 16, 13, 33).

It is now well known that the free iron oxide content and the state of alumino-ferruginous complexes in the soil seem to underlie the deviation of engineering behavior of laterite materials from the expectations of conventional soil mechanics as developed (in Europe and North America) for the temperate zone soils (34, 22, 30).

Grant and Aitchison (15) on the basis of their experiences in Australia have suggested a positive distinction between dehydrated laterite materials in which the iron has been fully immobilized to the ferric state and the hydrated ones in which at least some of the iron is still mobile. In the first case the soil is inert and should be subjected to standard soil index tests, and in the second case the material has a stabilization prop-

Sponsored by Committee on Exploration and Classification of Earth Materials.

erty and should be tested as such in order to reap the greatest benefit from this property. Serious engineering and construction problems may arise through failure to distinguish between hydrated and dehydrated laterite materials.

In Ghana the grading and plasticity limits as well as procedures for field compaction are based on the specifications (28) used for the selection and compaction of subbase, base, and special fill materials. These specifications have been used indiscriminately for both the highly dessicated dry savannah and the nondessicated wet forest soils. However, observations on the behavior of pavements with similar traffic patterns in the 2 climatic-vegetational zones have revealed different levels of performance. The use of uniform field-compaction procedures in the 2 zones could partly account for different pavement-behavior patterns.

In this study, an attempt has been made to assess the implications of different degrees of dessication of the dry savannah zone and wet forest zone soils in the laboratory evaluation of some index properties of those soils. It is hoped that this study will lead to a better appreciation of the effect of pretest preparations on the laboratory test results of some laterite materials and the field engineering implications of the sensitivity to pretreatment procedures.

SOME ENGINEERING SIGNIFICANCE OF TROPICAL SOIL GENESIS

Extensive literature available on the chemistry and mineralogy of the processes of primary and secondary (laterization) weathering has revealed that the genesis of residual laterite materials may be divided into 3 stages. The first stage (primary weathering) involves the partial or complete physical and chemical breakdown of the parent rock and the release of small primary particles and iron and alumina gels. The second stage (secondary weathering or laterization) involves partial or complete leaching of bases and combined silica and after that the coating or coagulation and impregnation or both of the residuals by iron and alumina gels. The level to which the second stage has been carried out depends to a large extent on the weathering system. Under certain conditions, the weathering processes may be so intense and may continue for so long that even the clay minerals, which are primary hydrous aluminum silicates, are destroyed in the continued weathering; the silica is leached, and the remainder consists merely of aluminum oxide, such as gibbsite, or of hydrous iron oxide, such as limonite or goethite derived from the iron.

The third stage involves partial or complete hardening either in situ or on exposure to air of the sesquioxide-impregnated materials due to dehydration of the hydroxides of the iron and aluminum. The free iron oxide is believed to play a major role in the hardening of the laterite materials. It is believed that the state of the sesquioxide gels, the free iron oxide, and the mineralogy considerably influence the engineering behavior of the laterite materials (34, 22, 12, 14, 32, 16, 31). One major result of the tropical weathering and laterization is the formation of a unique granular or concretionary (or both) structure of these materials. Alexander and Cady (2) have postulated that the development of the structure of laterite materials is due to the mechanism involving the migration and segregation of the major constituents, and they have identified several structure patterns. The gelatinous colloidal oxides of iron and alumina contribute to the formation of a concretionary soil structure by coating and coagulation or flocculation of the clay, silt, or sand particles and the subsequent dehydration of the coagulated material into clusters (modules) and stable aggregates (19). D'Hoore and Croegaert (9) have described "pseudosilt" and "pseudosand" formations in Congolese soils. Oxide-coated clay particles are bound by alumino-ferruginous binding agents or organic complexes or both to form stable aggregates of silt size, which in turn may be compounded to form particles of sand size. Millard (18) has also reported the structure of halloysitic red clays of central and east Africa and the engineering implications of this property during soil compaction.

Laboratory studies backed by field experience with laterite materials (13, 18) have revealed that with some soils the structure is persistent and with others it breaks down when the soil is worked. Such soils are difficult to classify by textural tests because their properties are changed by manipulation during testing.

Laterite materials formed over basic rocks and volcanic ash or in regions of continuously wet climate (rainfall of more than 60 in. per year) are characterized by high natural water content, high liquid limits, and high contents of gibbsite, halloysite, and allophane types of minerals that undergo irreversible changes on drying. Two factors that are related but different caused changes in the properties with drying: (a) the tendency to form aggregations on drying and (b) the loss of water in the hydrated minerals. The tendency to form aggregations was perhaps first described by Hirashima (16) and later, in more detail, by Terzaghi (32) for the red clays at the Sasumua Dam site in Kenya.

The aggregating effect of free iron oxide in the Sasumua clay was later demonstrated by Newill (22). Newill removed the iron chemically and found that the aggregations had been dispersed. This did not reform as had been the case after mechanical manipulation. The Atterberg limits were determined before and after chemically removing the free iron oxide, and the plasticity was found to increase considerably.

The unique structure of some laterite materials has led to difficulties in achieving adequate dispersion during grading and sedimentation tests. Consistent results of variations in the particle-size distribution with method of pretesting preparations have been widely reported. Drying causes the particle size to increase such that much of the clay-sized material becomes the size of silt (19).

Regarding the effect of pretreatment, it was found, for example, that using sodium oxalate as a dispersing agent on typical halloysite clay (in Kenya) gave 20 to 30 percent clay fraction and that using sodium hexametaphosphate gave 40 to 50 percent clay fraction with the same soil (23).

The liquid limit of a typical red clay from Kenya was found to vary with the mixing time required to break all the aggregations caused by free iron binding (30).

The effect of the iron oxide in binding smaller particles into larger ones is considered to account partly for the successful performance under tropical conditions of road bases having a silt and clay content considerably higher than that accepted by ASTM standards. Terzaghi (32) and Newill (22) attributed the properties of low compressibility, high permeability, and high angle of shearing resistance of the Sasumua clay (in Kenya) to the iron content that bound the clay minerals existing in the form of tube-shaped crystals into aggregations.

Millard (18) and Bhatia and Hammond (3) also showed that the strength of concretionary aggregates (hardness) correlates well with the amount of iron enrichment. The higher the iron content is, the higher the specific gravity is (21, 23). The low colloidal activities in laterite soils has also been attributed to the existence of considerable iron in these soils (10). Tateishi (31) and Brand et al. (5) have described variations in the values of maximum dry density tests, depending on whether the tests were performed after air-drying or without air-drying, by determining the points backward along the moisture-density curve as the soil dries. This was confirmed by Quinones (26) on a variety of materials from South America and laterized micaceous materials from Liberia. The clay minerals of tropical weathering profiles that are most susceptible to changes in properties with drying are allophane (12, 14), halloysite, especially hydrated halloysite (12, 29, 32, 22), and gibbsite (12). These minerals generally occur either over volcanic extrusives or at locations where the rainfall is more than 60 in. per year. In a recent lecture on the engineering implications of tropical weathering and laterization, Peck (25) emphasized that, when dealing with laterite soils sensitive to drying, the engineer may need to determine the index and engineering properties on the basis of tests run at natural moisture content and again at various degrees of air-drying in order to evaluate fully the range of properties associated with the physical conditions that may prevail on the job.

SCOPE OF STUDY AND GENERAL CHARACTERISTICS OF MATERIALS

The aim of the study reported here was to contribute to the standardization of laboratory test procedures for laterite materials. The object of a standardization study is to establish on the basis of existing standards and new tests a set of test procedures that take into account the inherently genetic characteristics resulting from the processes

of tropical weathering and laterization and the different chemical and mineralogical contents formed in different environments. The application of such a system would involve the use of simple tests that yield reproducible results. Two approaches to this problem are readily obvious. The first one involves a long-term program of selection of physical properties indicative of engineering behavior of laterite materials and the establishment of suitable simple but reproducible tests for evaluating them. This approach seems more difficult and requires a lot of time. The second approach, which was adopted here, is to accept the standard laboratory tests as a basis for evaluating index properties and to select testing conditions that ensure reproducibility of the test results using these test procedures.

A major contribution to the study of laterite materials was perhaps an observation implying a reversible mobilization and immobilization of alumino-ferruginous complexes leading to the hardening and softening of laterite materials in oxidizing and reducing environments respectively (2). Moreover it seems that the state of the sesquioxides and in particular of the free iron oxide in laterite materials may underlie the anomalous engineering behavior of some laterite materials (32, 30, 22).

The study investigated the effects of drying, soaking, and kneading on the Atterberg limits of typical wet forest zone and dry savannah zone laterite materials; and the effect of drying and compaction procedures on the moisture-density curves of those materials. The nature and general characteristics based on pedological data of the soils studied are given in Table 1. The forest ochrosols (FO) and the savannah ochrosol-groundwater laterites (SO-GWL) cover more than 80 percent of the surface of Ghana and form the most important road-making materials in the wet forest and dry savannah zones of the country. A rough assessment of the degree of dessication (dehydration) in terms of average natural moisture contents (based on long laboratory experience) and field studies is suggested as follows:

1. Forest ochrosols are of low degree of dessication due mainly to the forest vegetation cover;
2. Surface (up to about 6 ft) materials in the savannah ochrosol and groundwater laterite areas are highly dessicated; and
3. Deeper (below 7 ft) materials in the savannah ochrosol-groundwater laterite areas are also of low degree of dessication.

SAMPLE PREPARATION AND TESTING PROCEDURES

The samples used in the Atterberg limit tests were subjected to the pretest treatment given in Table 2 .

The laboratory tests were carried out according to the specifications described in the British Standard 1377 of 1961. The British standard particle-size scale was adopted in the study. The samples were compacted according to the Ghana standard (samples are compacted in 5 layers in a CBR mold, each layer receiving 25 blows with a 10-lb hammer falling 18 in.). The soil types studied in the program are typical naturally occurring lateritic base (2FO, 1SO-GWL), subbase (1FO, 4FO, 2SO-GWL), and fill (3FO) materials in dry savannah and wet forest zones. The results of the identification, chemical composition, and loss-on-ignition tests on soil fractions (passing No. 200 British standard sieve) and the aggregate impact test results (British Standard 812) on gravel fraction are given in Table 3. The results of Atterberg limit tests on 24 samples from each site are given in Table 4; the data show that in terms of plasticity the wet forest zone soils as well as soils from a deeper layer in the dry savannah zone are similar. Materials from the shallow depth in the dry savannah zone (1SO-GWL) are less plastic than the rest probably because they have been highly dehydrated and dessicated in situ.

DISCUSSION OF TEST RESULTS

Effect of Preheating and Drying on Plasticity of Soils

The variation of Atterberg limits for the wet forest and dry savannah zone soils is given in Table 5 and shown in Figures 1 and 2. The wet forest zone soils (Fig. 1) are

Table 1. General characteristics of residual profiles studied.

Soil[a]	Climate[b]	Zone	Topography and Drainage	Parent Material	Nature of Weathering System	General Characteristics of Profiles
1FO 2FO 3FO 4FO	P = >50 in./year T = 70 to 89 F H = 83 percent E = P	Medium rain to semideciduous wet forest	Gentle undulating to strongly rolling; upland soils are well drained and highly leached	Intermediate to acidic rocks, peneplain drafts covering intermediate erosion surface and upland terrace alluvia	Acidic to neutral in residual profiles studied	High-level peneplain surfaces covered with aluminous (bauxitic) hardpans; clay fraction contains high proportion of sesquioxides and kaolinite; highly leached profiles; soils generally wet
1SO-GWL 2SO-GWL	P = 40 to 50 in./year T = 71 to 82 F H = 65 percent E > P	Deciduous woodland dry savanna	Undulating to very gently rolling; well drained over sandstones; drainage impeded over shales and mudstones	Sedimentary sandstones or sandstone-shale-mudstone deposits	Mainly acidic in residual profiles studied	Friable and porous materials over sandstone to clayey mottled materials over mudstone-shales; surface materials generally dry (dessicated); clay fraction rich in kaolinite and iron oxides

[a]FO = forest ochrosol, SO = savannah ochrosol, and GWL = groundwater laterite.
[b]P = precipitation, T = temperature, H = humidity, and E = evaporation.

Table 2. Pretest treatment of samples.

Test	Treatment	Code
Atterberg limit	Molded at natural moisture content	NMC
	Air dried, 4 days, 34 C	AD4
	Air dried, 4 days, and	
	Soaked 1 day	AD4 S1
	Soaked 2 days	AD4 S2
	Soaked 4 days	AD4 S4
	Soaked 7 days	AD4 S7
	Air dried, 4 days, and	
	Soaked 1 day and intermittently kneaded[a]	AD4 SK1
	Soaked 2 days and intermittently kneaded	AD4 SK2
	Soaked 4 days and intermittently kneaded	AD4 SK4
	Soaked 7 days and intermittently kneaded	AD4 SK7
	Air dried, 5 days	AD5
	Air dried, 5 days, and	
	Soaked 1 day	AD5 S1
	Soaked 2 days	AD5 S2
	Soaked 4 days	AD5 S4
	Soaked 7 days	AD5 S7
	Oven dried	
	6 hours, 50 C	OD6-50
	24 hours, 50 C	OD24-50
	6 hours, 100 C	OD6-100
	24 hours, 100 C	OD24-100
	Oven dried, 6 hours, 100 C and	
	Soaked 1 day and intermittently kneaded	OD6 SK1
	Soaked 2 days and intermittently kneaded	OD6 SK2
	Soaked 4 days and intermittently kneaded	OD6 SK4
	Soaked 7 days and intermittently kneaded	OD6 SK7
Compaction	Molded at natural moisture content with addition of water or subtraction by air drying	CT-NMC
	Air dried, 4 to 5 days, 30 C	CT-AD
	Oven dried, 24 hours, 105 to 110 C	CT-OD

[a]About 3 min with spatula.

Table 3. Index properties and chemical composition of soils.

Soil	Location of Profile	Grading			Plasticity[b] (percent)			Chem. Composition[a] (percent)			Aggregate Impact Value[c] (percent)	Loss on Ignition[a] (percent)
		Gravel Size (percent)	Sand Size (percent)	Silt and Clay[a] (percent)	WL	Wp	Ip	SO_2	Al_2O_3	Fe_2O_3		
1FO	Patasi Road	61	13	26	45	19	26	40.3	16	33.4	26.5	10
2FO	Barekese	70	9	21	31	15	16	56.2	7.7	19.4	27.9	7.0
3FO	Okodie Road	—	26.4	73.6	65	27	39	44.7	16.9	15.9	—	12.0
4FO	Kumasi-Bekwai Road	56	16	28	43	19	24	50.5	12.1	23.4	35	7.0
1SO-GWL	Tamale-Yapei Road	57	18	25	38	18	20	59	26.9	29.3	30 to 35	6.8
2SO-GWL	Tamale-Yapei Road	42	24	34	43	18	25	—	—	—	—	—

[a]Fraction passing No. 200 BS sieve. [b]Fraction passing No. 36 BS sieve. [c]British standard 812.

Table 4. Plasticity characteristics of soils.

Soil	Liquid Limit (percent)	Plastic Limit (percent)	Plasticity Index (percent)	Frequency (percent)
2FO	40 to 75	20 to 40	20 to 40	95
3FO	40 to 65	20 to 30	20 to 35	95
1SO-GWL[a]	40 to 50	20 to 30	20	95
2SO-GWL[b]	40 to 60	15 to 30	25 to 30	95

[a]0 to 6 ft. [b]7 to 9 ft.

Table 5. Effect of drying, soaking, and kneading on soil plasticity.

		Liquid Limit				Plastic Limit				Plasticity Index		
Soil	Treatment	X_M	X	X_m	σ	X_M	X	X_m	σ	X_M	X	X_m
3FO	NMC	72	65.0	56.8	5.94	28.0	27.2	26.2	0.76	44.8	38.8	30.1
	AD4	68.0	62.9	57.0	4.8	29.3	27.8	25.8	1.46	38.7	38.5	31.2
	OD6-50	62.5	58.3	54.8	3.7	31.0	29.4	27.9	1.48	31.5	28.9	26.9
	OD24-50	62.3	58.5	53.6	3.68	32.2	28.5	25.3	2.87	31.2	30.0	28.3
	OD6-100	52.0	49.4	46.8	2.33	25.5	24.4	23.8	0.77	26.5	25.0	23.0
	OD24-100	48.5	46.0	43.2	2.26	27.1	25.9	25.0	0.92	21.4	20.1	17.8
	AD4 S1	68.7	64.4	59.5	3.86	28.6	24.6	21.0	4.01	42.4	39.8	36.9
	AD4 S2	70.7	66.8	61.2	4.09	29.5	26.4	22.5	3.04	46.5	40.4	33.5
	AD4 S4	71.0	65.5	61.5	4.04	29.0	25.9	22.5	2.76	44.1	40.5	36.4
	AD4 S7	69.7	64.8	60.5	4.11	30.0	25.6	24.5	2.92	39.7	39.2	36.0
	OD6 SK1	63.5	59.4	55.0	3.70	31.0	28.4	20.5	2.0	32.5	31.0	25.5
	OD6 SK2	69.7	65.0	62.8	3.24	32.5	29.2	26.2	3.03	37.5	36.4	34.3
	OD6 SK4	67.8	63.3	60.3	3.21	29.5	26.4	23.3	2.62	38.3	36.9	36.0
	OD6 SK7	72.2	67.5	62.9	4.28	30.0	27.2	25.0	2.14	42.2	40.3	36.7
	AD4 SK1	69.5	65.0	61.2	3.88	29.5	26.8	24.2	2.39	40.0	38.2	37.0
	AD4 SK2	70.7	65.5	62.5	3.48	31.3	28.8	26.1	2.36	39.4	36.7	34.7
	AD4 SK4	69.6	65.8	61.2	3.56	32.2	29.2	16.6	2.47	37.4	36.6	34.6
	AD4 SK7	70.5	66.5	63.0	3.24	33.0	30.2	26.6	2.7	37.5	36.3	35.1
4FO	NMC	64.7	61.6	56.4	3.75	31.4	28.2	25.3	2.51	35.5	33.4	31.1
	AD4	50.0	53.4	49.7	2.67	29.3	25.5	22.5	2.87	30.0	27.9	26.7
	OD6-50	56.4	54.4	51.9	1.89	31.3	26.2	23.0	3.55	29.4	28.2	25.1
	OD24-50	56.5	53.9	52.5	1.84	28.6	24.8	20.0	3.84	32.5	29.1	27.2
	OD6-100	47.5	44.4	40.5	2.9	27.2	23.6	19.3	3.32	25.3	20.8	15.7
	OD24-100	44.5	42.7	40.7	1.60	27.5	23.8	20.2	3.97	24.0	18.9	13.2
1SO-GWL	NMC	60.4	56.1	52.8	3.18	26.8	23.8	21.3	2.41	33.6	32.3	31.5
	AD5	53.0	49.1	43.5	4.0	22.5	20.2	16.3	2.7	30.5	28.9	27.2
	OD6-50	52.5	48.5	45.0	3.3	22.3	21.1	17.8	2.1	30.5	27.4	27.0
	OD6-24	50.0	47.5	45.6	2.24	22.2	20.6	18.0	2.27	27.8	26.9	25.4
	OD6-100	46.2	44.1	41.5	1.99	20.5	19.3	17.5	2.86	25.7	24.9	24.0
	OD24-100	46.2	44.2	42.5	1.86	20.8	19.2	17.5	1.65	25.4	25.0	24.7
	AD5 S1	59.9	57.7	55.6	1.81	24.9	24.0	22.8	0.95	37.1	33.7	31.9
	AD5 S2	61.7	60.0	58.8	1.36	22.6	21.3	20.9	1.04	41.6	38.7	37.4
	AD5 S4	62.3	60.5	59.2	1.31	23.4	22.1	20.6	1.15	40.0	38.4	37.9
	AD5 S7	62.4	61.2	59.9	1.08	32.2	22.2	21.0	1.0	39.8	39.0	38.2
2SO-GWL	NMC	48.5	45.7	42.5	2.49	25.7	23.2	18.5	3.24	24.0	22.5	21.5
	AD5	47.3	44.2	40.0	3.08	26.2	23.5	20.5	2.42	23.6	21.4	19.5
	OD6-50	47.3	44.4	42.5	2.0	28.0	25.9	21.8	1.9	20.1	18.5	19.8
	OD24-50	47.3	44.4	42.0	2.4	28.0	25.9	23.2	2.08	20.1	18.5	16.1
	OD6-100	45.3	43.4	41.9	1.45	28.2	26.2	24.8	1.48	18.8	17.2	17.1
	OD24-100	47.0	44.4	41.3	2.34	27.5	26.1	24.5	1.34	19.5	18.3	16.8

Note: X_M = maximum value; X_m = minimum value; X = mean value; and σ = standard deviation.

more sensitive to drying and heating than the highly dessicated dry savannah zone materials from shallow depths. Materials from a deeper layer in the dry savannah zone (Fig. 2) are also more sensitive to drying than those from shallow depths. Oven drying at 100 C for 6 hours or more reduces the dispersion of the test results considerably. The plastic limit seems to vary little with preheating and drying methods. Figure 3 shows the variation of average values of liquid and plastic limits for some of the samples. The variation of liquid limit is almost nil for the highly dessicated material.

Effect of Soaking of Samples on Atterberg Limits

Table 5 also gives typical results of statistical analyses of data on the effect of soaking on the plasticity of typical wet forest and dry savannah zone soils. The maximum and minimum plasticity values and also the means and standard deviation values of the effect of soaking on the air-dried samples are not significant for wet forest zone soils. The Atterberg limits vary between the same range, and the standard deviation values are almost the same for different periods of soaking. There is a definite increase for the dry savannah zone soil when soaked for the different periods.

Effect of Soaking and Kneading on Atterberg Limits

Air-dried soils from the wet forest zone are not affected much by soaking and kneading. Samples preheated to 100 C and then soaked and kneaded showed appreciable variation. The soaking and kneading led to the breakdown of the artificial aggregation produced during heating, and this increased plasticity. Table 5 gives the results of statistical analysis of test data for typical wet forest zone samples. The wet forest and dry savannah zone soils react differently to preheating and drying methods as revealed by the results of Atterberg limit tests.

Wet forest zone soils are fairly sensitive to preheating and drying probably because there is very little dehydration of these soils in the wet environment. Dry savannah zone materials from shallow depths are not affected much by the preheating and drying probably because these materials are highly dessicated in the field and, hence, most of the dehydration has already taken place in situ.

Soaking and kneading have very little effect on the air-dried materials but affect preheated materials considerably, for some degree of dehydration and aggregation has occurred during heating.

Effect of Preheating and Drying on Compaction Characteristics

The oven drying consistently gave highest maximum dry densities and lowest optimum moisture contents for both the wet forest and dry savannah zone soils. Figures 4 and 5 show the effect of using fresh and reused samples. Figure 5 shows that materials from the deeper layer in the dry savannah zone vary widely among compaction characteristics with different pretreatment methods. Soils from the shallow depth in the dry savannah zone (highly dessicated materials) show practically no difference in compaction test results obtained on oven-dried and undried soils. Failure to recognize the effective depth of highly dessicated topsoil may lead to serious disparities between specified and obtained field compaction results.

Effect of Compaction on Particle Breakdown

The effect of the level of compaction on the degree of breakdown of concretionary laterite gravel fractions was also investigated. This was to explain why reuse of samples during compaction gave in some cases lower and in other cases higher maximum dry densities with corresponding optimum moisture contents. When the breakdown of particles led to improvement in grading, higher maximum dry densities were noted; and when the breakdown of particles led to poorer grading, lower maximum dry densities were noted. It was also found that the weak concretionary gravels do break down considerably, and that confirmed the need for a criterion for selecting laterite gravels based not only on the grading and plasticity characteristics but also on the strength of the coarse aggregates (7).

Figure 1. Effect of drying on Atterberg limits of 3FO soils.

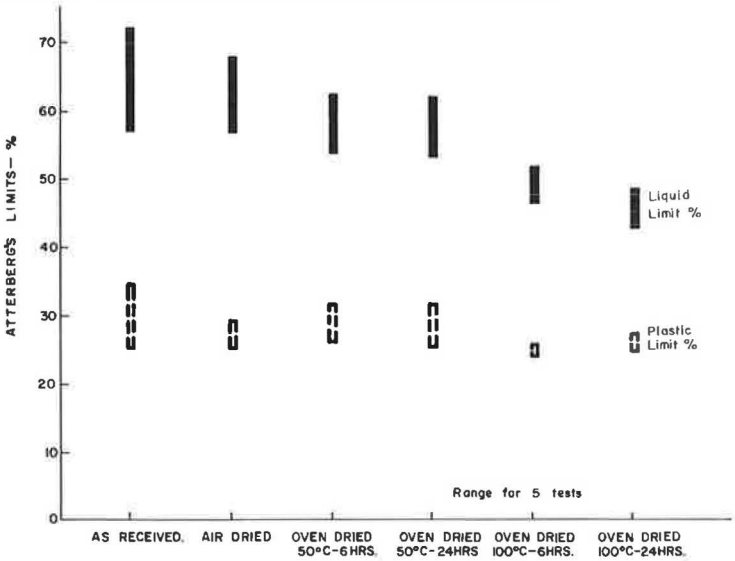

Figure 2. Effect of drying on Atterberg limits of 1SO-GWL and 2SO-GWL soils.

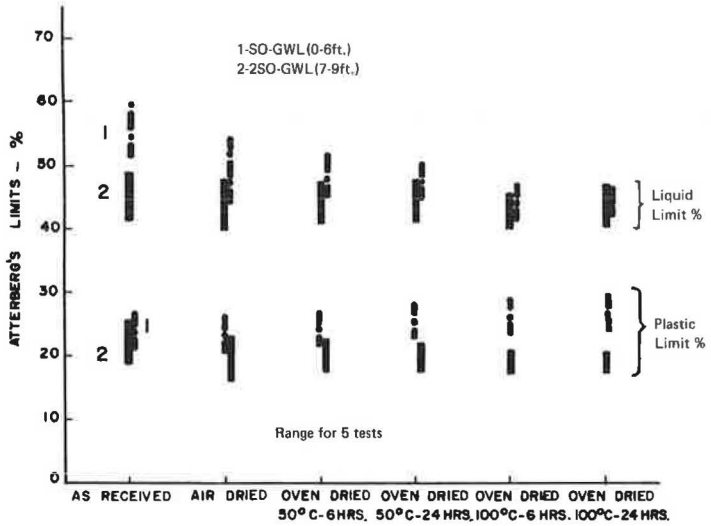

Figure 3. Effect of drying on mean Atterberg limits of 3FO, 4FO, 1SO-GWL, and 2SO-GWL soils.

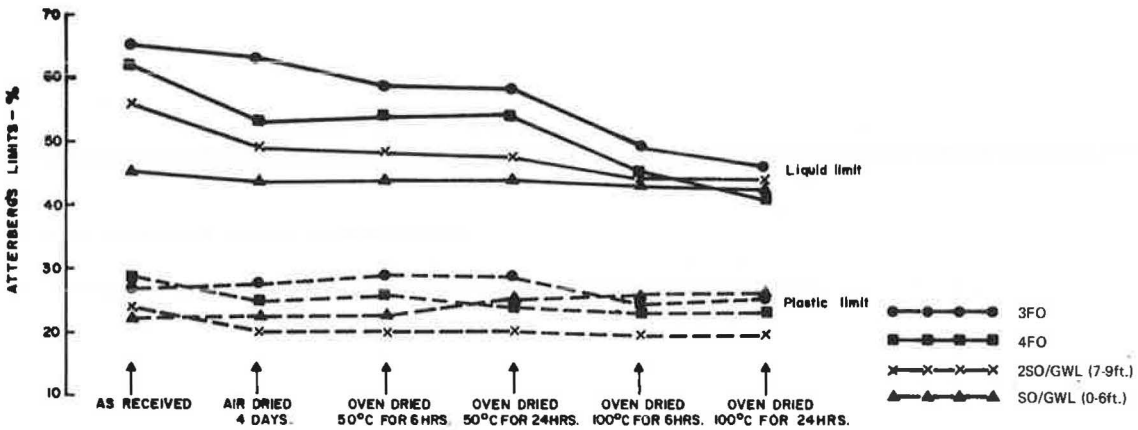

Figure 4. Moisture-density curves for 1FO, 2FO, and 3FO soils.

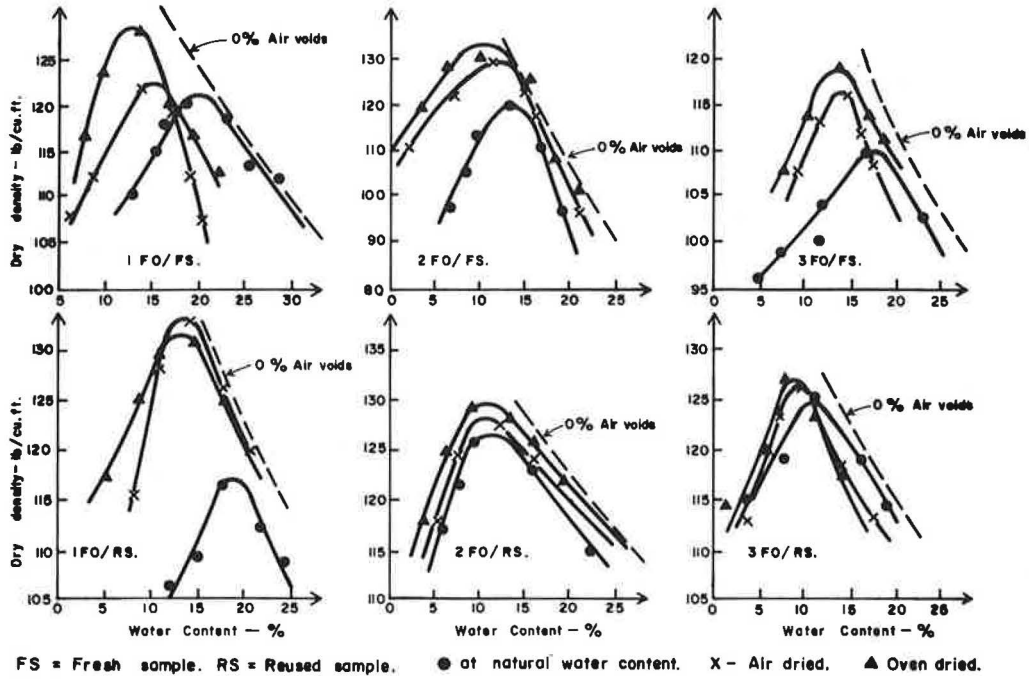

Figure 5. Moisture-density curves for 1SO-GWL and 2SO-GWL soils.

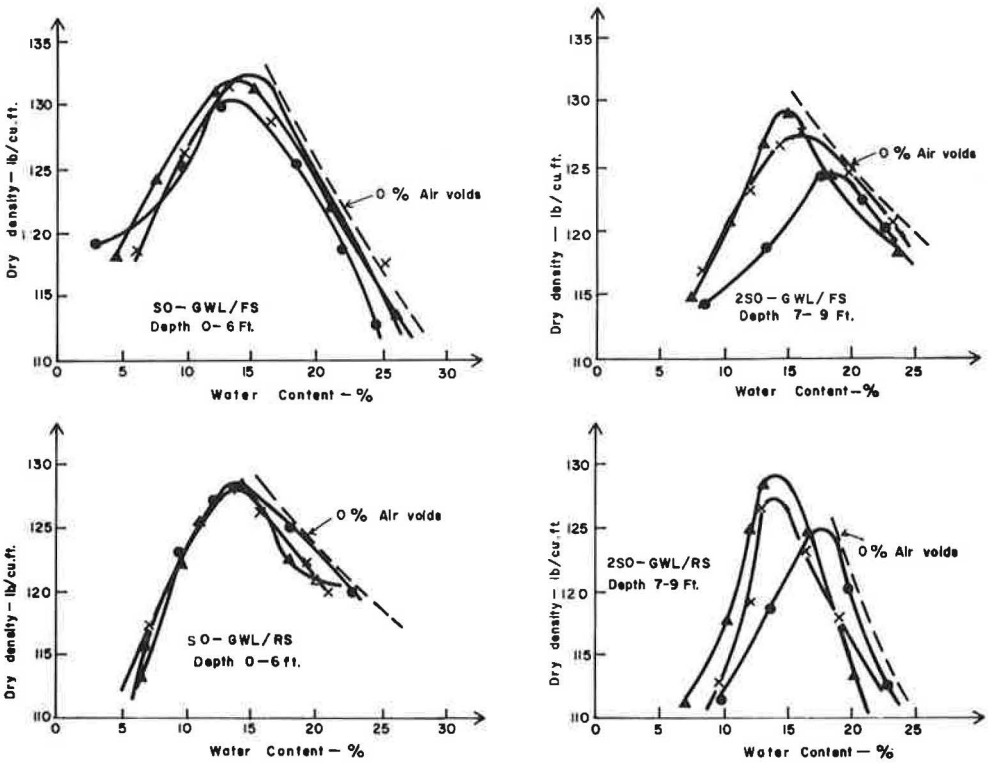

CONCLUSIONS

1. Highly dessicated shallow soils from the dry savannah zone react quite differently to heating and drying as well as to other pretesting preparation procedures than the less dessicated wet forest zone and deep dry savannah zone soils.
2. Although the less dessicated soils are highly affected by drying, the dessicated soils are not very much affected, as revealed by the variation of Atterberg limits with the preheating and drying methods.
3. The effect of soaking and kneading on Atterberg limits is very small in the case of air-dried wet forest soils and deep savannah zone soils. The difference in the effect of drying or preheating, soaking, and kneading on the Atterberg limits for the different soil types is attributed to the degree of in situ dehydration or dessication. The poorly dessicated soils are very sensitive to drying because of the relatively small in situ dehydration of the soils, and the highly dessicated (or dehydrated) soils are not very sensitive to drying. Because the dehydration (dessication) process seems to be associated with some degree of aggregation, the conclusions reached follow logically from the implications of the relation between dispersion and increase in liquid limit values.
4. With respect to moisture-density relations, it was found (as might be expected) that the oven-dried samples generally registered the highest maximum dry densities and corresponding lowest optimum moisture contents and that the soils compacted at natural moisture contents registered the lowest maximum dry densities and corresponding highest optimum moisture contents. The oven drying of samples before compaction is only of academic significance, but the relation between the oven-dried and natural moisture content compaction characteristics may be indicative of the degree of sensitivity to drying of a particular soil. Information like this will be useful for deciding the best laboratory test procedures to be adopted to simulate field moisture conditions likely to prevail on a job.
5. The reusing of samples during compaction led to either higher or lower maximum dry density with corresponding optimum moisture content depending on whether the breakdown of particles improved or worsened the grading curves. The degree of breakdown of gravel particles during compaction is a function of the strength of the aggregates, which may be assessed in terms of aggregate impact value or Los Angeles abrasion value.
6. The generalized approach to the evaluation and utilization of all laterite materials based on standard procedures can hardly be commendable. Each laterite material must be considered on its own merit. The degree of dessication or sensitivity or both to drying should be assessed vertically in the soil profile; and, after due consideration of genesis, mineralogical composition, and physicochemical processes that may occur when these materials are used in construction, tests should be designed that are appropriate to their nature.

ACKNOWLEDGMENTS

The work described in this paper is part of a long-term study on the engineering properties of laterite soils and was carried out as part of the laterite study sponsored by the U.S. Agency for International Development. The authors are grateful to J. W. S. de Graft-Johnson and H. S. Bhatia for their support during the study. The paper is contributed by permission of the Director of the Ghana Building and Road Research Institute.

REFERENCES

1. Ackroyd, L. W. The Engineering Classification of Some Western Nigerian Soils and Their Qualities in Road Building. Gt. Brit. Road Research Laboratory, Overseas Bull. 10, 1959, 32 pp.
2. Alexander, L. F., and Cady, J. G. Genesis and Hardening of Laterite in Soils. U.S. Dept. of Agriculture, Tech. Bull. 1282, 1962, 90 pp.
3. Bhatia, H. S., and Hammond, A. A. Durability and Strength Properties of Laterite Aggregates in Ghana. Ghana Building and Road Research Institute, Kumasi, Proj. Rept. SM9, 1970, 19 pp.

4. Birrell, K. S. Physical Properties of New Zealand Volcanic Ash Soils. Conf. on Shear Testing of Soils, Melbourne, 1952.
5. Brand, F. W., and Hongsnoi, M. Effect of Method of Preparation on the Compaction and Strength Characteristics of Lateritic Soils. Proc., Seventh Internat. Conf. on Soil Mech. and Found. Eng., Mexico, Vol. 1, 1969, pp. 107-116.
6. Correia, J. A., Antunes, A. M. C., and Teixeira, J. A. P. G. Results of Fractional Identification of Three Lateritic Gravels. Proc., Seventh Internat. Conf. on Soil Mech. and Found. Eng., Mexico, Vol. 1, 1969, pp. 37-51.
7. de Graft-Johnson, J. W. S., Bhatia, H. S., and Gidigasu, M. D. The Engineering Characteristics of Lateritic Residual Clays of Ghana for Earth Dam Construction. Symposium on Earth and Rockfill Dams, Nat. Soc. of Soil Mech. and Found. Eng., India, Vol. 1, 1968, pp. 94-107.
8. D'Hoore, J. L., and Fripiat, J. J. Tropical Clays and Their Iron Coverings. Proc., Second Inter-African Soils Conf., Leopoldville, 1954.
9. D'Hoore, J. L., and Croegaert, J. The Meaning of the Silt Fraction in Some Congo Soils. Proc., Second Inter-African Soils Conf., Leopoldville, 1954.
10. Dumbleton, M. Y., and Newill, D. A. A Study of the Properties of 19 Tropical Clay Soils and the Relation of These Properties With the Mineralogical Constitution of the Soils. Gt. Brit. Road Research Laboratory, unpublished Note LN/44, 1962.
11. Forster, C. R. Reduction in Soil Strength With Increase in Density. Trans., ASCE, 1957.
12. Frost, R. J. Importance of Correct Pretesting Preparation of Some Tropical Soils. Proc., First Southeast Asian Reg. Conf. on Soil Eng., Bangkok, 1967, pp. 43-53.
13. Fruhauf, B. A. Study of Lateritic Soils. HRB Proc., Vol. 26, 1946, pp. 579-593.
14. Gradwell, M., and Birrell, K. S. Physical Properties of Certain Volcanic Soils (From New Zealand). New Zealand Jour. of Sci. and Tech., No. 36B, 1954.
15. Grant, K. A., and Aitchison, G. D. Engineering Significance of Fericrete and Silcrete in Australia. Engineering Geology, Amsterdam, Vol. 4, 1970, pp. 93-120.
16. Hirashima, K. B. Highway Experiences With Thixotropic Volcanic Clay. HRB Proc., Vol. 28, 1948, pp. 481-496.
17. Portuguese Studies on Engineering Properties of Lateritic Soils. Seventh Internat. Conf. on Soil Mech. and Found. Eng., Mexico, Vol. 1, 1969, pp. 85-96.
18. Millard, R. S. Road Building in the Tropics. Jour. of Applied Chemistry, London, Vol. 12, 1962, pp. 342-357.
19. Moh, S. C., and Maxhar, F. M. The Effects of Method of Preparation on Index Properties of Lateritic Soils. Proc., Seventh Internat. Conf. on Soil Mech. and Found. Eng., Mexico, Vol. 1, 1969, pp. 23-35.
20. Mohr, E. C., and Van Baren, F. A. Tropical Soils. Interscience, New York, 1954, 498 pp.
21. Nascimento, U., De Castro, E., and Rodrigue, M. As Laterites de Ultramar Portugues. Lisbon, Memoria 141, 1964. (In Portuguese.)
22. Newill, D. A Laboratory Investigation of Tropical Red Clay From Kenya. Geotechnique, Vol. 11, 1961, pp. 303-318.
23. Novais-Ferreira, H., and Correia, J. A. The Hardness of Lateritic Concretions and Its Influence in the Performance of Soil Mechanics Tests. Proc., Sixth Internat. Conf. on Soil Mech. and Found. Eng., Montreal, Vol. 1, 1965, pp. 82-86.
24. Novais-Ferreira, H., and Meireles, J. M. F. The Influence of Temperature of Humidification on the Geotechnical Properties of Lateritic Soils. Proc., Seventh Internat. Conf. on Soil Mech. and Found. Eng., Mexico, Vol. 1, 1969, pp. 65-74.
25. Peck, R. B. Engineering Implications of Tropical Weathering and Laterisation. Seminar on Laterite and Other Problem Soils of Africa, Univ. of Science and Technology, Ghana, Jan. 1971.
26. Quinones, P. J. Compaction Characteristics of Tropically Weathered Soils. Univ. of Illinois, PhD thesis, 1963, 171 pp.

27. Remillion, A. Road Research in French Speaking African Countries. Technical Institute for Public Works and Buildings, Paris, No. 231-232, 1967, pp. 366-388. (In French.)
28. Soil Mechanics for Road Engineers. Gt. Brit. Road Research Laboratory, Her Majesty's Stationery Office, London, 1952.
29. Salas, J. A. J. Note on a Halloysite From Fernando Po Island. Proc., Third Reg. Conf. for Africa on Soil Mech. and Found. Eng., Salisbury, Southern Rhodesia, Vol. 1., 1963, pp. 85-88.
30. Sherwood, P. T. Classification Tests on African Red Clays and Keuper Marl. Quarterly Jour. of Engineering Geology, London, Vol. 1, No. 1, 1967, pp. 47-55.
31. Tateishi, H. Basic Engineering Characteristics of High Moisture Tropical Soils. Proc. WASHO conf., 1967, 19 pp.
32. Terzaghi, K. Design and Performance of the Sasumua Dam. Institution of Civil Engineers, London, Proc., Vol. 9, 1958, pp. 369-394.
33. Townsend, F. C., Manke, G. P., and Parcher, V. Y. Effects of Remolding on the Properties of a Lateritic Soil. Highway Research Record 284, 1969, pp. 76-84.
34. Winterkorn, H. F., and Chandrashekharan, E. C. Laterite Soils and Their Stabilization. HRB Bull. 44, 1951, pp. 10-29.

REGIONAL APPROACH TO HIGHWAY SOILS CONSIDERATIONS IN INDIANA

William J. Sisiliano, Indiana State Highway Commission; and
C. W. Lovell, Jr., Purdue University

It is hypothesized that a regional or physiographic subdivision approach can be effectively used in preliminary studies and investigations generally to predict the environment and to formulate the major soils problems to be considered in the design of a highway facility. Both generalized and specific quantifications of significant factors influencing a regional approach to highway soils considerations have been proposed. Available data from physiography, geology, pedology, remote sensing, and engineering soils mapping were used in the general approach. Data were compiled from completed Indiana State Highway Commission projects and roadway soil surveys performed by consultants, and statistical methods were applied to some of these data in the specific approach. If the findings and conclusions of this study are to be of practical consequence, they must be interpreted in terms of the present standards, policies, and procedures concerning roadway soil surveys used by the Indiana State Highway Commission. The physiographic subdivision approach is capable of contributing significantly and economically in the preliminary stages of planning, route location, and design of highway facilities in Indiana. Within the soil parent material areas in Indiana, the classes and severity ratings of highway soils problems can probably be generalized with confidence. This was accomplished for the Calumet Lacustrine Plain, a subsection of the Northern Lake and Moraine Region. The same procedure can be applied to the other physiographic units to provide similar information of practical value to the Indiana State Highway Commission.

• AMONG the factors to be considered in the planning, location, design, and construction of highway facilities are the soil and rock conditions within the corridor of the proposed route. These conditions are inherently complex and will need to be studied in detail before certain design and construction decisions are reached. However, there is considerable logic in deriving a generalized description of them prior to assessing details. This can be accomplished by examination of the factors of origin, parent material, topographic expression, and climatic environment. If the engineer has experience on projects where these general factors were similar, even though geographically removed from the route under study, he has a valid basis for the transfer of that experience. In other words, he can anticipate the likely challenges of the new project. A recognition of these interrelations and a concise recording of them will allow even an inexperienced engineer to exercise valuable insight. All of this occurs at the preliminary stage of investigation and is intended to enhance the interpretation of detailed physical studies, as opposed to replacing the studies.

As suggested above, the descriptors that appear most significant in a generalized assessment of route conditions are the geologic origin and complexity of the parent materials, the topographic expression, and the general texture of the soil, particularly clay content. The topographic expression is conveniently characterized by the branch

Sponsored by Committee on Exploration and Classification of Earth Materials.

of geology known as physiography or regional geomorphology, which defines units of unique landform combinations based on factors of structure, process, and stage. Therein lies the basis for the regional or physiographic subdivision approach. The physiographic units of Indiana adopted for this study are based on those defined by Malott (13), as shown in Figure 1. A further subdivision to the landform or an engineering soil parent material area level is needed to characterize the geologic origin and complexity of the soil parent materials and to afford a measure of the soil distribution throughout the physiographic region. Soil and landform maps (1, 25) were used for this purpose. The general texture of the soils is described by various soil index properties, which must be determined by physical tests.

PURPOSE

The objective of this paper is to show that a regional or physiographic subdivision approach may be effectively used in preliminary studies and investigations to predict the general soil and rock environment and to provide significant insight into the kinds of problems to be anticipated in the design and construction of a highway facility. A future goal is to indicate how the approach can be integrated into the present Indiana State Highway Commission's standards, policies, and procedures for performance of roadway soil surveys. In addition to the generalizations possible at the physiographic unit level, variability of soil characteristics was assessed for significant landforms within one unit. The purpose was to ascertain the variability of soil conditions within a landform and to frame correlative equations for selected soil characteristics for the landform unit.

That class of soils considerations peculiarly related to pavement design and construction has been omitted from this study because of its specialized nature and the complex and highly relevant soil-structure interaction effects.

GENERAL BACKGROUND

Physiography

As stated by Witczak (26):

> In the simple view, physiography permits subdivision into areas of contrasting or distinctive topographic expression. Such division is effected by an examination of three geomorphic control factors, viz., structure, process, and stage [22].
>
> Structure is a comprehensive term defined [by Thornbury, 22] as "... all those ways in which earth materials out of which landforms are carved differ from one another in their physical and chemical attributes." In a sense, structure expresses the type and arrangement of parent materials.
>
> Process describes the factors of origination and modification primarily responsible for the landscape. Processes may act constructively or destructively and may originate above the earth surface (e.g., wind, water, ice) or below it (viz., diatrophism or vulcanism). Thus process may be interpreted as origin.
>
> The operation of process upon structure in the development of the landscape involves various evolutionary phases or stages. Thus, this term conveys the notion of time of aging under ambient climate conditions, or the factor of age.
>
> In summation, the topographic expression is a function of the geologic parent material, the geomorphic processes acting, and the time and climate of action. These factors are highly relevant to landscape classification for engineering purposes, although they are probably not sufficiently quantified.

A physiographic unit is characterized by a mode of topographic expression that is different from those of adjacent units. However, certain variations from the modal pattern occur, and these variants are included as a matter of necessity. It is, therefore, logical that the physiographic subdivision becomes more "homogeneous" as the division becomes more limited in size. Malott (13) recognized this about 50 years ago when he outlined the basic physiographic subdivisions of Indiana and described them in considerable detail.

The state of Indiana lies physiographically within the Central Plains Province of North America as determined by Atwood (3). In the classical scheme of Fenneman (8), the maximum extent of glaciation is the boundary between the Till Plains Section of the Central Lowland Province and the Highland Rim and Bluegrass Section of the Interior Low Plateau Province to the south. Approximately the northern fourth of the state lies within the Eastern Lake Section of the Central Lowland Province.

Wayne (22) states that Indiana can generally be divided into 3 broad physiographic divisions trending in an east-west direction across the state. The central division, comprising about one-third of the state area, is a depositional plain of low relief, underlaid largely by thick glacial till and modified only slightly by postglacial stream erosion. It is called either the Central Drift Plain or the Tipton Till Plain.

The northern division is called the Northern Lake and Moraine Region and comprises slightly less than one-fourth of the state area. It is divided into 5 subdivisions, as shown in Figure 1. The northern division is characterized by greater relief than the central division, being very hilly in some areas; but even in those areas, the uplands are interrupted by lowlands and plains of little relief. Landforms in this division are mostly of glacial origin. A large variety of depositional forms are present, including end moraines, outwash plains, kames, lake plains, valley trains, and kettles; also present are many related postglacial features such as lakes, sand dunes, and peat bogs.

The roughest topography in Indiana is formed in the southern division, which is divided into 7 subdivisions (Fig. 1). Landforms in this division are primarily the result of normal degradational processes, such as weathering, stream erosion, and mass movement. The middle part of the southern division was not glaciated, and the topography strongly reflects the nature of the parent bedrocks. The units on either side were glaciated, but the influences of glaciation were minor, and the physiography is largely bedrock controlled. An exception in part is the Wabash Lowland where many lacustrine areas, valley trains, and outwash plains have developed as a result of glacial activity.

Geology

Most of the surface of Indiana has been glaciated to varying degrees by the various continental glacial advances. The south central portion of the state was not affected by the sculpturing effects of the ice sheet; thus, the topography, drainage, and soils have been formed through the weathering of the Paleozoic sediments. Wayne (25) shows the various glacial formations and landforms throughout the state. The lacustrine deposits resulting from Illinoian and Wisconsin glacial stages are mapped in some detail by Thornbury (29). A map of the thickness of drift north of the Wisconsin glacial boundary has been prepared by Wayne (24).

An excellent and thorough account of the bedrock geology and stratigraphy is presented by Cummings (7). The various bedrock formations along with their areal extent and several typical bedrock cross sections are shown by Parvis (16). Bedrock physiographic units as shown by Wayne (24) were originally developed by Malott (13). The bedrock physiographic units in southern Indiana generally have north-south boundaries that conform to the physiographic subdivisions previously discussed. It can be clearly seen, by comparison, that the east-west boundaries for the bedrock units extend much farther north, reflecting the subsurface geology. It can also be seen that the northern bedrock physiographic units have lateral limits very much modified from the previously discussed physiographic units. The dominant lithologies of the various bedrock physiographic units are given by Wayne (24). The formations and geologic age of these consolidated deposits are detailed by Cummings (7) and by McGregor (14).

Pedology

The pedologic approach to classification and distribution of Indiana soils (4, 6, 10, 19, 23, 27) and maps of the pedologic soil associations and soil series descriptions (1) are given in various reports. The Soil Conservation Service (SCS) has prepared the following 4 tabulations of soil indexes and interpretative ratings of those soils for various related fields of interest and practical applications: brief description of soils of

Indiana and their estimated physical and chemical properties, interpretation of the soils in Indiana for rural and urban development, interpretations of engineering properties of major soils in Indiana, nonagricultural (urban), interpretation of engineering properties of major soils in Indiana for agriculture. In addition, modern SCS county soil surveys contain simple engineering soil data.

Remote Sensing

Aerial photographic interpretation has been the dominant tool in the preparation of county engineering soils maps. These maps are available for many counties in Indiana, and have been summarized by McKittrick (15). Several other reports were very useful in this research (4, 9, 15, 17). Other excellent reports have been prepared as a part of the Joint Highway Research Project for air-photo interpretation of some major parent material regions in Indiana. These have also been summarized by McKittrick (15).

Engineering Soils

The mapping of soils and rocks depends most strongly in its form on the scale and the perspective and objective of the mapper. All maps are generalizations, and the smaller the scale is the greater is the degree of generalization. All mapping needs to be based on descriptors that are relatively simple and easy to determine. The descriptions chosen by the engineer are those that are both convenient and highly useful for framing the general nature of design and construction problems. Such maps provide valuable insight for preliminary studies such as locating a route and setting up a boring program for any given project. On occasion they may substitute for field studies, e.g., where the latter do not appear economically justifiable.

An outstanding effort to map and describe the soils of Indiana, drawing heavily on available pedologic data, was made by Belcher, Gregg, and Woods (4). This work led to a map of the engineering soil parent materials of Indiana (5).

As previously mentioned, certain county engineering soils maps have been prepared through interpretation of black and white aerial photography, usually supplemented by limited boring, sampling, and testing. As might be expected, the county maps give more detail because of the larger scale.

GENERALIZED QUANTIFICATION OF SIGNIFICANT FACTORS INFLUENCING REGIONAL APPROACH

Several original procedures were used generally to quantify the distribution of soil parent material areas or landforms within each physiographic region. Other related factors were also investigated.

A first and obvious step in generalized quantification was to compare the state physiographic regions with other state maps depicting topography, geology, pedologic units, engineering soil parent material areas, and thickness of drift. All of these maps were readily available. The comparisons are described in some detail below.

Topography

The topographic map by Logan (12) has a 100-ft contour interval and a scale of approximately 1:500,000 or about 1¼ in. to 10 miles. It is the largest scale state topographic map known to the authors. Because topography is considered to be a major factor, it was analyzed for each physiographic subdivision in a number of ways; e.g., the frequency distribution of elevation was defined. Areas within defined elevation intervals were planimetered, and curves of terrain elevation interval versus percentage of physiographic region were prepared. The curve obtained for the Calumet Lacustrine Plain is shown in Figure 2. Curves obtained for this phase of the study were typically of 3 types.

1. A high peak or mean value for percentage of physiographic region and a narrow range for terrain elevation interval characterize this group. Slight local relief and minor topographic expression are generally implied, i.e., almost level to gently undulating terrain.

2. Such curves have a moderate to high peak or mean value for percentage of physiographic region and a moderate to wide range for terrain elevation interval. Moderate variations in local relief and moderate topographic expression, viz., gently undulating to rolling terrain, are indicated.
3. A small to moderate peak or mean value for percentage of physiographic region and a wide range for terrain elevation interval characterize these curves. Large variations in local relief and major topographic expression are implied, i.e., rolling to rough terrain.

Thickness of Drift North of Wisconsin Glacial Boundary

The thickness of drift map was prepared by Wayne (24). The scale of this map is 1:500,000, or approximately 1¼ in. to 10 miles, and a contour interval of 50 ft is used. The thickness of unconsolidated deposits in Indiana south of the Wisconsin glacial boundary has not been mapped to the present time. Because depth to bedrock or thickness of drift is an important factor for many engineering projects, a frequency distribution of depth was developed for each physiographic region. Areas between defined depth intervals were planimetered and distribution curves drawn. These curves show the drift depth interval versus percentage of physiographic region. The curve obtained for the Calumet Lacustrine Plain is shown in Figure 3. Curves obtained for this phase of the study were typically of 2 types.

1. These curves showed an approximate normal distribution, with low percentages for extreme values and a peak at about the distribution mean. Such curves generally indicate the bedrock is well covered and will be encountered infrequently in an average project.
2. These distributions are skewed to the left; i.e., the curve peaks near the left extreme instead of near the mean value. Because the left extreme is the drift depth interval of 0 to 50 ft, bedrock may be encountered more than occasionally on an average project. The probability of encountering bedrock on a project is dependent on the actual percentage for the 0- to 50-ft interval and to a lesser extent on the percentage for the 50- to 100-ft interval.

Engineering Soil Parent Material Areas

A map of the engineering soil parent material areas was issued in 1943 (5) and revised in 1950. The scale is approximately ¾ in. equals 10 miles. The physiographic subdivisions were outlined on this map, and the area of each engineering soil parent material occurring within a physiographic region was planimetered. This information has been plotted and is shown in Figure 4 for the Calumet Lacustrine Plain.

Glacial Geology

The map of the glacial geology of Indiana was prepared by Wayne (25) in 1958. The scale is 1:1,000,000 or approximately ⅝ in. equals 10 miles. It shows the predominant soil areas of glacial origin for the glaciated part of the state. Again frequency distribution bar graphs were plotted, and the information for the Calumet Lacustrine Plain is shown in Figure 5.

Pedology

A map of Indiana soils (1) shows soil regions (parent material areas) and associations of soil series within the regions. In many areas of the state, the boundaries for the soil regions correspond to the boundaries given by Belcher, Gregg, and Woods (4), who emphasize the probable utility of such mapping for engineering purposes. The four tables prepared by the Soil Conservation Service are helpful in interpreting the pedologic mapping for engineering applications. The physiographic subdivisions were transferred to the state pedologic map, and the area of each series association within a physiographic region was planimetered. This information is shown in Figure 6 for the Calumet Lacustrine Plain.

Figure 1. Physiographic regions based on topography.

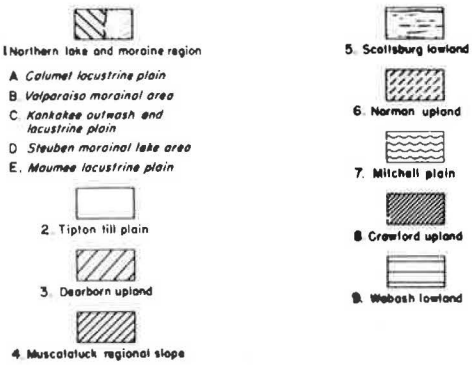

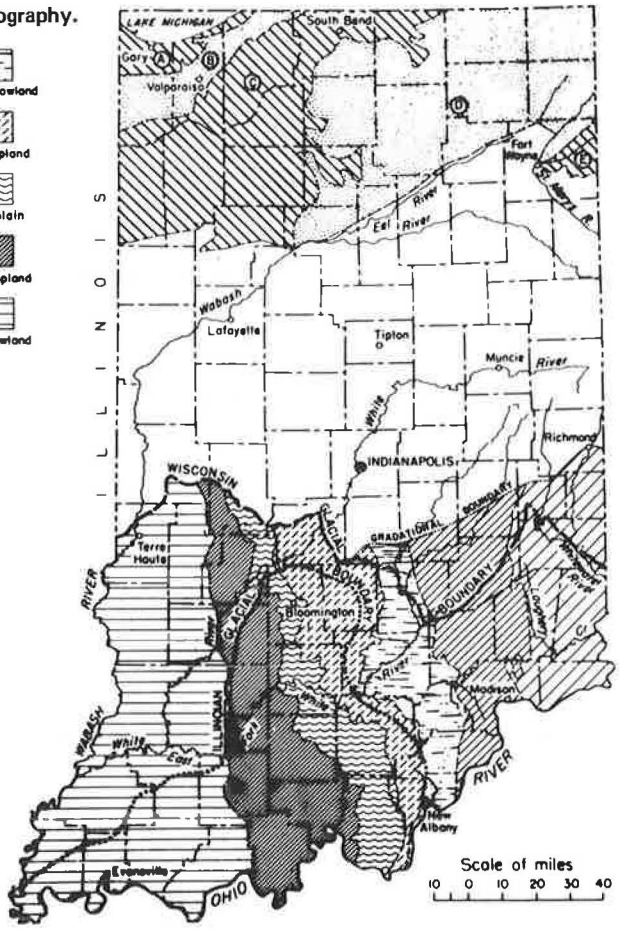

Figure 2. Terrain elevation interval for Calumet Lacustrine Plain.

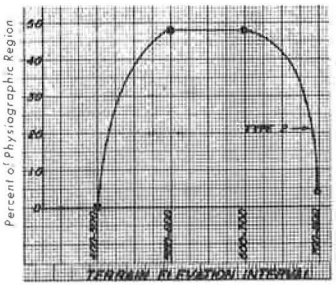

Figure 3. Drift depth interval for Calumet Lacustrine Plain.

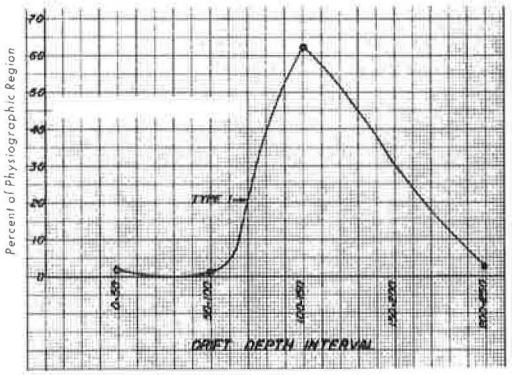

Figure 4. Engineering soil parent material in Calumet Lacustrine Plain.

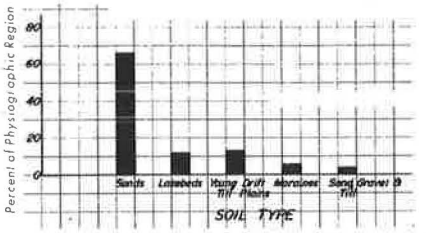

Figure 5. Glacial soils in Calumet Lacustrine Plain.

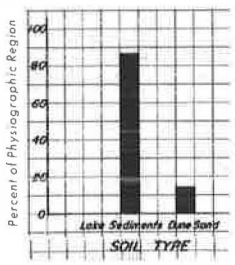

Figure 6. Soil regions and series association numbers for Calumet Lacustrine Plain.

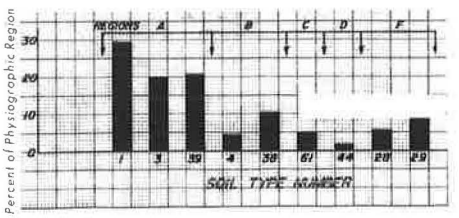

Earthwork Quantities by Physiographic Regions

A further generalized quantification involved tabulating the earthwork quantities for Indiana highway projects within each physiographic region for Interstate, primary, and secondary roads. Only those relatively recent projects for which data were readily available were used. A portion of the plotted data for the Interstate projects is shown in Figure 7. These data serve as indicators of topographic variation or roughness of terrain. However, they are also a function of the standard requirements for alignment, grade, and geometry of roadway cross section for the various classes of projects. An earthwork factor was defined as E, percent = [special borrow per mile/(special borrow per mile + excavation per mile)] × 100. The earthwork factor for the Calumet Lacustrine Plain was 96 percent for Interstate highways.

Aggregate Availability and Use Data

Rock quarry and sand and gravel pit data were also prepared for each physiographic region. The data may be used as indicators of (a) the occurrence of valley train and outwash plain sediments and (b) the occurrence of carbonate bedrock at relatively shallow depths.

Slope Instability

A survey of highway slope failures was conducted and analyzed with respect to the physiographic subdivisions (Table 1). The "normalization" of failures (square miles per failure) with respect to subdivision area is a convenient but approximate technique. The data given in Table 1 do indicate, however, that the parent materials and other environmental factors are more conducive to slope instability in some subdivisions than in others.

Other Aspects

At this point, let us consider the relative uniformity that is exhibited by the various physiographic subdivisions with respect to factors considered for generalization.

The relative percentages of significant soil parent material areas in the physiographic regions can be viewed as a first measure of uniformity. The logic of this premise can be illustrated by the following example. Consider the circumstance of a small number of significant soil parent material areas or landforms in a physiographic region (Figs. 4 and 5). "Significant" areas are those comprising more than 5 percent of the total physiographic region. Where the relative percentages are high, only a few soil parent material areas are present, and those are presumably repeating in a common or dominant pattern. This situation is viewed as a relatively uniform one. Such a first approximation of uniformity is shown by data given in Table 1, where 4 general ratings have been established.

A second degree of measure of uniformity within a physiographic region involves the soil series associations encountered within the soil parent material areas or landforms. Consider the data shown in Figure 6. A small number of significant associations within a soil parent material area are interpreted to mean a high degree of uniformity.

SPECIFIC QUANTIFICATION OF SIGNIFICANT FACTORS INFLUENCING REGIONAL APPROACH

As stated previously, the significant factors influencing a regional approach to highway soils considerations are the geologic origin and complexity of parent materials (or landforms), the topography, and the texture of the parent materials (particularly the percentage of the clay fraction). This section presents an approach for handling these factors in some detail.

Distribution of Interstate Mileage Within Physiographic Regions, Landforms, and Soil Types

The Interstate highway mileage within each landform or numbered soil area was determined as a percentage of the total Interstate mileage within the physiographic region.

Figure 7. Earthwork quantities by physiographic regions for Interstate projects.

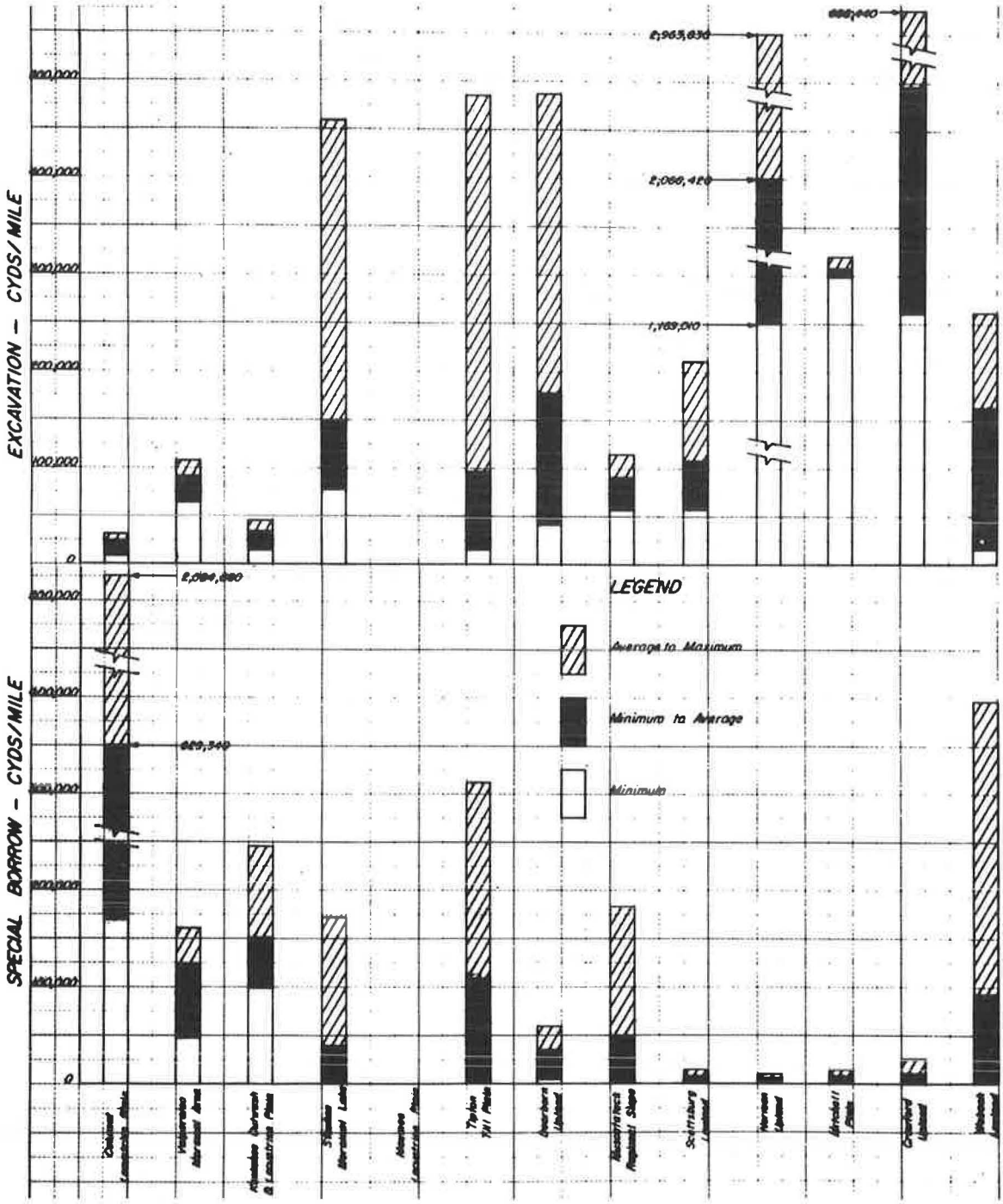

These data tend to answer the question, What landforms, soil types, or soil type numbers do existing or designed highways traverse? With this information, one can speculate as to the nature of the soils considerations and whether their magnitudes could be lessened by relocating routes to more desirable landforms. Economics is the criterion, and both initial cost and maintenance costs should be included. The information is included in detail in the original study (18).

Roadway Soil Survey Data for Cuts by Physiographic Region

One can make some very effective inferences about the nature of the terrain, the adequacy of standard design backslopes, and the amount of rock excavation required on a given project if one has a summary of the cut information for other projects in the same region. Therefore, a detailed study was made of the proposed cuts in the roadway soil surveys. Numerous cut statistics have been developed and included in the original study (18). The inferences that can be made are that (a) fewer cuts and shallower depth of cuts indicate more level terrain; (b) shallower average depth of cuts implies more stable backslopes; and (c) frequency of rock cuts is uniquely related to the physiographic region. The bedrock information is especially useful south of the Wisconsin glacial boundary, where thickness-of-drift maps are not applicable.

Specific Terrain Quantification Factors for Physiographic Regions

Several terrain descriptors were determined for the terrain elevation interval curves: coefficient of variation, V, in percent, and topographic coefficient, T, in percent, defined for the purpose of this study. These values were calculated for the curves obtained for each physiographic region and are given in Table 1. The significance and usefulness of these results are given in Table 2. The limits set for these values can be used to predict the general soil origin.

Typical Profiles and Physical Properties of Soils for Significant Landforms Within Physiographic Regions

Some degree of uniformity or frequency of occurrence for the soil types encountered within each significant landform within a physiographic region was demonstrated by typical profiles that were developed for the Calumet Lacustrine Plain. The data for the physical properties of the soils composing each significant landform were subjected to statistical methods and procedures in an attempt to characterize each significant layer or stratum within each typical profile. In addition to a typical profile, some pertinent relations and regression equations have been developed.

Typical Profiles—Typical profiles were prepared for each of the 3 significant landforms or soil parent material areas, as defined by the map of engineering soil parent material areas in Indiana, in the Calumet Lacustrine Plain. "Significant" has been defined as more than 5 percent of the physiographic region area. Thus, typical profiles were prepared for the dune sand, lake-bed, and ground moraine (Wisconsin) areas, which constitute about 66, 12, and 13 percent respectively of the approximate 279 square miles.

One needs to make use of all conveniently available sources to avoid erroneous conclusions. For example, consider the large area shown as dune sand on the map of engineering soil parent material areas in Indiana (5). If we consider this information, along with that on the map of Indiana soils (1), the impression is gained that sand is the engineering material. (Pockets, layers, and lenses of peat, marl, and other organic soils are expected in the depressions between the sand dunes.) However, the entire soil parent material area shown as dune sand is underlaid by a deep deposit of lacustrine sediments from glacial Lake Chicago, consisting of compressible fine-grained soils. This fact would be evident from the map of glacial geology of Indiana (25). The consolidation of these underlying deposits due to superimposed loading might well control the design of many facilities.

An important part of the typical profile is the statistical soil classification, which is based on average values for the pertinent physical characteristics used in the textural

Table 1. Measures of regional uniformity for physiographic regions.

Physiographic Region	Slope Failure			Coefficient of Variation (percent)	Topographic Coefficient (percent)
	Number	Square Mile per Failure	Rating[a]		
Northern Lake and Moraine Region					
Calumet Lacustrine Plain	0	—	II	22.5	9.6
Valparaiso Morainal Area	1	619	I to II	17.4	7.8
Kankakee Outwash and Lacustrine Plain	0	—	IV	23.6	10.6
Steuben Morainal Lake Area	2	1,842	III	23.8	8.3
Maumee Lacustrine Plain	0	—	I	0	100.0
Tipton Till Plain	1	13,435	II to III	22.8	3.7
Dearborn Upland	16	114	III to IV	29.8	2.4
Muscatatuck Regional Slope	0	—	III	25.8	3.1
Scottsburg Lowland	4	373	IV	25.3	5.0
Norman Upland	2	617	III to IV	26.5	2.9
Mitchell Plain	2	647	III	19.3	5.2
Crawford Upland	10	243	II to III	27.2	3.1
Wabash Lowland	3	1,646	IV	26.0	7.2
Total	41				

[a]For first degree of uniformity for soil parent material areas within each physiographic region: I = very uniform, 1 to 2 significant landforms; II = uniform, 2 to 3 significant landforms; III = slightly uniform, 3 to 4 significant landforms; and IV = complex, 5 or more significant landforms.

Table 2. Terrain quantification factors for physiographic regions.

Coefficient			Physiographic Regions		
V[a]	T[b]	Topography	V	T	Origin
<5	>25	Level to gently undulating	1E	1E	Lacustrine
≥5 ≤25	≤25 ≥ 5	Gently undulating to undulating	1A, 1B, 1C, 1D, 2, 7	1A, 1B, 1C, 1D, 5, 7, 9	Glacial
>25	<5	Undulating to rolling	3, 4, 5, 6, 8, 9	2, 3, 4, 6, 8	Residual

[a]Coefficient of variation, V = S(100)/x where S = standard deviation and $\bar{x}$ = mean value, from terrain elevation interval curves.
[b]Topographic coefficient, T = maximum ordinate/number of contour interval from terrain elevation interval curves.

Table 3. Statistical soil classification of dune sand landform of Calumet Lacustrine Plain.

Item	Passing Sieve (percent)		Sand (percent)	Silt (percent)	Clay (percent)	Liquid Limit	Plasticity Index	Classification	
	No. 40	No. 200						Textural	AASHO
Dune Sand, Stratum A									
Average value									
Method 1	85.7	5.9	94.1	4.0	1.9	N. P.	N. P.	Sand	A-3(0)
Method 2	91.1	3.5	96.5	2.4	1.1	N. P.	N. P.	Sand	A-3(0)
Method 3	91.5	3.2	96.8	2.4	0.8	N. P.	N. P.	Sand	A-3(0)
Standard deviation									
Method 1	19.3	6.3	6.3	4.5	3.4	N. P.	N. P.		
Method 2	14.7	5.0	5.0	3.4	2.6	N. P.	N. P.		
Method 3	14.1	4.6	4.6	3.3	2.2	N. P.	N. P.		
Maximum value	100	20	100	19	13	N. P.	N. P.		
Minimum value	1	0	80	0	0	N. P.	N. P.		
Range	99	20	20	19	13	N. P.	N. P.		
Lakebed, Stratum B									
Average value									
Method 1		87.6	12.4	58.6	29.0	28.4	12.5	Silty clay loam	A-6(9)
Method 2		87.1	12.9	54.7	32.4	28.4	12.5	Silty clay	A-6(9)
Method 3		87.8	12.2	55.0	32.8	28.4	12.5	Silty clay	A-6(9)
Standard Deviation									
Method 1		11.9	11.9	11.8	14.3	4.4	4.1		
Method 2		12.4	12.4	11.6	14.3	4.2	4.0		
Method 3		11.8	11.8	10.3	12.9	4.0	3.7		
Maximum value		100	34	80	55	38	21		
Minimum value		66	0	42	6	21	7		
Range		34	34	38	49	17	14		

and in the AASHO classification systems. These values were obtained from roadway soil surveys performed for the Indiana State Highway Commission. Three different methods were used in determining the statistical soil classification.

Physical Properties—Physical properties of the soils in each significant landform were subjected to statistical methods and procedures in an attempt to characterize each significant layer or stratum within each typical profile. Because economy is a major factor in the performance of any roadway soil survey, sufficient data were not always available. In areas where it was intuitively obvious that the proposed conditions would pose no challenge to the existing foundation soils, detailed information was not requested or supplied. This was the case for several of the strata involved in the typical profiles developed for this study.

The data compiled and the relations determined are given in Table 3 and shown in Figures 8, 9, 10, and 11 for the dune sand landform of the Calumet Lacustrine Plain. Development of similar information for landforms in other physiographic regions would be most useful but would be a major undertaking. All such summaries should be continually updated as more information becomes available.

Ratings of Highway Soils Considerations for Landforms Within Physiographic Regions

Ratings of highway soil considerations for landforms within physiographic regions in Indiana are given in Table 4 for the Calumet Lacustrine Plain. The authors consider that information of this type is potentially quite valuable for practicing soils engineers who are inexperienced in this geographical location. The usefulness of these data (shown for the entire state in the earlier study, 18) could be expanded if other practicing soils engineers who are experienced in this locale were to offer constructive criticisms and if their thoughts and experiences were to be reflected in a modified presentation. These ratings are primarily useful in the preliminary studies of highway planning, route location, and design. One must always keep in mind that (a) these ratings are generalizations within a landform and (b) they reflect the present standards, policies, and procedures used by the Indiana State Highway Commission for the design and construction of highway facilities. It is emphasized that detailed information is needed at a specific location before final decisions are made. The information in this study may influence but does not replace a detailed investigation. Only if a partial study of a project were to reveal conditions extremely similar to those developed within this investigation and if sufficient data were available in this study to lead to statistically sound conclusions may a complete detailed study be judged unwarranted for that particular project. This decision should always be made by a competent, experienced soils engineer.

CONCLUSIONS AND RECOMMENDATIONS

1. The physiographic subdivision approach outlined in this study can lead to meaningful and worthwhile implications and conclusions for use in the preliminary stages of planning, route location, and design of highway facilities in the state of Indiana.
2. To increase the usefulness of this approach, a further subdivision of the physiographic units (Fig. 1) is recommended. The landforms or engineering soil parent material areas (5) seem to define areas within which one can indeed generalize as to the class and severity of highway soil problems with which one must cope.
3. The significant factors influencing a regional approach to highway soils considerations are the geologic origin and complexity of parent materials (landforms), the topography, and the general texture of the parent materials (particularly the magnitude of the clay fraction).
4. Methods and procedures presented for a generalized quantification of significant factors influencing a regional approach provide a useful means for generally quantifying the factors of geologic origin and complexity of parent materials (landforms) and topography. Data developed in this phase of the study, and related to the frequency of occurrence of landforms, are the basis for what has been defined as the first dimension or degree for the measure of uniformity within physiographic regions.

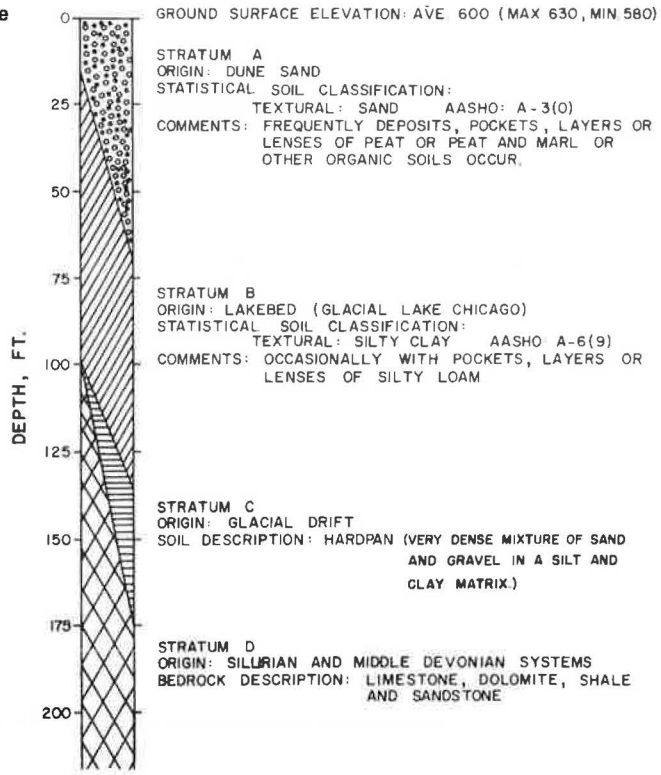

Figure 8. Typical profile of dune sand landform of Calumet Lacustrine Plain.

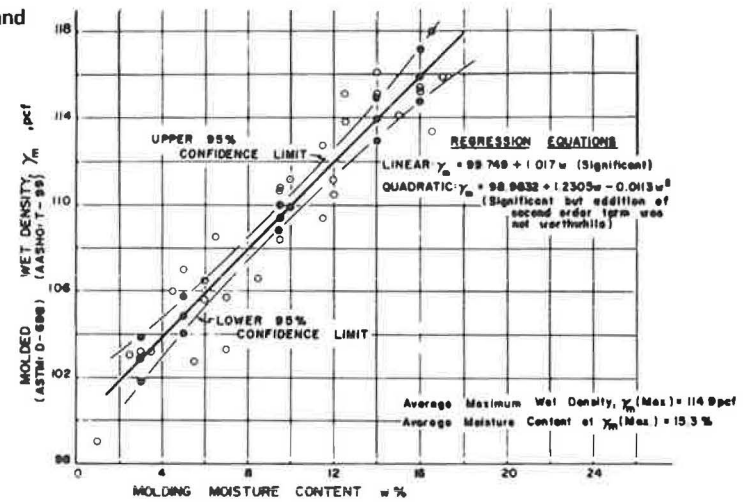

Figure 9. Molded wet density and molding moisture content, stratum A.

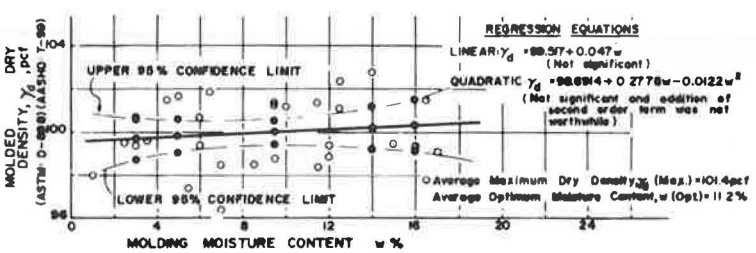

Figure 10. Molded dry density and molding moisture content, stratum A.

Figure 11. CBR and molded dry density, stratum A.

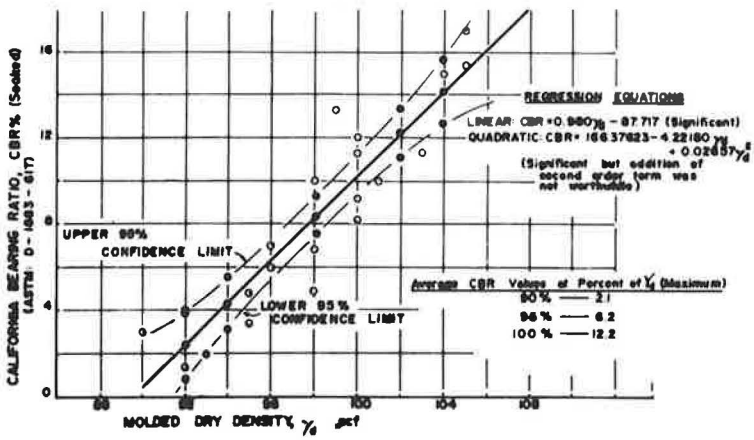

Table 4. Ratings of highway soils considerations for landforms of the Calumet Lacustrine Plain.

Soil Consideration	Dunes[a]	Lacustrine[b]	Depressions and Stream Channels[c]	Ground Moraine[d]
Cut design				
Soil backslope instability	L	M	H	L
Rock backslope instability	—	—	—	—
Groundwater control	L	L	L	L
Erosion potential	H	M	H	M
Surface drainage	H	M	H	M
Sinkholes and solution channels	—	—	—	—
Natural slope and river bank instability	L	M	H	M
Embankment design				
Soil sideslope instability	L	L	H	L
Rock sideslope instability	—	—	—	—
Soil type, compaction, and placement methods	L	M	H	L
Rock type, compaction, and placement methods	—	—	—	—
Erosion potential	H	M	H	M
Surface drainage	H	M	H	M
Embankment foundations				
Inadequate shear strength potential	L	M-L	H	M
Excessive settlement potential	L	M-H	H	M
Groundwater control	L	L	L	L
Organic deposit occurrences	L	L	H	L
Localized areas of unstable soils	L	M	H	M
Liquefaction potential	L	—	—	—
Sinkholes and solution channels	—	—	—	—
Surface drainage	L	H	H	M
Design and camber of culverts and conduits	L	M-H	H	M
Subgrades				
Support characteristics	H	L	L	M
Frost action potential	L	M	L	M
Pumping potential	L	H	H	M
Shrink and swell potential	L	H	H	M
Structure design with footings				
Instability potential	L	M	H	M
Excessive settlement potential	L	M-H	H	M
Scour potential	H	M-L	H	M
Structure design with piles				
Instability potential	L	L-L	M	L
Excessive settlement potential	L	L-M	M	L
Negative skin friction potential	L	M-H	H	M
Predetermination of pile lengths	L	H-H	H	M
Scour potential	H	M-L	H	M
Retaining structure				
Determination of lateral earth pressure	L	H	H	M

Note: L = low, M = medium, and H = high, and indicate little, average, and high likelihood respectively that major problems deserving detailed consideration will develop.

[a]Wisconsin, sand. [b]Wisconsin, sand and silty clay. [c]Recent-Wisconsin, peat and muck-marl. [d]Wisconsin, clay and silty clay.

5. The methods and procedures presented for the specific quantification of significant factors influencing a regional approach provide a useful means for specifically quantifying the 3 significant factors mentioned above. Data developed in this phase of the study, and related to the frequency of occurrence of soil types within landforms, are the basis for what has been defined as the second dimension or degree for the measure of uniformity within physiographic regions. The typical profiles and regression equations for pertinent relations, which were developed for landforms within the Calumet Lacustrine Plain physiographic region, could constitute a very valuable cataloging of soils experiences. If these relations were developed for the significant landforms within each physiographic region, they could lead to greater economy in the performance of soil and foundation investigations or at least a redistribution or concentration of any efforts to the known so-called problem landforms.

6. The authors consider the information given in Table 4 to have the greatest potential value for soils engineers inexperienced in this geographical location. The principal usefulness of these ratings is in preliminary studies related to highway planning, route location, and design. This usefulness would be expanded severalfold by the constructive criticism of other experienced soils engineers in this locality.

ACKNOWLEDGMENTS

The cooperation and interest of the Division of Materials and Tests, Indiana State Highway Commission, and its chief, W. T. Spencer, is gratefully acknowledged. Harold L. Michael of the Joint Highway Research Project also afforded helpful support for this work.

Any statements and conclusions made in this study represent the personal views of the authors based on their experience and should not be interpreted necessarily to represent the views of other personnel of the Indiana State Highway Commission.

REFERENCES

1. A Map of Indiana Soils. Department of Agronomy, Purdue Univ.
2. Raisz, E. Map of the Landforms of the United States. Institute of Geographical Exploration, Harvard Univ., Cambridge, Mass., 1939.
3. Atwood, W. W. The Physiographic Provinces of North America. Institute of Geographical Exploration, Harvard Univ., Cambridge, Mass., 1939.
4. Belcher, D. J., Gregg, L. E., and Woods, K. B. The Formation, Distribution and Engineering Characteristics of Soils. Eng. Exp. Station, Purdue Univ., Bull. 87, Jan. 1943.
5. Map of Engineering Soil Parent Material Areas of Indiana. Eng. Exp. Station, Purdue Univ., Bull. 87, Jan. 1943.
6. Bushnell, T. M. A Story of Hoosier Soils and Rambles in Pedological Fields. Peda-Products, Lafayette, Ind., Aug. 1958.
7. Cummings, E. R. Nomenclature and Description of the Geological Formations of Indiana. In Handbook of Indiana Geology, Indiana Dept. of Conservation, Pub. 21, Pt. 2, 1922.
8. Fenneman, N. M. Physiography of the Eastern United States. Univ. of Cincinnati, 1938.
9. Frost, R. E. The Use of Aerial Maps in Soil Studies and Location of Borrow Pits. Eng. Exp. Station, Kansas State College, Bull. 51, July 1946.
10. Agricultural Soils Maps. HRB Bull. 22-R, July 1957.
11. Ladd, C. C. Stress-Strain Behavior of Saturated Clay and Basic Strength Principles. Dept. of Civil Eng., M.I.T., Cambridge, Res. Rept. R64-17, April 1964.
12. Logan, W. N. Topographic Map of Indiana. In Handbook of Indiana Geology, Indiana Dept. of Conservation, 1922.
13. Malott, C. A. The Physiography of Indiana. In Handbook of Indiana Geology, Indiana Dept. of Conservation, Pub. 21, Pt. 2, 1922.
14. McGregor, D. J. High Calcium Limestone and Dolomite in Indiana. Geological Surveys, Indiana Dept. of Conservation, Bull. 27, 1963, 76 pp.

15. McKittrick, D. P. Subsurface Investigation for Indiana Highways. Purdue Univ., MSCE thesis, Sept. 1965.
16. Parvis, M. Regional Drainage Patterns of Indiana. Joint Highway Research Proj., Purdue Univ.
17. Patton, J. B. Geologic Map of Indiana. In Atlas of Mineral Resources of Indiana, Map 9, 1956.
18. Sisiliano, W. J. A Regional Approach to Highway Soils Considerations in Indiana. Purdue Univ., MSCE thesis, Aug. 1970.
19. Soil Survey Manual. U. S. Dept. of Agriculture, Handbook 18, Aug. 1951.
20. Terzaghi, K., and Peck, R. B. Soil Mechanics in Engineering Practice. John Wiley and Sons, New York, Oct. 1964.
21. Thornbury, W. D. Glacial Sluiceways and Lacustrine Plains of Southern Indiana. Div. of Geology, Indiana Dept. of Conservation, Bull. 4, June 1950.
22. Thornbury, W. D. Principles of Geomorphology. John Wiley and Sons, New York, 1954.
23. Ulrich, H. P. Soils. In Natural Features of Indiana, Indiana Academy of Science, July 1966, pp. 57-90.
24. Wayne, W. J. Thickness of Drift and Bedrock Physiography of Indiana North of the Wisconsin Glacial Boundary. Geological Surveys, Indiana Dept. of Conservation, Progress Rept. 7, June 1956.
25. Wayne, W. J. Glacial Geology of Indiana. In Atlas of Mineral Resources of Indiana, Map 10, 1958.
26. Witczak, M. W., and Lovell, C. W., Jr. Physiographic Subdivision for Engineering Purposes. Highway Research Record 276, 1969, pp. 60-63.
27. Woods, K. B., and Lovell, C. W., Jr. Distribution of Soils in North America. In Highway Engineering Handbook (Woods, K. B., ed.), McGraw-Hill, New York, 1960.

PROGRESS REPORT ON SOIL-BITUMINOUS STABILIZATION

Chester McDowell, University of Texas

• SOIL-BITUMINOUS stabilization, or soil-asphalt, as it is often referred to, has not been blessed with testing procedures that are an aid to the development and promotion of this product. This point has been reemphasized at meetings of the HRB Committee on Soil-Bituminous Stabilization during 1969 and 1970. The author does not wish to be any more critical of the work of others than he is of his own inasmuch as he was a prime mover in the development of 2 soil-asphalt test procedures, both of which fall far short of what is needed.

One of those methods was developed in the late thirties and was known as the modified bearing value (1). The second method known locally as the triaxial method (2) for soil-asphalt design was developed in the fifties. Both of these tests were of the waterproofing type and usually indicated the use of leaner mixtures than were realistic unless the "fat point" was crowded. They did not consider voids, percentage of moisture in compaction, aeration, and other pertinent data. Although neither of these 2 methods was very successful, it is believed that they did serve as a useful background in developing a third method that we believe will be far superior to either of them. The development of the large soils gyratory press and techniques in the late sixties for hot-mix black base gave promise that its utilization could improve soil-asphalt testing procedures.

The introduction of the large gyratory press for soils and its use for black-base design have paved the way for investigation of soil-bituminous mixtures, and the results of experiments with this new procedure and equipment constitute the bulk of this progress report on soil-bituminous mixtures. We tried to develop a test procedure employing use of the cohesiometer testing equipment. After doing a lot of unsuccessful work on this phase of testing, we abandoned the investigation in favor of a direct compression test. This report does not include that phase of the investigation.

The purpose of this investigation was to develop improved test procedures and techniques for the evaluation of soil-bituminous mixtures. It is believed that a good start in this direction has been made.

EXPERIMENTS AND RESULTS

For the experiments, a sand-clay soil (66-248-R) having a 5 plasticity index, 79 percent sand sizes, 5 percent silt, and 16 percent clay was selected from near Elgin, Texas. The materials (soil, water, and RC-2) were mixed at room temperature with a kitchen mixer and compacted into specimens having a 6-in. diameter and a 6-in. height. The compaction procedure is similar to test method Tex-126-E except for specimen height and molding temperature. Figures 1 through 5 show some of the testing equipment used. It is recognized that molding temperature is critical, and this is one of the reasons that the use of relatively small specimens (6-in. diameter by 6-in. height) in conjunction with the high efficiency of the gyratory press was selected for use especially for room-temperature molding. Another reason for the use of short specimens evolves from that portion of our procedure requiring pressure-wetting of the specimen at room temperature. It is believed that the shorter the specimen is, the less will be the time required to wet the specimen in the pressure pycnometer. Pressure-wetting temperatures will be discussed more thoroughly in a subsequent section of this report. The results of these tests are shown in Figure 6. Two sets of moisture-density

Sponsored by Committee on Soil-Bituminous Stabilization.

Figure 1. Compaction mold and base plate.

Figure 2. Gyratory compaction machine.

Figure 3. Caster-mounted dolly.

Figure 4. Ejection press.

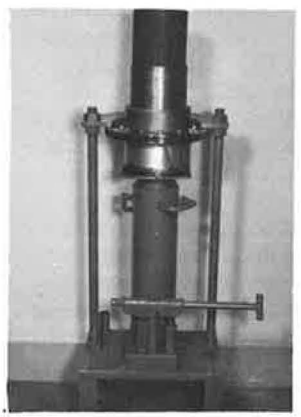

Figure 5. High-speed testing machine.

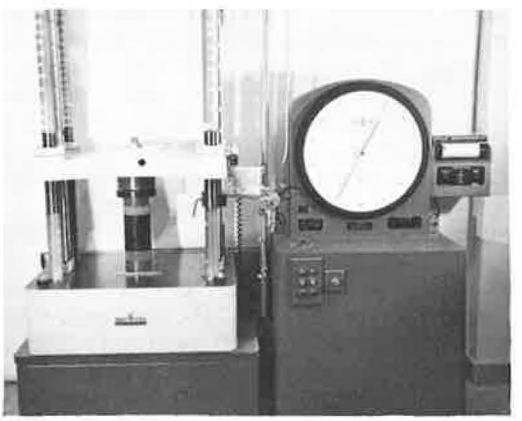

Figure 6. Density-moisture curves.

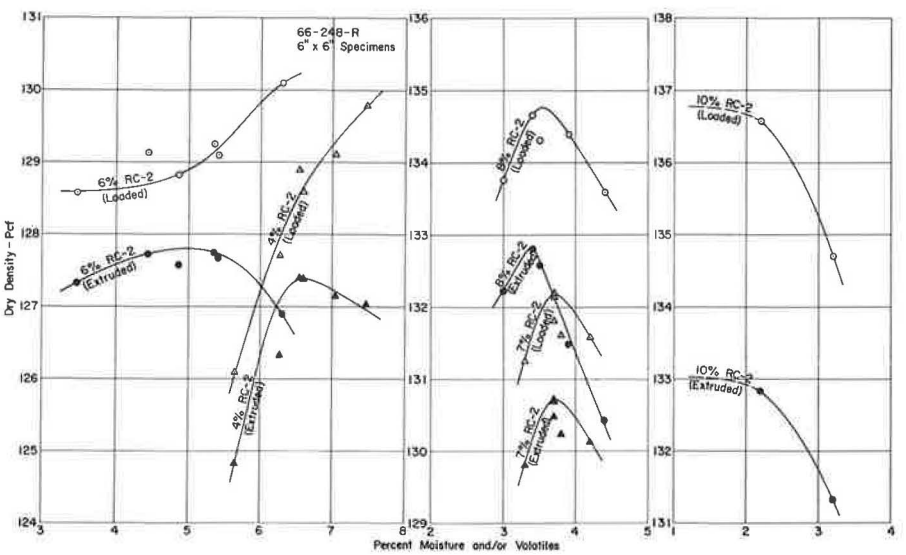

curves are shown: one with the specimen held under a load of 500 psi and the other after the specimen is extruded and its height measured after rebound. It was interesting to note that some of the leanest mixtures would not produce a reasonable optimum moisture content when measured in a loaded condition but did when measured after extrusion. Apparently certain mixtures, i.e., 4 and 6 percent, hold water tenaciously enough that little is squeezed out under load. The use of percentages of water in excess of optimum for extruded specimens was unreasonable because rebound cracked specimens so badly that low compressive strengths were obtained. We made hundreds of specimens and used more than a thousand pounds of mixtures before we found out part of what was happening to compaction rebound.

One of the important problems in soil-asphalt testing is to determine the desirable amount of moisture to add without doing an extensive amount of testing. For the soil tested, we have discovered an easy way to make this determination. Figure 7 shows that optimum moisture content can be determined by merely subtracting the percentage of stabilizer to be used from the optimum moisture content of the raw soil. It is hoped that this moisture-density relation will remain the same for other soils and other asphalts. Only a continued investigation will verify the workability of the method for all soil-asphalt mixtures. The percentage of air voids at optimum moisture content when plotted against percentage of asphalt reveals an S-shaped curve containing 2 hooks (Fig. 8). The left hook at slightly more than 6 percent (where the curve steepens) indicates the point in richness at which the mixtures begin to be capable of being compacted easier than are leaner mixtures. As asphalt content is increased, compaction (removal of voids) continues until a reversing curve hook shows danger that voids are being overfilled at about 9 percent. It would seem that the best percentage of RC-2 in this case would range between 6.5 and 9 percent. It is also interesting to note that, if the minimum void content in percentage obtained is increased by 5 percent (the average difference between laboratory-gyratory molding and field cores found on black-base projects) and this line shown in Figure 9 is projected horizontally to the voids curve and then downward, the use of 7.3 percent is suggested in this case.

Mixtures containing 0, 2, 4, 6, 7, 8, 9, and 10 percent RC-2 were mixed at room temperature and at optimum moisture, molded as previously described, and cured in a 140 F drying oven for 5 days. After dry-curing, the specimens were cooled to room temperature, placed in plastic bags, and then pressure-wet as described in test method Tex-119-E except that room temperature wetting without restrainers was used. Many tests were run that showed that some cutback asphalts are too soft to withstand pressure-wetting at 140 F (Fig. 9). Wetting with restrainers produced what is believed to be false high compressive strengths for very lean mixtures because of firm restraint. Had we known these facts we could have saved the effort in making a ton or two of these mixes.

After the wetting, the ends of the plastic bags were folded over the ends of the specimens, and porous stones were placed on the specimen ends. After they were placed in triaxial cells, the specimens were placed in a 140 F oven for 24 hours before being tested in unconfined compression at a rate of loading of 0.15 in./min. The results of compression tests are shown in Figure 10. The rising half of the strength curve covers the range of RC-2 that is desirable to use (Fig. 8).

A few specimens were made of mixtures that had been aerated 30 to 90 min and that had molding moisture replaced. Densities obtained were lower than those obtained from fresh mixtures as indicated by the voids shown by Figure 8. Although densification was reduced several pounds per cubic foot, it was gratifying to see that no strength loss accompanied this loss in density due to aeration. It would seem that consideration of a practical working moisture content is essential before a selection is made of percentage of asphalt to be used. For instance, the optimum moisture for 9 percent RC-2 is 1.8 percent, but, as lower percentages of RC-2 are used, the optimum moisture increases to as high as 4.3 percent for 6.5 percent RC-2. It may be that conditions are such that the soil cannot be dried enough to be compatible with the use of high amounts of stabilizer. On the other hand, water may be high priced in the deserts where the use of rich mixtures may be most practical.

Previous portions of this report pertain primarily to mix design. Because success of asphalt-treated bases depends greatly on compaction, it is necessary that proper

Figure 7. Relation of percentage of RC-2 and optimum moisture.

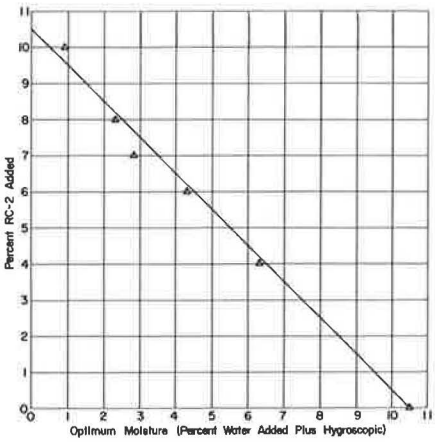

Figure 8. Relation of voids and percentage of RC-2

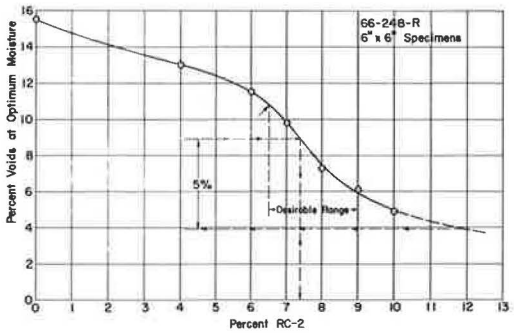

Figure 9. Detrimental effects on specimens containing 6 percent RC-2 when pressure-wet with hot water.

Figure 10. Relation of unconfined compressive strength and percentage of RC-2.

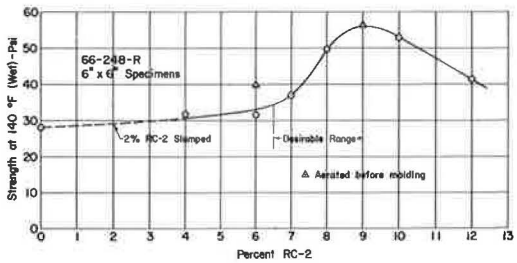

Figure 11. Density-moisture-strength curves (each sample aerated to desired molding moisture content).

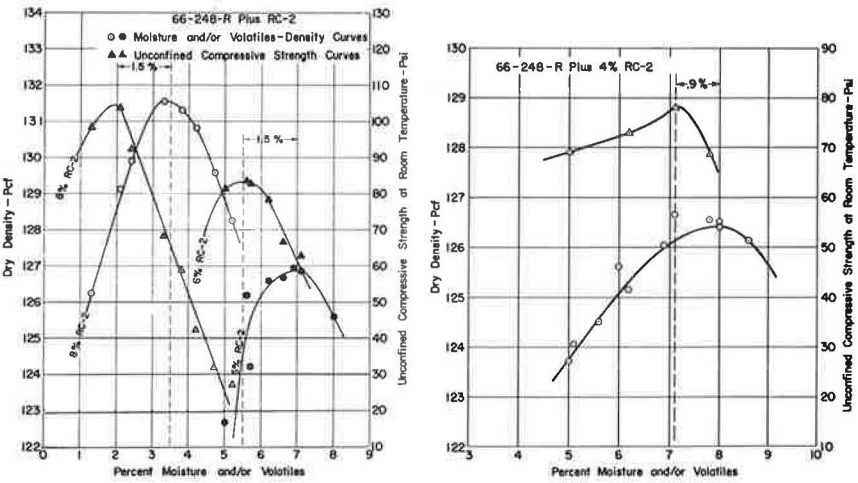

aeration of moisture or volatiles or both just prior to compaction be determined. The following simple field test procedure to determine optimum liquid contents for compaction is recommended for use.

1. After field mixing at a liquid content above optimum has been completed, select a 100-lb sample and divide into at least 7 portions of approximately 14 lb each. Place portions where temperature will fluctuate very little.
2. Mold one sample, which has not been aerated, in the gyratory press and determine density as previously described.
3. Place remainder of portions on trays and aerate in the sun or by stirring under a fan until various increments of water and volatiles have been removed and then compact in gyratory compactor.
4. Repeat step 3 for various portions until a moisture-density curve has been completed. (Keep the molding temperature as uniform for all portions as is practical, i.e., ±2 F.)
5. Plot the density data as shown in Figure 11 and select optimum liquid content.
6. When the field mixture is aerated to a liquid content between the optimum liquid content mentioned in step 4 and an amount not to exceed 1.5 percent below the optimum, begin rolling.

The data shown in Figure 11 indicate that compaction at moisture or liquid contents of 0.9 to 1.5 percent below optimum will produce maximum apparent unconfined compressive strengths. There may be some cases where this rule does not apply and, in such cases, both densities and strengths should be determined in the field, and temperatures should be kept as uniform as practical, i.e., ±2 F. [Similar procedures such as that of Marais (3) have been proposed.] Additional samples molded at optimum moisture, air-dried 5 days, and pressure-wet were equally as strong as those molded at a liquid content of 1.5 percent below optimum.

SUMMARY

It is believed that we are beginning to develop some test procedures that can help evaluate soil-bituminous mixtures, inasmuch as they appear to have a realistic approach to determination of the role that the percentage of stabilizer, moisture, volatiles, curing, and compaction play in the building of soil-asphalt bases.

RECOMMENDATIONS

It is recommended that the proposed procedure be used to test several soils of varying characteristics when mixed with several types of asphalt stabilizers. After obtaining these results, we should be able to write adequate test procedures and specifications for construction of soil-asphalt subbases and bases.

ACKNOWLEDGMENTS

The author is indebted to many who have contributed and encouraged the development of this report. The work of the members of the Soils Section and other members of the Materials and Tests Division of the Texas Highway Department, under the able guidance of A. W. Eatman, is gratefully acknowledged. The major factors in making this report possible consist of performance of tests and contribution of advisory consultations by A. W. Smith, C. E. O'Dell, and Clarence Stark of the Soils Section.

REFERENCES

1. The Development of Equipment and Testing Procedure for the Design of Bituminous Stabilized Roads. Texas Highway Department, Test Procedure THD-98, 1940.
2. Manual of Soil Testing Procedures. Texas Highway Department, Test Method Tex-119-E.
3. Marais, C. P. A New Technique to Control Compaction of Bitumen-Sand Mixes on the Road Using a Vane Shear Apparatus. Trans., South African Institution of Civil Engineers, Vol. 8, No. 3, March 1966.

ROAD CAPABILITY STUDY ON IMPROVED EARTH ROADS

John H. Grier and C. H. Perry, U. S. Army Transportation Engineering Agency, Newport News, Virginia

•DURING the past several years, personnel from the U. S. Department of Defense, civilian agencies, and highway agencies concluded that opinions differed on estimating methods of road capacity. A research analysis program was, therefore, conducted for refining factors for assessing road capability.

Field tests in the continental United States (CONUS) involved operating as many as 10 two-axle resupply vehicles in convoy on closed single-lane loops on a 24-hour basis for several consecutive days. Tests were conducted on improved earth roads with surface soils composed of silty sand (SM), lean clay (CL), and fat clay (CH) at dry, moist, and wet conditions. The tests on silty sand and lean clay were conducted during May 1971, and tests on fat clay were conducted during September 1971.

The field tests in Southeast Asia (SEA) involved monitoring operational convoy moves as well as conducting controlled tests on lateritic soils. These tests were conducted in accordance with the same test plan that was used in the CONUS test programs.

TEST SITES

Tests on silty sand and lean clay roads were conducted at Camp Wallace, Virginia, located on the James River. The terrain consists of rugged woodland with heavy growths of underbrush and is representative of mountainous terrain where there are improved earth roads. Because no fat clay was found at a suitable location in Virginia, arrangements were made with the U. S. Army Corps of Engineers to conduct tests on a fat clay road near Vicksburg, Mississippi. Relevant data on soils of volcanic origin in tropical areas of the world (lateritic soils) were obtained in tests conducted in the Long Binh area of the Republic of Vietnam. Typical views of these test sites are shown in Figure 1. The detailed characteristics of all the test roads, which were closed loops with 1-way traffic only, are given in Table 1.

TEST VEHICLES

It was desired that the test vehicle simulate 2-axle resupply truck with a gross weight of 16,260 lb, rear-axle drive only. This was accomplished in the Virginia test by using M35A2 trucks with the intermediate-axle wheels removed and the drive shaft to the front axle disconnected. Twenty M35A2 trucks were temporarily modified and driven in the tests. The Mississippi tests were conducted with commercial 2-axle flatbed trucks because these were readily available and required no modifications to meet the requirements for test truck characteristics. The test vehicles used in the Long Binh tests were commercial 2-axle dump trucks with flatbeds.

TEST PROCEDURES

All of the test courses were in the form of closed loops with single-lane traffic in 1 direction. The test vehicles were run on a 24-hour basis. In the CONUS tests, there were three 8-hour shifts; and in the SEA tests, there were two 12-hour shifts. Approximately 6.5 hours were lost during a 24-hour period because of required stops for rest, meals, and vehicle maintenance.

During each test period, the vehicles were driven at maximum speeds, consistent with safe driving conditions. Several times during each shift a check was made of the

Sponsored by Special Committee on International Cooperative Activities.

average speed around a given test loop, and also an instantaneous check was made of the average vehicle lead and speed of the lead and rear vehicles in the convoy.

Road maintenance equipment at each test site in CONUS consisted of a motor grader, a bulldozer, and a water distributor. Practically all road maintenance was accomplished by use of the motor grader. The bulldozer was used only to muck out the low soft spots that slowed the operations following any rains. Maintenance was performed when rutting exceeded 6 to 8 in., washboarding occurred, or potholes caused driving to become more difficult and speed to be reduced. This was accomplished during meal and vehicle stops and during short periods when road capability could be substantially increased. Road maintenance was kept to a minimum throughout the entire test periods. Time and type of equipment used to perform road maintenance were recorded in the test data records.

There was no road maintenance performed on the SEA test loop because the surface soils were more stable inasmuch as they contained ferrous oxides and deteriorated at a slower rate than the CONUS soils. Operations were sustained when vehicles straddled ruts in the small sections of road that had failed. As these ruts progressively worsened, the speeds of vehicles were reduced, but a substantial volume of traffic could be maintained. Adequate road maintenance equipment was available on site, but the tests concerned keeping operations as close to actual enemy combat conditions as possible.

Soil borings for classification in accordance with the United Soil Classification System were taken in all test loops in order to identify the soil types in the test loops and at critical points. All soil tests and laboratory analyses were conducted in accordance with the current test procedures of the U. S. Army Corps of Engineers. Frequent moisture, density, and cone penetrometer readings were taken before, during, and after all test periods to document the test conditions under which each test was performed.

DETERMINATION OF ROAD CAPABILITY

Road conditions that affect road capability include factors such as vertical and horizontal alignment, surface type and width, visibility, and roadway maintenance. Traffic conditions, consisting of factors that influence vehicle movements and those that are generated by all vehicles using the road, include crossing and turning movements, movements of additional vehicles not normally associated with supply movements, interference caused by opposing vehicular movement, and diversity in sizes of vehicles composing the traffic stream. Certain factors that are normally of major importance in estimates of the capacity of an uncontrolled high-density roadway are not applicable to controlled supply movements. More rigid control is normally exercised in supply movements than in movements of freely moving civilian passenger vehicles. Despite this control, there will be some variation in vehicle spacing and speed, owing largely to the influence of roadway alignments. To develop an accurate capacity estimate for supply vehicle movements requires that all factors pertaining to the type of roadway under consideration be weighed in proper perspective. The factors cannot be established as exact figures but are to be judiciously applied in accordance with related conditions.

The results in this test program are based on a strictly controlled, 1-way supply movement where there was no other traffic permitted on the supply route and where vehicle lights were on during night operations. Many of the factors that affect capability were built in the selected test loops. Factors such as vertical and horizontal alignment, width, and surface type are constants for a given test loop and can be related to a type of improved earth road supply route. Factors that are variables include moisture condition of the surface soil, road maintenance, vehicle speed and lead, driver behavior and experience, and fixed time loss (10-min rest stops). Because maximum road capability is significant in supply movements, the maximum speed and the minimum lead consistent with safe driving conditions were striven for. Test road characteristics, speed and lead, vehicle rates, road maintenance data, and computed road capacities are given in Table 2.

Figure 1. Road sections tested.

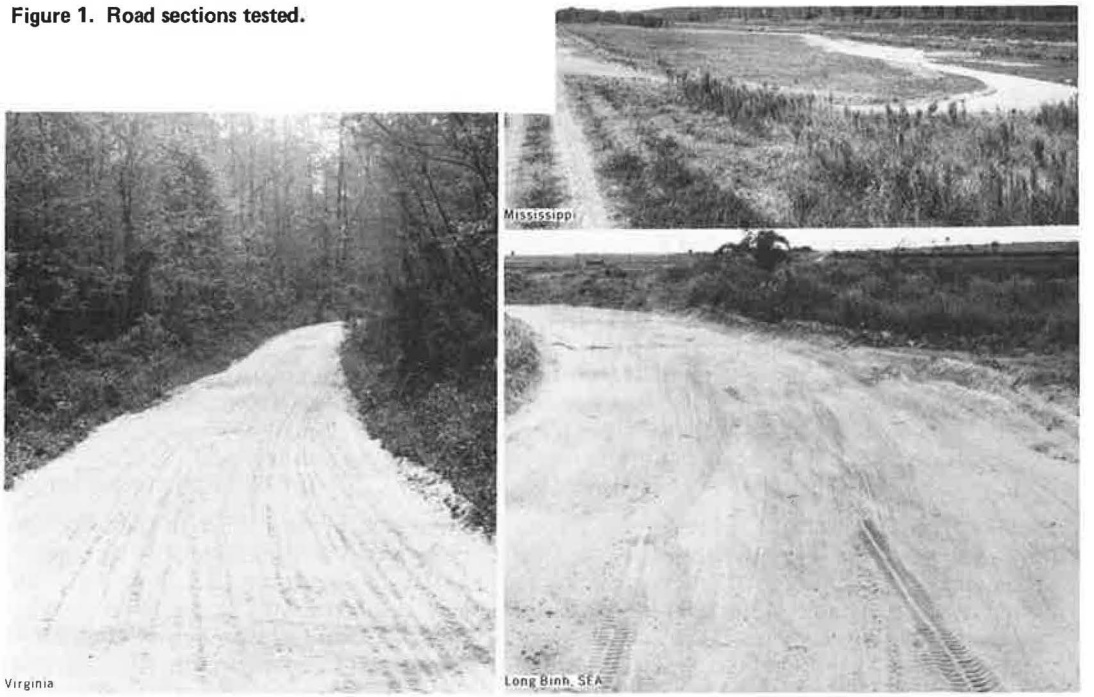

Table 1. Test loop characteristics.

Location	Test Loop	Soil Type[a]	Length (ft)	Avg Width (ft)	Maximum Width (ft)	Minimum Width (ft)	Maximum Grade (percent)	Minimum Radius Curve (ft)
Virginia	1	SM	2,420	20.2	24.0	16.5	10 to 7	61
	2	CL, SM, SC	4,700	19.0	39.0	12.1	8 and 20	48
	3	SM	3,717	40.0	40.0	40.0	1.5	240
Mississippi	1	CH	2,670	18.0	18.0	18.0	12.0	75
Long Binh	1	SC, SM, SP, SW, CL, CH	3,070	20.1	38.0	18.3	9.0	202

[a]United Soil Classification System, where CL = lean clay, CH = fat clay, SC = clayey sands, SM = silty sands, SP = poorly graded sands or gravelly sands, and SW = well-graded sands or gravelly sands.

Table 2. Road capabilities.

Location	Soil Type	Soil Condition	Avg Width (ft)	Maximum Grade (percent)	Minimum Radius Curve (ft)	Avg Lead[a] (ft)	Avg Speed[a] (mph)	R	C_a	M	P_v
Virginia	CL, SC, SM	Dry	19.0	8 and 20	48	207.0	15.8	402.0	1,337	11.2	1,600
Virginia	CL, SC, SM	Moist	19.0	8 and 20	48	171.1	14.1	433.0	1,337	11.2	1,630
Virginia	CL	Wet	19.0	8 and 20	48	0.0	0.0	0.0	0	0.0	0
Virginia	SM	Moist	20.2	10 and 7	61	111.8	18.8	888.0	1,573	8.1	2,780
Virginia	SM	Wet	20.2	10 and 7	61	147.1	20.5	735.0	1,021	10.9	1,450
Virginia	SM	Moist	40.0	1.5	240	134.0	27.8	1,100.0	3,414	14.2	3,440
Virginia	SM	Wet	40.0	1.5	240	140.5	21.6	809.0	2,104	5.7	4,410
Mississippi	CH	Dry	18.0	12.0	75	89.0	21.0	1,240.0	1,032	5.2	2,980
Mississippi	CH	Moist	18.0	12.0	75	101.0	20.0	1,040.0	724	12.2	976
Mississippi	CH	Wet	18.0	12.0	75	0.0	0.0	0.0	0	0.0	0
Long Binh	SM, SW, SP, SC	Wet	20.1	9.0	202	429.0	2.9	24.6	NA	0.0[b]	366[c]
Long Binh	CL, CH	Wet	20.1	9.0	202	0.0	0.0	0.0	0	0.0[b]	0[c]
Long Binh	SM, SW, SP, SC, CL, CH	Moist	20.1	9.0	202	179.0	19.8	584.0	NA	0.0[b]	8,687[c]
Long Binh	SM, SW, SP, SC, CL, CH	Dry	20.1	9.0	202	145.0	22.2	809.0	NA	0.0[b]	12,034[c]

[a]Based on numerous tests throughout 24-hour periods.
[b]No road maintenance was required on lateritic soils due to slow rate of deterioration versus CONUS soils.
[c]$P_v = f(24 \cdot L_t)R$ when no maintenance is accomplished as in SEA.

The equation for computing road capacity is as follows:

$$P_v = f\ C_m \left\{ \frac{(24 - L_t)}{[(C_m/R) + M]} \right\} \text{ when } [(C_m/R) + M] \leq (24 - L_t)$$

where

P_v = vehicle passes/24-hour period;
f = reduction factor (0.85) to compensate for contingencies such as egress and ingress of vehicles;
C_m = number of vehicle passes before road maintenance is required;
R = theoretical number of vehicles per hour that can pass a fixed point in 1 direction (5.280 × avg speed/avg lead);
M = time loss due to road maintenance/fixed number of passes; and
L_t = fixed time loss due to rest stops (10-min stops), 3.5 for CONUS and 6.5 for SEA.

The term $[(C_m/R) + M]$ represents 1 road maintenance cycle. That is the total time for C_m vehicles moving at a rate of R per hour to pass plus the time required to repair the road. The term $(24 - L_t)$ fixes the amount of time available in a 24-hour day. Division of the available time by the road maintenance cycle time gives the number of cycles that can be accomplished in one 24-hour day; multiplying this by the number of vehicle passes per cycle and modifying the result by f give the maximum road capacity. The data given in the last column of Table 2 are considered to be realistic maximums for the road characteristics given in the table.

The vehicle maintenance records for the tests indicate that 2 vehicles would be required to keep 1 operation in a continuous short-haul resupply operation over the same short closed-loop route. A large maintenance float would be required to sustain this type of operation because the vehicles would take continuous pounding on the same mechanical components. On a long-haul convoy operation this would not be prevalent. Some maintenance support would be necessary but not to the extent as required in the closed-loop operation. In addition to the maintenance float required, adequate road maintenance equipment must also be available. The test records indicate that the equivalent of 1 motor grader per 4 miles of road is needed for minimum road maintenance. It was also noted that road maintenance was not necessary if one is willing to reduce vehicle capacity gradually based on percentage of the road that has deteriorated. Thus, the analysis of the test records clearly indicates that to sustain the maximum road capacity requires adequate maintenance float vehicles and road maintenance equipment.

This analysis indicates that the ability of a given country to sustain a large resupply operation is dependent not only on the type of roads available but also on the supply of vehicles and ability to keep them operational. Under wet conditions the road would be the controlling factor.

TYPICAL SOIL FAILURES IN THE ROAD SURFACE

The types of failures that require road maintenance to improve capacity, to reduce hazardous driving conditions, or to minimize mechanical damage to the vehicles (or all of these) are discussed below under the various soil types.

Silty Sand

Figure 2 shows the situation that existed after a dry test with 1,320 vehicle passes, i. e., on a curve to the left, downgrade, potholes to 10 in. deep, and fine powdery soil piled along the outside of the curve 18 to 24 in. high.

Figure 3 shows a straight, level, poorly drained, highly consolidated silty sand where there is a deep pothole near the center. It was necessary to muck out this section of road several times after rains (note pile of soil in the left of photograph); however, the vehicles were never immobilized here. This situation existed after a moist test.

On a level, slightly banked curve to the right, severe washboarding occurred after 1,573 vehicle passes (Fig. 4). (Note piles of soil near the top of photograph.)

Figure 2. Potholes in Virginia road.

Figure 3. Poorly drained section in Virginia road.

Figure 4. Washboarding in Virginia road.

Figure 5. Deep depressions in Virginia road.

Figure 6. Deep rutting in Virginia road.

Figure 7. Deep potholes in Mississippi road.

Figure 8. Deep depressions and potholes in Mississippi road.

Figure 9. Deep rutting and deterioration in SEA road.

Figure 10. Deep depression, washboarding, and soil buildup in SEA road.

Figure 11. Dust along SEA road.

Lean Clay

Figure 5 shows a failure that occurred at the bottom of a downhill grade on a slight curve to the right. This section of road was constructed on a low fill. Note the deep depressions in the left wheel track after 1,320 vehicle passes.

Deep rutting occurred at this location on a sharp curve to the left at the bottom of an uphill grade after moist tests (Fig. 6). Although the undercarriage of the vehicles often touched the center of the road surface, no vehicles were immobilized here during the moist tests. The vehicles were immobilized here during a wet test because of slipperiness, not sinkage.

Fat Clay

Deep potholes developed at this location on a downhill grade and curve to right as a result of a dry test. Traffic moved to the left, as shown in Figure 7.

Deep depressions and potholes developed at the bottom of an uphill grade and a curve to the right as a result of a moist test (Fig. 8).

Lateritic Soils

Deep rutting and complete deterioration of surface at this location of CL-CH soil on an uphill grade, and a curve to the left developed as a result of a wet test. Vehicles were immobilized during monsoon. Traffic moved to the right, as shown in Figure 9.

Deep depressions, washboarding, and buildup of soil to the right on an uphill grade and a curve to the right developed as a result of moist test (Fig. 10).

On a downhill grade, slightly curving to the right, dusty condition, rutting, and buildup of soil to the left of road occurred as a result of dry test (Fig. 11).

CONCLUSIONS

1. Roads in CONUS composed of silty sands, lean clay, or fat clay in the dry or moist condition, compacted to 90 to 100 percent of maximum density, and maintained at periodic intervals can support the passage of a thousand or more vehicles of the 2-axle type in a 24-hour period.
2. Roads in SEA composed as indicated above and having the same conditions were able to achieve and sustain maximum density without any road maintenance because of the high humidity, which provides moisture, and the ferrous oxides in laterites, which reacted as soil stabilizers. The traffic provided the necessary compactive effort.
3. Roads in CONUS composed of silty sands in the wet condition, compacted to 90 to 100 percent of maximum density, and maintained at periodic intervals can support the passage of a thousand or more vehicles of the 2-axle type in a 24-hour period.
4. Roads in SEA composed of silty sand in the wet condition, compacted to 90 to 100 percent of maximum density, and not maintained can support the passage of several hundred vehicles of the 2-axle type in a 24-hour period.
5. Roads in CONUS and SEA composed of lean clay or fat clay in the wet condition and having uphill grades of approximately 6 and 8 percent or more respectively will immobilize vehicles of the 2-axle type because of slipperiness. On roads with grades less than approximately 6 percent, some traffic can travel at very low speeds provided penetration of surface moisture has not exceeded more than approximately 3 in.
6. Vegetation that provides a canopy over a road prolongs moisture retention in the road surface soil after rains. This condition will have a significant effect on road usage.
7. Assuming that a given improved earth road is in a trafficable condition, a large maintenance float and adequate road maintenance will be required to support volume movements of vehicles because of the effects of dust, road roughness, frequent shifting of gears, and frequent braking actions that cause rapid mechanical failures such as fractured radiator connections and mountings, failure of wheel axle seals and brake lines, and clutch component failures. This will be prevalent for short-haul, closed-loop operations but reduced for long-haul operations.
8. The ability of a given country to mount and support maximum resupply movements over improved earth roads is not dependent on the roads available but on the number and quality of resupply vehicles and the ability to maintain the vehicles and road.

UNCERTAINTY OF SETTLEMENT ANALYSIS FOR OVERCONSOLIDATED CLAYS

Raymond J. Krizek, Department of Civil Engineering, Northwestern University; and J. Neil Kay, School of Civil and Environmental Engineering, Cornell University

The uncertainty associated with using the Skempton-Bjerrum method for settlement determination in overconsolidated clays is evaluated by means of a probabilistic procedure wherein the usually deterministic parameters are represented by appropriate probability distribution functions. Some of these distributions are determined subjectively and combined with others that are based on measured data to deduce a probability distribution function for the settlement-layer thickness ratio. The uncertainty is characterized in terms of a 90 percent confidence interval, and values are presented graphically for a wide range of parameters. Engineering judgment was used in the selection of the subjectively determined parameter distribution, and the ensuing analysis and interpretation provide the design engineer with a rational and logical procedure whereby the reliability of a given settlement prediction can be assessed. Accordingly, the gross intuitive estimate of uncertainty associated with a conventional deterministic calculation is obviated.

• THE TOTAL settlement of an overconsolidated clay may be arbitrarily divided into (a) immediate settlement, or that settlement which occurs before dissipation of excess pore-water pressure has begun, (b) primary consolidation settlement, or that settlement which occurs while excess pore-water pressure is being dissipated, and (c) secondary consolidation settlement, or that settlement which occurs after excess pore-water pressure has been dissipated. However, the distinction between the above-mentioned classifications of settlement becomes vague in a field situation and renders the settlement determination for foundations on overconsolidated clay a very complex problem. Owing to the uncertainty associated with the determination of an undrained stress-strain modulus for soil, the computation of immediate settlement is subject to considerable skepticism; in addition, it is difficult to ascertain the extent to which immediate settlement is influenced by partial dissipation of pore-water pressure during the loading process. Although the prediction of secondary consolidation is also very difficult, such settlement generally constitutes only a minor part of the total settlement of an overconsolidated clay provided a sufficient margin of safety against bearing capacity failure has been employed. Accordingly, the following analysis is restricted to a quantitative evaluation of the uncertainty associated with primary consolidation settlement, as determined by use of the method proposed by Skempton and Bjerrum (6).

NOTATION

The notation used in this paper is defined as follows:

A = Skempton pore-pressure parameter;
b = half-width of strip load or radius of circular load;
C_r = recompression index;

Sponsored by Committee on Soil and Rock Properties.

$\overline{C}_r$ = mean recompression index;
D = layer thickness;
E = error function for pore pressure parameter;
e = void ratio;
$\overline{e}$ = mean void ratio;
F_c = horizontal deformation factor for circular load;
F_s = horizontal deformation factor for strip load;
f = probability distribution function;
G = error function for horizontal deformation;
$\overline{G}$ = mean error function for horizontal deformation;
H = difference between high end of 90 percent confidence interval and $\overline{R}$;
H_R = $H/\overline{R}$;
L = difference between low end of 90 percent confidence interval and $\overline{R}$;
L_R = $L/\overline{R}$;
N = 0.866A + 0.211;
n = number of test values;
OCR = overconsolidation ratio;
p_c = preconsolidation pressure;
p_o = overburden pressure;
Δ_p = pressure increase;
Q = uncertainty factor for C_r - e relation;
R = settlement layer thickness ratio;
$\overline{R}$ = value of R obtained from mean parameter values;
V = coefficient of variation;
$Z = [\overline{C}_r - C_{r(t)}]/[VC_{r(t)}/\sqrt{n}]$;
z = depth below foundation base;
$\alpha = \left(\int_0^D \sigma_3\, dz\right) \Big/ \left(\int_0^D \sigma_1\, dz\right)$;
δ = consolidation settlement;
δ' = one-dimensional consolidation settlement;
ξ = standard normal deviate;
μ = settlement reduction factor;
μ_c = settlement reduction factor for circular load;
μ_s = settlement reduction factor for strip load;
σ_1 = vertical stress; and
σ_3 = horizontal stress.

SKEMPTON-BJERRUM PROCEDURE

In order to account for dilatancy in determining settlements of overconsolidated soils, Skempton and Bjerrum (6) proposed a method that utilizes the A pore-pressure parameter, obtained from conventional triaxial tests, and a factor α, determined from the relation

$$\alpha = \left(\int_0^D \sigma_3\, dz\right) \Big/ \left(\int_0^D \sigma_1\, dz\right) \tag{1}$$

α depends primarily on the geometry of the system, and tabulated values are readily available (given subsequently in Table 1). Next, a factor μ is given by

$$\mu_c = A + \alpha_c(1 - A) \tag{2}$$

for a circular footing, or

$$\mu_s = N + \alpha_s(1 - N) \tag{3}$$

for a continuous footing, where

$$N = 0.866A + 0.211 \tag{4}$$

is calculated. Then, the settlement δ for the overconsolidated soil is determined by taking the product of μ and the settlement δ', determined on the basis of the conventional, one-dimensional approach, or

$$\delta = \mu\delta' \tag{5}$$

Skempton and Bjerrum have indicated a correlation between the A pore-pressure parameter at working loads and the in situ overconsolidation ratio, and, more recently (1), curves have been presented to facilitate the direct determination of μ from these same parameters.

PROBABILISTIC APPROACH

The accuracy of the above-described Skempton-Bjerrum procedure is evaluated here by use of a probabilistic treatment that is similar to that previously employed (2) to study the one-dimensional consolidation of normally consolidated soils. This treatment consists essentially of representing the independent parameters by probability distribution functions instead of deterministic values in order to derive a probability distribution function for settlement; from this latter function, the uncertainty associated with computed settlement values may be inferred.

Deterministic Formulation

Combination of the probability distribution functions is achieved by Monte Carlo simulation, and, since this process requires formulation of the problem in terms of continuous functions, some curve-fitting of the tabulated relations presented by Skempton and Bjerrum is necessary. Accordingly, it is proposed to replace the discontinuous relation shown in Figure 1 by the empirical equation

$$A = 1.3(0.63)^{OCR} \tag{6}$$

Similarly, the factor α for a uniformly loaded circular area may be expressed by

$$\alpha_c = 1/\exp\{\exp[0.33 - 0.34(2b/D)]\} \tag{7}$$

in which b is the radius of the loaded area. Discussion (4) of the Skempton-Bjerrum work indicates that it is necessary to correct their data for a continuous strip load, and these corrected data can be closely represented by

$$\alpha_s = 1/\exp\{\exp[0.05 - 0.42(2b/D)]\} \tag{8}$$

in which b is the half-width of the strip load. Table 1 compares the previously tabulated values with those calculated from Eqs. 7 and 8.

Although the method does not account for the effect of horizontal strains, Skempton and Bjerrum claim, on the basis of numerical studies, that the error in computed settlements will not exceed approximately 20 percent; this error will be greatest when 2b/D is small and least when 2b/D is large. To account for this error in the formulation developed here, we propose the multiplying factors F_c for a circularly loaded area and F_s for a strip load, where

$$F_c = 1 + 0.01 \exp[2.753 - 0.45(2b/D)] \tag{9}$$

and

$$F_s = 1 + 0.01 \exp[1.654 - 0.45(2b/D)] \tag{10}$$

Typical values for F_c and F_s for various values of 2b/D are as follows:

2b/D	F_c	F_s
0.1	1.150	1.050
1.0	1.100	1.033
10	1.002	1.001

Although entirely empirical, Eqs. 9 and 10 allow the settlement computations to be realistically adjusted to account for the error associated with neglecting horizontal strains, and they form a sound basis for considering this aspect of uncertainty. Equations 2 and 3 may now be modified to

$$\mu_c = [A + \alpha_c(1 - A)] F_c \tag{11}$$

and

$$\mu_s = [N + \alpha_s(1 - N)] F_s \tag{12}$$

and values of μ are shown in Figure 2 as a function of OCR and 2b/D for both circular and strip loads.

The one-dimensional settlement for overconsolidated soils may be determined from

$$\delta'/D = [C_r/(1 + e)] \log [(p_o + \Delta p)/p_o] \tag{13}$$

Equation 13 may be combined with Eq. 5 to obtain the dimensionless settlement-layer thickness ratio, R, given by

$$R = \delta/D = \mu [C_r/(1 + e)] \log [(p_o + \Delta p)/p_o] \tag{14}$$

and the probability distribution function for R can be determined by use of the preceding relations for any given set of conditions.

Application of Monte Carlo Simulation

A convenient means of obtaining the distribution function for R, f(R), is by use of Monte Carlo simulation (7). If each uncertain variable is represented by an appropriate probability distribution function, a simulated sample of the variable may be taken by generating for each a random number and then processing it in accordance with the associated distribution. Combination of the sample values in accordance with the foregoing formulas leads to a sample value for R. If this is repeated a large number of times, we obtain a frequency distribution histogram from which the uncertainty associated with settlement determination may be inferred. An example of such a histogram is shown in Figure 3.

The spread of the histogram is characterized by use of a 90 percent confidence level; this entails the determination of a range that has a 90 percent probability of including the true settlement. As shown in Figure 3, a reference value of R, designated $\overline{R}$, is determined by substituting into the deterministic formulas the mean values of the relevant parameters. From the differences between $\overline{R}$ and the upper and lower 5 percent levels (H and L respectively, as shown), the ratios $H/\overline{R}$ (designated H_R) and $L/\overline{R}$ (designated L_R) are determined.

DISTRIBUTION FUNCTIONS FOR INPUT PARAMETERS

Figure 4 shows a diagrammatic summary of the various parameters that influence the settlement determination for an overconsolidated clay and the manner in which they combine to do so. The variables associated with the system geometry, b and D, are considered to be known without error, and they are represented deterministically. Probability distribution functions are applied to soil properties (C_r and e), to soil stresses (p_o, p_c, and Δp), and to formulation uncertainty.

Soil Properties

For the recompression index, C_r, a previously proposed (3) distribution form is used. Although little supporting evidence in the form of measured data is available for C_r, the physical nature of the phenomenon and its similarity to phenomena for which data are available indicate that both (a) a consistency in the value of the coefficient of variation would exist and (b) the specimen test results would display a normal distribution. Provided these 2 assumptions are satisfied, the distribution for possible values of the true recompression index may be given by

$$f[C_{r(i)}] = \lim_{C_{r(i+1)} \to C_{r(i)}} \left\{ \int_{Z_{i+1}}^{Z_i} f(Z)\, dZ \Big/ [C_{r(i+1)} - C_{r(i)}] \right\} \tag{15}$$

in which

$$Z_i = [\overline{C}_r - C_{r(i)}]/[VC_{r(i)}/\sqrt{n}] \tag{16}$$

and

$$f(Z) = (1/\sqrt{2\pi}) \exp(-0.5\, Z^2) \tag{17}$$

For Monte Carlo simulation, each sample of C_r may be obtained from

$$C_r = \overline{C}_r/[1 - (\xi V/\sqrt{n})] \tag{18}$$

where ξ is the standard normal deviate generated from a normal distribution having a mean of zero and a standard deviation of unity. In this study the value of $V/\sqrt{n}$ is taken as 0.2, which, for example, corresponds to $V = 0.4$ and $n = 4$ or to $V = 0.2$ and $n = 1$.

Determining the probability distribution function for the void ratio, e, gives rise to a complication. Although the uncertainties associated with the other variables are essentially independent of one another and the random variables generated in the simulation process are correspondingly independent, the void ratio is at least partially dependent on the recompression index. However, very little information is available to establish a quantitative relationship between the two, and it is unlikely that a reasonable value of the recompression index could be determined from void ratio alone. Nevertheless, within the same soil mass, there is some indication that a change in the recompression index is related to a change in the void ratio. For example, Schmertmann (5) has suggested the following equation to relate, for a particular soil, any 2 void ratios at the start of rebound (e_{r1} and e_{r2}) to the corresponding recompression indices (C_{r1} and C_{r2}).

$$\log (C_{r1}/C_{r2}) = 2.5 \log [(e_{r2} + 1)/(e_{r1} + 1)] \tag{19}$$

If the inaccuracy associated with this relation is taken into account by a factor Q, which is generated from a normal distribution with a mean of 1.0 and a standard deviation of 0.05, the sample value of the void ratio, e, to be used in the simulation process is given by

$$e = (\overline{e} + 1)\, (\overline{C}_r/C_r)^{0.4/Q} - 1 \tag{20}$$

in which $\overline{e}$ is the mean initial void ratio obtained from the test specimens, C_r is the sample recompression index generated in accordance with Eq. 18, and $\overline{C}_r$ is the mean recompression index. The value of 0.05 for the standard deviation in the formulation given above was determined by considering the experimental data presented by Schmertmann.

Soil Stresses

Considerable uncertainty is encountered when the stresses associated with settlement determinations are evaluated; and, since there are few data to serve as a guide

in establishing the form or spread of probability distribution functions that represent stress uncertainties, a subjective approach is necessary. In addition to the convenience afforded by normal distributions, they appear to offer quite reasonable representations of the phenomena under consideration, as the following examples will indicate. Accordingly, normal distributions with values of 0.1, 0.05, and 0.025 for the coefficients of variation are used for the preconsolidation stress, the overburden stress, and the stress increase respectively. The implications of normal distributions with the indicated coefficients of variation are given in Table 2; for this example, the most likely value of the stress in each case is 1,000 psf.

Formulation Uncertainty

Determination of the A parameter from the table of Skempton and Bjerrum is only approximate, and a graphical indication of the approximation is shown in Figure 1. A degree of uncertainty similar to that indicated by the rectangular blocks is incorporated in the suggested formulation (Eq. 6) by adding an error function, E, which is normally distributed with a mean of 0 and a standard deviation of 0.1; thus, Eq. 6 becomes

$$A = 1.3\ (0.63)^{OCR} + E \tag{21}$$

The effect of this error function on the resulting values of A is shown in Figure 1. Generated values of A are influenced by the distributions associated with E, p_c, and p_o.

Equation 6 provides an empirical means for considering the error associated with lateral strains in the Skempton-Bjerrum approach. Since the uncertainty in the formulation becomes greater as the error increases, one appropriate probabilistic treatment for the case of a uniformly loaded circular area is to generate the random variable F_c from the equation

$$F_c = 1 + G \tag{22}$$

in which G is normally distributed with a mean $\overline{G}$ where $\overline{G} = 0.01 \exp [2.753 - 0.45 (2b/D)]$ in accordance with Eq. 9, and a standard deviation of $0.4\overline{G}$; the large value for the standard deviation is indicative of the considerable degree of uncertainty involved. One implication for the extreme case where $2b/D = 0$ is that there is a 67 percent probability of F_c falling within the range 1.12 to 1.20. This corresponds approximately with the possible error of 20 percent indicated by Skempton and Bjerrum.

ANALYSIS OF UNCERTAINTY

The influence of various parameters on the uncertainty associated with settlement determinations for uniformly loaded circular areas is evaluated by making several series of computations in which many of the parameters are varied over a wide range of values. Subject to the elimination of any case wherein the overconsolidation ratio is less than $(p_o + \Delta p)/p_o$ (that is, the implied settlement extends beyond simple recompression), 81 combinations of the following parameters were utilized to establish distributions, f(R):

Parameter	Various Values Used
$(p_o + \Delta p)/p_o$	1.5, 2, 5, 10
OCR	2, 6, 15
$C_r/(1 + e)$	0.15, 0.04, 0.004
2b/D	0.1, 1, 10

In each case the high and low deviation ratios, H_R and L_R, were determined, and multiple regression techniques were employed to develop the following relations:

$$H_R = 0.96 - 0.001 \{1.163\ OCR [\log (2b/D) - 1] + 16.63\ (2b/D)\} \tag{23}$$

and

Figure 1. Relation of parameter A and OCR.

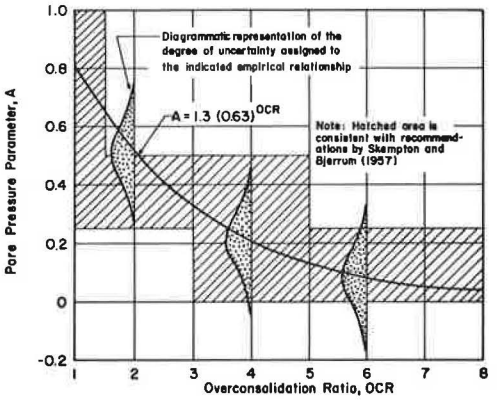

Figure 2. μ determined from OCR and load.

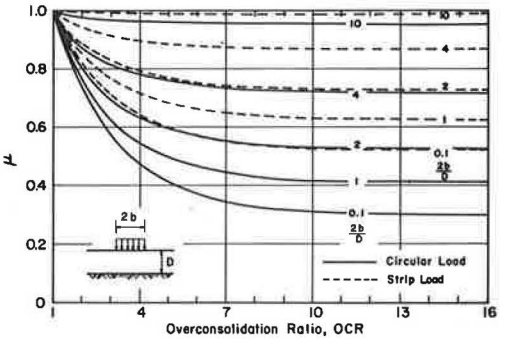

Figure 3. Typical probability distribution of R.

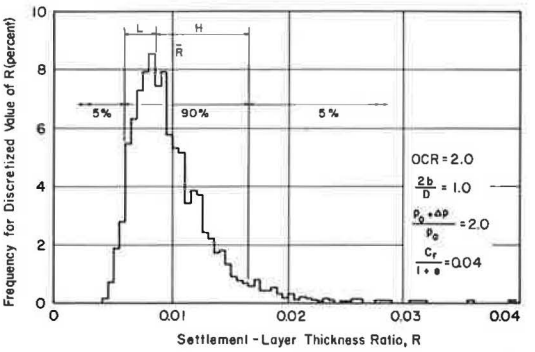

Figure 4. Parameters influencing settlement.

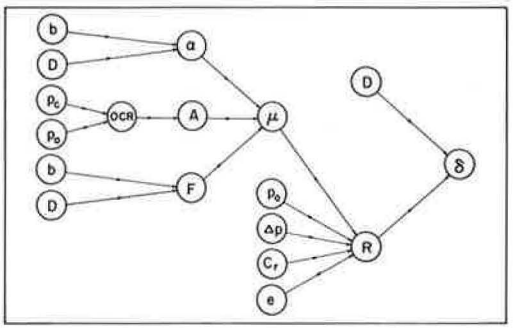

Figure 5. Uncertainty as a function of OCR and depth parameter.

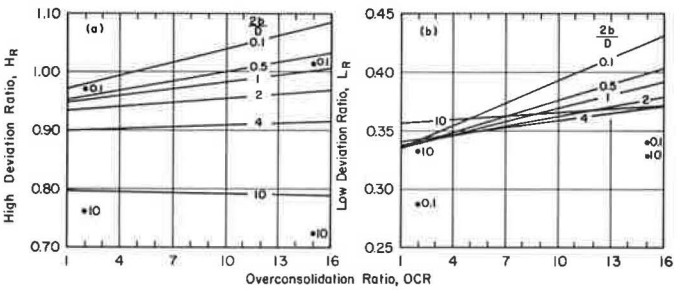

Table 1. Values of a.

2b/D	Circularly Loaded Area: Reported Value (6)	Circularly Loaded Area: Calculated From Eq. 7	Continuous Strip Load: Reported Value (4)	Continuous Strip Load: Calculated From Eq. 8
∞	1.00	1.00	1.00	1.00
4.00	0.67	0.69	0.80	0.81
2.00	0.50	0.49	0.63	0.64
1.00	0.38	0.37	0.53	0.50
0.50	0.30	0.31	0.45	0.43
0.25	0.28	0.28	0.40	0.39
0.10	0.26	0.26	0.36	0.36
0	0.25	0.25	0.25	0.35

Table 2. Probability that indicated stress range includes true value of stress.

Stress Parameter	Coefficient of Variation	67 Percent	95 Percent	99 Percent
Preconsolidation stress	0.1	900 to 1,100	800 to 1,200	742 to 1,258
Overburden stress	0.05	950 to 1,050	900 to 1,100	871 to 1,129
Stress increase	0.025	975 to 1,025	950 to 1,050	935 to 1,065

Note: Stress ranges are in psf.

$$L_R = 0.328 - 0.001 \{0.718\ OCR\ [\log (2b/D) - 1] - 2.78\ (2b/D)\} \quad (24)$$

which are shown graphically in Figure 5. As implied by Eqs. 23 and 24, the magnitudes of both H_R and L_R are relatively insensitive to variation in $(p_o + \Delta p)/p_o$ and $C_r/(1 + e)$.

Application of the results given above is limited to cases where the expected value of the total stress falls somewhat below the expected value of the preconsolidation stress, since the analysis does not take into account the possibility of virgin consolidation settlement that may occur when these 2 expected stress values are similar. Obviously, for cases where the total stress probability distribution overlaps the preconsolidation stress probability distribution, the settlement will depend on the virgin compression index, C_c, as well as the recompression index, C_r. Therefore, the true deviation ratio, H_R, under these circumstances should be higher than that shown in Figure 5.

Illustrative Problem

Application of the above-described procedure can be best explained in terms of an example problem. Suppose a 10-ft-square foundation rests on a 20-ft-thick layer of overconsolidated clay with an overconsolidation ratio of 8, an average in situ void ratio of 0.5, and a recompression index of 0.03. If the average initial overburden stress is 1,500 psf and the stress increase due to loading is 6,000 psf, determine the probable range of settlement.

From Eq. 13, we obtain

$$\delta' = D[C_r/(1 + e)] \log [(p_o + \Delta p)/p_o]$$

$$= (20 \times 12)[0.03/(1 + 0.5)] \log [(1,500 + 6,000)/1,500]$$

$$= 3.4 \text{ in.}$$

From data shown in Figure 1 for OCR = 8 and 2b/D = 0.5, we get $\mu = 0.4$, which, when used in conjunction with Eq. 5, yields

$$\delta = \mu\delta' = 0.4\ (3.4) = 1.36 \text{ in.}$$

Finally, from data shown in Figure 4 for OCR = 8 and 2b/D = 0.5, we determine $H_R = 0.99$ and $L_R = 0.37$, which lead to the following relations:

$$(1 + H_R)\delta = (1 + 0.99)\ 1.36 = 2.7$$

and

$$(1 - L_R)\delta = (1 - 0.37)\ 1.36 = 0.9$$

Therefore, there is a 90 percent probability that the consolidation settlement of the foundation will lie within the range from 0.9 to 2.7 in.

Discussion of Problem

For the parameter values utilized, the upper end of the 90 percent probability range varies from 79 to 109 percent above the deterministically computed settlement, while the lower end varies from 33 percent to 44 percent below the deterministically computed settlement. Since the uncertainty indicated by these values is considerable, it is important to discuss some of the factors that may contribute to this situation.

The first point of interest concerns the crudeness of the correlation between the A pore-pressure parameter and the overconsolidation ratio; in fact, Skempton and Bjerrum specifically advise against the use of such a correlation for formal calculations, and they suggest that A be determined by means of a triaxial test. Therefore, in order to study the effect of the 2 different approaches on the uncertainty associated with the end result, the simulation process was repeated with an A value generated from a distribution that is representative of the uncertainty associated with A as

determined from a triaxial test. Since few data are available on which a distribution for A may be based, a normal distribution with a standard deviation of 0.05 is subjectively selected; this implies a 67 percent probability that the true value for A lies within ±0.05 of the mean value of A determined from tests or a 95 percent probability that the true value lies within ±0.1. Then, H_R and L_R were determined for overconsolidation ratios of 2 and 15 and 2b/D values of 0.1 and 10; the results are shown in Figure 5. The average reductions in the deviation ratios are 5 percent on the high side and 14 percent on the low side. Since it is unlikely that the distribution given above for A is too broad, it appears that little is gained by determining A from a triaxial test.

It is also interesting to compare the preceding results with those reported (2) for the case in which a similar approach is taken to the simpler problem of one-dimensional consolidation due to a stress in excess of the preconsolidation stress. In the earlier study for cases where the ratio of the total stress to the preconsolidation stress exceeds about 2 (and for $V/\sqrt{n} = 0.2$), the high deviation ratio is in the range of 35 to 40 percent and the low deviation ratio is about 25 percent. However, a considerable increase over these values is not unexpected because of the uncertainties associated with the use of the A pore-pressure parameter and the effect of horizontal displacements. On the other hand, when the ratio of total stress to preconsolidation stress is less than about 2 in the previous study, the uncertainty associated with the settlement computation approaches that associated with foundations on overconsolidated soils; this is due to the greater influence of the less certain preconsolidation stress under these conditions.

CONCLUSION

Probability theory has been used to develop a rational procedure for evaluating the uncertainty associated with the computation of settlement for foundations resting on overconsolidated soils. Although every effort was made to incorporate well-founded and representative expressions in the probabilistic formulation, the lack of measured data in many cases necessitated the use of considerable subjective judgment; however, the developed procedure is readily adaptable to modification if and when appropriate data become available. In the meantime, a quantitative, even though subjective, assessment of the individual aspects of the problem in terms of accepted probabilistic procedures, such as Monte Carlo simulation, seems to provide the best available solution to such problems. This approach is particularly useful when mathematical complexities preclude an intuitive evaluation of uncertainty, as is the case for settlement computations involving overconsolidated soils.

REFERENCES

1. HRB Committee A2L02. Estimating Consolidation Settlements of Shallow Foundations on Overconsolidated Clay. Applications Bull., Jan. 1971.
2. Kay, J. N., and Krizek, R. J. Analysis of Uncertainty in Settlement Prediction. Jour. of Southeast Asian Society of Soil Engineering, Vol. 2, No. 2, Dec. 1971, pp. 119-129.
3. Kay, J. N., and Krizek, R. J. Estimation of the Mean for Soil Properties. Proc., Conf. on Application of Statistics and Probability to Soil and Structural Engineering, Hong Kong, Sept. 1971.
4. Muir Wood, A. M. Correspondence on "A Contribution to the Settlement Analysis of Foundations on Clay" by A. W. Skempton and L. Bjerrum. Geotechnique, Vol. 9, No. 1, March 1959, pp. 29-30.
5. Schmertmann, J. H. The Undisturbed Consolidation Behavior of Clay. Trans. ASCE, Vol. 120, Closure to discussion, 1955, pp. 1229-1233.
6. Skempton, A. W., and Bjerrum, L. A Contribution to the Settlement Analysis of Foundations on Clay. Geotechnique, Vol. 7, No. 4, Dec. 1957, pp. 168-178.
7. Warner, R. F., and Kabaila, A. P. Monte Carlo Study of Structural Safety. Jour. of Structural Division, Proc. ASCE, Vol. 94, No. ST12, Dec. 1968, pp. 2847-2859.

USE OF INFRARED PHOTOGRAPHY TO IDENTIFY FAULTING IN PIERRE SHALE

E. R. Hoskins, D. W. Hammerquist, and P. H. Rahn,
South Dakota School of Mines and Technology

ABRIDGMENT

•SOIL expansion and the accompanying pavement distress in roadways constructed on the Pierre formation have been a serious problem for the South Dakota Department of Highways for many years. Because of the distribution of the Pierre formation, most highways in the western half of the state have been affected. In the past decade, a great deal of research has been carried out by the highway department and other agencies to find a suitable design for primary roadways that would eliminate or at least minimize roadway heave and the subsequent breakup of the pavement. The investigation summarized in this report has been a continuation of this major research effort.

Along Interstate 90 from Wasta west to Rapid City, there are many sections of portland cement concrete pavement that have buckled and broken. Various post-construction treatments were attempted (1, 2), but eventually those areas required extensive overlays and patching. In 1968 and 1969 an investigation of pavement distress in roadways in western South Dakota was carried out by Hammerquist and Hoskins (3). These investigators were able to correlate severe pavement distress with faulting and jointing in the underlying Pierre shale. They also observed that pavement heave was still possible in sections of the primary roadway in which the subgrade had been lime-treated prior to paving. Moisture apparently could get down through the subgrade (or come up if the water table rose) into the faulted and jointed material under the subgrade and cause swelling along the strike of the faults. When the strike of a fault crossed the roadway at approximately a right angle, a prominent sharp bump in the surface resulted.

It follows that one of the key problems associated with the design and construction of smooth, maintenance-free highways in western South Dakota should be the identification of faults and joints as well as seasonal variations in the depth of the water table in the Pierre shale prior to the design and construction of existing routes. If these potentially troublesome areas can be identified beforehand, it might be possible to relocate the route to avoid those areas; or, if relocation were not feasible, a more extensive (and more effective) design and construction procedure might be used in just the faulted and jointed areas to secure better highways and eventually lower overall costs.

The purpose of the investigation we now report on was to try to identify faults and joints and water table depths in the Pierre shale from terrestrial and low-altitude aerial photographs. We used a multispectral photographic approach with black and white panchromatic, natural color, and infrared color film. The areas selected for photographic coverage were 3 test sites east of Rapid City previously investigated (trenched, with the faults and joints mapped in detail) by Hammerquist and Hoskins (3). The terrestrial photographs were taken at intervals of approximately 1 month for 1 year. Our initial premise was that the color infrared film would show relative changes in the health of the vegetation growing in the faulted zones compared to that growing on the undeformed shale. The fault and joint zones should serve as areas where more moisture is available to plant roots. Areas with a permanently higher water table should similarly be covered with more luxuriant vegetation.

Sponsored by Committee on Exploration and Classification of Earth Materials.

We took the photographs at regular intervals for a full year to find out whether these differences in plant vigor were easier to identify at any particular time of the year. Terrestrial instead of aerial photographs were used initially for 2 reasons.

1. We were looking for lineaments whose total width was known from our previous work to vary from a fraction of an inch to a maximum of 5 to 6 in. We felt that it would be difficult to reliably identify such narrow features from conventional aerial photography.
2. It was much less expensive to take the photographs from the ground. Because this was a preliminary investigation we were not sure at the start what combination of filters and films and processing tricks would be required to give us the most useful display of information. With a limited amount of money available we could try many more combinations and repeat them if necessary under different lighting conditions with ground-based photography than we ever could have accomplished with commercial aerial photography.

Toward the end of the project we did contract for 2 flights of low-altitude (500 to 1,500 ft) coverage; one of the principal investigators rode on the flight to take the photographs.

The 3 areas selected for detailed study in this investigation are all located in the Pierre shale in 25- to 40-ft deep cut sections along Interstate 90 in Pennington County, South Dakota. These are sites 5, 6, and 8 (3). All 3 sites were in clay shale with field moistures of approximately 30 percent and liquid limits between 70 and 100. The concrete pavement was badly warped and broken by differential swelling of the shale along the strike of the faults at all 3 sites. The roadway has subsequently been patched and repatched several times at each location. The area is in rolling terrain with ridges approximately parallel and trending northwest to southeast. The highway grades in the road cuts are low angle to almost level, and the drainage in the cuts is generally poor.

The following cameras, film, and filter combinations were used for the terrestrial photography: Kodak Panatomic-X black and white film with no filter on the camera, Kodak Ektachrome-X reversal color film with a UVa (ultraviolet absorption) filter, Kodak Ektachrome Infrared Aero film No. 8443 with a No. 12 (minus blue) filter, and Kodak Ektachrome Infrared Aero film No. 8443 with No. 12 (minus blue) and No. 80B (light blue) filter used together. All of the Ektachrome and Ektachrome Infrared photographs were taken with 35-mm hand-held cameras. The Ektachrome and Ektachrome Infrared films were developed in our laboratory by using Kodak E-3 processing solutions. We also processed the black and white film. Both types of color film yield positive color transparencies. These are difficult to interpret even when projected, and so several different techniques were used to make prints. Color prints were made of a few of the transparencies; however, inasmuch as we produced more than 1,000 color transparencies, it would have been prohibitively expensive and time-consuming to make color prints of them all. Accordingly, we made negative black and white prints of the color slides on panchromatic enlarging paper (Kodak Panalure). To attempt to enhance the data presentation, we also selectively filtered the color slides during the printing process with No. 47 (dark blue), No. 64 (deep green), and No. 29 (deep red) filters on the enlarger. Each color slide (normal and infrared color) then yielded 4 different black and white paper negatives, one with no filters used on the enlarger, one with the dark blue filter, one with the green filter, and one with the red filter. These paper negatives were then used to make positive prints on ordinary photographic paper.

In general the terrestrial photographs were about as effective as we had anticipated. They show a wealth of detail with good resolution, and they are simple and inexpensive to take. However, they are very low angle obliques and are difficult to quantitatively interpret. Also, because these are photographs of artificially cut hillslopes, they should not be expected to show as much information as photographs of a natural hillslope where time has allowed the slow evolution of plants, each dependent on subtle soil-moisture changes. However, the fact that fracture traces are visible on the artificial slopes serves to indicate the usefulness of the techniques.

The low-altitude (500 to 1,500 ft), high-resolution aerial photographs yielded the most useful and easiest to interpret display of information. Most of the fine-scale

lineaments were still visible, and they are relatively simple to interpret. Conventional higher altitude aerial photography was only of limited use to us. The lineaments visible on conventional air photos are mostly the major drainages, and these are the fill areas on the highway and so are not directly related to the problem of pavement roughness in the cut areas.

We have recommended that a small project be started in which low-altitude aerial color infrared photographs are taken of a section of a highway route in Pierre shale prior to construction. Lineations found on the photographs should then be checked by a geologist on the ground during the excavation of the cuts. Once the lineations are identified and mapped, the performance of the pavement in these areas would be checked and recorded by highway maintenance personnel for several years. In this way a direct relation between the presence of the lineaments and the ultimate maintenance costs would be found and the cost effectiveness of the aerial photography as an investigative tool established.

REFERENCES

1. McDonald, E. B. Lime Research Study, South Dakota, Interstate Routes (16 Projects). South Dakota Department of Highways, Final Rept., 1969, 33 pp.
2. Whyte, R. M. I-90-2(9)77, Pennington County Water Induction Tests. South Dakota Department of Highways, Final Rept., 1965, 7 pp.
3. Hammerquist, D. W., and Hoskins, E. R. Correlation of Expansive Soil Properties and Soil Moisture With Pavement Distress in Roadways in Western South Dakota. South Dakota School of Mines and Technology, Rapid City, Final Rept., 1969, 61 pp.

SPONSORSHIP OF THIS RECORD

Special Committee on International Cooperative Activities
Robert O. Swain, International Road Federation, chairman
Donald S. Berry, A. Carl Cass, William H. Glanville, James R. Golden, Lucius M. Hale, Perry Leaming, H. Jack Leonard, Morris S. Ojalvo, Clyde H. Perry, Ralph E. Rechel, Wilbur S. Smith, Clifton G. Stoneburner, W. Murray Todd

GROUP 2—DESIGN AND CONSTRUCTION OF TRANSPORTATION FACILITIES
John L. Beaton, California Division of Highways, chairman

COMPACTION AND STABILIZATION SECTION
Eugene B. McDonald, South Dakota Department of Highways, chairman

Committee on Soil-Bituminous Stabilization
Anwar E. Z. Wissa, Massachusetts Institute of Technology, chairman
K. O. Anderson, M. Barrett Clisby, David D. Currin, Donald G. Fohs, C. W. Heckathorn, Moreland Herrin, James E. Kelly, Larry L. Kole, Sidney Mintzer, A. H. Neunaber, Vytautas P. Puzinauskas, Ronald L. Terrel, Thomas D. White, Walter H. Zimpfer

SOIL MECHANICS SECTION
Carl L. Monismith, University of California, Berkeley, chairman

Committee on Strength and Deformation Characteristics of Pavement Sections
John A. Deacon, University of Kentucky, chairman
Richard D. Barksdale, Bert E. Colley, Hsai-Yang Fang, Frank L. Holman, W. Ronald Hudson, Melvin H. Johnson, Bernard F. Kallas, William J. Kenis, Wolfgang G. Knauss, Milan Krukar, H. Gordon Larew, Fred Moavenzadeh, Carl L. Monismith, William M. Moore, Keshavan Nair, Eugene L. Skok, Jr., Ronald L. Terrel

Committee on Embankments and Earth Slopes
Lyndon H. Moore, New York State Department of Transportation, chairman
Philip P. Brown, Raymond A. Forsyth, David S. Gedney, Wilbur M. Haas, C. W. Heckathorn, Raymond C. Herner, William P. Hofmann, Henry W. Janes, Martin S. Kapp, Philip Keene, Richard E. Landau, Ivan C. MacFarlane, Harry E. Marshall, Glen L. Martin, R. M. Mattox, Melvin W. Morgan, Robert L. Schuster, Robert T. Tierney, David J. Varnes, Walter C. Waidelich, William G. Weber, Jr.

Committee on Foundations of Bridges and Other Structures
M. T. Davisson, University of Illinois, chairman
David R. Antes, Edwin C. Beethoven, Bernard E. Butler, Harry M. Coyle, Jacob Feld, David S. Gedney, Bernard A. Grand, Robert J. Hallawell, Horace E. Hoy, Hal W. Hunt, Martin S. Kapp, Philip Keene, Richard E. Landau, Clyde N. Laughter, G. A. Leonards, Thomas D. Moreland, A. Rutka

SOIL AND ROCK PROPERTIES AND GEOLOGY SECTION
L. F. Erickson, Idaho Department of Highways, chairman

Committee on Exploration and Classification of Earth Materials
Robert L. Schuster, University of Idaho, chairman
Robert C. Deen, Albin D. Hirsch, William P. Hofman, Robert B. Johnson, Ralph W. Kiefer, Robert D. Krebs, Clyde N. Laughter, R. V. LeClerc, Robert H. Mattox, Donald E. McCormack, Olin W. Mintzer, R. Woodward Moore, Arnold C. Orvedal, David L. Royster, A. Rutka, William W. Shisler, Preston C. Smith, Ernest G. Stoeckeler, Walter H. Zimpfer

Committee on Soil and Rock Properties
W. H. Perloff, Purdue University, chairman
William F. Brumund, Richard W. Christensen, George B. Clark, Wilbur I. Duvall, Charles L. Emery, Emmericus C. W. A. Geuze, Bernard B. Gordon, James P. Gould, Ernest Jonas, Robert L. Kondner, Charles C. Ladd, G. A. Leonards, Victor Milligan, Vladimir Obrcian, Shailer S. Philbrick, Gerald P. Raymond, Hassan A. Sultan, Harvey E. Wahls, T. H. Wu

Roy C. Edgerton and John W. Guinnee, Highway Research Board staff

The sponsoring committee is identified by a footnote on the first page of each report.